

**PHOTOCHEMISTRY
OF
2,3-PENTANEDIONE**

TO MY FAMILY

PHOTOCHEMISTRY
OF
2,3-PENTANEDIONE

By

ANTHONY WILLIAM JACKSON, B.Sc.

A Thesis

Submitted to the School of Graduate Studies

in Partial Fulfilment of the Requirements

for the Degree

Doctor of Philosophy

McMaster University

May 1971

DOCTOR OF PHILOSOPHY (1971)
(Chemistry)

McMASTER UNIVERSITY
Hamilton, Ontario

TITLE: The Photochemistry of 2,3-pentanedione

AUTHOR: Anthony William Jackson, B.Sc. (London)

SUPERVISOR: Professor A. J. Yarwood

NUMBER OF PAGES: xii, 247

SCOPE AND CONTENTS:

When excited in the region 365-436 nm in the gas phase, 2,3-pentanedione is shown to emit fluorescence and phosphorescence. The absolute emission yields have been determined and the radiationless processes removing the excited singlet and triplet states have been considered.

The radiationless processes removing the triplet state have been investigated at different temperatures and concentrations and are shown to be intersystem crossing to the ground state, a temperature dependent unimolecular reaction and a temperature dependent bimolecular self-quenching reaction.

Excitation at 365 nm causes emission from vibrationally excited levels of the singlet state. The variation of the fluorescence yield with pressure at this excitation wavelength is compatible with either a strong or weak collision mechanism for vibrational deactivation within the singlet manifold. Phosphorescence yield measurements support this conclusion.

A consistent mechanism is proposed to describe the system and is tested with fluorescence, phosphorescence, and lifetime measurements at various temperatures and concentrations.

The interaction of the triplet state of pentanedione with various classes of substrate has been investigated. Emphasis has been placed on the temperature dependence of the reaction modes. The possibility of energy transfer from the triplet pentanedione molecule has been investigated with 1,3-butadiene and cyclopentadiene at different temperatures. The butadiene quenching system is kinetically simple at all temperatures studied, whereas the cyclopentadiene is simple at high temperatures but complex at lower temperatures. This behaviour has been reconciled with reversible energy transfer in the gas phase triplet pentanedione/cyclopentadiene system at the lower temperature. A mechanism is proposed which demonstrates directly the intermediacy of the triplet cyclopentadiene species and, therefore, confirms the energy transfer nature of the interaction. The energy transfer rate constants are discussed with respect to the current models of energy transfer to dienes.

ACKNOWLEDGEMENTS

I would like to express my gratitude to Dr. A. J. Yarwood for his guidance and encouragement throughout the course of this work. My thanks go to Dr. Hari S. Samant and Mr. Gerald M. White for their stimulating and helpful conversations.

I must pay tribute to the patience and understanding encouragement provided by my wife, Ruth, who has always been a source of comfort.

I would like to thank Miss Jan Iverson for her excellent cooperation in the typing of this thesis.

Financial support from the Province of Ontario and McMaster University is gratefully recognised.

TABLE OF CONTENTS

	Page	
Chapter 1	Introduction	1
Chapter 2	Apparatus and Technique	23
Chapter 3	Absorption spectrum and natural radiative lifetime of 2,3 pentanedione.	40
Chapter 4	Luminescence spectra	51
Chapter 5	Triplet lifetime experiments with 2,3 pentanedione	74
Chapter 6	Self-quenching of Q_f and Q_p for 436 nm excitation.	103
Chapter 7	Vibrational deactivation: photolysis at 365 nm at 90°C.	113
Chapter 8	Variation of fluorescence and phosphorescence yields with temperature.	145
Chapter 9	Quenching of triplet pentanedione by α,β unsaturated carbonyl compounds.	165
Chapter 10	Quenching of triplet state by a variety of molecules.	178
Chapter 11	Quenching of triplet pentanedione by conjugated diolefins.	197
Conclusions		231
Appendices		233
References		238

LIST OF TABLES

Table	Title	Page
1.	Energies of biacetyl electronic states	45
2.	Absolute Quantum yields of emission at 365, 405, 436 nm, at 24°C.	54
3.	Q_p and Q_f for biacetyl and pentanedione at 30°C, $\lambda_{ex} = 436$ nm.	54
4.	Phosphorescent lifetime in different phases at 77°K.	82
5.	Values of Q_f and Q_p at 50, 70, 90°C, $\lambda_{ex} = 436$ nm.	105
6.	Comparison of self-quenching rate constants at 50, 70, 90°C.	110
7.	Values of Q_f and Q_p at 90°C with 365 nm excitation.	117
8.	Rate constants for quenching of triplet 2,3 pentanedione by eneones.	171
9.	Quenching constants for various substrates with pentanedione triplets.	188
10.	Slope and intercept data for quenching of pentanedione by cyclopentadiene at 30°C.	213

LIST OF FIGURES

Figure	Title	Page
1.	The Jablonski diagram showing the modes of disappearance of electronically excited states.	4
2.	Sensitivity correction curve of photomultiplier-monochromator used in quantum yield determination.	26
3.	Narrow band pass filters used in this study.	27
4.	Proportionality between transmitted light signal and displayed monitor signal.	28
5.	Optical arrangement used in determination of Q_f and Q_p .	31
6.	Response of 935 photocell at different light intensities.	33
7.	Geometry of cell for calculation of inner filter effect at 460 nm.	34
8.	Correction factor for inner filter effect at 460 nm.	36
9.	Visible/u.v. absorption of 2,3-pentanedione in the gas phase at 24°C.	41
10.	The n, π configurations for biacetyl.	46

11.	Uncorrected emission spectrum of 2,3-pentanedione excited at 405 nm, temperature is 23°C.	52
12.	Corrected total emission spectrum of pentanedione excited at 405 nm.	55
13.	Corrected fluorescence emission spectrum of pentanedione excited at 405 nm.	56
14.	Schematic representation of potential energy curves of S_0 , S_1 and T_1 states.	60
15.	Showing "mirror-image" relationship between fluorescence and absorption.	62
16.	Variation of phosphorescent lifetime with temperature, concentration of pentanedione is 6.6×10^{-4} M.	75
17.	Variation of triplet lifetime with concentration at 25, 30, 40, and 50°C.	77
18.	Variation of triplet lifetime with concentration of pentanedione at 60, 70, 80, and 90°C.	78
19.	Variation of τ_p with pressure of perfluoroethane at 80°C.	79
20.	Variation of triplet lifetime with incident light intensity at 63.9°C.	80
21.	Variation of the Bimolecular Quenching rate constant with temperature.	86
22.	Showing the non-linear behaviour of $\log 1/\tau_0$ with $1000/T$	90

23.	Showing the asymptotic variation of $1/\tau_0$ with $1000/T$.	91
24.	Variation of Q_p^0/Q_p with concentration of pentanedione at 50, 70, and 90°C; $\lambda_{ex} = 436$ nm.	104
25.	Variation of fluorescence intensity with pressure of added C_2F_6 ; pentanedione pressure is 26.4 torr, temperature is 40°C, $\lambda_{ex} = 436$ nm.	107
26.	Variation of Q_f with concentration of pent- anedione in the gas phase at 90°C, $\lambda_{ex} = 365$ nm.	115
27.	Variation of Q_p with concentration of pent- anedione in the gas phase at 90°C, $\lambda_{ex} = 365$ nm.	116
28.	Variation of total emission yield with pressure of SF_6 at 30°C, 23PD = 10.7 torr, $\lambda_{ex} = 365$ nm.	119
29.	The dimensionless fluorescence function for $\lambda_{ex} = 365$ nm at 90°C.	123
30.	Test of the modified three-level fluorescence Scheme C, $\lambda_{ex} = 365$ nm at 90°C.	129
31.	Variation of Q_p^{-1} with $[M]^{-1}$ at 90°C, $\lambda_{ex} = 365$ nm.	132
32.	Variation of f with $[M]^{-1}$ at 30°C, $\lambda_{ex} = 365$ nm.	137
33.	Variation of $Q_p + f$ and Q_f with temperature; 23PD = 4.2 torr, $\lambda_{ex} = 405$ nm.	148
34.	Variation of Q_p with temperature; 23PD = 4.2 torr $\lambda_{ex} = 405$ nm.	149
35.	Variation of $Q_p + f$ with temperature; 23PD = 23 torr, $\lambda_{ex} = 365$ nm.	150

36.	Variation of Q_p with temperature; 23PD = 23 torr, $\lambda_{ex} = 365$ nm.	151
37.	Variation of $Q_p + f$ and Q_f with temperature; 23PD = 115 torr, $\lambda_{ex} = 436$ nm.	152
38.	Variation of Q_p with temperature; 23PD = 115 torr $\lambda_{ex} = 436$ nm.	153
39.	Variation of $Q_p + f$ and Q_f with temperature; 23PD = 115 torr, $\lambda_{ex} = 365$ nm.	154
40.	Variation of Q_p with temperature; 23PD = 115 torr $\lambda_{ex} = 365$ nm.	155
41.	Quenching of pentanedione triplets by acrolein at 42.2°C and 50.8°C.	167
42.	Quenching of pentanedione triplets by acrolein at 68.3°C and 88.3°C.	168
43.	Quenching of pentanedione triplets by croton- aldehyde at 60.2, 71.5, and 84.4°C.	169
44.	Quenching of pentanedione triplets by methyl vinyl ketone at 62.5, 70.8, and 80.5°C.	170
45.	Arrhenius plots for eneone quenching rate con- stants.	173
46.	Quenching of pentanedione triplet by O_2 at 30 and 60°C.	179
47.	Effect of Xenon on the triplet lifetime of pentanedione at 30°C.	181

48.	Quenching of pentanedione triplets by isobutane at 30°C and 50°C.	182
49.	Quenching of pentanedione triplets by germane at 30°C and 67.8°C.	184
50.	Quenching of pentanedione triplets by furan at 30°C and 72.4°C.	185
51.	Quenching of pentanedione triplets by perfluorobutene-2 at 59.2°C and 80.0°C.	186
52.	Quenching of triplet pentanedione by 1,3-butadiene at 30°C.	198
53.	Quenching of triplet pentanedione by 1,3-butadiene at 70°C.	199
54.	Quenching of triplet pentanedione by cyclopentadiene at 68 and 83°C.	201
55.	Quenching of triplet pentanedione by cyclopentadiene at 30°C, 23PD = 6.1 torr.	202
56.	Quenching of triplet pentanedione by cyclopentadiene at 30°C, 23PD = 12.1 torr.	203
57.	Quenching of triplet pentanedione by cyclopentadiene at 30°C, 23PD = 20.2 torr.	204
58.	Quenching of triplet pentanedione by cyclopentadiene at 30°C, 23PD = 26 torr.	205
59.	Quenching of triplet pentanedione by cyclopentadiene at 30°C, 23PD = 32 torr.	206

60.	Variation of $(\tau^{-1} - \tau_0^{-1})^{-1}$ with pentanedione pressure at 30°C.	209
61.	Variation of $(\tau^{-1} - \tau^{-1})^{-1}$ with pentanedione pressure, CPD pressure is 20 torr.	210
62.	[Intercept from Figs. 60 and 61] ⁻¹ vs CPD pressure at 30°C.	214
63.	[Slope of Figs. 60 and 61 x CPD] ⁻¹ vs CPD pressure at 30°C.	216
64.	Clausius-Claypron plot for 2,3 pentanedione in the region 300-370°K.	236

CHAPTER 1

INTRODUCTION

Light has always been a part of man's existence (1) yet it is only within the last seventy years that he has begun to understand the nature of the interaction of light with matter. This understanding is based on the quantum mechanical description of events and has resulted in a vocabulary which has its origins in this theory. The nature of the interaction will depend on the wavelength of the electromagnetic radiation, a feature which has given rise to many areas of investigation. As with any subdivision in the study of a phenomenon, the field of photochemistry has no exact limits, but, in general, deals with the interaction of matter with radiation in the range 100-700 nm, which corresponds to photon energies in the region 300-40 Kcal/Einstein. As most chemical bonds have energies greater than 40 Kcal/mole, the possibility of bond rupture and chemical rearrangement is apparent.

The early development of the subject was hindered by a lack of an adequate theoretical model and problems associated with the analysis of the sometimes diverse products of photochemical systems. However, in the 1950's, important theoretical advances were made in the understanding of electronically excited states, which together with improvements in analytical and spectroscopic technique have given rise to a surge of interest in this field. This has resulted in immense gains in the knowledge of the processes occurring in photochemical systems.

A historical review will not be presented, since a number of books (2,3) and reviews (4,5,6) have recently considered the general area of photochemistry. What will be presented is the current framework within which the mechanisms of photochemical systems are considered. The interdisciplinary nature of this area of activity will be revealed in the variety of physical and chemical processes which are necessary to explain the behaviour of these systems.

The behaviour of photochemical systems incorporates three general features which have become known as the "Laws of Photochemistry". These are:

- (a) Only the light which is absorbed by a material can be effective in producing photochemical change.
- (b) The absorption of light by a molecule is a one-quantum process, so that the sum of the primary process quantum yields must be unity. This statement needs the qualifying definitions of primary process and quantum yield.

The primary process has been defined by Noyes (7) as "The primary photochemical process comprises the series of events beginning with the absorption of a photon by a molecule and ending either with the disappearance of that molecule, or with its conversion to a state such that its reactivity is statistically no greater than that of similar molecules in thermal equilibrium with their surroundings".

The quantum yield may be defined by,

$$\text{Quantum yield, } \phi = \frac{\text{Number of molecules undergoing a particular process}}{\text{Number of quanta absorbed by the system}}$$

This law may only be applied at moderate light intensities where the concentration of excited molecules is small. Biphotonic processes have been identified in laser and flash photolysis systems using high light intensities ($\sim 10^{23}$ photons/cc/sec).

(c) The amount of monochromatic light absorbed by a system will be governed by the combined Beer-Lambert law,

$$\log \frac{I_0}{I} = \epsilon cl$$

The incident intensity is represented by I_0 , the transmitted intensity after passage through 1 cm containing c mole/litre of material is I . The quantity ϵ is a constant characteristic of the material at a given wavelength and temperature. The law strictly applies to cases where molecular associations are absent. This is usually the case in the gas phase and dilute solution phase.

These generalisations are to be borne in mind in considering the behaviour of chemical systems absorbing the light and behaving in a manner described by the Jablonski energy level diagram shown in Fig. (1).

Jablonski Energy Level Diagram:

This is a schematic representation of the various energy levels which exist for the molecule in the energy region of interest. The molecular orbital theory of chemical bonding can be used to predict these levels, some of which can be correlated with observed spectroscopic transitions. For clarity, only the lowest two, the first excited singlet state S_1 and the lowest triplet state T_1 , in addition to the ground state, S_0 , of the molecule have been shown. The sequence of photochemical events begins with the absorption of a photon by the ground state molecule.

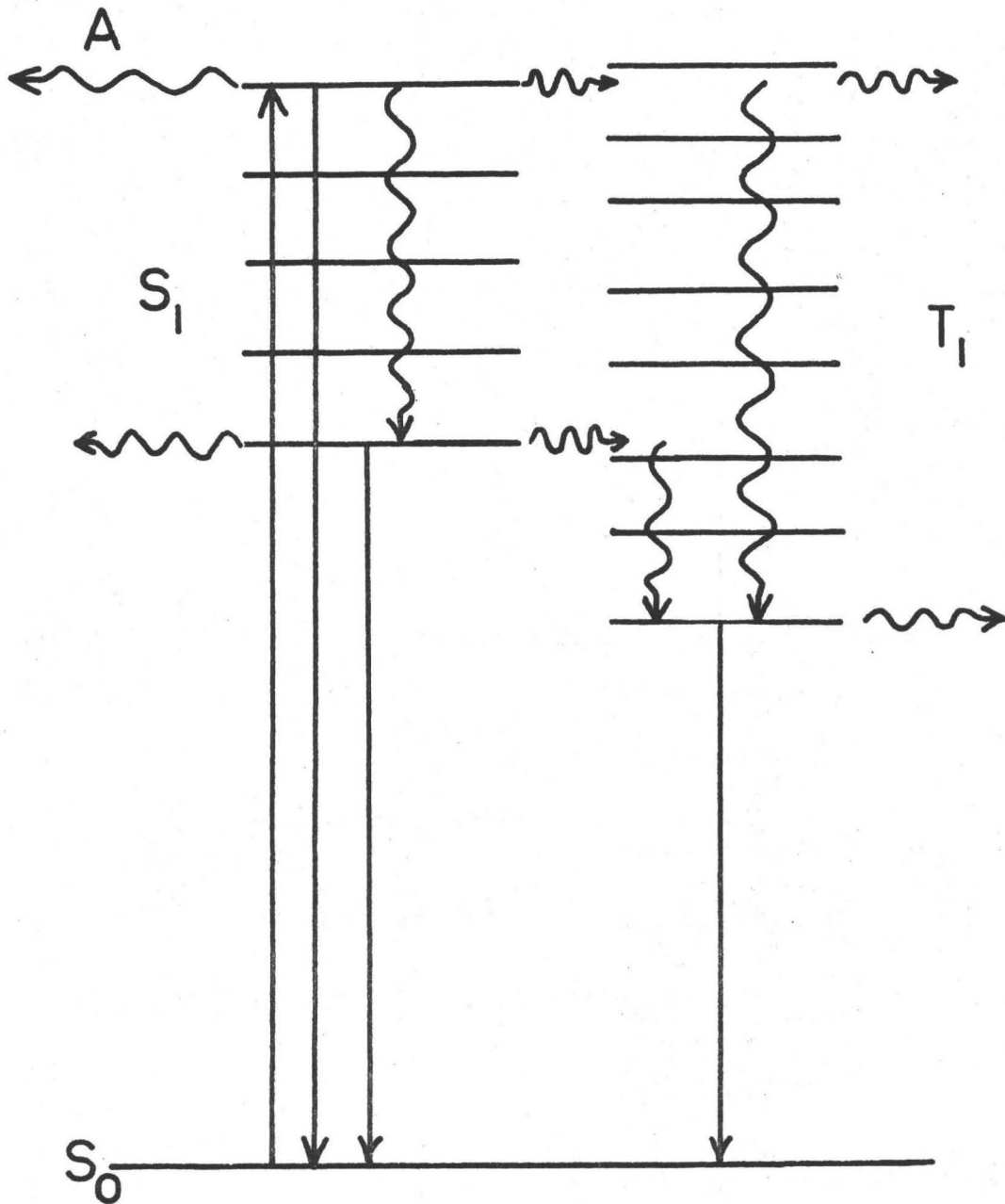


Fig. 1 The Jablonski Diagram showing the modes of disappearance of electronically excited species.

This is assumed to form the molecule in its S_1 excited state as this will be the transition responsible for the absorption spectrum in this energy region. The vibrational energy level of this excited state will be determined by the wavelength (energy) of the exciting radiation. The many paths open for the removal of this initially formed species will determine the behaviour of the system. In the diagram, the solid lines represent radiative processes, whereas the wavy lines represent non-radiative processes.

Intramolecular Processes

The processes represented by the wavy arrow A could represent any of the following.

(a) Photodecomposition

This occurs when the vibrational level reached by absorption is one of a continuous set lying above the dissociation energy of S_1 . It is characterised by a continuous rather than discrete absorption at the exciting wavelength.

(b) Predissociation

Excitation from the ground state forms an excited level of S_1 which would be stable in the absence of another state X_1 . In the presence of this state, which is not unlikely in a large polyatomic molecule, the initially formed state will decay into the X_1 state by a radiationless process. This X_1 state can be repulsive (dissociative), or the level at which the isoenergetic radiationless change of identity takes place can be above the dissociation energy of X_1 . In either case, this process

will result in dissociation of the initially formed state.

(c) Photoisomerization

A radiationless process which can be thought of as the decay of the initially formed state into a manifold of vibrational levels corresponding to a different geometry of nuclei.

(d) Photoionization

This can be considered as a special case of the photodecomposition case (a) except here the excitation is to a continuum level of states corresponding to the free electron and the ionized molecule.

(e) Internal Conversion to S_0 Manifold

This is a radiationless process, whereby the initially formed level will decay into the manifold of vibrational levels corresponding to the ground state S_0 . Vibrational deactivation of this state will occur and the ground state will be retrieved.

(f) Intersystem Crossing to T_1 Manifold

This is the analogous process to (e) except that the state will decay into the manifold corresponding to the triplet state T_1 . Successful vibrational deactivation will form the triplet state in its vibrationally equilibrated level.

In addition to the radiationless processes removing the excited singlet level, there is also a radiative process for return to the ground state.

Fluorescence Emission

If this occurs directly from the level formed upon absorption,

then it will be resonance fluorescence at the wavelength of the absorption. However, if there is a rearrangement of energy within the molecule, then the wavelength region of emission cannot be predicted.

In competition with these processes (a) - (f) and fluorescence emission, there will be vibrational deactivation of the initially formed state. This will form the singlet state in its vibrationally equilibrated level. The processes removing this state can be:

(i) Internal conversion to S_0 in the same manner as for the initially formed state.

(ii) Intersystem crossing to T_1^V .

(iii) Emission of fluorescence in a spin conserved process which will be allowed by quantum mechanical selection rules. The probability of this process occurring can be related to the intensity of the absorption process forming the S_1 state from S_0 . As the process is allowed, the fluorescence emission is characterised by a short lifetime, 10^{-6} s or less.

If intersystem crossing to a vibrationally excited level of T_1 takes place, and if the vibrationally excited level of the triplet is successfully deactivated to the equilibrated level, then a variety of processes will be available to account for its removal.

(a) Intersystem crossing to the adjacent isoenergetic manifold of the ground state.

(b) Emission of phosphorescence in a formally spin-forbidden process which will, therefore, be characterised by a smaller probability for emission than the $S_1 \rightarrow S_0$ transition. That it occurs at all is evidence

of the breakdown of the separability of spin and orbital angular momentum in the model, which originally gave rise to the selection rule. As this same effect, spin-orbit coupling, is responsible for the intersystem crossing process $T_1 \rightarrow S_0^V$, the triplet state is metastable with respect to the ground state.

Consideration of the Intramolecular Processes

- (i) The system is complex and identification of the precursors of products and correlation of behaviour will not be a simple matter.
- (ii) References have been made frequently to "radiationless processes". The understanding of these processes is one of the present enigmatic problems of photochemical phenomena, and has been the source of much interest. The last decade has seen vigorous development of theories describing these events (8,9). These theories have a common feature in that they require the breakdown of the Born-Oppenheimer approximation for a state coupled to an adjacent manifold of vibrational levels via a perturbation operator. In the case of a spin-allowed process, for example internal conversion, the perturbation is provided by the nuclear kinetic operator.

In the case of a spin forbidden process, intersystem crossing, the perturbation is provided by a contribution from the nuclear kinetic operator and the spin-orbit coupling operator, H_{SO} . The degree to which the spin-orbit perturbation affects the system will depend on the quality of the Russell-Saunders coupling description for the system.

The most general theory developed by Jortner et al (10-13) predicts that for an isolated molecule, the behaviour towards radiationless processes can fall into three categories depending on the magnitude of a term ρV . Where ρ is the density of available vibronic states in the perturbing manifold and V is the magnitude of the average perturbing matrix element,

$$\bar{V} = \langle \Psi | H' | \Psi_i \rangle$$

where Ψ represents the isolated level undergoing the process, H' is the perturbing operator and Ψ_i is a vibronic level in the adjacent manifold.

It should be pointed out that not all levels in the adjacent manifold will be available for interaction. This is a result of the selection rules for non-vanishing vibronic matrix elements, which demand that $\Psi_1 \otimes \Psi_i$ have the same representation under the molecular point group as H' . This makes the effective value of the ρ less than the actual value. The three categories described by Jortner are:

(a) $\rho V \gg 1$.

This is the statistical limit in which the density of vibronic states in the adjacent manifold is extremely high. Radiationless processes occur as an intramolecular phenomenon and are independent of external perturbations. The radiationless rate constant k_{nr} is given by the expression,

$$k_{nr} = \frac{2\pi}{h} \rho V^2$$

(b) $\rho V \ll 1$.

This is the small molecule or resonance limit in which the vibronic levels in the adjacent manifold are coarsely spaced. A small number of these states will be accidentally degenerate (or quasi-degenerate) and will be split by the perturbation into discrete stationary levels. These levels cannot relax unless level broadening or some quasi-continuum is provided (by collisions in the gas phase or coupling with the lattice vibrations in a matrix).

(c) $\rho V \sim 1$.

This is the intermediate case in which the density of states is not sufficiently high to put the system in the large molecule category. The fluorescence decay is only approximately exponential, and sensitive to collisions, showing a decrease in "lifetime" compared to the isolated molecule situation.

(iii) The magnitude of the fluorescence and phosphorescence yields will depend upon the fraction of molecules reaching the emitting level and also the magnitude of the emission rate constant compared to the other processes removing the emitting states. This explains the diversity of luminescence behaviour shown by photochemical systems, where the quantum yield of emission can be from approximately unity to an undetectable level, presumably less than 1×10^{-5} . It also emphasizes the utility of fluorescence and phosphorescence measurements in elucidating the mechanism of a photochemical system. In conjunction with the measurement of these emissions, other techniques have been used to monitor the concentrations of reactive intermediates. These could be

physical methods such as electron paramagnetic resonance spectroscopy (14) or kinetic optical spectroscopy (15), (flash photolysis).

No mention has been made of bimolecular activity except in the context of a heat bath for the dissipation of vibrational energy. Other processes are indeed possible.

Intermolecular Processes

The interaction of an electronically excited species with a molecule in its ground state is a process of fundamental importance in the understanding of photochemical systems. These interactions, which result in the destruction of the original electronic state, can be considered in two categories even though the validity of this division is in question in some systems.

Chemical Interactions

The electronically excited state has a different configuration from the ground state and is, therefore, a different chemical entity. The promotion of an electron to a higher energy molecular orbital destroys the strong electron pair correlation that exists in the ground state and as the behaviour of the electrons is more independent, it can be expected to give rise to increased chemical reactivity. The form of this reactivity will depend on the structure of the substrate molecule and can take the form of an abstraction reaction in a saturated molecule or bond formation with an unsaturated molecule.

Physical Interactions

In this case, the physical interaction of the excited state with the substrate does not have the net effect making or breaking chemical bonds, but results in the dissipation of the excitation energy in the form of vibrational energy of the pair (16) or electronic energy of the substrate (2). Electronic energy transfer is common in both atomic (17) and molecular systems (3) and has caused much interest in the nature of these sensitized reactions. Apart from the nature of the interaction which is of fundamental importance in the explanation of the system (18), this energy transfer ability has made possible the study of photochemical systems by indirect means. If the reactions of the excited substrate are known from other sources, then the processes controlling the fate of the energy donor can be deduced from the sensitized system. This method has found wide application in the elucidation of the processes occurring in photochemical systems, which show no emission or simple chemical products.

While these energy transfer processes have been a great importance in the recent understanding of photochemical systems, the nature of the interaction by which the processes occur is not known. In fact, the arbitrariness of the division into 'chemical' and 'physical' interactions has been emphasized by the simultaneous occurrence of these reactions within a system, e.g. excited ketone/olefin systems (19). This only serves to underline the need for further work into the nature of interactions between excited state molecules and ground state substrate.

An Illustration of a Photochemical System

In the light of the preceding remarks, interest in the processes of emission and sensitization as tools for the elucidation of photochemical mechanisms can be understood. A system which has received much attention with respect to both of these phenomena is the α -diketone, 2,3-butanedione, commonly known as biacetyl.

Biacetyl Photosystem

The behaviour of the biacetyl photosystem depends on the wavelength of excitation. In the short wavelength band, 230-320 nm, the main result is photodecomposition, whereas in the long wavelength band, 360-470 nm, photodecomposition and emission occur from the excited states of the system. This difference in behaviour can be associated with the different electronic states formed by excitation in these two regions (20). In terms of relevance to this discussion, the behaviour in the long wavelength region is of more importance. However, as the mode of photodecomposition at the longer wavelengths can be correlated with the behaviour at shorter wavelengths, some comments regarding the short wavelength photolysis are appropriate.

(a) Photolysis in the 230-320 nm absorption region

The products of the reaction are carbon monoxide, ethane, methane, and acetone, all of which have been determined quantitatively from photolysis at wavelengths less than 320 nm (21). Ketene and 2,3 pentanedione are known to be present in the reaction products particularly at higher temperatures.

The following overall reactions occur (22),



There is some doubt as to the primary process but for the present it can be represented by



Secondary reactions of the radicals formed in the primary scission are important and constitute a complex radical chain mechanism. The extent of this reaction will depend upon pressure and temperature.

Excitation in the short wavelength region will form an excited state S_2 . With reference to the Jablonski diagram above, the behaviour of the system is consistent with efficient dissociation from the initially formed level competing with vibrational deactivation and internal conversion to the S_1 manifold (23). This level of the S_1 manifold can then dissociate or be collisionally deactivated to the equilibrated level of the singlet manifold. Fluorescence and phosphorescence emission are observed from the S_1 and T_1 states, the latter being formed by intersystem crossing from S_1 . The magnitude of these yields depended upon temperature and pressure. Due to the complexity of the system and the intermediacy of several states capable of decomposing, the primary decomposition mode has not been definitely determined. It can be expressed as



where α lies between 0 and 1, and seems to depend on the excitation wavelength (7).

(b) Excitation in the 350-460 nm absorption region

The behaviour of the biacetyl photosystem when excited in this region is of direct importance to the interpretation of the work to be described later.

As with the absorption at shorter wavelengths, the behaviour of the system depends upon the excitation wavelength and can be considered in conjunction with the Jablonski diagram, Fig. 1. At 365 nm excitation, the promotion of the ground state molecule is to a vibrationally excited level of the S_1 manifold. The processes removing this state are consistent with:

- (i) Decomposition, presumably through a pre-dissociative mechanism to give radicals which can undergo secondary reactions similar to those in the short wavelength photolysis;
- (ii) Internal conversion to the S_0 manifold;
- (iii) Vibrational deactivation to the equilibrated level of the S_1 manifold. Fluorescence emission occurs from the S_1 manifold and the insensitivity of the profile to exciting wavelength has been taken as evidence for emission from only the equilibrated level of the S_1 manifold (24).

Intersystem crossing from the equilibrated level of the S_1 manifold is very efficient (25) and followed by vibrational deactivation in the triplet manifold results in the formation of the vibrationally equilibrated level of the triplet state. The process removing this T_1

level are:

- (i) Emission of phosphorescence;
- (ii) Intersystem crossing to S_0 ;
- (iii) Thermal decomposition (26);
- (iv) Decomposition by an unusual annihilation process (27).

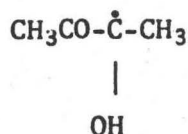


As the quantum yields of these processes depend upon the degree of collisional deactivation in the S_1 manifold, i.e. the pressure and the temperature, the description of the system is quite complex. However, an elegant correlation of phosphorescence and decomposition experiments has been suggested by Noyes (7) in terms of the mechanism given above.

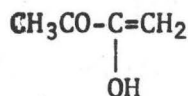
At longer wavelength excitation, i.e. at 405 and 436 nm, the S_1 state is formed in a lower vibrational level (20) and decomposition from this level is not important (26). Fluorescence occurs from the S_1 manifold with low yield, $\phi_F = 0.002$ (28), and more than 99% of the excited molecules are successfully deactivated to the equilibrated level in the gas phase (29) and in solution (25). In the gas phase at 25°C, the phosphorescence yield is high (30), 0.18, and together with the phosphorescent lifetime (31), 1.8×10^{-3} s, has allowed the rate constants to emission and intersystem crossing from $T_1 \rightarrow S_0$ to be calculated.

The ability of biacetyl to fluoresce and phosphoresce in fluid solution as well as in the gas phase has made this compound the object of much attention with respect to the bimolecular processes it may undergo. In particular, the relatively high phosphorescence yield in fluid solution,

~ 0.05 , has been associated with the relative chemical inertness of the triplet biacetyl molecule. At the time this work was begun, the only characteristic bimolecular chemical reaction known for this state was hydrogen atom abstraction, leading to the radical.



which could lead to products by dimerization (32) or further abstraction (3). There had also been a suggestion that photoenolisation could take place (33) to give



by an unknown mechanism.

The non-chemical interactions of biacetyl had received much more attention as it was known that biacetyl could act as a donor in its excited state, or an acceptor in its ground state, in singlet-singlet (34) and triplet-triplet (25,35,36,37) energy transfer processes. These processes can be represented by,



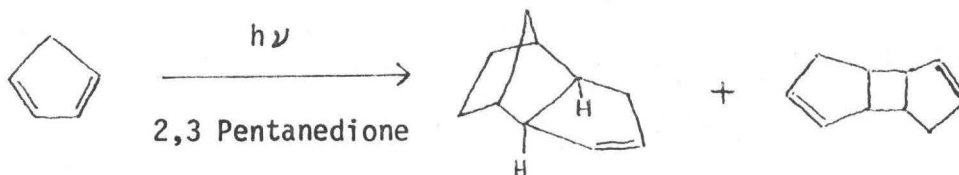
where D is the donor and A is the acceptor, the numerical superscripts are the spin multiplicities of the states, and the asterisks represent electronic excitation.

The excited singlet and triplet biacetyl molecules formed in these processes would then act in the same manner as if formed by photo-excitation. The measurement of sensitised yields of fluorescence and phosphorescence of biacetyl has allowed many important conclusions to be made concerning the behaviour of the donor states in many photochemical systems (2,3).

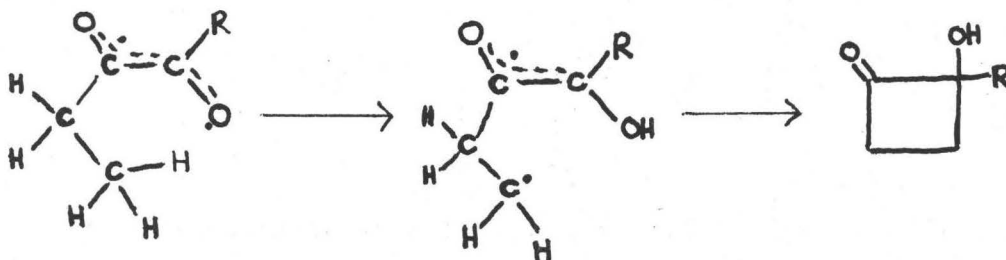
Extension to Pentanedione

It seems that the emission properties of 2,3 pentanedione (herein after referred to as pentanedione) were discovered by Lewis and Kasha in 1944 (38). The green emission observed by these workers was later investigated (in a rigid glass of 77°K) by Hammond et al (39) in 1964, when it was characterised as phosphorescence by analogy with biacetyl. The triplet energy estimated under these conditions was 54.7 Kcals.

In between these two determinations of the triplet energy at low temperatures, Hammond et al (40) successfully demonstrated the sensitized dimerisation of cyclopentadiene using pentanedione as an energy donor. It was implied that the reaction occurred through the triplet state of the pentanedione. The reaction could be represented by,



The photochemical reactions of a series of diketones including pentanedione were investigated in 1962 by Urey and Trecker (41) who showed, using broad band excitation, that 2-hydroxy-2-methyl cyclobutane was the major product in pentanedione photolysis. It was proposed that this product occurred via intramolecular abstraction of a hydrogen atom followed by ring closure in the resulting diradical.



Quenching experiments (42) using low triplet energy acceptors demonstrated that the reaction occurred via the triplet state.

The phosphorescence in rigid media at 77°K and in fluid solution at room temperature of a series of α -diketones, including pentanedione, was studied by Richtol and Klappmeier in 1966 (43). The decreasing phosphorescence yield with increasing side chain length in these molecules was ascribed to an increased probability of $T_1 \rightarrow S_0$ intersystem crossing.

During the course of the current work, this explanation was thrown in doubt by the experiments of Turro and Lee (44), which demonstrated that the probability of 2-hydroxycyclobutanone formation was increased as the side-chain was extended in a series of α -diketones. Increased competition from this reaction mode would reduce the emission yields, as observed by Richtol and Klappmeier.

This example illustrates the high level of activity in the field of photochemistry and in the study of diketones in particular (45).

The Current Work

It was decided to investigate the processes controlling the fate of electronically excited pentanedione molecules using the fluorescence and phosphorescence techniques which had been applied so fruitfully to biacetyl. The gas phase was chosen for this study of the molecular interactions and their efficiencies. Even though the gas phase limits the compounds that can be studied, it does provide a simpler environment than the solution phase and should allow a clearer interpretation of the factors that control the rate processes.

It was recognized that electronically excited states might react at a rate that depends on the ambient temperature (27,46). This prompted the investigation of the dependence of the reaction rate on temperature.

The studies carried out on pentanedione can be divided into two classes.

(a) Intramolecular Processes

These are the processes which control the fate of the excited species and can be considered with respect to the Jablonski diagram, Fig. 1. The role of any added gas is in this context to act merely as a heat bath. The intramolecular processes were investigated in the following categories:

(i) The radiative fluorescence process and radiationless conversion $S_1 \rightarrow T_1$ were studied with reference to the absorption spectrum and the

fluorescence emission spectrum at long wavelength excitation. The results obtained from the experiments are presented and discussed in Chapters 3 and 4.

(ii) The radiative phosphorescence process and the radiationless processes removing the triplet state were investigated by use of the phosphorescent yield and the phosphorescent lifetime. Emphasis was placed on the temperature dependence of the radiationless processes removing the triplet state. These experiments are described and discussed in Chapters 4 and 5.

(iii) The processes controlling the magnitude of the emission yield, when excitation is to a low vibrational level of the S_1 manifold, were investigated using 436 nm excitation at various temperatures with different pressures of diketone. These experiments are presented and discussed in Chapter 6.

(iv) The radiative and non-radiative processes controlling the emission yields when excitation is to a vibrationally excited level of the S_1 manifold were determined by measurement of these yields at various pressures at constant temperature. The nature of the collisional deactivation mechanism of the initially formed level is discussed in terms of the weak and strong collision mechanisms in Chapter 7.

(v) The temperature variations of the radiative and non-radiative processes controlling the emission yields when excitation is at short and long wavelengths are presented in Chapter 8. This information consolidates the mechanism which had been tentatively proposed on the basis

of conclusions from the preceding chapters.

(b) Intermolecular Processes of the Triplet Pentanedione

The molecules used to interact with the triplet pentanedione molecule were chosen so as to represent variations in structure and interaction mode.

(i) The interaction of several conjugated carbonyl compounds with the triplet pentanedione at different temperatures was studied in an effort to diagnose the nature of this interaction. The results and conclusions of this work are presented in Chapter 9.

(ii) The effect of atomic, paramagnetic, and 'chemical' substrate molecules on the triplet pentanedione molecule is discussed in Chapter 10.

(iii) The nature of the energy transfer process in the gas phase is inspected with respect to the triplet pentanedione molecule in the presence of butadiene and cyclopentadiene. This phenomenon, which has not received the attention it merits in the gas phase, is studied at various temperatures. The results and conclusions are presented in Chapter 11.

CHAPTER 2

APPARATUS AND TECHNIQUE

Gas-handling equipment

Gases were manipulated in a mercury-free, greasefree apparatus of conventional design constructed from Pyrex. The system was evacuated by an oil diffusion pump and a roughing pump. Cold traps maintained at -196°C were used to prevent vapours from the pumps contaminating the operational part of the apparatus. Provision was made for distillation of gases through a series of U-traps and storage was in 5-litre bulbs having positions maintained at -196°C . Glass stopcocks, supplied by Delmar, fitted with 3 ethylene/propylene rubber O-rings (recommended for use with ketones and diketones) were used throughout the apparatus. Low pressure measurement was by means of a thermocouple gauge and ionisation gauge; higher pressures were measured using a Bourdon spoon gauge in opposition to a mercury manometer.

Chemicals

The chemicals which were used in this work together with their purifications are described in Appendix A.

Emission Measurements with Wavelength Resolution

Light from a 1000 W Hg/Xe lamp was focussed through a Bausch

and Lomb monochromator (1200 grooves/mm blazed at 400 nm) and allowed to fall on the sample contained in a 1 cm square Hellma Suprasil cell. Emitted light was analysed at right angles to the incident light using a 0.5 m Ebert Jarrell-Ash scanning monochromator with 1180 grooves/mm grating blazed at 400 nm, fitted with an RCA 8575 photomultiplier cooled to -78°C . The signal from the photomultiplier was amplified by a Keithley model 610 C electrometer and displayed on a pen recorder.

Absolute Emission Quantum Yields

The absolute emission spectrum of a specimen is a plot of luminescence intensity measured in quanta per unit frequency (or wavenumber) interval, against frequency (or wavenumber) i.e. if q represents the total number of quanta of all wavenumbers emitted per unit time, the $\frac{dq}{d\bar{\nu}}$ represents the intensity of a wavenumber $\bar{\nu}$, and the plot of $\frac{dq}{d\bar{\nu}}$ against $\bar{\nu}$ is the true luminescence emission spectrum.

When the emission spectrum is scanned at constant slit width and constant photomultiplier sensitivity, the curve obtained is the apparent or uncorrected emission spectrum. To determine the true spectrum, the apparent curve has to be corrected for three wavenumber-dependent factors; the quantum efficiency of the photomultiplier, the band width of the monochromator, and the transmission factor of the monochromator. These may be combined into a factor $S_{\bar{\nu}}$ which is the relative sensitivity of the monochromator-photomultiplier combination. This factor was determined using a standard tungsten lamp Type L101 with a P101 current supply, obtained from Electro Optics Associates. The lamp was arranged

approximately 5 meters from the entrance slit of the monochromator with all settings as in the emission experiments. The emission spectrum was scanned and the recorder trace was compared with the known absolute emission spectrum as supplied by the manufacturer. The correction factor was normalised at $22,500 \text{ cm}^{-1}$ and is shown in Fig. 2. This allowed the experimentally acquired emission curve to be corrected.

The absolute quantum yield of emission was determined using a quinine sulphate solution in 1N H_2SO_4 of known optical density as a relative standard. The quinine sulphate sample in a 1 cm square Hellma Suprasil cell was irradiated at 313 nm using the same mounting as for the gas emission studies. The emission spectrum was recorded and corrected. The relative intensities of emission by the Hg-Xe lamp-monochromator combination were determined using the ferrioxalate actinometer described by Parker (47) at 313, 365, 405, 436 nm.

Relative Quantum Yield Measurements of Fluorescence and Phosphorescence in Gas Phase

The light source was a 60 W medium pressure mercury lamp operated from a Gates Omnirange power supply. The light was focussed to produce parallel light which passed through a filter holder. Interference filters supplied by Baird-Atomic were used to isolate 3130, 3650, 4047, 4358 nm emission lines (see Fig. 3). A portion of the light passed by the filter was reflected by a quartz plate mounted 45° to the axis of the system onto the cathode of a G.E. Type 935 photocell. The signal was displayed on a pen recorder and gave a measure of the intensity of the light entering the system, (see Fig. 4). The majority of the light was transmitted

Fig. 2. Sensitivity correction curve of photomultiplier-monochromator used in quantum yield determination.

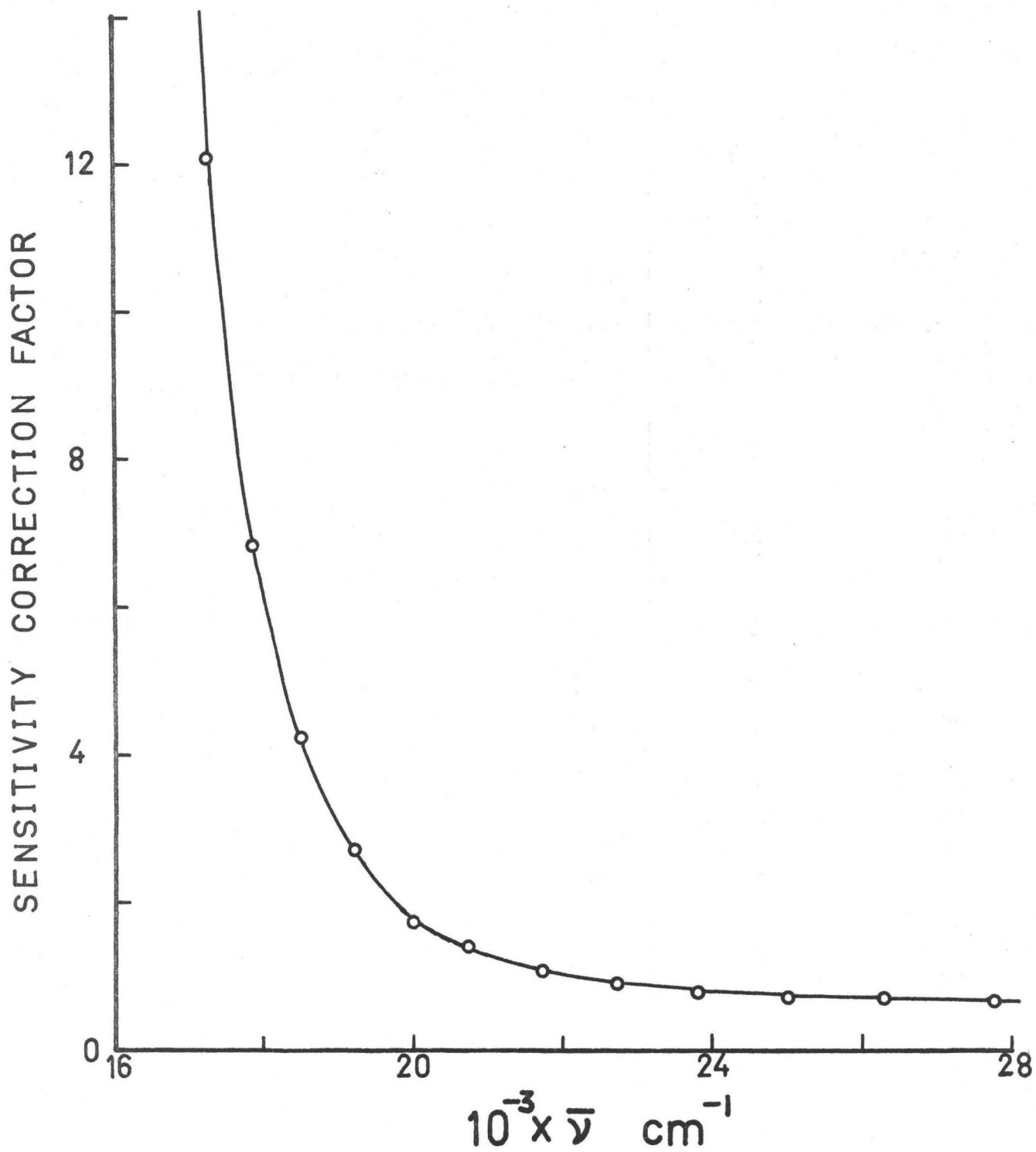


Fig. 3 Narrow band pass filters used in this study.

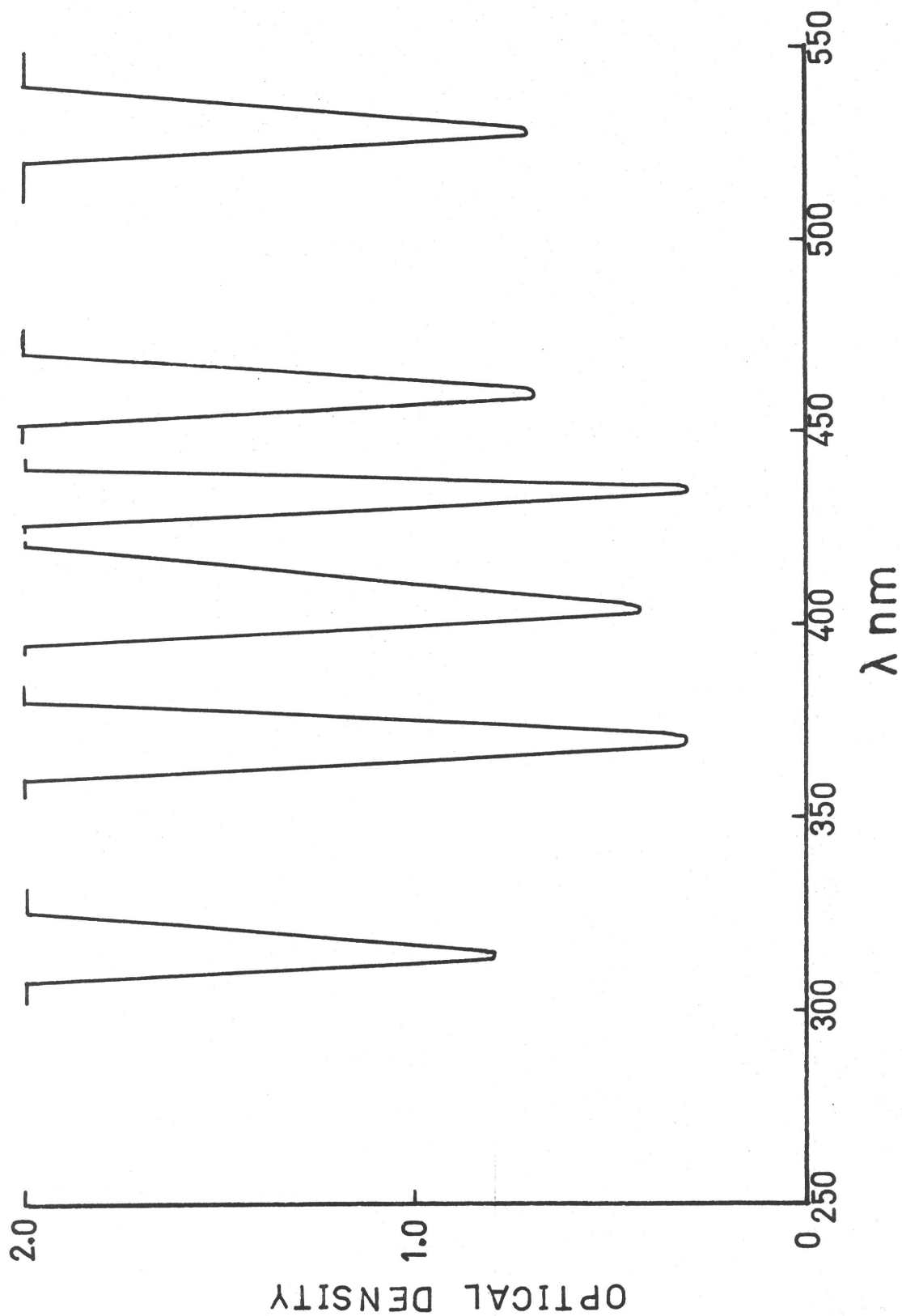
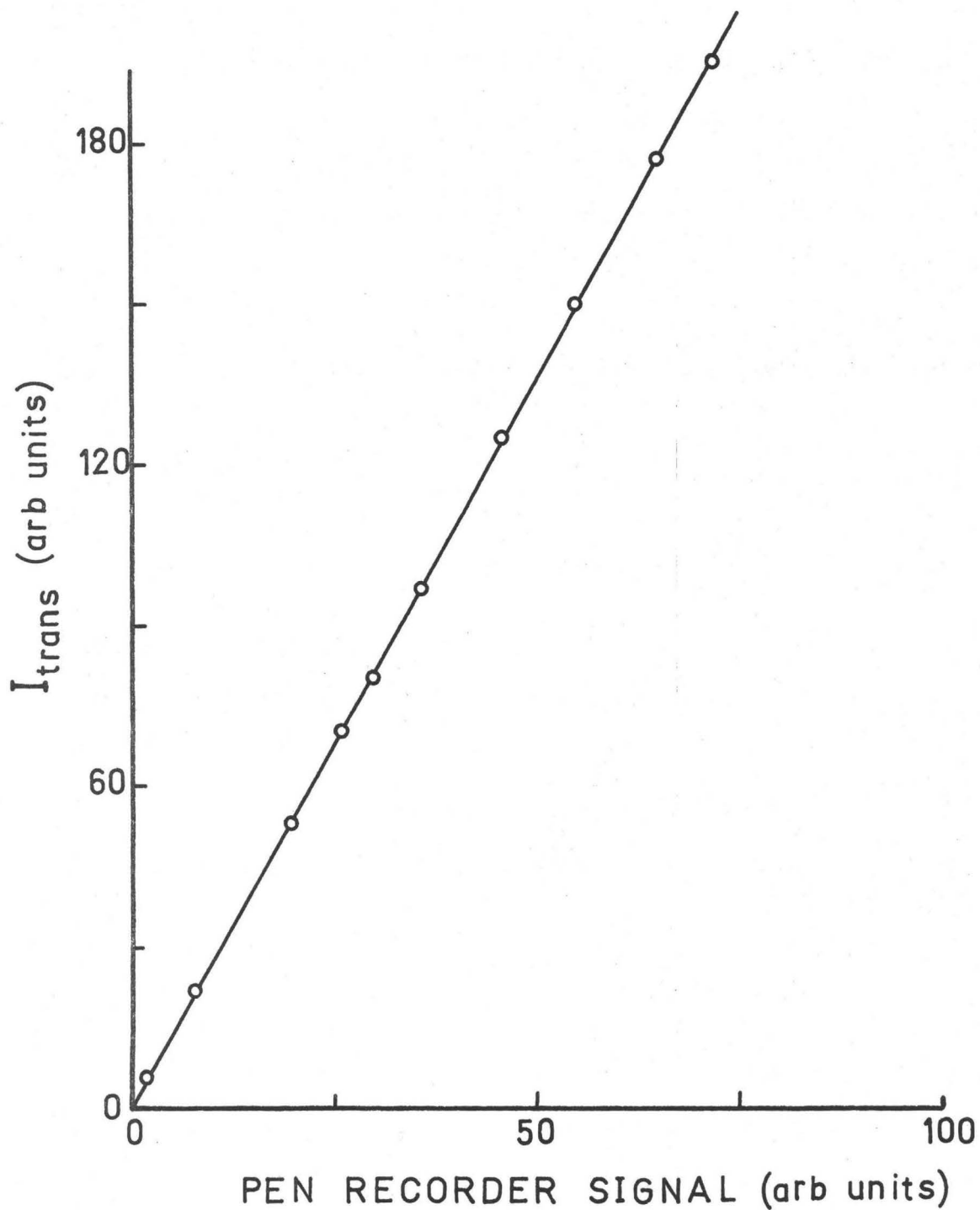


Fig. 4 Proportionality between transmitted light signal and displayed monitor signal.



by the plate, passed through the cell and was focussed onto a second G.E. Type 935 photocell, the output of which was read by a Keithley model 610 C electrometer.

The cell was constructed of quartz with Suprasil windows (54 mm diameter) fused onto the ends to give a path length of 10 ± 0.05 cm. A smaller window (25 mm diameter) was attached at the midpoint of the cell at right angles to the axis. Experiments were often performed with mixtures of gases, whereby each component would be distilled into the cell and trapped at -196°C . It was found that unaided thermal diffusion was very inefficient in forming a homogenous gas solution and many hours were necessary to give reproducible results. Therefore, a gas circulating pump was fitted. Two designs were used: the first consisted of a Teflon paddle wheel fitted with a Teflon encased permanent magnet through its axis such that an externally mounted rotating permanent magnet would cause the paddle wheel to rotate. Although this improved equilibration times (compared to unaided diffusion), the axis support points deteriorated and the design was changed.

The second design incorporated an external cam-driven permanent magnet which moved the internal glass-encased permanent magnet along the cylinder of the pump and by simultaneous compression and rarefaction of the gas, operated valves. The valves were constructed from microscope slide covers ground to fit. This design proved to be much more efficient and would successfully operate at 0.1 torr.

The cell and stirrer were mounted in a thermostatically controlled

box constructed from wood with glass-fibre insulation and fitted with a fan and heating coil (200 W). Thermal equilibrium was maintained by a Durro thermometer that controlled a switching device for the heating coil. Quartz windows in the box allowed the cell to be mounted in an optical train. Thermocouples attached to the cell measured the temperature, which was constant $\pm 0.1^\circ\text{C}$.

Light emitted by the sample through the side window passed down a tube 10 cm in length, mounted to reduce scattered light and restrict the portion of the cell viewed. The intensity of the emission at 460 nm and 528 nm was measured using narrow band filters (see Fig. 3) and a cooled photomultiplier (EMI 6256S cooled to -80°C with cold N_2 gas). The signal from the photomultiplier was measured using a Keithley model 610C electrometer. A schematic diagram of the optical apparatus is shown in Fig. 5.

The quantity measured in these experiments was the relative quantum yield of emission at the wavelengths 520 or 528 nm, defined by,

$$Q_\lambda = \frac{I_\lambda - I_\lambda^\circ}{g (I_{\text{trans}}^\circ - I_{\text{trans}})}$$

where $I_\lambda - I_\lambda^\circ$ is the difference between the emission reading with and without sample in the cell. $I_{\text{trans}}^\circ - I_{\text{trans}}$ is the difference between the transmitted photo-cell readings with and without sample in the cell. The readings of I_λ , I_{trans}° , I_{trans} were taken simultaneous with readings of the light monitor recorder. The electrometer reading was then corrected to some arbitrary value of incident intensity for all readings

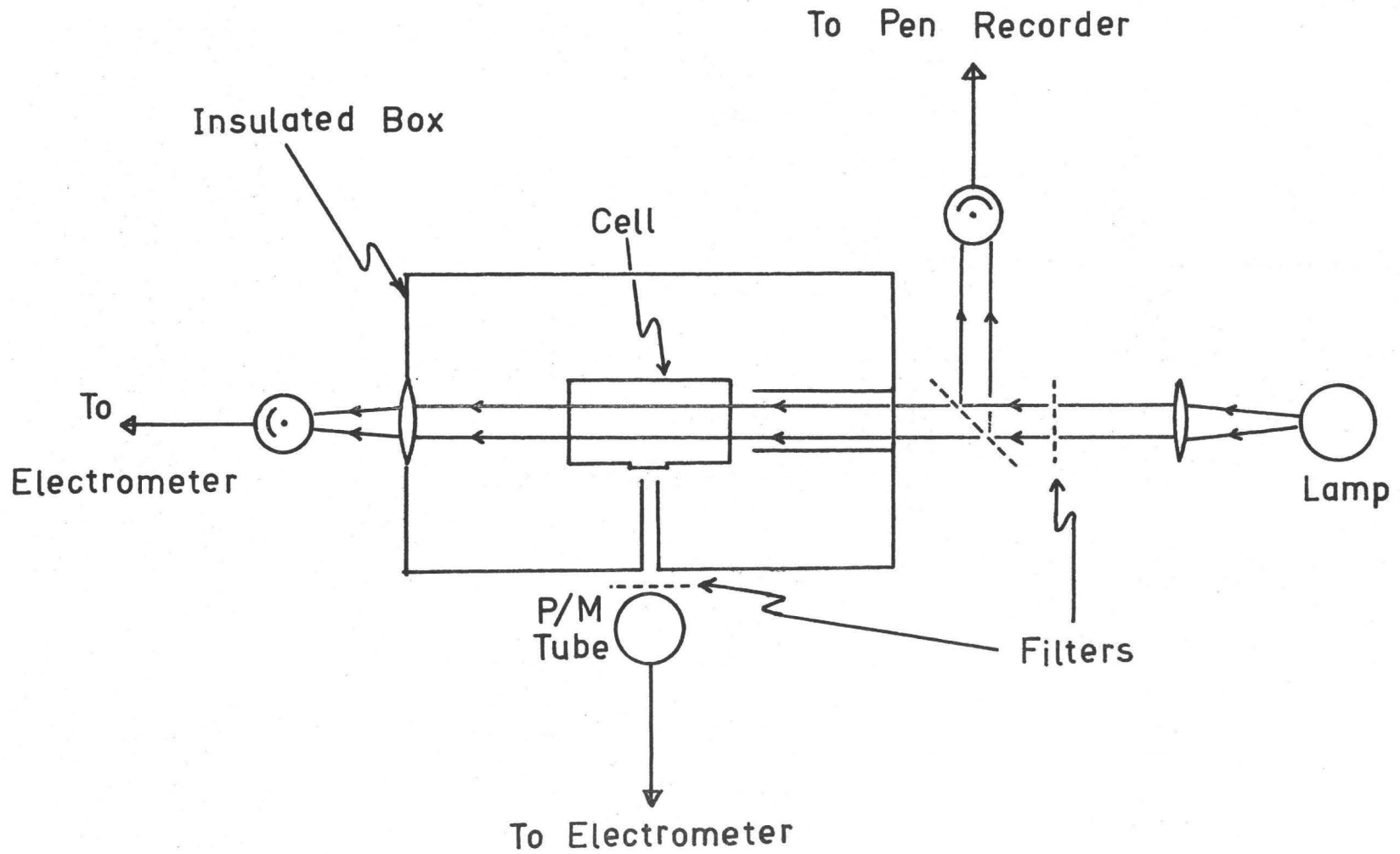


Fig. 5 Optical arrangement used in determination of Q_f and Q_p .

taken at a particular exciting wavelength. In this way, small variations in the incident light intensity were corrected. The linear response of the transmitted light photocell was checked using neutral density filters (Fig. 6).

The quantity g is a factor depending on the geometry of the apparatus and takes into account that the actual incident light causing emission in the region viewed by the photomultiplier varies as the amount of light absorbed varies. For the geometry shown in Fig. 5, the formula is:

$$g = \frac{\text{Sinh } \epsilon c \delta / 2}{\text{Sinh } \epsilon c \ell / 2}$$

where ϵ is the natural extinction coefficient, c is the concentration in mole/litre, $\delta = 1$ cm, $\ell = 10$ cm.

The value of Q was also corrected for reflection effects in the cell. This phenomenon has been studied by Hunt and Hill (48) who showed that the measured fraction of light absorbed in the cell ($I_{\text{trans}}^{\circ} - I_{\text{trans}}$) is always less than the actual amount due to multiple traverses of the cell by the parallel beam of light. A correction table given by Calvert and Pitts (2) was used.

A further correction was necessary for the emission data collected at 460 nm. This is due to reabsorption of the emitted light by the sample before its detection by the photomultiplier. The geometry of the excitation system is shown in Fig. 7. The incident flux is assumed to uniformly strike the shaded region. The light emitted by the region of thickness δx a distance x from the cell wall is:

$$I_x = A e^{-\epsilon c x} \delta x$$

Fig. 6 Response of 935 photocell at different light intensities.

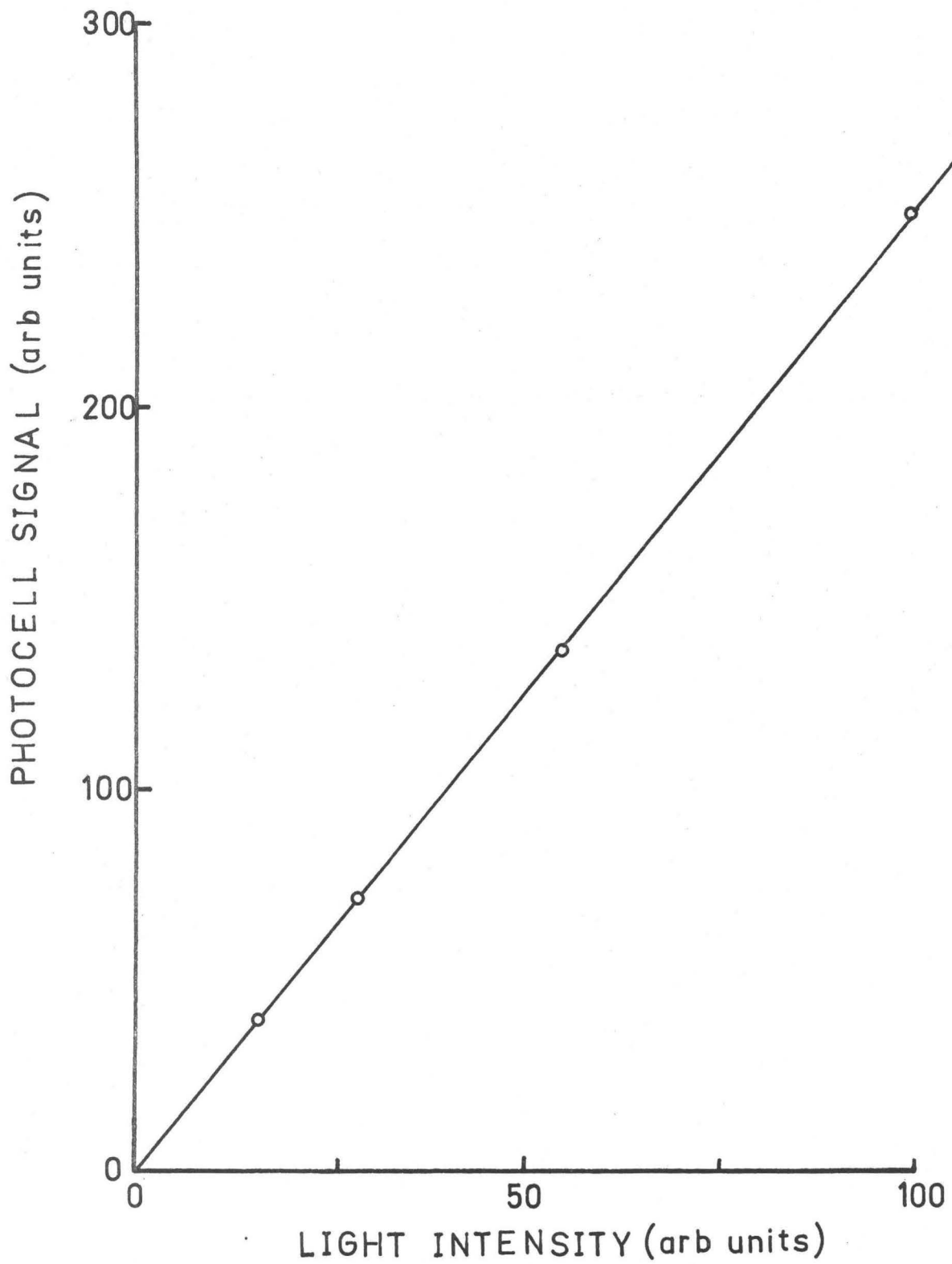
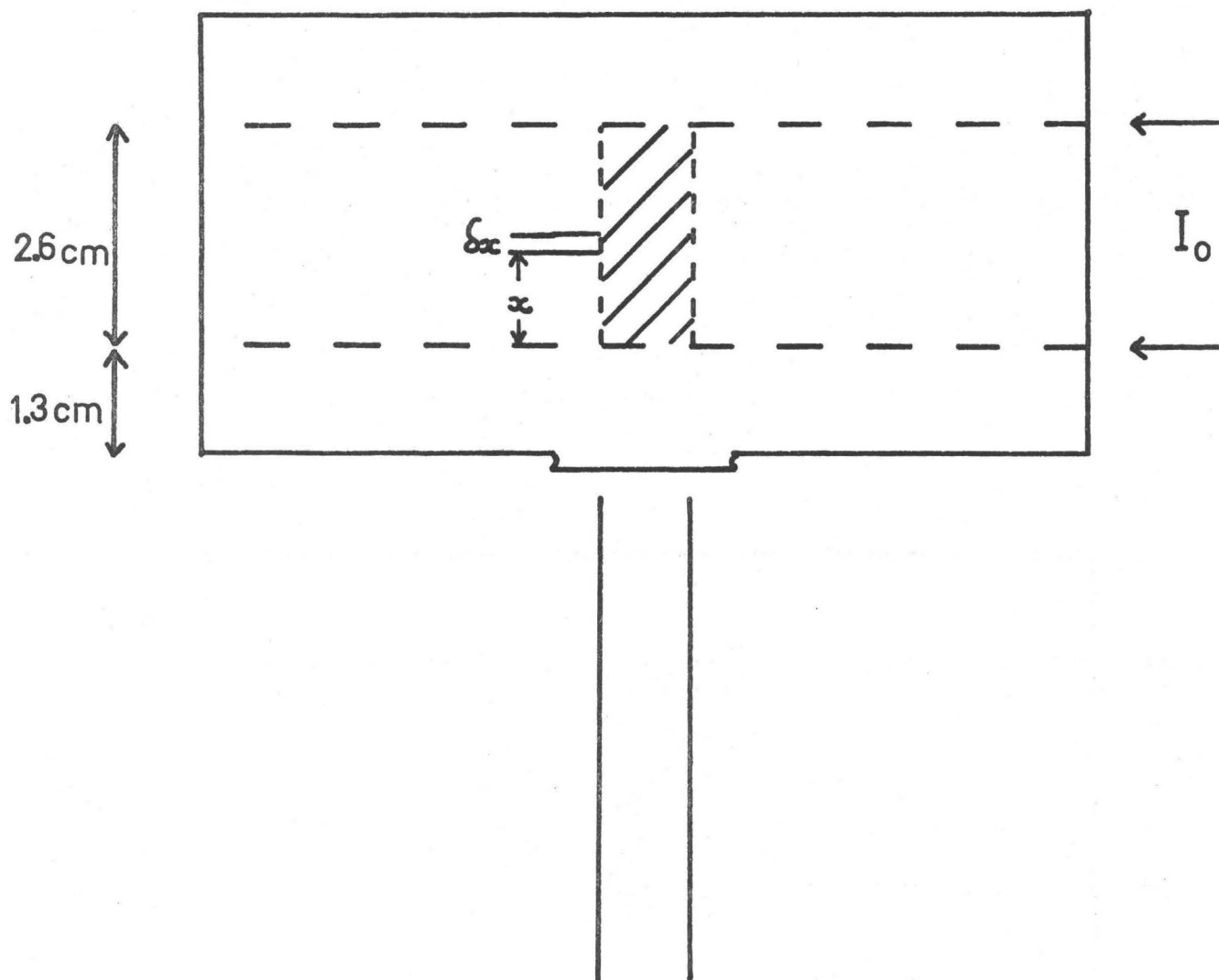


Fig. 7 Geometry of cell for calculation of inner filter effect at 460 nm.



The total light emitted by the region is:

$$I_{\text{tot}} \int_0^a = 3a \int_0^a \exp(-\epsilon c x) dx$$

$$\therefore I_{\text{total}} = \frac{A}{\epsilon c} [e^{-\epsilon c a} - e^{-3\epsilon c a}]$$

This is to be compared to the emitted light in the absence of the inner filter effect, $2aA\epsilon c$. Therefore, the correction factor is given by,

$$\frac{I_{\text{true}}}{I_{\text{exp}}} = \frac{2a\epsilon c}{e^{-\epsilon c a} - e^{-3\epsilon c a}}$$

The variation of this correction factor with concentration is shown in Fig. 8, using $\epsilon_{4600} = 2.303 \times 4$ (see Chapter 3), $a = 1.3$ cm.

As the fluorescence and phosphorescence overlap, the signal measured at 528 nm contains some contribution from fluorescence. To determine this overlap an experiment was performed in which the signals were measured at 460 nm and 528 nm, oxygen was added and the signals measured again. The quenching rate constant of oxygen with triplet pentanedione was known, which allowed the contribution of the fluorescence at 528 nm to be calculated.

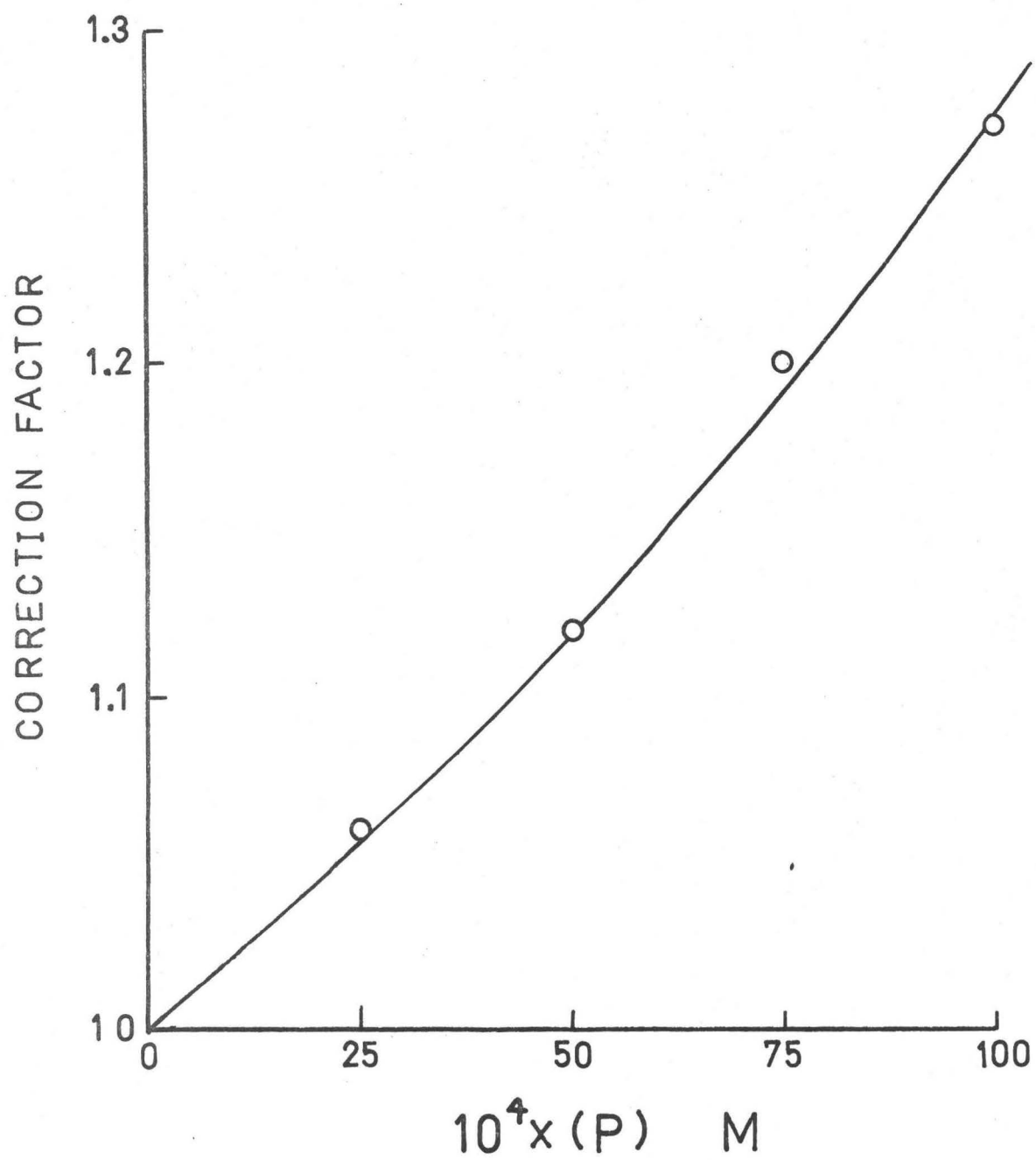
The absolute emission yield, ϕ_e , is related to the relative quantum yield of emission Q_e by the equation

$$Q_e = \beta \phi_e$$

where β is a constant provided the following conditions are met:

(1) The emission profile does not vary. The signal measured at wavelength λ will always be proportional to the total area under the

Fig. 8 Correction factor for inner filter effect at 460 nm.



emission curve.

- (2) The geometry of the apparatus remains the same.
- (3) The measurement conditions are unchanged, i.e. potential to photomultiplier, potential to the photocells.
- (4) The wavelength of excitation is not changed. If the wavelength is changed, then appropriate sensitivity corrections must be applied to the Q values for the photocell recording the transmitted light.

Phosphorescence Lifetime Experiments in Gas Phase

The apparatus used for the relative emission yield experiments was used with modifications. The light source was a xenon discharge lamp (Strobotac Type 1531-AB 0.018 J/flash) which had a decay time of 3.8×10^{-6} s. This was mounted at right angles to the optical axis and light entered the system through a positioned mirror. The lamp triggered at about 2Hz from the time base of an oscilloscope. The incident light was restricted to the region 360 nm to 520 nm using a Corning CS5-60 filter. The emitted light passed through a glass filter (Corning CS3-71) and was detected by the photomultiplier with a response time of about 2×10^{-6} s. The output of the photomultiplier was displayed on an oscilloscope and photographed (about 100 flashes per photograph were required). The photograph was measured and the lifetime derived from a plot of log signal vs time. No lifetimes shorter than 20×10^{-6} s were measured. In separate experiments, the effect of incident light intensity (100% to 15%) on the lifetime was investigated using neutral density filters supplied by Baird-Atomic and whose optical density had been determined using a Cary 14 u.v./vis spectrophotometer.

(i) Measurements on 2,3-Pentanedione

For a particular concentration of pentanedione in the cell, the lifetime was measured at temperatures between 20° and 90°C in about 10° intervals. At higher concentrations measurements were possible only at higher temperatures. In these cases to attain the required concentrations, the cell was filled the appropriate number of times at room temperature and then heated to a temperature at least 10°C above the temperature at which liquid and vapour were in equilibrium (see Appendix B). To ensure quenching by decomposition products did not interfere, the lifetimes were occasionally remeasured at a low temperature after a usual sequence of experiments was complete. No attempt was made to reproduce the same temperatures for the different concentrations. The lifetimes at the experimental temperatures were calculated, and a cubic polynomial was fitted, using a least-square technique, to the experimental data in the form $\log \tau^{-1}$ vs $\frac{1000}{T}$. From the polynomial that fitted the smoothly varying experimental data, the lifetimes at 25, 30, 40,....., 90° were calculated. There was no evidence of problems associated with liquid diketone using this procedure. The concentration of diketone in the cell was checked using the transmitted light intensity from the 60 W medium pressure mercury lamp. No variation in the amount of light absorbed was found over the temperature range. If condensation were a problem, the amount of light absorbed might be expected to vary.

(ii) Triplet Quenching Experiments

The temperature was fixed for a particular experiment. A sample of pentanedione filled the cell at a known concentration. Quenching material filled a calibrated volume at a known pressure and was condensed into the cell with the pentanedione. Phosphorescence lifetimes were measured for mixtures of the fixed amount pentanedione and various amounts of quenching material. The pressure of quenching material never exceeded the vapour pressure at a temperature $\sim 10^{\circ}\text{C}$ below that at which the experiment was carried out.

The experiment was repeated using fresh materials at different fixed temperatures.

Phosphorescent Lifetime at 77°K

The sample in an open 2 mm quartz tube was immersed in boiling liquid nitrogen contained in a quartz optical dewar. Excitation was provided by the xenon discharge lamp described above fitted with a Corning CS 5-60 filter. Emitted light was detected at right angles to the axis of excitation by an 1P28 photomultiplier fitted a response time of 2×10^{-6} s. The signal from the photomultiplier was displayed on an oscilloscope and photographed.

CHAPTER 3

ABSORPTION SPECTRUM AND NATURAL RADIATIVE LIFETIME OF 2,3 PENTANEDIONE

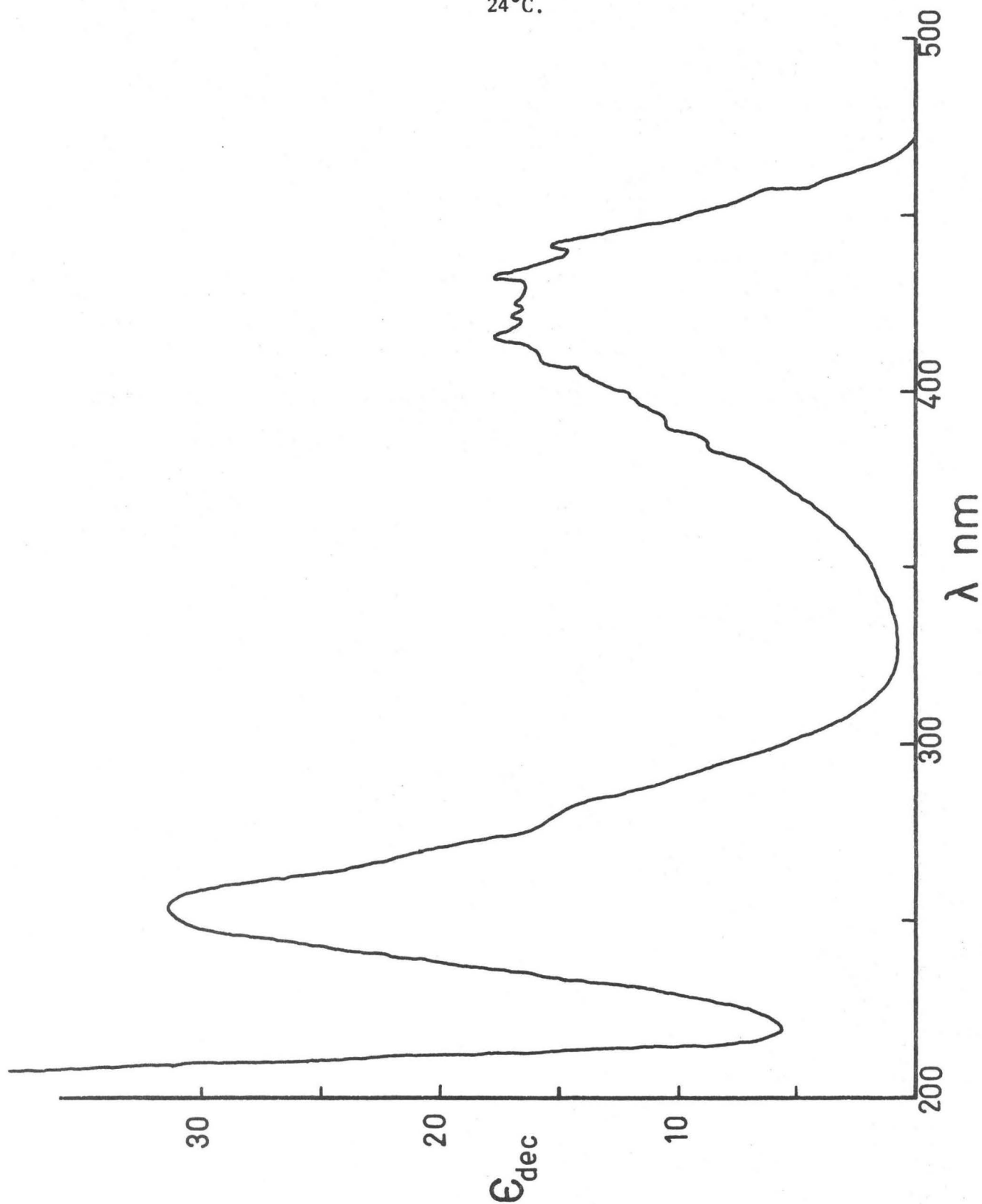
Results

The absorption spectrum of 2,3 pentanedione in the ultraviolet-visible region was taken on several different occasions in a 10 cm cell fitted with quartz windows using a Cary model 14 spectrophotometer. The pressure varied from 10 torr to 18 torr. Average values of the decadic extinction coefficient calculated from the Beer-Lambert Law are shown in Fig. 9. The spectrum consists of two systems. The one at shorter wavelengths extends from less than 220 nm to greater than 320 nm with a maximum at 253 nm ($\epsilon = 31.5 \text{ M}^{-1}\text{cm}^{-1}$). No structure was observed except for a shoulder at 280 nm. The longer wavelength system extends from less than 340 nm to greater than 470 nm. Some structure in the form of bands was observed at 442, 433, 423, 416 and possible at 410 nm. No absorption was observed at wavelengths longer than 470 nm.

Liquid phase absorption spectra of 2,3 pentanedione, biacetyl and chloro-biacetyl were measured in 3-methyl-pentane solution at concentrations of approximately 10^{-2} M using 1 cm quartz cells. The long wavelength absorption band extending from less than 340 nm to greater than 480 nm was very similar in all three cases.

The short wavelength band was featureless, the characteristics

Fig. 9 Visible/u.v. absorption of 2,3-pentanedione in gas phase at 24°C.



are tabulated below.

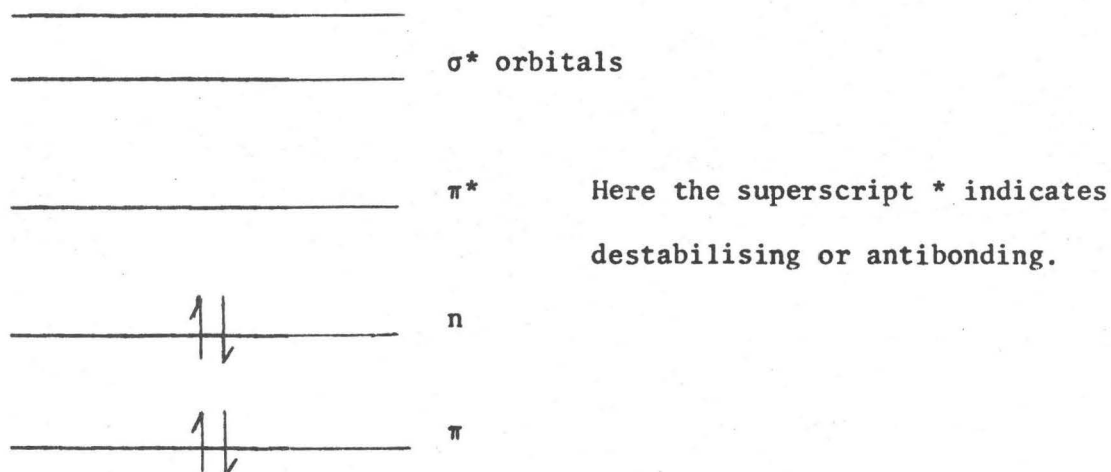
Compound	λ_{max} nm	ϵ_{max}
Biacetyl	270	~12
Chlorobiacetyl	265	~240
2,3 Pentanedione	255	~30

Discussion

The electronic transitions observed in conjugated dicarbonyl molecules can be explained in terms of the energy levels associated with an isolated carbonyl system. It is found in many branches of chemistry that certain properties may be associated in isolation with a particular functional group of atoms, and the electronic configuration of the carbonyl system is included in this generalisation.

The prototype bonding scheme involves the carbon atom in a sp^2 hybrid. Overlap of bonding orbitals on R_1 and R_2 with the $2p_x$ orbital of the carbon atom gives the σ -bonding framework of the molecule. The $2p_z$ orbital of the carbon atom and the $2p_z$ orbital of the oxygen atom combine to give a π -bond between these atoms. This leaves the doubly occupied $2s$ orbital of the oxygen and the doubly occupied $2p$ orbital of the oxygen. The energy of the doubly occupied $2s$ orbital of the oxygen is such that it is essentially non-bonding. Similarly, the doubly occupied $2p_y$ orbital contains two non-bonding electrons, but is of higher energy.

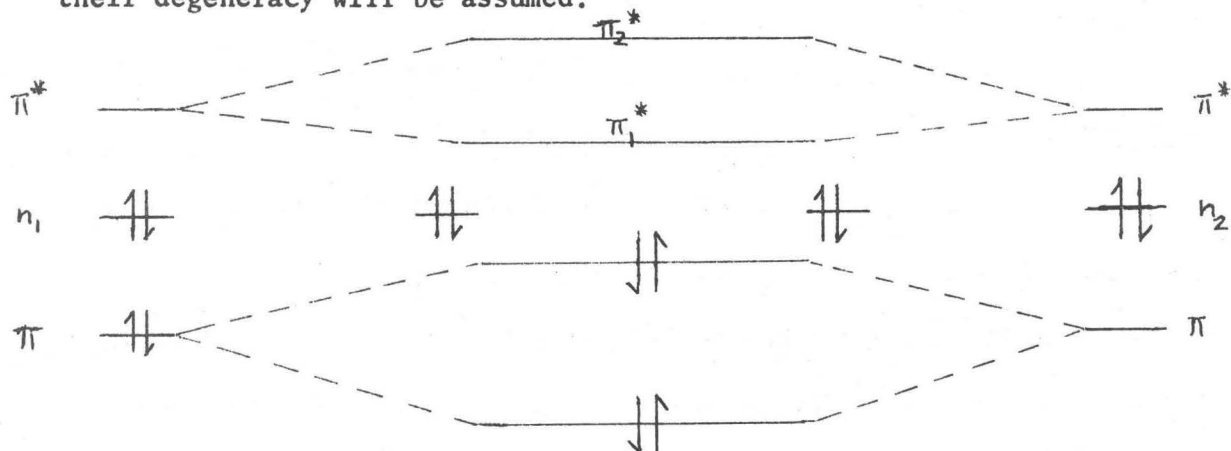
The ordering of the molecular orbitals is represented schematically by,



{ σ -bonds, doubly occupied}

This simple theory can be used to explain many of the observed spectroscopic properties of carbonyl systems (49).

The effect of placing two carbonyl systems in conjugation can be predicted by the simple interaction of the prototype carbonyl systems, in which two degenerate π bonds are split to give one orbital of higher energy and another of lower energy than the original pair. The interaction between the oxygen atoms will be small, and in this discussion their degeneracy will be assumed.



The absorption spectrum of α -dicarbonyls characteristically consists of two absorption systems of low intensity. The simple members

of the group, glyoxal (50,51), methyl glyoxal (52), and biacetyl (20) have been studied. The conclusion on the basis of intensity (49) and symmetry arguments (50) is that the long-wavelength transition involves the promotion of a non-bonding electron in the oxygen $2p_y$ orbital to the anti-bonding π^* , orbital. In the notation of Kasha (53), this is an $n\pi^*$ transition. Brand (50) concludes that the transition in glyoxal is from a trans-planar geometry to an approximately trans-planar geometry. The simple model described here demonstrates how the n orbitals on the oxygen atom will have little mutual interaction in a trans α -dicarbonyl system. This is reinforced by the lack of any experimental evidence for the splitting of the degenerate n levels in this class of molecules (54).

The low intensity of the transition can be understood in terms of the local symmetry of the simple conjugated system, in that the n orbital on the oxygen atom and the π -system are orthogonal. In practice, however, the orbitals are not "pure" and can be considered as containing common contributions which make the transition probability a finite quantity. There is also an effect whereby vibrational modes in the molecule which are of the appropriate symmetry couple with the electronic transition to give vibronically allowed transitions (Hertzberg-Teller effect (55)).

This simple model predicts that an electron in the π^* orbital and an electron in the n orbital will have little interaction with each other due to their small overlap. This would be expected to produce excited electronic states which do not differ greatly in energy in the singlet and triplet states. This prediction is confirmed by the analysis

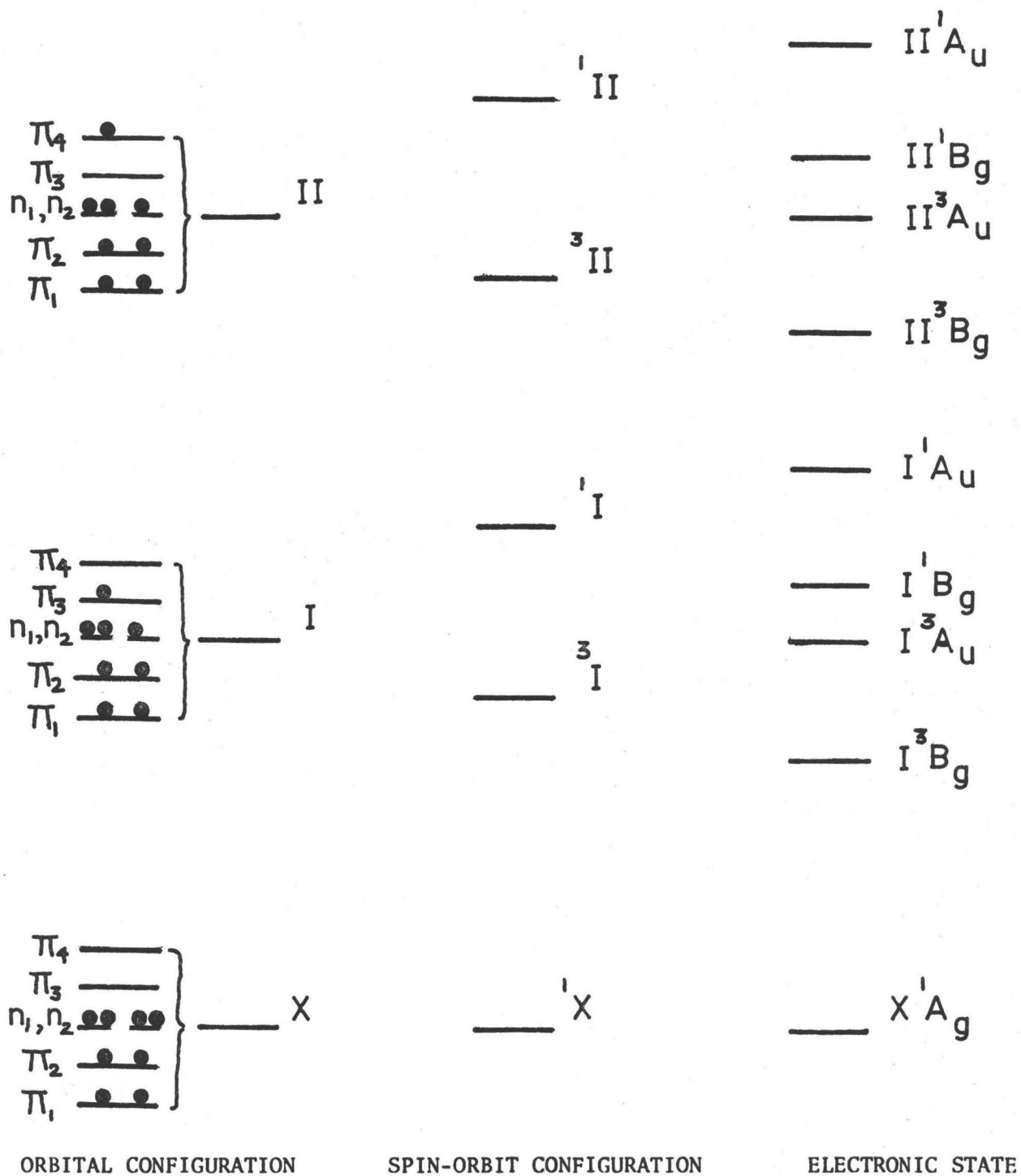
of Sidman and McClure (20) on the absorption spectrum of biacetyl at 4°K which assigns the 0-0 transitions shown in Table 1.

TABLE 1

State	Energy in cm^{-1} above ground State 1A_g
I^3B_g	>19,700, <20,355 v. weak
I^3A_u	20,421 v. weak
I^1B_g	22,359
I^1A_u	22,873
II^1A_u	31,475

The states are shown on the schematic energy diagram in Fig. 10.

The assignment of the transition at 31475 cm^{-1} to the $\pi^1A_u \leftarrow X^1A_g$ is on the basis of molecular orbital calculations by McMurry (49). McClure comments that for this transition the band is much broader than the long wavelength band and is attributed to predissociation of the molecule in this state. This can be related to the photochemical dissociation observed when biacetyl is excited in this region (21,22). The vibrational fine structure is also in agreement with an unstable upper state. The intensity of this transition increases towards higher energies indicating that the dimensions of the upper and lower states must differ considerably.

Fig. 10 The n, π configurations for biacetyl.

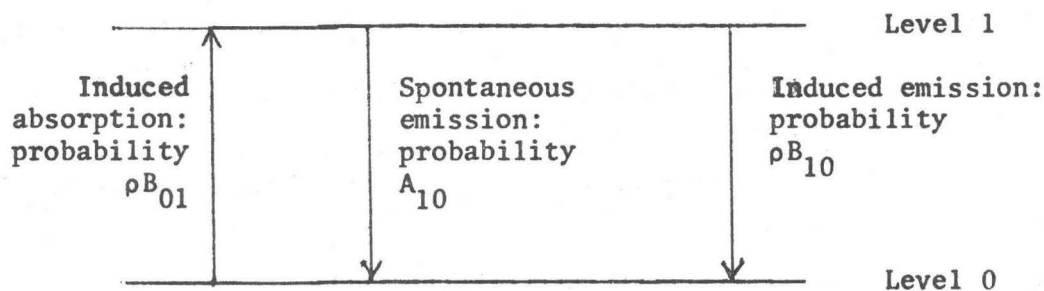
However, an interesting comparison can be made between biacetyl and 2,3 pentanedione. There is little doubt that the long wavelength transition in both molecules corresponds to the formation of a singlet $n\pi^*$ excited state. For the absorption at shorter wavelengths, the maximum for biacetyl in the vapour phase is 270 nm ($\epsilon \sim 12 \text{ M}^{-1}\text{cm}^{-1}$) (2) and for 2,3 pentanedione in the vapour phase is 255 nm ($\epsilon \approx 30 \text{ M}^{-1}\text{cm}^{-1}$). This shift in maximum and intensity is rather surprising as the long wavelength absorption are almost identical in the two molecules. A further point of interest is the case of chlorobiacetyl, which shows a long wavelength band very similar to 2,3 pentanedione and biacetyl. For this molecule, however, the short wavelength absorption is at 265 nm ($\epsilon \approx 240 \text{ M}^{-1}\text{cm}^{-1}$). It is interesting to conjecture that the shorter wavelength absorption is not that of the second $n\pi^*$ transition. The effect of substituting a methyl and a chlorine atom in the biacetyl molecule has been to increase the intensity of the transition. This is the kind of behaviour that would be predicted for a formally spin-forbidden spectral transition. The presence of the internal heavy atom, chlorine, has through the agency of its larger spin-orbit coupling constant, increased the intensity of a transition which is forbidden in the absence of spin-orbit coupling. Calculations carried out by Kidd and Santry (56) on oxalyl fluoride suggest that the short wavelength transition could be $^3\sigma^* \leftarrow n$. The intermediacy of an $n\sigma^*$ state in the photochemistry of hexafluoroacetone has been proposed by Kutchke (57) and calculations by White, Santry and Yarwood (58) indicate that an $n\sigma^*$ state could be important in explaining the photochemical behaviour of formaldehyde.

While it is interesting to question the original assignment of the short wavelength transition, the suggestion that it is of an $^3\sigma^* \leftarrow n$ type is speculative. The enhancement of the transition in pentanedione compared to biacetyl is not large and the substitution effect of the chlorine atom in chlorobiacetyl could be explained in terms of the interaction of the d-orbitals on the chlorine atom with the π -system and the n-orbitals, rather than a spin-orbit induced forbidden transition.

Calculation of the Natural Radiative Lifetime

The fundamental equations governing the probabilities of various interactions of a system with electromagnetic radiation were derived by Einstein (59).

The processes considered are summarised in the diagram.



Application of the Maxwell-Boltzmann distribution law and the Planck radiation density equation allow the probabilities of induced absorption and spontaneous emission to be correlated. The probability of induced absorption can also be associated with the experimental absorption spectrum.

The derivation gives the probability of spontaneous emission A_{10} as,

$$A_{10} = \frac{8\pi^2 302}{N} c \bar{\nu}_{10}^2 \int \epsilon(\bar{\nu}) d\bar{\nu} = 2.88 \times 10^{-9} \bar{\nu}_{10}^2 \int \epsilon(\bar{\nu}) d\bar{\nu}$$

where N is Avagadro's Number, $\epsilon(\bar{\nu})$ is the molar extinction coefficient at wavenumber $\bar{\nu}$ and c is the velocity of light. The mean frequency of the transition is $\bar{\nu}_{10}$.

If there are no other processes other than emission removing the state 1 then the lifetime of the emission, called the natural radiative lifetime τ_{10} is given by,

$$\tau_{10} = \frac{1}{A_{10}}$$

Therefore, from a knowledge of the absorption process, the natural radiative lifetime can be calculated. However, this derivation has been applied to a system having sharp transitions where $\nu_{01} = \nu_{10}$. It can only be strictly applied to systems such as atomic absorptions with resonance fluorescence. In practice this equation is often applied to molecular fluorescence systems where the absorption band is broad and the fluorescence emission is shifted to longer wavelengths (23). It must be understood that results obtained using this method are only approximate. More detailed theories have been developed (60), but their application to a system which involves vibronically allowed transitions (51) is not justified (61).

Application of the approximate formula given above to the long wavelength absorption system of pentanedione (Fig. 9) gave a value of $A_{10} = 1.23 \times 10^5 \text{ s}^{-1}$. This can be compared to the value, $A_{10} = 1.18 \times 10^5 \text{ s}^{-1}$, found for biacetyl (62) using the same formula. The similarity

is striking and attests to the assumption that the same electronic transition is being considered in both cases. Furthermore, as the magnitude of the fluorescence yield depends upon the success of spontaneous emission in competition with radiationless processes, the close correlation of emission probabilities in biacetyl and pentanedione will allow useful conclusions to be made in Chapter 4.

CHAPTER 4

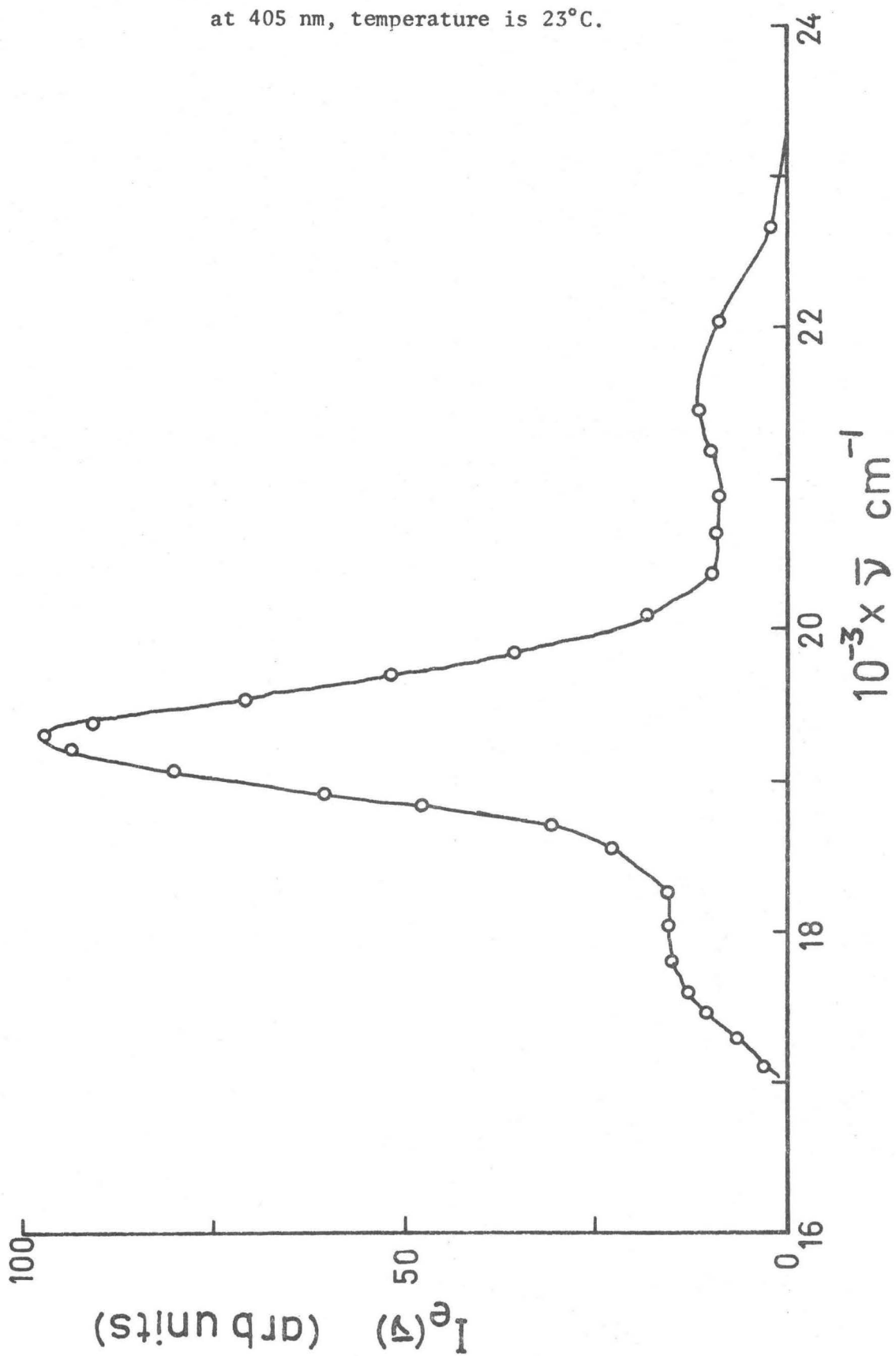
LUMINESCENCE SPECTRA

Preliminary investigations using an Aminco-Bowmann spectrofluorometer showed that when 2,3 pentanedione is excited in its long wavelength absorption band in the gas phase at room temperature, luminescence is observed. Experiments using a phosphoroscope attachment showed that the emission consisted of two components: a short-lived weak blue emission and a longer lived emission with a maximum in the green-yellow region. On the basis of these exploratory experiments, a detailed study was carried out to determine the nature of the emissions, their absolute magnitude and their dependence on exciting wavelength and pressure of added gases. The apparatus used in these studies has been described in Chapter 2.

Results of Experiments with 2,3-Pentanedione

When irradiated at 365, 405, and 436 nm, a sample of 15 torr of 2,3 pentanedione in the vapour phase at 24°C gave rise to emission extending from less than 430 nm to greater than 610 nm. The uncorrected spectrum obtained directly from the apparatus is shown in Fig. 11. The emission profile was identical at the three excitation wavelengths used. No fine structure was discernible, but maxima were observed at 460, 520, and 560 nm.

Fig. 11 Uncorrected emission spectrum of 2,3-pentanedione excited at 405 nm, temperature is 23°C.



Addition of 20 torr of oxygen caused the emission at longer wavelengths, already associated with a long-lived species from the phosphoroscope experiments, to disappear completely. In all cases, the profiles of the emission after the addition of oxygen were identical at the three excitation wavelengths used. The emission spectra obtained by irradiation in the long wavelength region at 365, 405, and 436 nm were corrected for the sensitivity factors described in Chapter 2. The corrected emission spectra at 24°C for the pure material and for a mixture of 2,3 pentanedione with 20 torr of oxygen are shown in Fig. 12 and Fig. 13.

To determine the absolute quantum yield of emission in the absence and presence of oxygen at room temperature, quinine sulphate was used as a relative standard as described in Chapter 2. The absolute quantum yields of the emissions, ϕ_e , were calculated using the following formula:

$$\frac{\phi_e}{0.55} = \frac{\text{Area}_{\text{PD}}}{\text{Area}_{\text{QS}}} \times \frac{(\text{OD})_{\text{QS}}}{(\text{OD})_{\text{PD}}} \times \frac{\text{Flux}_{313}}{\text{Flux}_{\lambda}}$$

where Area is the area under the corrected emission curve with frequency as abscissa, and OD is the absorbance of the sample. The subscripts PD and QS refer to 2,3 pentanedione sample and quinine sulphate sample, respectively. The relative flux emitted by the lamp-excitation monochromator at the wavelengths 313 nm and λ (where $\lambda = 365, 405, 436$ nm) is denoted by $\text{Flux}_{313}/\text{Flux}_{\lambda}$. The absolute values of the quantum yields of emission at the three excitation wavelengths are shown in Table 2.

A further check of the absolute quantum yield of emission was carried out using relative quantum yield apparatus described earlier, Fig. 5. The relative standard used here was biacetyl and the experiment

TABLE 2. ABSOLUTE EMISSION YIELDS AT 23°C

SAMPLE	λ_{ex}	ϕ_f	ϕ_p
15 torr 23PD	436	0.0011	0.019
	405	0.0011	0.019
	365	0.00063	0.010
15 torr 23PD + ~ 1000 torr SF ₆	436	0.0011	0.019
	504	0.0011	0.019
	365	0.0012	0.020

TABLE 3. RELATIVE EMISSION YIELDS AT 30°C.

SAMPLE	Q_{p+f}	Q_f	Q_p
Pentanedione (14 torr)	6.8	0.4	6.4
Biacetyl (25 torr)	56	1.0	55

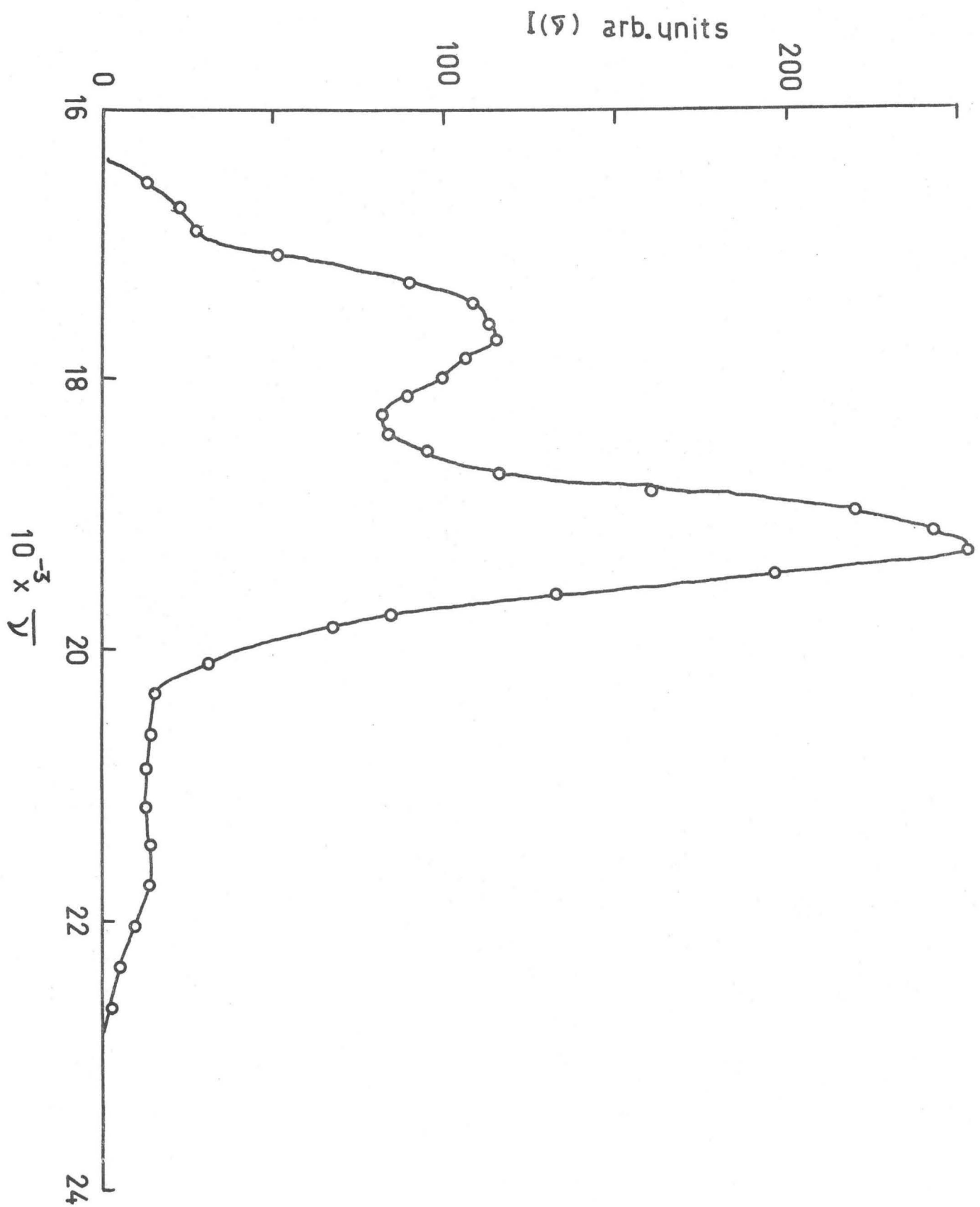


Fig. 12 Corrected total emission spectrum of pentanedione excited at

405 nm.

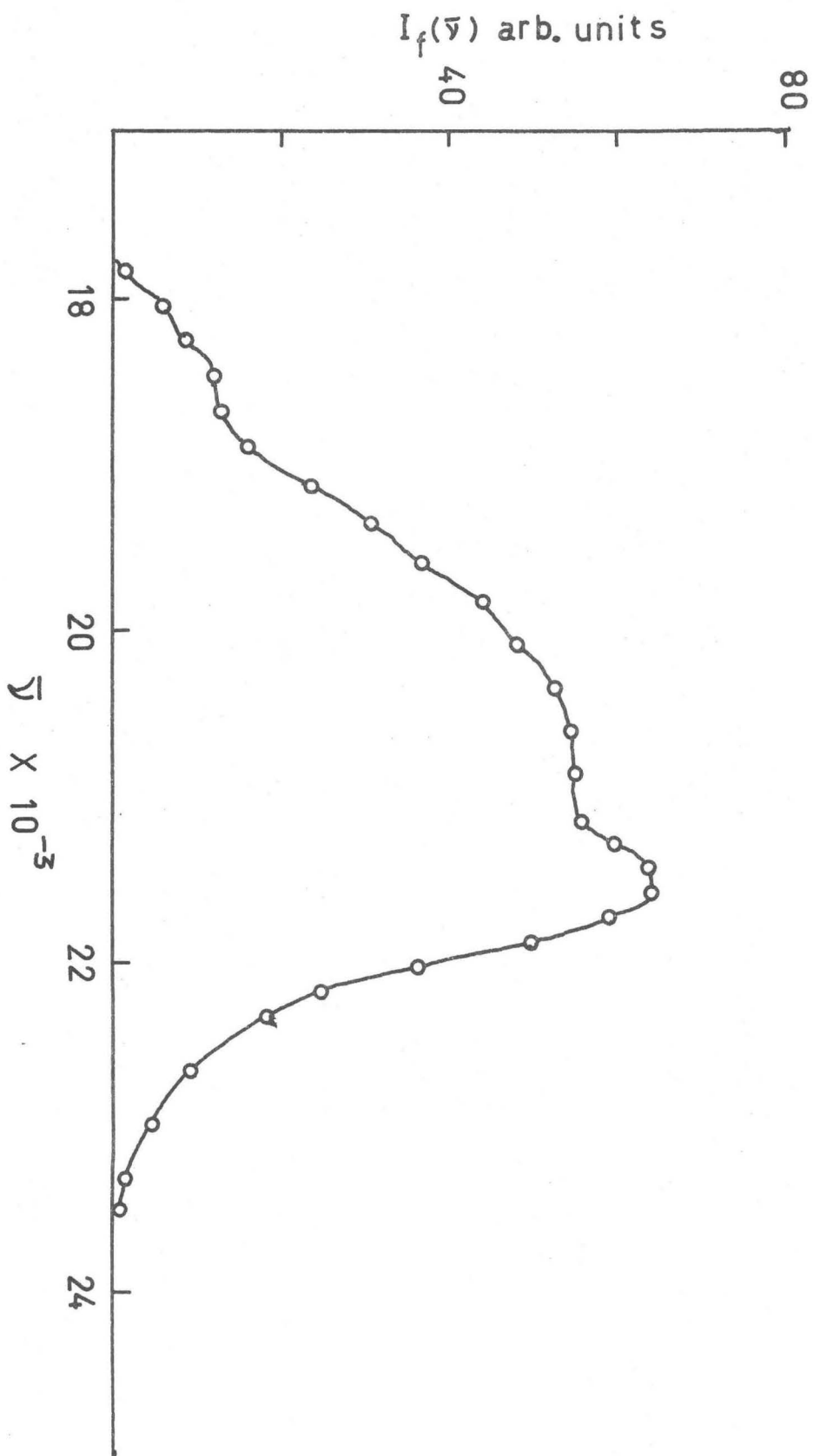


Fig. 13 Corrected fluorescence emission spectrum of pentanedione excited at 405 nm.

was performed at 30°C. The Q values were calculated for 2,3 pentanedione and biacetyl with and without 20 torr of oxygen and are shown in Table 3. The absolute quantum yield of emission of biacetyl has been determined by several workers (30,64). The value of 0.18 was used in this work. As the emission profiles of 2,3 pentanedione and biacetyl are very similar, the Q values can be compared directly, using the formula:

$$\frac{\phi_{PD}}{\phi_{Biacetyl}} = \frac{Q_{PD}}{Q_{Biacetyl}}$$

where ϕ 's refer to the absolute emission yields and Q's refer to relative yields. This comparison gave a value for the total emission yield of 2,3 pentanedione at 30°C of 0.022. This compares well with the value obtained using quinine sulphate as a standard.

Effect of Added Inert Gas on Emission Spectra

The same apparatus geometry and sample of 2,3 pentanedione was used as in the studies of the emission spectrum of the pure material. The effect of adding a high pressure of inert gas ($\text{SF}_6 \sim 1000$ torr) on the emission yields is included in Table 2. The emission profiles were unchanged in the presence of the added gas at all excitation wavelengths. As can be seen from Table 2, the absolute yields are unaffected by the addition of gas at 436 nm and 405 nm. However, at 365 nm excitation, the absolute value of ϕ_f and ϕ_p are increased to those found when 405 and 436 nm excitation is used.

Discussion

Absolute Emission Yields at 24°C

The emission of 2,3 pentanedione has been shown to consist of two components by use of the rotating-shutter phosphoroscope attachment. This experiment reveals that the emission at longer wavelengths, with a maximum at 520 nm, is due to a species having a lifetime approximately equal to the period of rotation of the shutter in the phosphoroscope ($\sim 10^{-4}$ sec). The species giving rise to emission in the blue region, being undetectable by this method, has a shorter lifetime than this. The addition of 20 torr oxygen causes only the yellow-green emission to disappear. Therefore, the following conclusions can be made:

- (1) The weak blue emission extending from less than 430 nm to greater than 550 nm is associated with a relatively short lived species and is not quenched by 20 torr of oxygen.
- (2) The stronger green emission extending from less than 480 nm to greater than 610 nm is associated with a species which has a lifetime $\sim 10^{-4}$ s or longer and is quenched by 20 torr of oxygen.

The conclusions of Kasha (65) predict that the most probably radiative transitions will be from the lowest energy state of a particular spin multiplicity. Now it has already been shown in Chapter 3 that the lifetime of the S_1 state of 2,3 pentanedione cannot be longer than $\sim 8 \times 10^{-5}$ s, whereas the lifetime of the T_1 state can be considerably longer due to the spin-forbidden nature of the $T_1 \rightarrow S_0$ transitions. This feature, to-

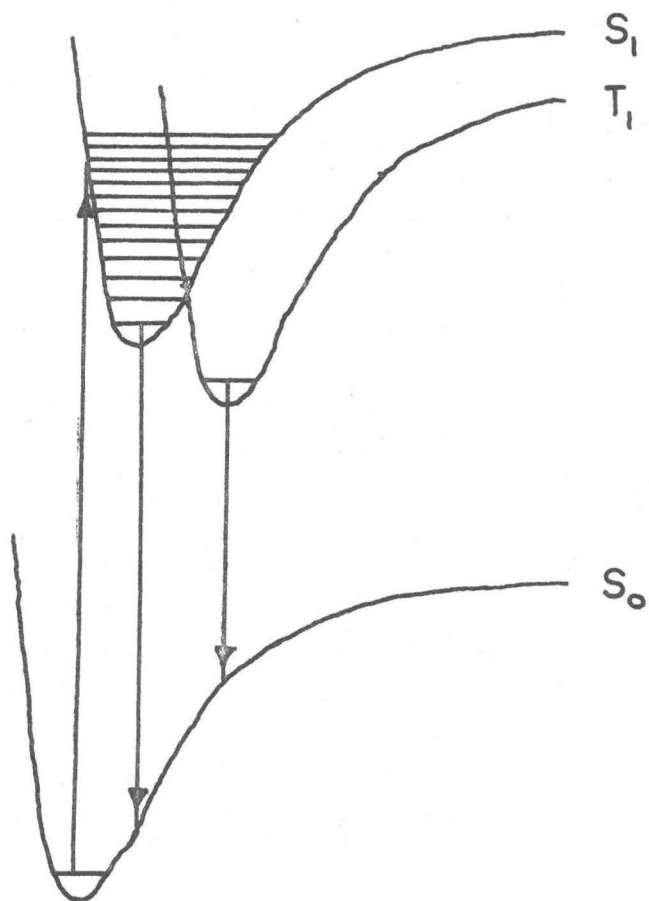
gether with the condition that the triplet state of a system will always be of lower energy than the singlet (66), suggests that the short-lived blue emission (high energy) is associated with the S_1 state, whereas the longer-lived green emission (lower energy) is associated with the T_1 state.

Further support for this suggestion is gained from the effect of oxygen which will efficiently quench triplet states of many organic molecules in solution and in the gas phase (2,3). In particular, the triplet state of biacetyl is quenched by oxygen (31,67). The similarity in structure between biacetyl and pentanedione is such that it is reasonable to assume that the T_1 state of pentanedione will also be efficiently quenched by oxygen. One can conclude, therefore, that the total emission spectrum consists of fluorescence from the S_1 state and phosphorescence, from the T_1 state.

Determination of S_0-S_1 and S_1-T_1 Energies

The energies of the 0-0 transitions from the S_0 manifold to the S_1 and T_1 manifold can be obtained from a detailed analysis of the absorption spectrum. In the absence of such an analysis for pentanedione, the fluorescence and phosphorescence spectra can be used in conjunction with the absorption spectrum to obtain estimates of these quantities. It is known from the absorption spectra of glyoxal and biacetyl that the 0-0 transition $S_1 \leftarrow S_0$, lies at longer wavelength than the most intense absorption. Assuming that the Franck-Condon vertical transition will be the strongest in absorption, the situation can be portrayed in the schematic potential energy diagram in Fig. 14.

Fig. 14 Schematic representation of potential energy curves of S_0 , S_1 and T_1 states.

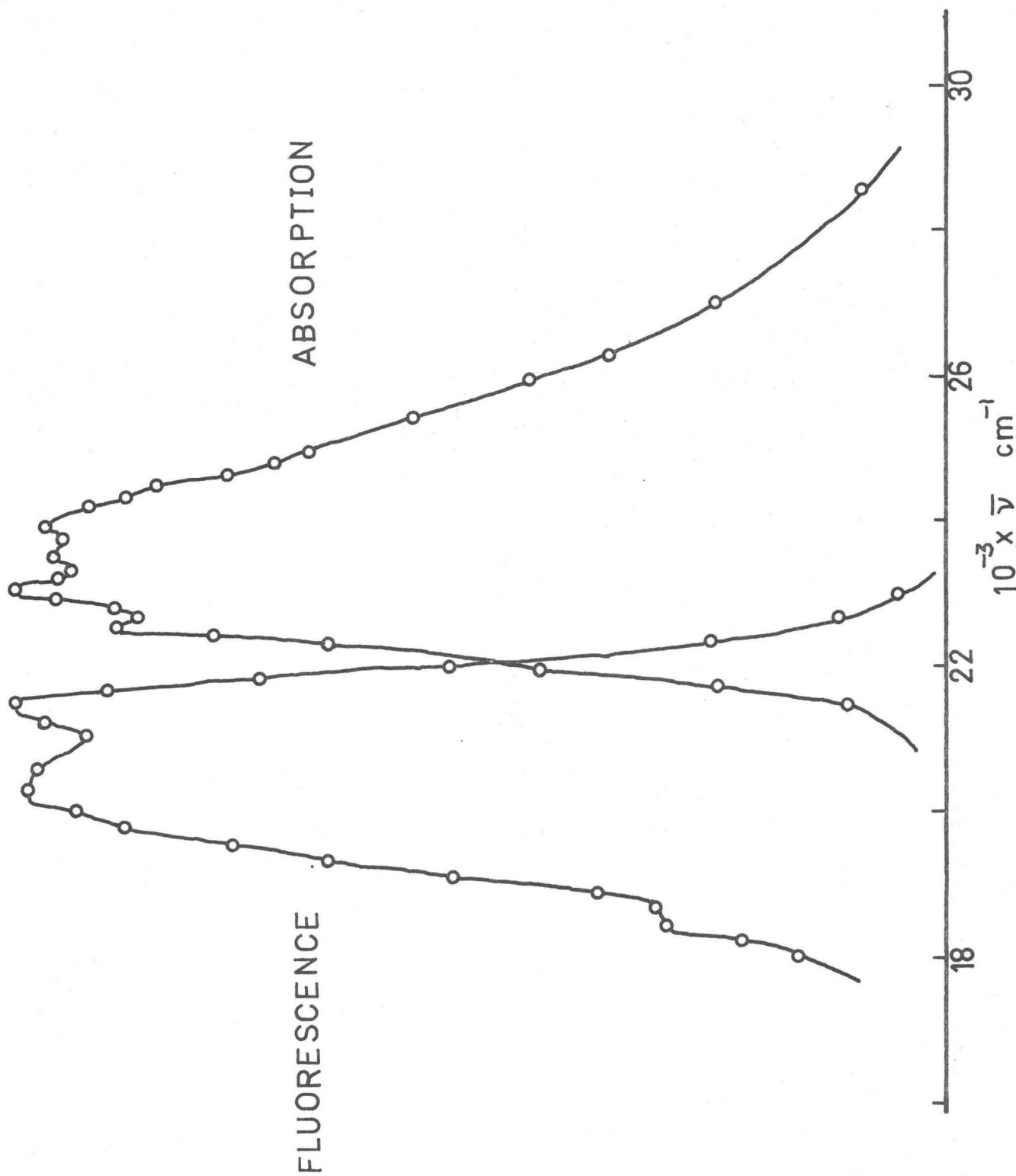


It is assumed that fluorescence emission at high pressure occurs from the zeroth vibronic level of the S_1 manifold. The displacement of the T_1 curve is not a prerequisite and is merely to retain clarity in the diagram.

The absorption spectrum will represent the variation of the Franck-Condon vibrational overlap integrals between the zeroth vibrational level of S_0 and the vibrational levels of the S_1 manifold. As such, it will be characteristic of the topography of the S_1 hypersurface. Whereas the fluorescence spectrum will represent the variation of the Franck-Condon factors between the zeroth vibronic level of S_1 and the vibronic levels of the S_0 manifold. This will, therefore, be characteristic of the topography of the S_0 hypersurface. The similarities between the hypersurfaces of S_1 and S_0 are revealed by the approximate "mirror image" relationship existing between the absorption spectrum and the fluorescence spectrum as shown in Fig. 15. This method of normalised plotting allows the 0-0 transition to be identified immediately. The simple ideas presented above predict that the 0-0 transition is as intense in absorption as it is in emission. It is, therefore, the point of intersection of the two spectra shown in Fig. 15. The value obtained by this method is $22,100 \text{ cm}^{-1}$ (63.2 Kcal).

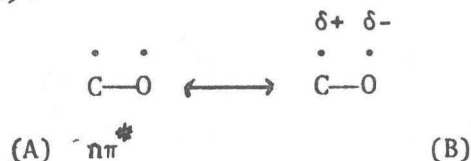
To determine the S_1 - T_1 0-0 splitting energy, some assumptions are necessary concerning the characteristics of the T_1 hypersurface. If the geometry of this state is similar to that of the S_1 and S_0 states, then the Franck-Condon factors for the radiative transition $T_1 \rightarrow S_0$ will be approximately the same as for the radiative $S_1 \rightarrow S_0$ transition. The onset of the fluorescence will give the magnitude the highest vertical energy change between the hypersurfaces S_1 and S_0 . Similarly, the onset of the phosphorescence will give the highest vertical energy change between the hypersurfaces T_1 and S_0 . As it is assumed that emission from

Fig. 15 Showing "mirror-image" relationship between fluorescence and absorption.



S_1 and T_1 takes place from the zeroth vibronic level, the S_1-T_1 0-0 energy can be estimated as the difference between the onset of the fluorescence and the onset of phosphorescence. From the spectra shown in Figs. 12 and 13, the S_1-T_1 0-0 splitting is calculated as 3220 cm^{-1} (9.2 Kcal). Therefore, by difference the T_1-S_0 0-0 energy is calculated as 18880 cm^{-1} (54.3 Kcal) in the gas phase. This value can be compared with the value of 54.7 Kcal obtained by Hammond (39) in a 3,Me-pentane matrix at 77°K .

The value determined in this study is comparable to the energy levels determined spectroscopically for other diketones. The effect of substitution in the pentanedione molecule is not large and can be rationalised in terms of the inductive effect of the methyl and ethyl groups stabilising the $n\pi^*$ excited state. The electron distribution in the carbonyl system will be asymmetric due to the greater electronegativity of the oxygen atom compared to the carbon atom. This can be described in valence bond terms by including in the resonance structure a contribution from (B).



Inductive redistribution of electron density from the alkyl groups will tend to delocalize this asymmetry and lead to stabilization of the state.

The small singlet-triplet splitting energies of diketones can be reconciled with the nature of the electronic transition involved. The difference in energy between singlet and triplet of the same electronic

state is given by twice the exchange integral (69),

$$E_{S_1} - E_{T_1} = 2 \int \phi_1^*(r_1) \phi_2(r_1) H \phi_1^*(r_2) \phi_2(r_2) \Delta r_1 \Delta r_2$$

where ϕ_1 is the wavefunction of the orbital from which the electron is promoted and ϕ_2 is the orbital that it is promoted to. The asterisks imply complex conjugate and the integration is over volume elements Δr_1 and Δr_2 with H the electronic coulombic repulsion operator

$$\frac{e^2}{|\mathbf{r}_1 - \mathbf{r}_2|}$$

This can be thought of as twice the coulomb repulsion energy of two charge distributions $\phi_1^*(1) \phi_2(1) \Delta r_1$ and $\phi_1^*(2) \phi_2(2) \Delta r_2$. As was pointed out earlier, in the carbonyl group the overlap between the n orbital of the oxygen and the π^* system is small. In addition, the transition involves the redistribution of charge over a large region in the delocalised π^* orbital, i.e. the coulombic repulsion operator will be smaller, as $|\mathbf{r}_1 - \mathbf{r}_2|$ is larger. These two factors both act to make the S_1 - T_1 energy gap small in diketones.

One of the results of the small S_1 - T_1 energy gap is considerable interstate mixing of the S_1 and T_1 states via the spin-orbit operator, which is enhanced by the presence of the relatively heavy hetero atom, oxygen, in the molecule. This result follows from the first-order perturbation treatment of interstate mixing (70,71,72).

$$T_1' = T_1 + \frac{\int S_1 H' T_1 d\tau}{E(T_1) - E(S_1)} \cdot S_1$$

where T_1' is the first order perturbed wave function, T_1 is the wavefunction of the unperturbed triplet, H' is the perturbing operator (in the case of carbonyl compounds, the spin-orbit operator), S_1 is the perturbing singlet wavefunction, and $E(T_1)$, $E(S_1)$ are the energies of the unperturbed triplet and singlet states, respectively. Therefore, we would expect to find intersystem crossing to be efficient in diketones, as is confirmed by experiment.

Effect of Added Gas on Emission Properties

The data summarising the effect of ~ 1000 torr of SF_6 on the absolute quantum yields of fluorescence and phosphorescence is included in Table 2. Important conclusions can be drawn from these experiments.

At 436, 405, 365 nm, the fluorescence and phosphorescence profiles are independent of pressure. This can be interpreted either as:

- (a) The same species are giving rise to emission in the pure diketone as in the presence of added gas, or,
- (b) There are different species (in the S_1 and T_1 manifolds) giving rise to the emission but the profiles are coincident.

It has already been shown that the phosphorescence is relatively long-lived. Therefore, a molecule in the triplet state will undergo many collisions in the average lifetime ($\sim 10^{-3}$ sec) before it emits. This will be sufficient time to equilibrate any excess vibrational energy it possesses. Therefore, it is safe to assume that the species giving rise to emission from the triplet manifold will be in its Boltzmann

thermalized level (i.e. zeroth vibronic level for ambient temperatures $\sim 300^\circ\text{K}$). These arguments need not apply to a molecule in the S_1 state. Excitation at 435 nm will form an excited singlet state in a vibronic level near to the zeroth vibronic level. If the only processes governing the fate of such a molecule are fluorescence and intersystem crossing to the triplet manifold (26), then the fluorescence yield is given by

$$\phi_f = \frac{k_f}{k_f + k_{isc}}$$

where k_f is the emission constant for $S_1 \rightarrow S_0$, and $k_{isc_{S_1 \rightarrow T_1}}$ is the intersystem crossing rate constant. Inserting values for ϕ_f and k_f ,

$$10^{-3} = \frac{1 \times 10^5}{1 \times 10^5 + k_{isc_{S_1 \rightarrow T_1}}}$$

gives the value of $k_{isc_{S_1 \rightarrow T_1}}$ as $\sim 10^8 \text{ sec}^{-1}$. Consider a molecule formed by excitation at a shorter wavelength (i.e. a higher vibronic level of the S_1 manifold). If the processes which this species S_1^v undergoes are:

- (1) emission with rate constant $\sim 10^5$.
- (2) vibrational deactivation in collisions with rate constant = $Z[M] \sim 10^{11} \times 10^{-3} \sim 10^8 \text{ s}^{-1}$ at torr pressures where Z is of the order of the collision frequency and M is the pressure.
- (3) intersystem crossing with rate constant $\sim 10^8 \text{ s}^{-1}$ then the emission yield from that level will be given by,

$$\phi_{f_{S_1^v}} = \frac{k_f}{k_f + k_{isc} + Z(M)} \sim \frac{10^5}{10^5 + 10^8 + 10^8} \sim 10^{-4}$$

This approximate calculations shows that, provided the rate constants are of the magnitude suggested, emission from vibrationally excited levels is possible. This could be the behaviour when excitation is at 365 nm. The subject of vibrational deactivation will be dealt with in detail in Chapter 7 and the various diagnostic tests for mechanisms will be discussed. The simple experiment described above, however, does permit the conclusion that the presence of added gas makes the emission process more efficient for excitation at 365 nm and this can be interpreted in terms of collisional deactivation of the initially formed vibronic level into a condition where fluorescence is more efficient.

The magnitude of the ϕ_f/ϕ_p ratio is also the source of another important conclusion concerning the processes taking place in the singlet and triplet manifolds in the presence of added gas. It was shown above that the energy gap between the S_1^0 and T_1^0 levels was relatively small (~ 10 Kcal) and this was correlated with the small exchange integral associated with the $n\pi^*$ state. Systems displaying small S_1 - T_1 splitting and relatively long lived T_1 states may display delayed fluorescence as characterised by Parker (73). This process occurs when molecules in the triplet manifold may be returned to the S_1 manifold, by two processes. These are represented as:

(a) P-type delayed fluorescence to

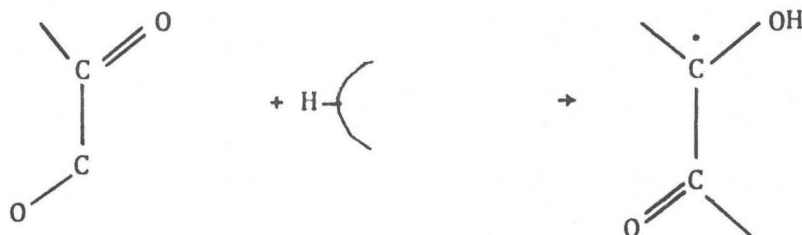


(b) E-type delayed fluorescence to



In the gas phase at low light intensities (i.e. low T_1 concentrations) the more probable of these processes is (b). This is the process which has been observed in an α -diketone in the condensed phase (74) and has been suggested as being important in the photolysis of biacetyl, in the gas phase in the presence of high pressures of added gas (75). If this were an important process in the photochemistry of 2,3 pentanedione, then the ratio of ϕ_f/ϕ_p would be expected to increase with pressure of inert gas at long wavelengths. As can be seen from Table 2 this is not detectable within experimental error. Therefore, one can conclude that this process is an unimportant process under the conditions studied. This subject will be discussed later in further detail as the results of other experiments are described.

For pentanedione in the gaseous phase at 24°C, excited at 405 nm and 436 nm, the ratio ϕ_f/ϕ_p is 0.05 (see Table 2) for a concentration of 10^{-3} M, whereas, Richtol and Klappmeier (43) report that in hexane solution at 25°C at a similar concentration, the ratio is about 0.60. This discrepancy can be understood in terms of the other processes influencing the removal of the triplet state in solution. In particular, one process which is known to occur with hydrogenated molecules is abstraction of a hydrogen atom by the triplet state of the diketone (76,77).



If the rate of removal is increased in solution relative to the gas phase, ϕ_p will decrease, and a larger value of ϕ_f/ϕ_p will result.

Emission Behaviour of aliphatic α -diketone systems

As was pointed out earlier, the investigation of the emission properties of 2,3 pentanedione would allow interesting comparisons with the emission behaviour of the first two members of the series of α -diketones: glyoxal and biacetyl. In particular, interesting variations in radiationless processes might occur with increasing complexity.

The glyoxal emission system has received little attention with respect to elucidating the processes removing the excited singlet and triplet species. It was reported in an early study (78) that at 80°C the fluorescence yield ϕ_f is high ~ 0.30 while the phosphorescence yield ϕ_p is $\sim 10^{-3}$. In a recent report, Parmenter et al (79) describe certain interesting features of the photolysis of this molecule. It appears that the intersystem crossing process $S_1 \rightarrow T_1$ is collisionally induced, leading to a dependence of ϕ_f/ϕ_p on pressure.

Biacetyl luminescence in the gas phase has been the subject of much study (23,24,26,80). It has been shown by several workers (7,80) that with excitation at 436 nm, the fluorescence and phosphorescence quantum yields are independent of pressure of inert added gas with the values $\phi_p = 0.18$ (30), $\phi_f = 2.3 \times 10^{-3}$ (28). This has been interpreted as showing the intersystem crossing process in biacetyl is not collisionally induced (80). The fluorescence lifetime in the gas phase at 436 nm and

24°C has been measured as 1.0×10^{-8} s (81). In the absence of other radiationless processes removing the level formed under these conditions (26,29), this represents the lifetime controlled by the intersystem crossing process $S_1 \rightarrow T_1$ i.e. $k_{isc_{S_1 \rightarrow T_1}} = 1.0 \times 10^8 \text{ s}^{-1}$.

It has been shown in Chapter 3 that the long wavelength absorption system in pentanedione is very similar to that of biacetyl. The probabilities for spontaneous emission were the same using the same method of estimation. Reference to Table 2 shows that the fluorescence yield of pentanedione excited at 436 nm shows the same insensitivity to added gas as does that of biacetyl. It is reasonable to assume that the behaviour of the two compounds when excited at 436 nm is the same. The fluorescence yields of pentanedione and biacetyl can be represented by,

$$\phi_{f_{PD}} = \frac{k_{f_{PD}}}{k_{isc_{S_1 \rightarrow T_1 PD}}} = 1.0 \times 10^{-3}, \quad \phi_{f_{BA}} = \frac{k_{f_{BA}}}{k_{isc_{S_1 \rightarrow T_1 BA}}} = 2.3 \times 10^{-3}$$

as $k_{f_{PD}} = k_{f_{BA}}$, then

$$k_{isc_{S_1 \rightarrow T_1 PD}} = 2.3 k_{isc_{S_1 \rightarrow T_1 BA}} = 2.3 \times 10^8 \text{ s}^{-1}$$

The difference in behaviour of glyoxal, biacetyl and pentanedione present an interesting problem to the current theories of radiationless events. These processes were discussed in Chapter 1, where emphasis was placed on the treatment of Jortner et al and the limiting cases which their theory describes. The behaviour of the diketones can be viewed in

terms of the criteria presented there. It should be mentioned that as the process under consideration is a formally spin-forbidden process, $S_1 \rightarrow T_1$, the magnitude of the perturbation operator will be smaller than for a formally spin-allowed process. However, with respect to intersystem crossing in other molecules, it will be favoured due to the presence of the relatively heavy hetero-atom, oxygen, and the small singlet-triplet splitting energy, leading to a relatively high degree of mixing. The small value of the singlet-triplet splitting will, however, be reflected in a lower value for ρ , the density of states in the adjacent manifold. The states associated with emission have been identified as the 1A_u and the 3A_u (20) in glyoxal and biacetyl. However, the presence of closely lying 1A_g and 3A_g has been confirmed by analysis of the absorption spectrum (20). The presence of such states can be an important factor in the promotion of the intersystem crossing process, as pointed out by Bixon and Jortner (9).

In the case of glyoxal excited at 436 nm, Parmenter (79) calculates that the maximum value for the density of states, ρ , in the 3A_u manifold at this excitation level in 1A_u is 6 per cm^{-1} . This small value, while V is not known, indicates the product ρV will be less than unity. Therefore, this corresponds to the small molecule limit described by Jortner et al. The occurrence of collisionally induced intersystem crossing is consistent with this conclusion.

The behaviour of biacetyl is at present under debate. The fluorescent lifetime at a pressure of 20 torr (81) is the same as that found in solution (82). The fluorescent quantum yield for 436 nm excitation

is independent of pressure to as low as 0.04 torr (80) where the excited singlet molecule is unperturbed during its lifetime and is effectively isolated. These are the properties to be expected of a large molecule in the statistical limit. This allows use of the formula,

$$k_{nr} = \frac{2\pi}{h} \rho \bar{V}^2$$

Using a value of $\rho \sim 100$ states/cm⁻¹ based on estimates of vibrational frequencies in the T₁ state Parmenter (80) uses this equation to calculate \bar{V} . However, the value of ρV obtained is $\sim 10^{-1}$. This clearly is outside the limit provided by the theory. An explanation of the lack of success of the theory in this case is suggested by Parmenter and involves the use of the average matrix coupling element, \bar{V} , in the equation above. This may be a poor approximation in biacetyl, as the singlet-triplet splitting energy is small, and may give rise to large Franck-Condon overlap factors in some matrix elements. Furthermore, the use of the equation is based on the interaction of only two manifolds whereas it is known that there are two singlet states and two closely lying triplet states in close proximity in biacetyl. The application of the simple theory to this case may be invalid.

The case of 2,3 pentanedione offers an opportunity to observe the radiationless processes in a diketone where the parameters ρ and \bar{V} have been modified. The singlet-triplet splitting energy and the absorption spectrum and emission spectra are very similar to those of biacetyl. Therefore, one would expect that the matrix elements connecting the singlet

and triplet manifolds would be of similar magnitude. However, in the case of pentanedione, the density of states ρ has been modified, due to the increased complexity of the molecule. Therefore, qualitatively, the increase in the radiationless process $S_1 \rightarrow T_1$ in the case of pentanedione could be ascribed to the increase in the density of states in the triplet manifold in the region of the cross-over. This kind of qualitative argument has to be used carefully, however, as various formulae exist (83) for calculation of the density of vibrational levels at a point in a manifold. If these formulae are based on an harmonic model, they are to be suspected, because of the probably anharmonicity of the accepting potential surface at the crossover point. Combined with this reservation it must be remembered that the density of states calculated using such a formula is an upper limit to the value of ρ to be used in the equation above as $\rho_{\text{effective}}$ is probably less than ρ_{total} because of matrix element selection rules.

Nevertheless, we suggest that in pentanedione, there is an example of a large molecule with a high density of states, ρ , apparently behaving in a manner consistent with it being in the statistical limit of radiationless transitions.

CHAPTER 5

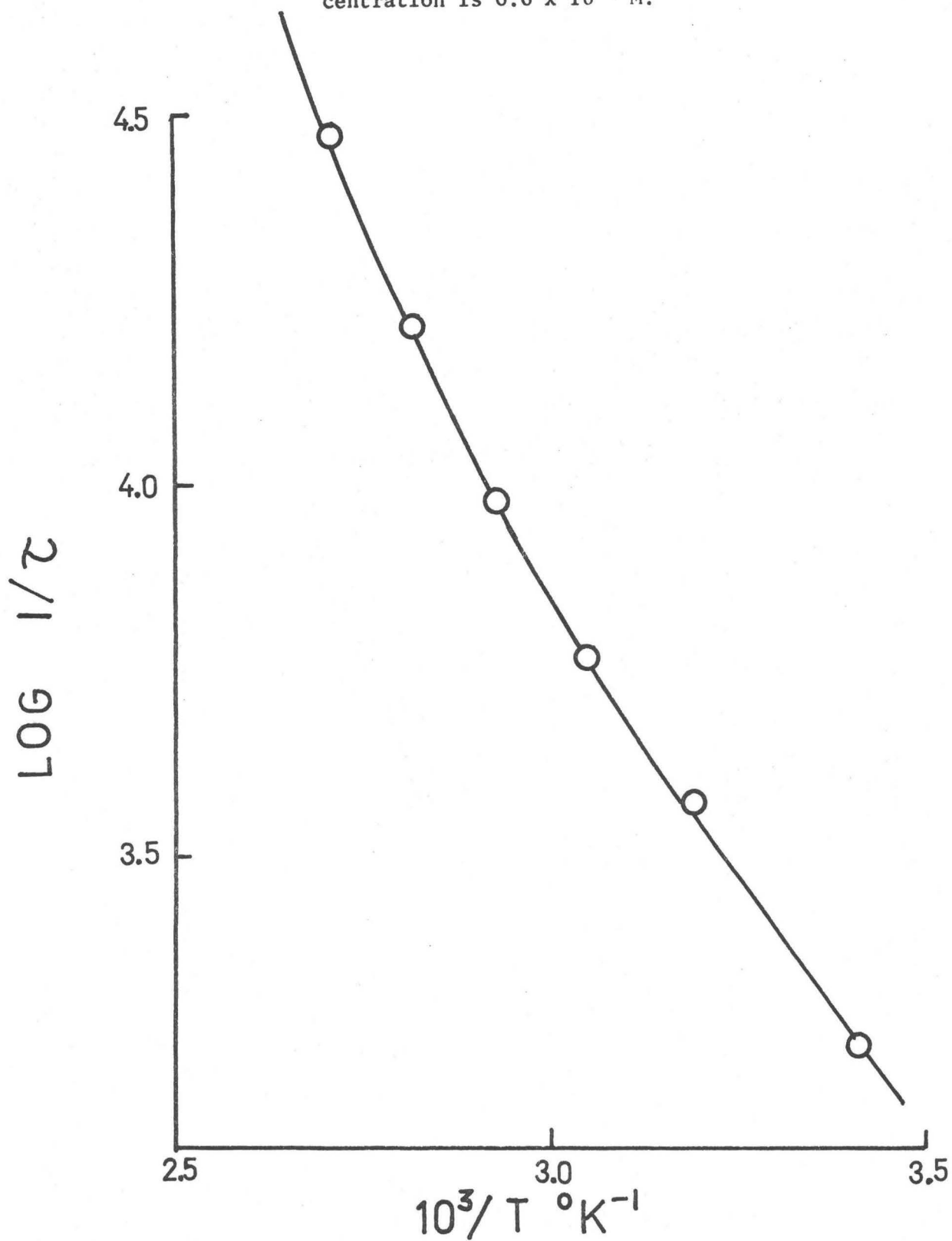
TRIPLET LIFETIME EXPERIMENTS WITH 2,3 PENTANEDIONE

Results

The phosphorescent decay of pentanedione in the gas phase was studied using the apparatus described in Chapter 2. The object of the study was to determine the factors controlling the fate of the phosphorescent species in the gas phase at temperatures in the range 300-370°K.

In all experiments, the decay of the emission was of a simple exponential form. It was found in all experiments that as the temperature of the system was increased the phosphorescent lifetime decreased. The results of a typical experiment are shown in Fig. 16. They are presented in the form of $\log \frac{10^{-3}}{\tau}$ vs $\frac{1000}{T} \text{ } ^\circ\text{K}^{-1}$. This form was chosen because it lent itself to the polynomial interpolation procedure described earlier. Data was obtained for concentrations in the range 6.6 to 900×10^{-5} M, but not at all temperatures due to the limitations of the vapour pressure (Appendix B). For some concentrations, the lifetime was remeasured at a lower temperature after completing the sequence of lifetime measurements at increasing temperatures. In each case the remeasured lifetime was in good agreement with the data obtained in the initial sequence, so that the problems associated with the formation of a quenching product were not encountered.

Fig. 16 Variation of phosphorescent lifetime with temperature, concentration is 6.6×10^{-4} M.



Using the polynomial interpolation procedure described in Chapter 2, the phosphorescent lifetime was calculated at a series of temperatures for each sample concentration. In Fig. 17 and Fig. 18, the reciprocal of the lifetime obtained in this manner varies with concentration at a series of temperatures. The behaviour of the plots is linear at all temperatures, however, the lack of a wide concentration range at the lower temperatures places wide statistical limits on values of the slope and intercept.

Effect of Inert Gas

The effect of inert gas on the triplet lifetime in the gas phase was studied using a pentanedione concentration of 1.0×10^{-3} M (18.5 torr). Addition of 1.1 and 2.0×10^{-2} M of sulphur hexafluoride did not change the triplet lifetime from that of the pure pentanedione over the temperature range 25 to 90°C. This effect was confirmed using a sample of pentanedione (0.5×10^{-3} M) and perfluoroethane over a wider pressure range at 80°C. The results are summarized in Fig. 19. There is no variation of the lifetime within the experimental limits of the measurement over the pressure range 0-950 torr.

Effect of Light Intensity

The effect of light intensity on the lifetime in the gas phase was studied using a pentanedione concentration of 6.8×10^{-3} M at 63.9°C. The data are presented in Fig. 20, the lifetimes show no trend with incident intensity, and within experimental error, are the same.

Fig. 17 Variation of triplet lifetime with concentration at 25, 30, 40, and 50°C.

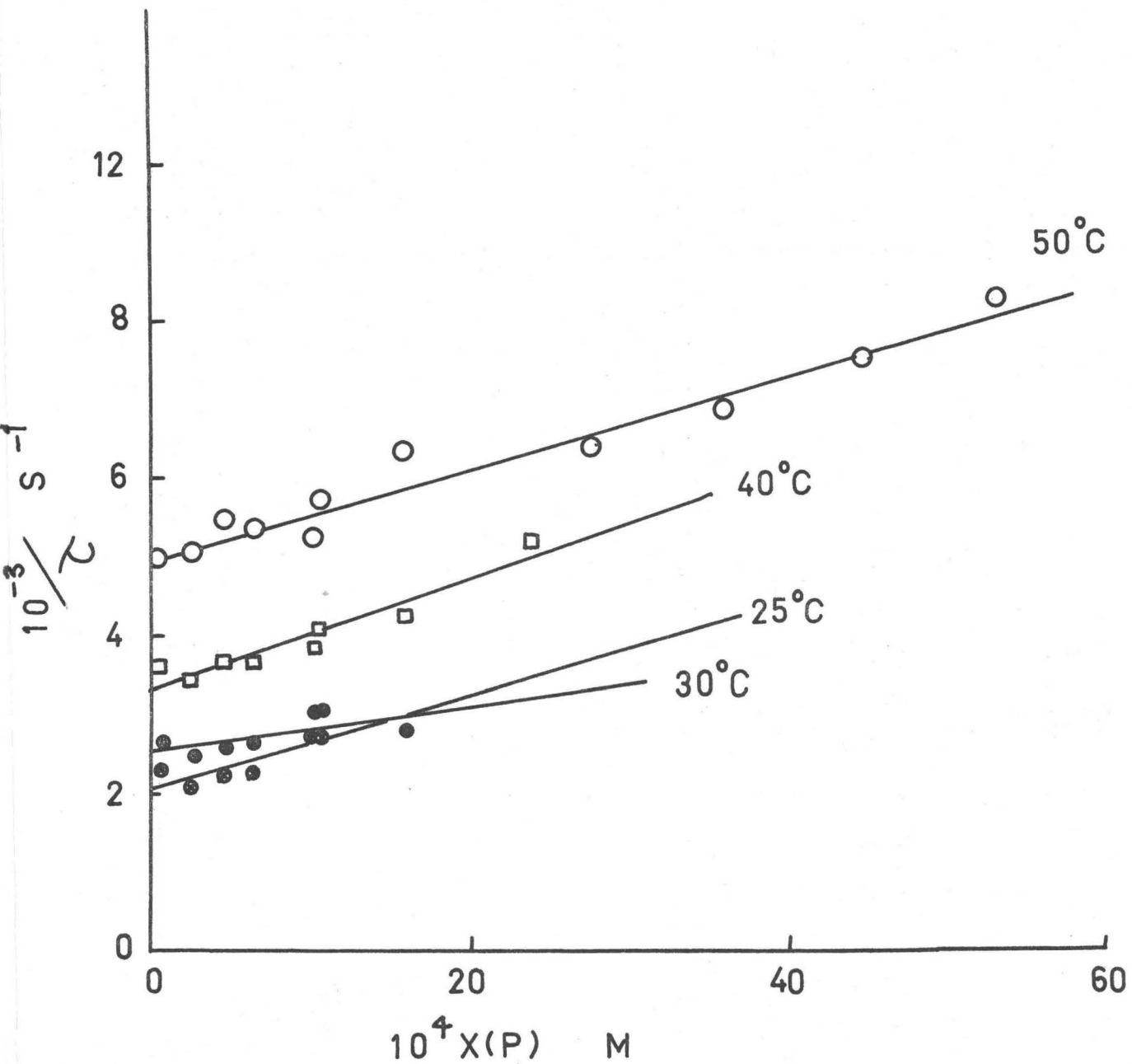
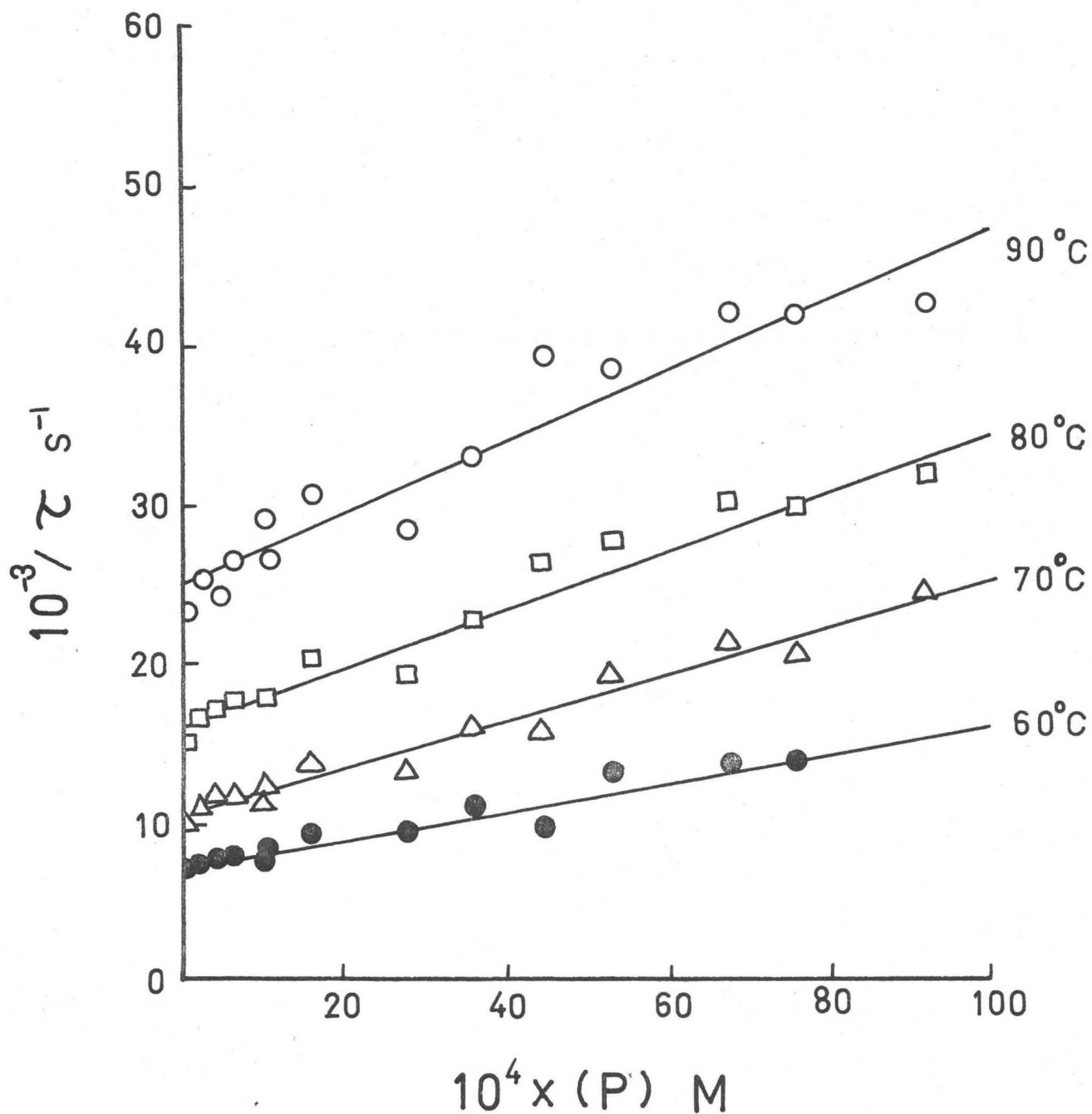


Fig. 18 Variation of triplet lifetime with concentration at 60, 70, 80, and 90°C.



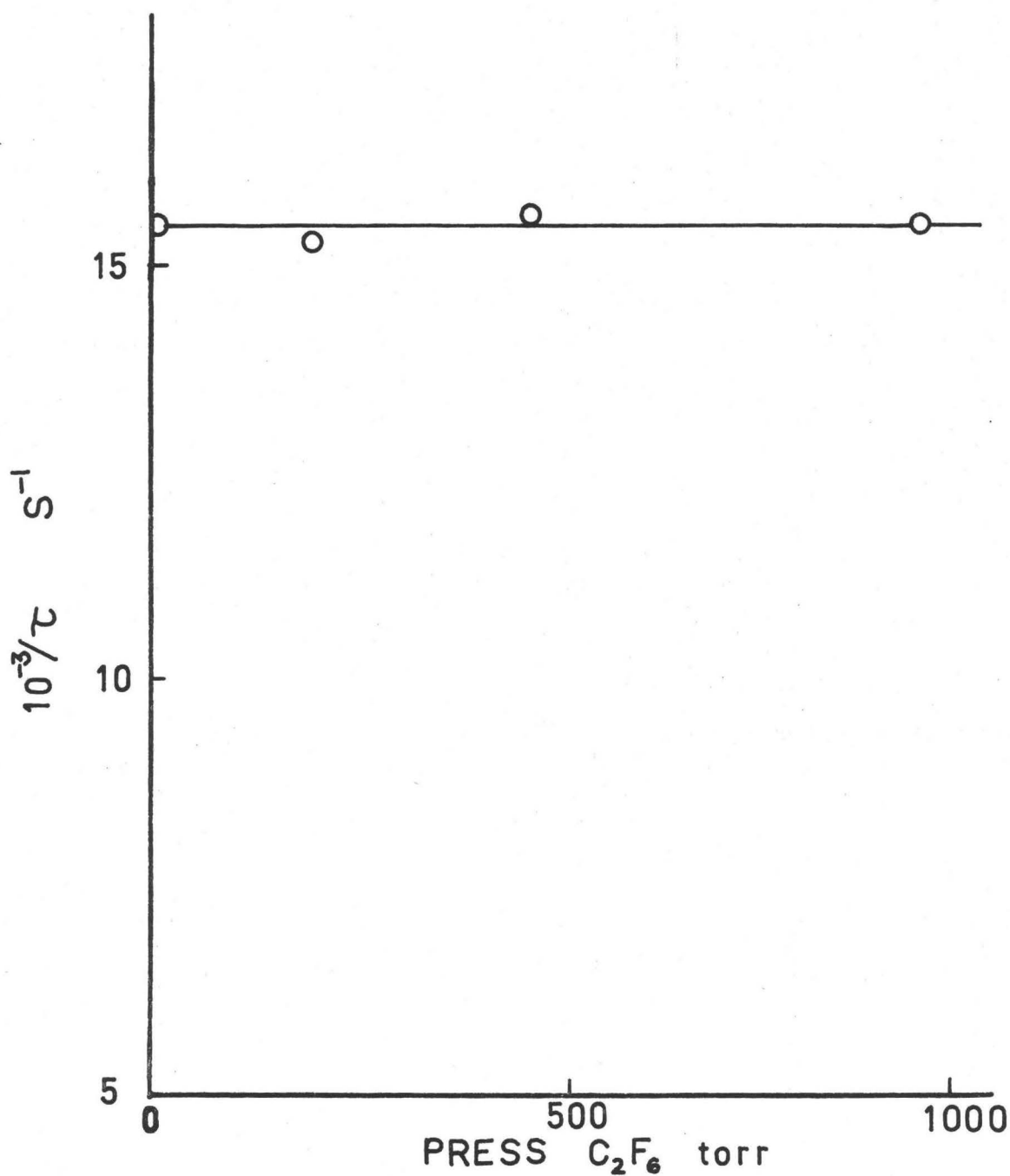
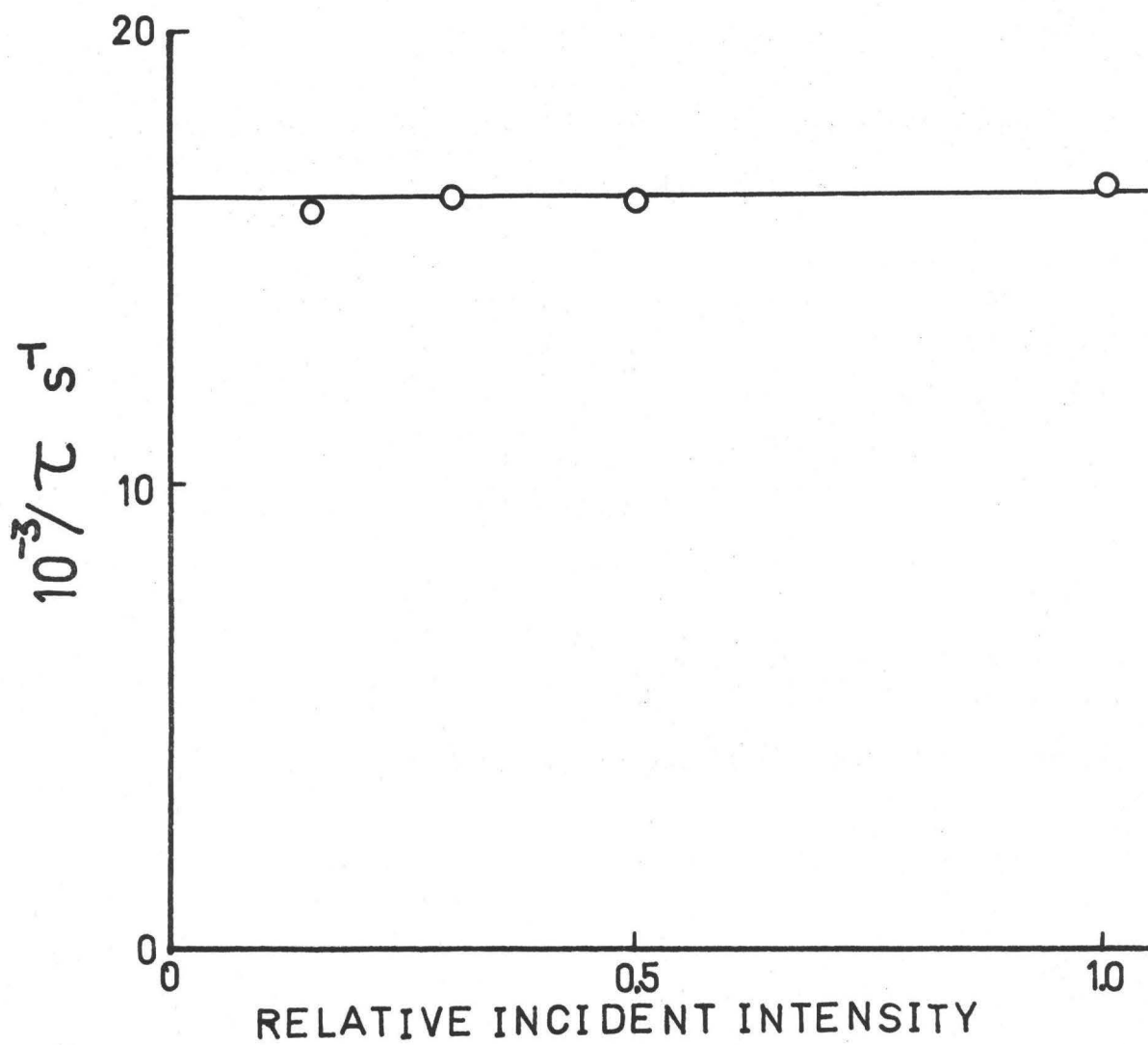


Fig. 19 Variation of phosphorescent lifetime of pentanedione with added C_2F_6 at $90^\circ C$.

Fig. 20 Variation of triplet lifetime with incident light intensity
at 63.9°C, 23PD = 6.8×10^{-3} M.



Triplet Lifetime at 77°K in various media

The phosphorescence lifetime at 77°K was measured in a variety of phases. It was necessary to leave the quartz sample tube immersed in the Dewar for at least 20 minutes to attain thermal equilibrium. An interesting effect was observed in the gases of neat pentanedione: rapid cooling of the liquid gave a sample having the appearance of a cracked glass with $\tau_{\text{phos}} = 0.97 \times 10^{-3}$ s whereas slow cooling of the sample resulted in a crystalline phase having a $\tau_{\text{phos}} = 4.6 \times 10^{-3}$ s.

In all media the decay of the emission was exponential. The phosphorescent lifetimes found under the various conditions are shown in Table 4.

Discussion

The experiments described in this section used the lifetime of the phosphorescent emission of the T_1 state as a monitor of its concentration. As all the lifetimes reported are longer than 20×10^{-6} s and as pressures in the region ~ 1 torr were used, it can be assumed that the T_1 state undergoing emission in the gas phase is in its equilibrated state at any particular temperature. Therefore, the data presented

TABLE 4. PHOSPHORESCENT LIFETIMES AT 77°K

Phase	$\tau_o^3 \times 10^{-3}s$	$10^3 \times \tau_{ave}$
Neat, cracked glass	0.948, 0.963, 0.954, 1.03	0.97
Neat, crystalline	4.27, 4.65, 4.52, 4.56	4.86
$\sim 5 \times 10^{-4}$ M in 3-Me pentane	2.43	2.43
$\sim 5 \times 10^{-4}$ in crystalline perfluoromethylcyclo- hexane	1.55	1.55

here describe the fate of the equilibrated T_1 state, and it should be emphasized that no information can be deduced concerning the processes forming this T_1 state.

For a species, T_1 , undergoing a series of simultaneous first and second order irreversible removal processes, the variation of its concentration with time is given by,

$$-\frac{d[T_1]}{dt} = \sum_i k_i [T_1] + \sum_j k_j [Q]_j [T_1]$$

where k_i is a first order rate constant, k_j is a second order rate constant for the reaction of Q_j and T_1 , and $[Q]_j$ is the concentration of Q_j . If the concentration of T_1 is small compared to the concentration of Q , the decay of the T_1 species will be a simple exponential having a lifetime, τ , given by,

$$\tau^{-1} = \sum_i k_i + \sum_j k_j [Q]_j$$

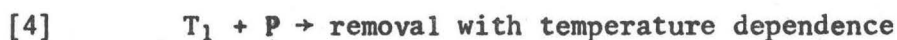
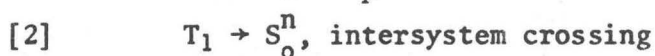
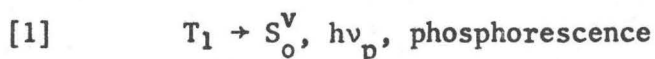
This is a form of the well-known Stern-Volmer relationship (84).

The data shown in Fig. 17 and Fig. 18 clearly follow this dependence for the case of a single quencher to the lowest concentration used (~ 1 torr). Several important conclusions can be made from this observation.

- (i) At the low pressures (~ 5 torr) spurious effects due to interaction of the T_1 species with the wall of the vessel are not important. As the lifetime of the T_1 species is comparatively long, at low pressures it is possible that diffusion to and destruction at the

wall of the vessel could be an important mode of removal for the T_1 species. This is the case for biacetyl (80), where it is found that at low pressures, destruction at the wall was an important process leading to an abrupt change in the variation of lifetime with pressure.

- (ii) The intercept value, τ_0 , decreases with increasing temperature. This indicates that a first-order process removing T_1 has a significant temperature dependence.
- (iii) The value of the second-order self-quenching rate constant, k_j , determined from the slope of the plots shown in Fig. 17 and Fig. 18, increases with increasing temperature. This indicates that this second-order quenching process has a significant temperature dependence. A mechanism which has all the necessary features for the removal of the thermally equilibrated T_1 species is given below:



where T_1 is the triplet pentanedione and P is the ground state pentanedione.

A steady state treatment of this system gives the following expression,

$$\tau^{-1} = k_1 + k_2 + k_3 + k_4[P]$$

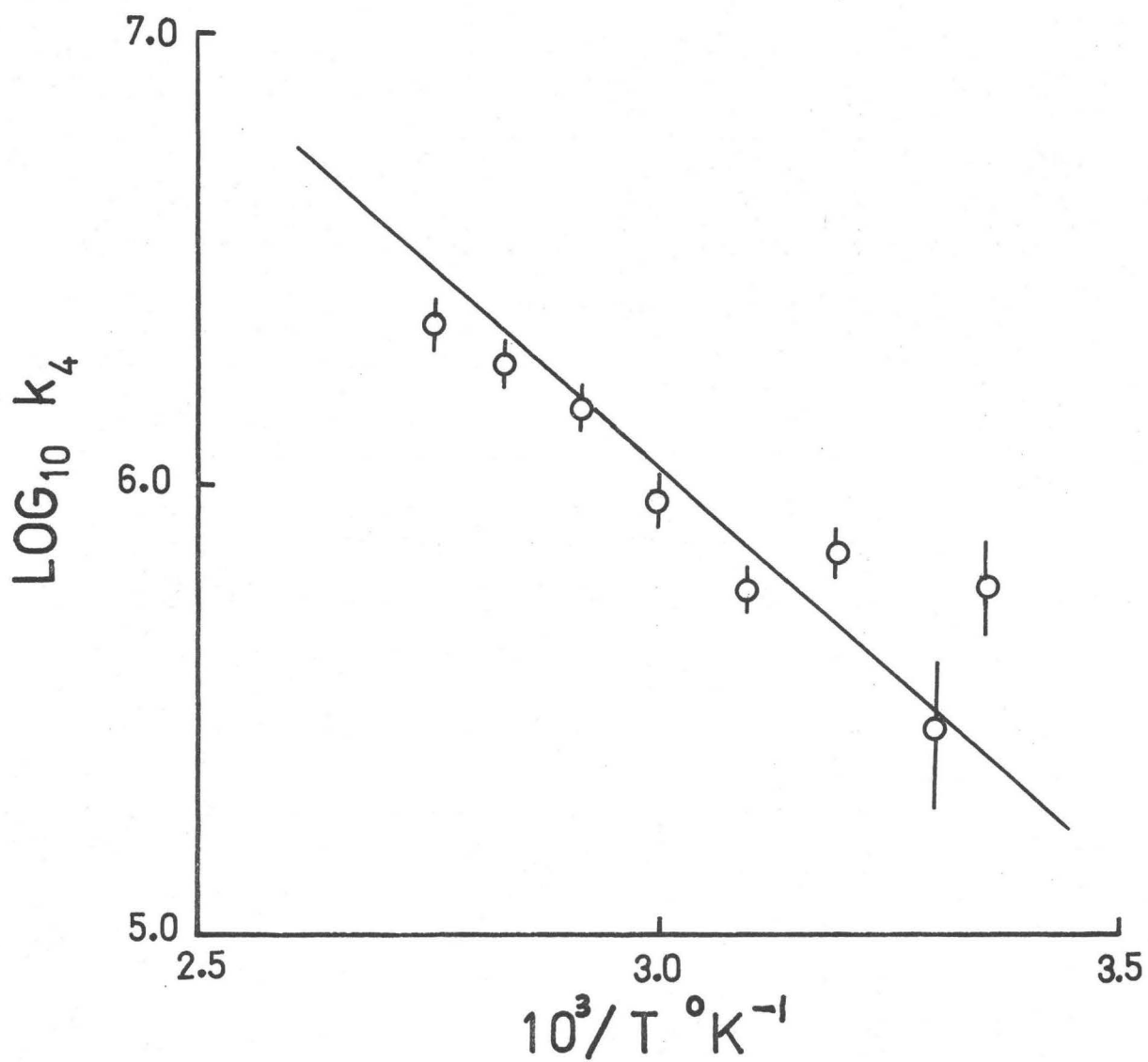
This demonstrates the expected form of the Stern-Volmer plots shown in Fig. 17 and Fig. 18.

The Second Order Removal Process

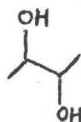
To examine the nature of the second order removal process [4], a plot of $\log k_4$ vs $1000/T$ is shown in Fig. 21 at various temperatures. A weighted least squares fit of k_4 to the Arrhenius equation gave the pre-exponential factor as $9 \times 10^{10} \text{ M}^{-1}\text{s}^{-1}$ and the activation energy as $7.5 \text{ Kcal mole}^{-1}$. The value of the pre-exponential factor is larger than might be expected for the chemical reaction of a polyatomic molecule with an activation energy of $7.5 \text{ Kcal mole}^{-1}$. However, a lower value of the pre-exponential factor is possible. The values derived from Fig. 21 depend significantly on the precision of the data at lower temperatures. Unfortunately, in this region the precision of the derived values of k_4 decreases rapidly. This is due to the low value of the constant k_4 in this region and the limitation of the concentration range by the low vapour pressure of the diketone at the low temperatures. (The error bars shown in Fig. 21 are the standard deviations of the slopes derived from Fig. 17 and Fig. 18.)

No studies were made in this work of the decomposition products so the reaction [4] cannot be associated with product formation. However, interesting parallels can be drawn with other studies of aliphatic diketone systems. At 25°C the value of k_4 determined in this study is $3 \times 10^5 \text{ M}^{-1}\text{s}^{-1}$. This is close to the estimate by Turro (44) of $2 \times 10^5 \text{ M}^{-1}\text{s}^{-1}$, for pentanedione, in a solution phase study. The analogous rate constant for biacetyl in the gas phase was determined by Garabedian and Dows (86) as $7 \times 10^4 \text{ M}^{-1}\text{s}^{-1}$ at 25°C .

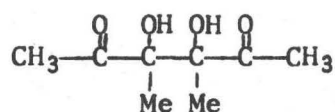
Fig. 21 Variation of the Bimolecular Quenching rate constant with temperature.



On the basis of this limited evidence, one can suggest that bimolecular quenching reactions are characteristic of aliphatic diketones. The type of reaction, however, is open to conjecture. Photolysis of biacetyl in 2-propanol (41) yields 2,3 dihydroxybutane (A) and 3,4 dihydroxy-3,4 dimethyl hexane 2:5 dione, (B), (86).



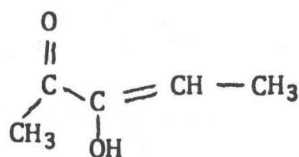
(A)



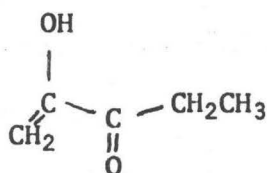
(B)

Both of these products have been associated with reactions of the T_1 state. They are typically photoreductions and can be correlated with electrophilic nature of the carbonyl oxygen atom in the T_1 state resulting in hydrogen atom abstraction. Whether these are present in the gas phase photolysis is open to question (87).

An interesting aspect of the photolyses of α -diketones is the occurrence of photoenolization. This has been suggested for biacetyl (33) and reported for 1-phenyl-1,2-alkanediones (88). While interference from photolysis has been shown to be unimportant in this study of pentanedione, the presence of semi-enol species could explain the bimolecular quenching observed in this case. The important provision is that production of the semi-enol species should be a "dark" thermally induced process. Such an enol, (C) or (D), might be expected to have a low-lying

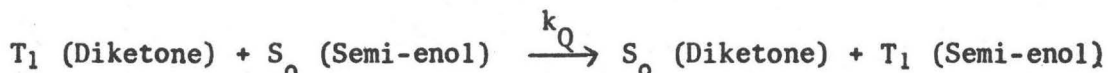


(C)



(D)

triplet π^* energy level (33). Energy transfer would then be efficient between the triplet diketone and the ground state semi-enol according to the equation,



Although keto-enol equilibria of cyclic α -diketones have been studied in solution (89), no experiments have been carried out in the gas phase. However, it is known that the attainment of the keto-enol equilibrium in α -diketones is promoted by glass surfaces (90,91). The uncatalysed thermal enolization of the diketone would require a symmetry forbidden suprafacial (1,3) sigmatropic shift according to Woodward-Hoffmann nomenclature (93), and, therefore, in the gas phase would be of low efficiency compared to the surface catalysed reaction.

The First Order Removal Processes

According to the steady state treatment of the mechanism shown above, the intercepts on Fig. 17 and Fig. 18 are $k_1 + k_2 + k_3$ at the appropriate temperatures. It is expected that the temperature dependence of k_1 will be small (93), as the transition will be symmetry allowed under the C_s point group for pentanedione. Similarly, the intersystem crossing rate constant k_2 will be expected to have a small temperature dependence over the range used in this study. Although the temperature dependence of intersystem crossing rate constants has not been studied extensively, there is theoretical and experimental evidence to substantiate this assumption. The theory of Siebrand (94) suggests a very

small temperature effect on the intersystem crossing rate constants in molecules with large energy gaps between states. Similarly, the theory of Hochstrasser and Jortner (95,95) predicts that the variation of k_2 will be small in this case. Experimentally the work of Jones and Siegel (97) on aromatic compounds in a polymethacrylate matrix has shown little variation in $k_{isc_{T_1 \rightarrow S_0}}$, and the research of Kutschke and co-workers (98), on the triplet state of hexafluoroacetone in the gas phase has shown that in that system a temperature independent $k_{isc_{T_1 \rightarrow S_0}}$ can explain the experimental data.

This leaves only the rate constant k_3 as a function of temperature. The mechanism thus requires that a plot of the logarithm of the intercepts of the lines in Fig. 17 and Fig. 18 versus the reciprocal of the temperature should be non-linear. This is demonstrated in Fig. 22. The intercepts of Fig. 17 and Fig. 18 were fitted using a weighted least-squares technique to the form,

$$\text{Intercept} = \tau_0^{-1} = a + b \cdot \exp(-c/Rt)$$

where "a" is the sum of the rate constants k_1 and k_2 and "b" and "c" are the pre-exponential factor and activation energy for the rate constant k_3 . The results using this method are:

$$k_1 + k_2 = 1.40 \times 10^3 \text{ s}^{-1}$$

$$k_3 = 1.0 \times 10^{11} \exp(-11,000/RT) \text{ s}^{-1}$$

Explicit values of k_1 and k_2 can be obtained using the quantum yield data in Chapter 4. The quantum yield of phosphorescence, ϕ_p , is

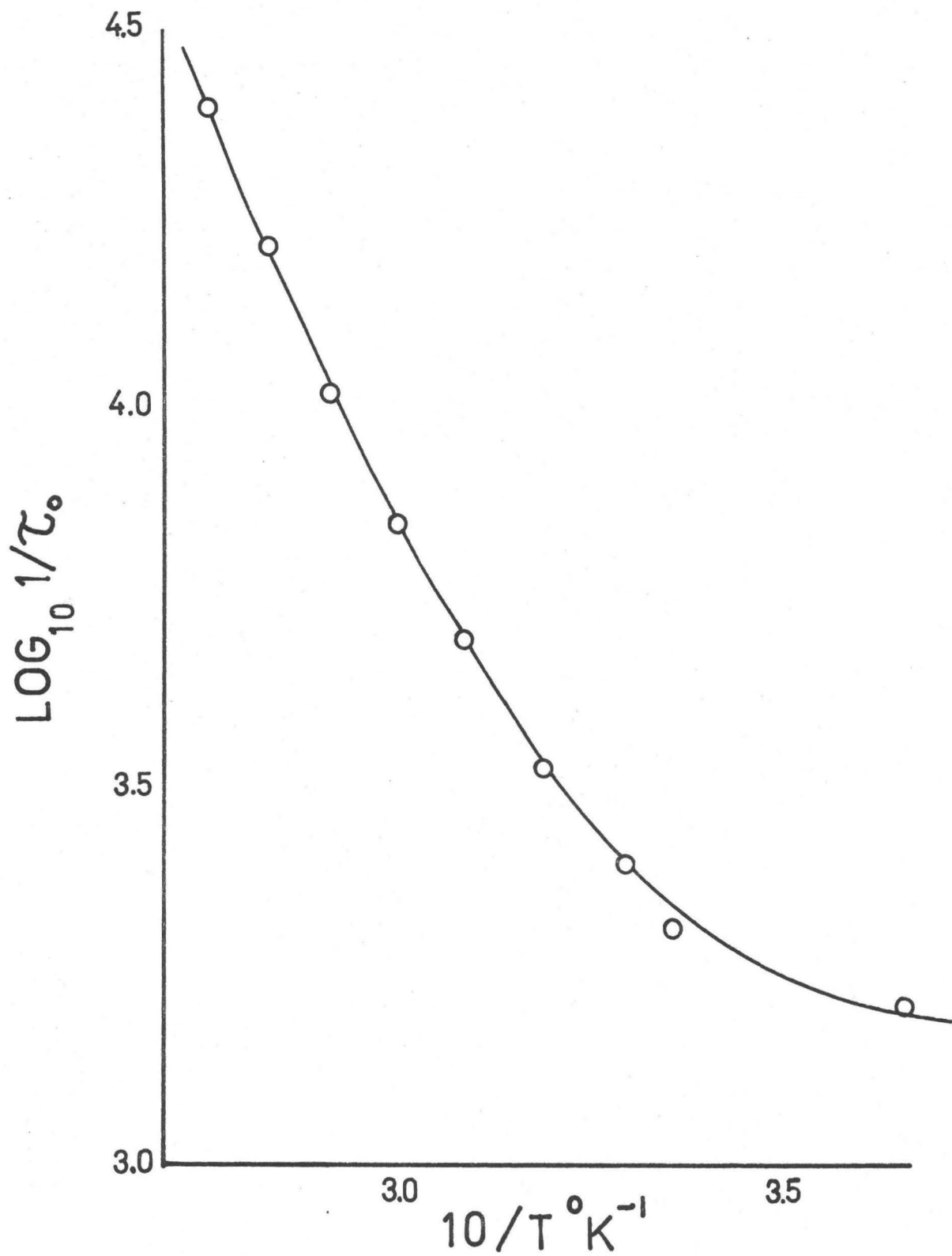


Fig. 22 Showing the non-linear behaviour of $\log 1/\tau_0$ with $1000/T$.

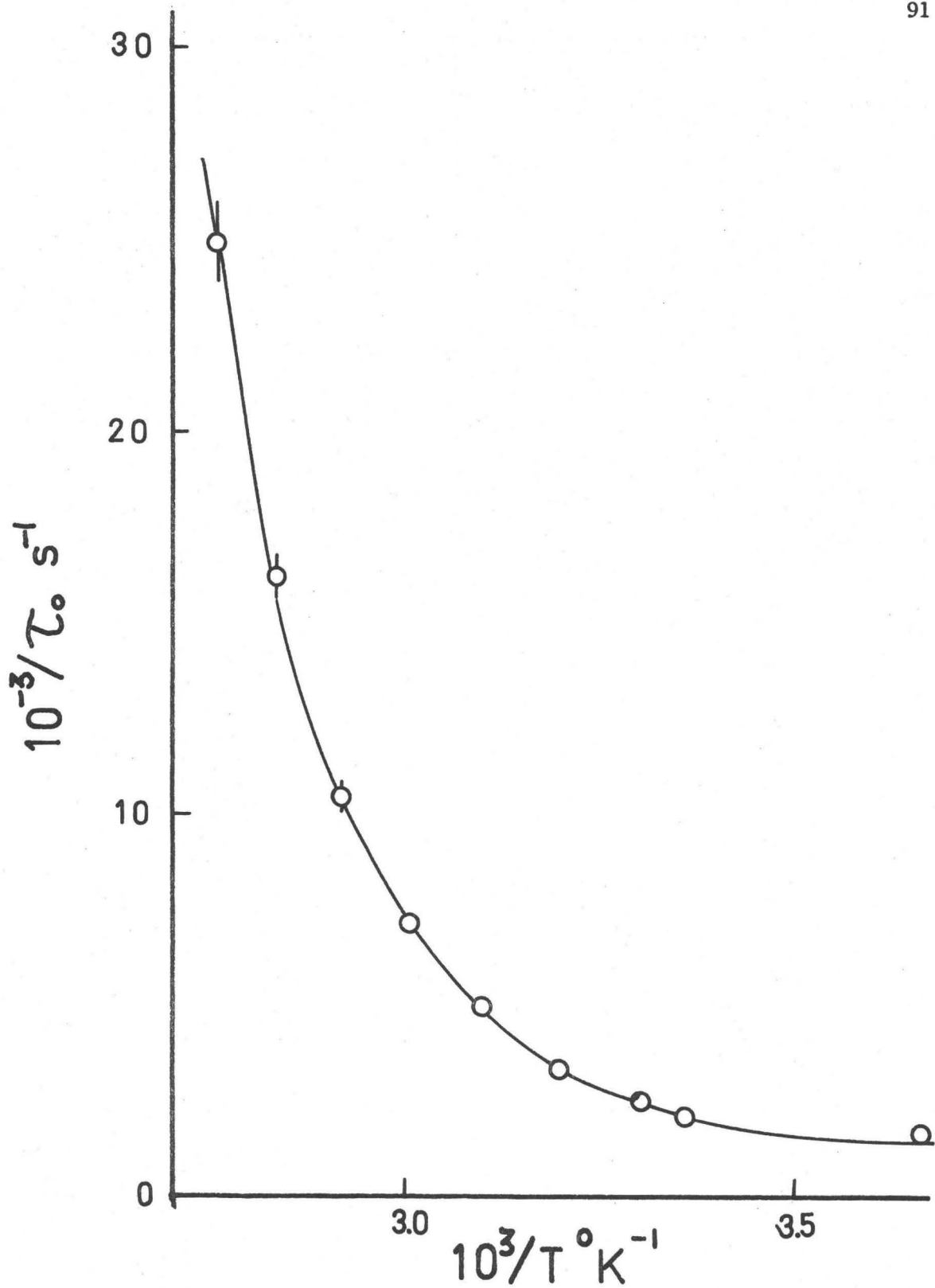


Fig. 23 Showing the asymptotic variation of $1/\tau_0$ with $1000/T$.

given by,

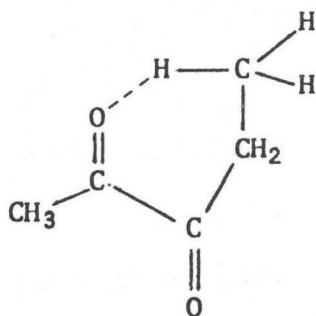
$$\phi_p = \phi_{T_1} \tau_p k_1$$

where τ_p is the phosphorescent lifetime and ϕ_{T_1} is the quantum yield of triplet. It has been shown that the quantum yield of triplet pentanedione for 436 nm is high (0.98) in solution (43) and the behaviour of biacetyl (25,29) suggests that the yield in the gas phase will also be high. If ϕ_{T_1} is assumed to be unity, then substitution into the equation gives $k_1 = 47 \text{ s}^{-1}$ and $k_2 = 1.3 \times 10^3 \text{ s}^{-1}$.

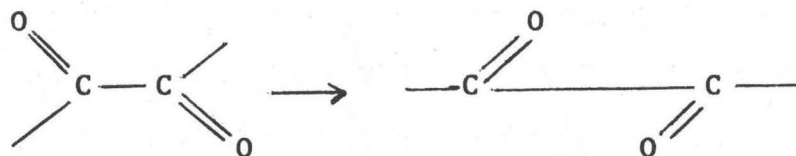
These values can be compared with analogous constants known for biacetyl in the gas phase. From the phosphorescence quantum yield determined by Kutschke and Gandini (30) and the triplet lifetime data of Kaskan and Duncan (31), $k_1 = 100 \text{ s}^{-1}$ and $k_2 = 460 \text{ s}^{-1}$ for biacetyl. This suggests that the effect of substituting a methyl group for a hydrogen atom in aliphatic acyclic α -diketones is to increase the rate constant for intersystem crossing from T_1 to S_0 . This is opposite to the effect observed in aliphatic acyclic monoketones at low temperature in a matrix (99). In the case of monoketones, the effect was correlated with the importance of α C-H modes in the intersystem crossing process (100). In monoketones, the geometry of the triplet state is suspected to be non-planar (103). The magnitude of the intersystem crossing rate constant will reflect the magnitude of matrix elements coupling this out of plane species with the planar ground state. Substitution onto the α -carbon atoms will increase steric interaction and could affect the magnitude of the matrix elements so as to produce the observed effect.

In the case of α -diketones, the excited states are probably planar (50). However, the other geometry changes are not known and, therefore, there are no clues to the potentially important normal modes which might promote the radiationless processes to the ground state. The effect of deuteration in biacetyl is to increase the phosphorescent lifetime by $\sim 25\%$ in benzene solution at 25°C (102). This increase has been attributed to a reduction in the intersystem crossing constant $T_1 \rightarrow S_0$. This suggests that the $\alpha\text{C-H}$ modes are involved in this process. However, no drastic effect is observed with perfluorination (103), (τ_{phos} for perfluorobiacetyl = 1.9×10^{-3} sec. at 25°C compared to τ_{phos} for biacetyl = 1.80×10^{-3} sec. at 25°C (31)). This tends to argue against the importance of C-H modes or of an inertial effect of heavy atom substitution on the bending modes in the molecule.

Comparing the structures of pentanedione and biacetyl, substitution of a methyl group apart from reducing the number of C-H mode, α to the diketone group, introduces a potentially important intramolecular effect. This is an interaction between the carbonyl group and a hydrogen atom on the terminal carbon atom.



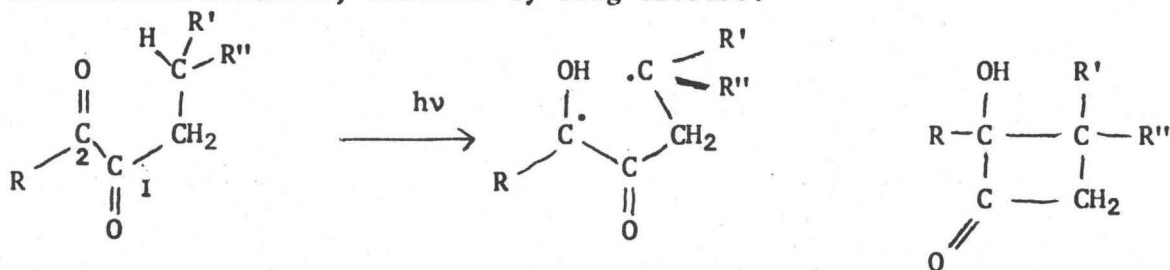
For the time being, emphasis will be placed on the photophysical repercussions of this interaction. The presence of the hydrogen atom close to the carbonyl group in the triplet excited state could allow the bending and stretching modes of the carbonyl system to couple with the C-H stretching and bending modes of the γ -hydrogen atom. There is a suggestion (56) that the excited states of glyoxal could have the oxygen atoms shifted in the manner shown below. This can be expected to be accomplished by a lengthening of the C-O bond length because of the promotion of an electron to a π^* orbital which has a node between the C and O atoms.



If this is the case, then not only would interaction between carbonyl and γ -H be significant, but the carbonyl bending mode would be expected to be important in promoting the radiationless transition to the ground state. The substituent effect in pentanedione can then be rationalized, if the radiationless process $T_1 \rightarrow S_0$ in diketones involves carbonyl bending modes and their interactions with other C-H modes in the molecule, in particular, γ C-H modes in pentanedione.

The nature of the reaction k_3 is suggested by the work of Urrey and Trecker (41,42). These workers showed that long wavelength photolysis of aliphatic diketones containing hydrogen atoms attached to a γ -carbon atom resulted in 2-hydroxy-cyclobutanone formation. The mechanism, involving the triplet diketone, suggested that intramolecular hydrogen atom

abstraction occurred, followed by ring closure.

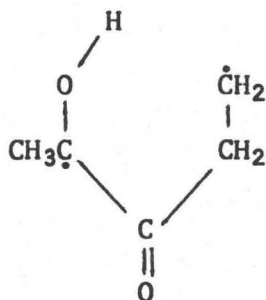


In this way, the transition state for abstraction would consist of a relatively strain-free six-membered ring. This geometry was aided by the multiple bond character of the 1-2 carbon bond, in the excited state. These studies have been extended by Turro (44), who determined the quantum yield of 2-methyl, 2-hydroxycyclobutanone formation from 2,3-pentanedione in benzene solution at 25°C as 0.054.

The magnitude of the Arrhenius parameters of k_3 are consistent with an intramolecular hydrogen atom abstraction involving a six-membered transition state (104). The low value of the A-factor compared to kT/h can be associated with a "tight" transition state in which the two internal rotations of the methylene and terminal methyl group have been restrained into torsional modes of the cyclic structure. The value of the activation energy (11.0 Kcal) is within the range found for hydrogen atom abstraction by an organic radical from an organic molecule (104). As knowledge of the Arrhenius parameters of excited carbonyl molecules reactions is sparse, comparisons cannot be made directly with other cases.

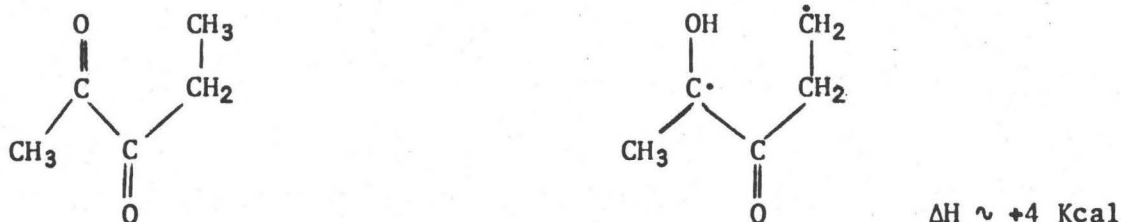
A possible analogous situation is the pronounced temperature effect noted for the photolysis of phenyl-glyoxalates in alcoholic solution (105). At room temperature, the reaction is mainly intermolecular photoreduction. At 80°C intramolecular photoreduction predominates

The stability of the triplet diketone towards the intramolecular H atom abstraction ($k_{\text{intramol}} \sim 10^{3.5}$ around room temperature), relative to the triplet monoketone ($k_{\text{intramol}} \sim 10^9 \text{s}^{-1}$ (106)) initially surprising, One might expect that in the diketone the electron withdrawing effect of the adjacent carbonyl group would enhance the reactivity of the $n\pi^*$ state (111). Also, the intermediate biradical, shown below,

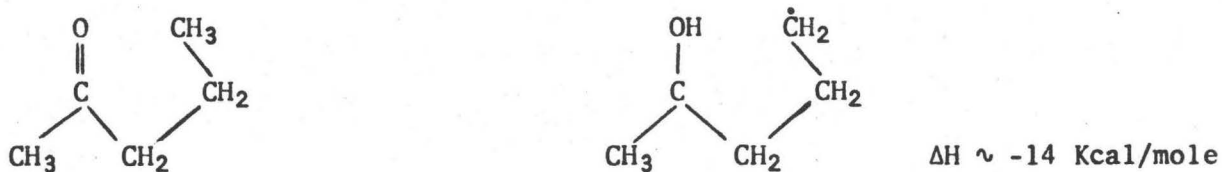


is enolic and, therefore, resonance stabilised (112). However, the activation energies of the two processes appears to be the limiting feature. The value determined in this study, of 11.0 Kcal for the reaction of the diketone, can be compared with the low values, ~ 3 or 4 Kcal, for the reactions of alkoxy radicals (113). The indication (106) is that alkoxy radicals are very similar to triplet ketone molecules in their absolute rates and selectivity. Therefore, the activation energies for intramolecular abstraction reactions of monoketones are probably also low. This can be inferred from the magnitude of the rate constants at room temperature for monoketone intramolecular abstractions which are $\sim 10^{8,9} \text{s}^{-1}$. If it is assumed that the pre-exponential factor deduced for pentanedione can be applied, then the activation energy is ~ 1.5 Kcal for the monoketone case.

The difference in the activation energies of the intramolecular H-atom abstractions for monoketones and diketones is predicted to some extent by consideration of the thermodynamic properties. Using the group thermodynamic properties given by Benson (104), the conversion of triplet pentanedione $E_T \sim 55$ Kcal mole⁻¹ to the corresponding biradical is estimated to be endothermic by approximately 4 Kcal mole⁻¹.



Whereas, the conversion of triplet 2-pentanone (114) ($E_T = 78$ Kcal/mole) to its biradical is exothermic by approximately 14 Kcal.



The difference in the ΔH values can be mainly ascribed to the differences in the triplet energies of the molecules. Therefore, this treatment predicts that the activation energy for intramolecular abstraction in the diketone case is at least 4 Kcal mole⁻¹.

Effect of Light Intensity

The effect of light intensity on the triplet lifetime of pentanedione in the gas phase at 30°C and 6.8×10^{-4} M is shown in Fig. 23.

The variation is within the systematic error of the experiment and it can be concluded that the phosphorescent lifetime is independent of light intensity using the light source described in Chapter 2. This experiment was carried out as a preliminary experiment to determine the feasibility of the lifetime studies discussed above. It was prompted by the observation of Kaskan and Duncan (31) that the phosphorescent lifetime of biacetyl depended on the light intensity in their experiments. This observation was rationalized later by Noyes et al (26,27) who showed that a process for the removal of triplet biacetyl molecules involved interaction between two triplet species to give decomposition,



The lack of any effect in pentanedione may not be due to any intrinsic difference in its behaviour relative to biacetyl, but rather the comparatively low light intensity used in this study together with a shorter lifetime for the triplet state.

Effect of Added Gas

The experiments carried out using SF₆ and C₂F₆ as added gases over a range of temperatures and pressures indicate that the triplet lifetime is unaffected by the total pressure of the system. These results are significant for several reasons:

- (1) These experiments demonstrate that the behaviour of the pentanedione does not include a unimolecular decomposition process in its pressure fall-off region. The presence of one unimolecular process has already been demonstrated by the proposed intramolecular

hydrogen abstraction reaction. This reaction is in its 'high-pressure limit' even at the lowest experimental pressures used (~ 1 torr) and, therefore, in the language of the RRK unimolecular reaction rate theory (118) must involve a large number of degrees of freedom. However, a unimolecular reaction involving a smaller number of degrees of freedom might show the characteristic reduction of the unimolecular rate coefficient within an accessible pressure region. This has been proposed (119) to explain the behaviour of triplet acetone in the gas phase. The variation of the reciprocal of the phosphorescent lifetime of acetone with the pressure has distinct curvature (31). This is attributed to a thermal decomposition of the triplet acetone in its fall-off region.

Triplet biacetyl has been shown to undergo a unimolecular decomposition in the gas phase with an activation energy ~ 15 Kcal mole⁻¹. The rate constants of the system are such that the unimolecular rate coefficient drops to one-half its high pressure value at a pressure of about 12 torr. The activation energy indicates that unimolecular decomposition is an important mode of disappearance only at elevated temperatures, i.e. greater than 70°C.

The behaviour of pentanedione in not showing any signs of undergoing a thermal dissociation analogous to biacetyl can be rationalised by considering the shorter lifetime of the triplet pentanedione species. This makes detection of the effect more

difficult; even at elevated temperatures an increased contribution from the thermal dissociation would be swamped by the reduced lifetime of the triplet due to competing unimolecular and bimolecular reactions.

- (2) It would appear that an experiment of this kind would be useful in diagnosing the presence of E-type delayed fluorescence (73). This type of behaviour, in which a molecule in the T_1 state is thermally activated to the S_1 state, might occur in pentanedione, where the $S_1 \rightarrow T_1$ gap is $\sim 8 \text{ Kcal mole}^{-1}$. One might expect that, as this activation is most likely to come from collisions in the gas phase, the variation in the lifetime of the triplet would reflect this removal process, i.e. simple Stern-Volmer quenching might be expected. This is not so, as the simple kinetic model given in Appendix C demonstrates the reason for this can be associated with high value of $k_{isc_{S_1 \rightarrow T_1}}$ which returns any thermally activated molecules in a time scale which is short compared to the lifetime of the T_1 state.

Triplet Lifetime at 77°K

The results of the experiments carried out at 77°K indicate that the phosphorescent lifetime of pentanedione, varies markedly with phase (Table 4). At this low temperature the rates of chemical processes removing the triplet molecule will be slow and it is reasonable to assume that the triplet lifetime measured under these conditions represents control by the photophysical processes of emission and radiationless dissipation

of electronic excitation energy. From measurements of the phosphorescence yield and phosphorescent lifetime of biacetyl in different phases at different temperatures, it has been concluded (121) that the spontaneous emission probability for phosphorescence of biacetyl is independent of phase and temperature. Therefore, the observed variation in the triplet lifetime of pentanedione with phase at 77°K probably represents variation in the photophysical radiationless rate constant.

In Chapter 1 the radiationless processes of the electronically excited states were considered in terms of the matrix coupling elements and the density of states in the adjacent manifold. In the gas phase for the triplet level of a large molecule the adjacent manifold will correspond to the ground electronic state. However, in the condensed phase at low temperatures, there will be additional levels available which correspond to phonon levels of the host matrix. It is, therefore, not unexpected that the radiationless processes removing the triplet state will be modified (138). The sensitivity of the emission properties of the triplet state to effects of host matrix and temperature have been recognised (138) and conclusions which can be drawn from the experiments with pentanedione at 77°K are limited.

It is significant that the decay of the emission in different phases was exponential as this implies that a single species was responsible in each case. The difference in the lifetimes between the two phases of pentanedione also implies that in the crystalline phase the interaction of the excited triplet molecule with the matrix is such as to produce less efficient processes for its removal. The observation that the lifetime in the pure crystalline phase is longer than that observed in other phases, is not unusual and has been observed in several carbonyl compounds (139,140).

CHAPTER 6

SELF-QUENCHING OF Q_f AND Q_p FOR 436 NM EXCITATION

Measurement of Q_f and Q_p at various pressures of diketone will reveal the presence of self-quenching reactions within the singlet and triplet manifolds. If excitation is at 436 nm, where vibrational deactivation in the singlet manifold is expected to be efficient this variation can be interpreted directly to give values of quenching constants.

Results

The apparatus used in this study has already been described in Chapter 2. Experiments were carried out at a fixed temperature. The emission signals at 460 nm and 528 nm together with the transmitted light signal were measured for various pressures of diketone from a calibrated volume. The data was treated to correct for geometry, inner filter effects at 466 nm, reflection losses, and overlap of fluorescence and phosphorescence. The values of Q_f and Q_p at various pressures at 50°, 71°, 90.5°C are given in Table 5. The variations in Q_p are plotted in the form Q_p°/Q_p , where Q_p° is the yield at zero pressure, versus pressure at various temperatures in Fig. 24.

Search for delayed fluorescence

Experiments were carried out to determine if there was a process

Fig. 24 Variation of Q_p^0/Q_p with concentration of pentanedione at 50, 70, and 90°C; $\lambda_{ex} = 436 \text{ nm}$.

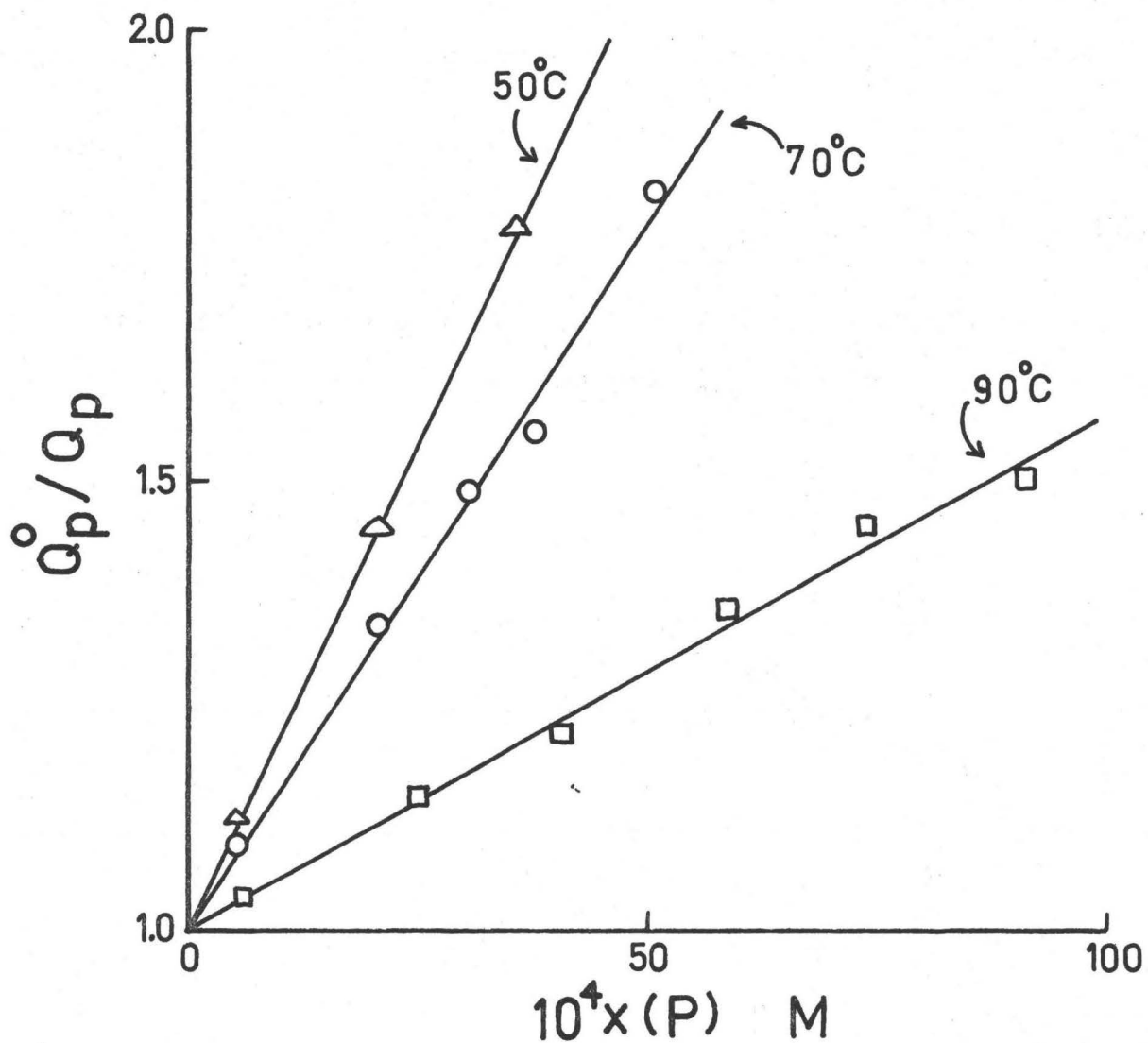


TABLE 5

At 50°C		At 70°C		At 90°C	
CONC $\times 10^{-4}$ M	Q _p ARB UNITS	CONC $\times 10^{-4}$ M	Q _p ARB UNITS	CONC $\times 10^{-4}$ M	Q _p ARB UNITS
4.8	1410	4.9	702	6.02	277
		20.8	575	25.6	230
20.3	1120	29.3	518	42.0	211
				58.6	190
35.5	1000	38.3	498	75.2	178
		51.9	422	91.7	171

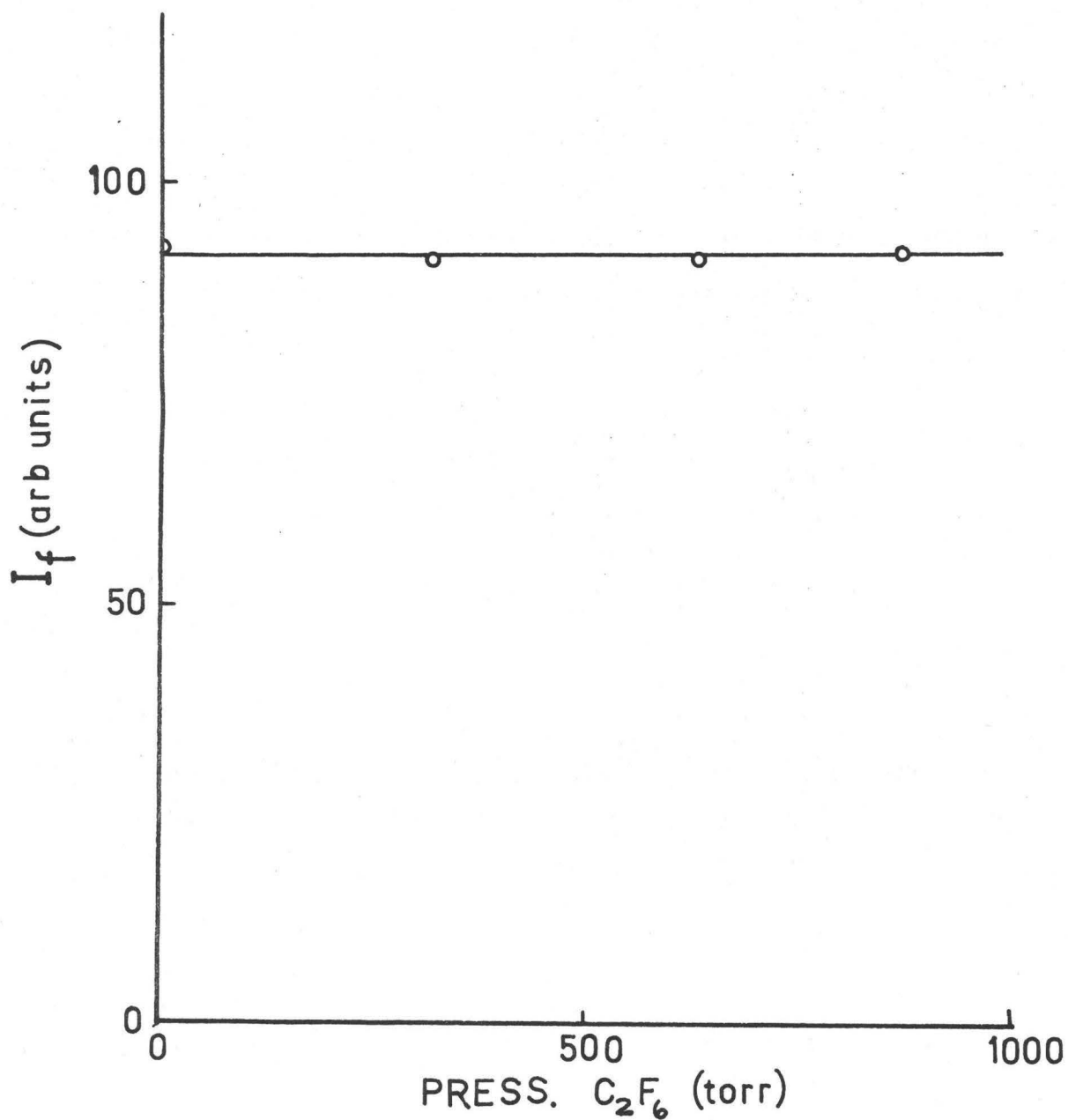
At 50°C		At 70°C		At 90°C	
CONC $\times 10^{-4}$ M	Q _f ARB UNITS	CONC $\times 10^{-4}$ M	Q _f ARB UNITS	CONC $\times 10^{-4}$ M	Q _f ARB UNITS
3.3	356	20.8	334	25.6	295
13.9	350	29.3	323	42.0	301
21.5	345	38.3	332	58.6	293
43.3	342	51.9	320	75.2	282
				91.7	287

operating in the photolysis of pentanedione such that triplet molecules could be excited to a vibrational level approximately isoenergetic with the singlet level and intersystem cross to the singlet manifold. This process would give rise to an anomalously high fluorescence yield, the enhancement has been termed E-type delayed fluorescence by Parker (73). This experiment was carried out at 40°C using a pentanedione sample pressure of 26.4 torr which allowed accurate measurement of the fluorescence intensity of the signals at 460 nm and 528 nm corrected as discussed in the earlier definition of Q_f and Q_p in Chapter 2. Inert gas, perfluoroethane, was added from a calibrated volume and the emission intensities were measured. The pressure of perfluoroethane varied from 0 to 870 torr. The results of this experiment are shown in Fig. 25.

Discussion

The absorption spectrum of pentanedione has not been studied in detail but its similarity with the spectrum of biacetyl suggests that the 0-0 transitions are probably at about the same energy. If this is so then excitation at 436 nm might be expected to form the singlet state approximately 3 Kcals above the 0-0 level. It is unlikely that this will represent sufficient energy to allow the spontaneous dissociation of the species and its likely fate is to be deactivated by collisions to the vibrationally equilibrated level of the singlet manifold. The quantum yield of the vibrationally equilibrated singlet level is then probably unity at this wavelength.

Fig. 25 Variation of fluorescence intensity with pressure of added C_2F_6 ; pentanedione pressure is 26.4 torr, temperature is $40^\circ C$ $\lambda_{ex} = 436$ nm.



It can be seen by inspection of Table 5, that the value of the relative quantum yield of fluorescence, Q_f , is effectively independent of the pressure of the pentanedione for 436 nm excitation at 50, 70 and 90°C. This confirms the assumption regarding the importance of vibrational equilibration and also indicates that there is no bimolecular process involving excited singlet and ground state molecules which can be detected for the concentration range 0-0.01 M using this technique. It should be remembered that for a simple Stern-Volmer quenching system having the form,

$$\frac{Q_f^\circ}{Q_f} = 1 + k_Q \tau_0 [\text{Quencher}]$$

the magnitude of the term $k_Q \tau_0 [\text{Quencher}]$ must be of the order of unity before quenching can be detected. As the lifetime of the excited singlet state is suspected to be short, $\sim 5 \times 10^{-9}$ s, then only quenching processes having a rate constant greater than $\sim 3 \times 10^9 \text{ M}^{-1} \text{ s}^{-1}$ can be detected.

Unfortunately, the behaviour of pentanedione with respect to self-quenching of the fluorescence cannot be compared directly with that of biacetyl. It seems that the variation of the fluorescence yield of biacetyl at 436 nm has not been studied at a variety of temperatures and pressures. However, from the results of photochemical decomposition experiments carried out under these conditions, the behaviour can also be described without inclusion of a bimolecular self-quenching step for the vibrationally equilibrated level of the singlet with ground state species (27).

The variation of Q_p for pentanedione with pressure of pentanedione shown in Fig. 24 is particularly interesting. That the variation follows a simple Stern-Volmer form indicates the self-quenching reaction is of a simple bimolecular form involving the vibrationally equilibrated triplet molecule and a molecule of pentanedione in the ground state. This is exactly the conclusion reached in the phosphorescence lifetime study described in Chapter 5. Furthermore, the bimolecular quenching rate constants derived from Fig. 24 can be compared with those found from the lifetime study. If the processes removing the emitting level of the triplet are:

1. ${}^3P \rightarrow$ phosphorescence
2. ${}^3P \rightarrow$ radiationless removal
3. ${}^3P + P \rightarrow$ removal

where 3P is the triplet pentanedione and P is the ground state pentanedione, then it can be easily shown that,

$$\frac{\phi_p^0}{\phi_p} = 1 + k_3\tau_0 [P]$$

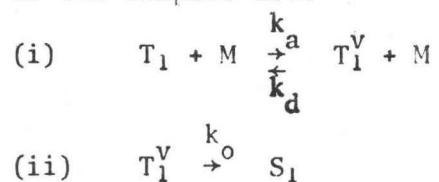
In this expression, τ_0 , is the phosphorescence lifetime of the pentanedione extrapolated to zero pressure. The variation of τ_0 with temperature is already known and in conjunction with the values of the slopes in Fig. 24 allows k_3 in the above mechanism to be calculated. The values of the bimolecular self-quenching rate constants derived from the Q_p measurements are compared with those derived from the phosphorescence lifetime measurements in Table 6. It can be seen that the agreement is good and serves as evidence for the internally consistent nature of the proposed quenching reaction for the emitting level of the triplet state.

TABLE 6. COMPARISONS OF TRIPLET SELF-QUENCHING
RATE CONSTANTS FROM τ_p AND Q_p EXPERIMENTS

Temp °C	k_Q from τ_p $M^{-1} s^{-1} p$	k_Q from Q_p $M^{-1} s^{-1} p$
50	5.3×10^5	7.5×10^5
70	1.5×10^6	2.5×10^6
90	2.5×10^6	2.0×10^6

The results of the experiment to detect the presence of E-type delayed fluorescence in the gas phase pentanedione system indicate that the intensity of fluorescence is independent of the pressure of added gas. The phenomenon of E-type delayed fluorescence which has been observed in rigid matrixes and fluid solution is associated with thermal excitation of the triplet state to the singlet state and has been detected in molecules characterised by small singlet-triplet splitting energy. This effect has been observed in a diketone, benzil (74) and has been suggested to occur in the gas phase biacetyl system (163). The experiment described above, was to see if this phenomenon could be detected in the gas phase in pentanedione.

The sequence of processes necessary for the successful excitation of the triplet are:



where M is any gas molecule and T_1^V is a vibrational level of the triplet with energy greater than or equal to that of the singlet. If it is assumed that the step (ii) is rate limiting and that the populations of T_1 and T_1^V obey the Boltzmann law then,

$$\text{Rate constant of (ii)} = k_c e^{-E_a/RT}$$

where $E_a \sim E_{T_1^V} - E_{T_1}$. In a detailed study of a delayed fluorescence system, eosin (162) in solution, it appears that $k_{isc_{T_1^V \rightarrow S}}$ is $k_{isc_{S_1 \rightarrow T_1^V}}$.

If this is the case in pentanedione, then the rate of activation to the S_1 manifold from the T_1 manifold will be given by,

$$\text{Rate constant of activation} \sim 10^8 e^{-9000/RT} \sim 50 \text{ s}^{-1}$$

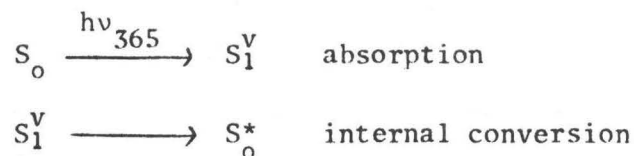
This process will, therefore, face strong competition from other radiationless processes removing the T_1 state and will be a minor pathway for dissipation of triplets in the system.

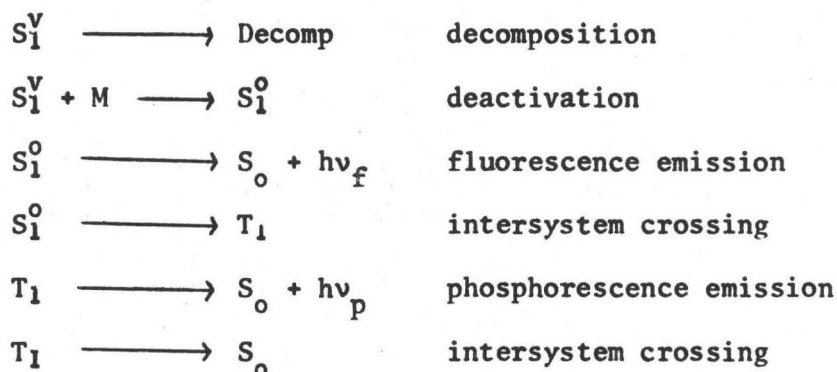
The lack of direct evidence for delayed fluorescence in pentanedione can be reconciled with the low magnitude of the reactivation process.

CHAPTER 7

VIBRATIONAL DEACTIVATION: PHOTOLYSIS AT 365 NM AT 90°C

In the experiments to determine the quantum yields of emission at various wavelengths described in **Chapter 3**, it was found that the yield at 365 nm depended on the pressure of the system. What is more, in the presence of a large amount of inert gas, the yields of fluorescence and phosphorescence were the same as found by excitation at longer wavelengths. This effect of enhancement of emission with total pressure is not unusual and has been observed in hexafluoroacetone (96) and pentafluoromonochloroacetone (123). In particular, the behaviour of biacetyl is similar and has been the object of much investigation (7,23,24,26,27,80) in the gas phase particularly by Noyes and coworkers who have correlated the phosphorescence emission and decomposition behaviour of this molecule. Their model of the photolysis system at 365 nm involves formation of the excited singlet species in a high vibrational level of the singlet manifold. The processes competing for this species are radiationless processes corresponding to fragmentation of the molecule, internal conversion to the S_0 manifold, and removal of vibrational energy through collisions within the S_1 manifold. The mechanism at low light intensities and temperatures below 70°C can be represented by,

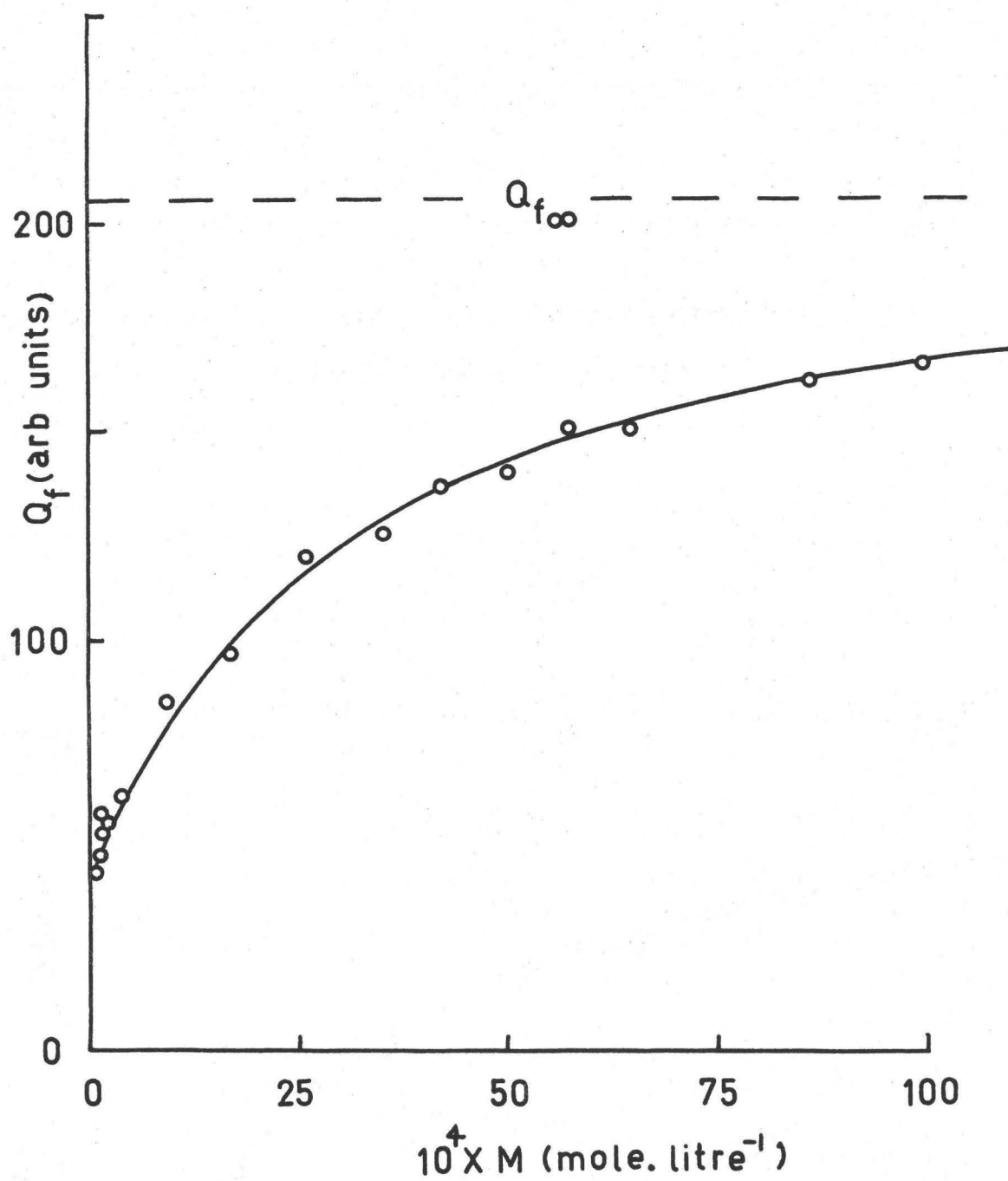




It can be seen from this mechanism that all the excess vibrational energy of the initially formed molecule is removed by one encounter in the gas phase. Furthermore, emission of fluorescence and intersystem crossing to the triplet manifold occur only from the vibrationally equilibrated (vibrationless at $T \sim 300^\circ\text{K}$) level of the excited singlet state. As the pressure is increased, the proportion of excited molecules successfully reaching this level increases and is marked by increased Q_f values.

It was decided to investigate collisional deactivation in electronically excited pentanedione using the relative quantum yield of emission technique. The apparatus has been described in Chapter 2. Pentanedione was used as its own vibrational quencher to avoid complications due to the relative efficiencies for removal of vibrational energy in the presence of foreign inert gas. The experiment was carried out at 90°C so that a considerable concentration range was available to the diketone. The pressure of diketone was varied from 1 to 200 torr. The relative quantum yields of fluorescence, Q_f , and phosphorescence, Q_p , were determined using the corrections described earlier in Chapter 2. The variations of these quantities with diketone pressure are shown in Fig. 26 and Fig. 27 and collected in Table 7. The value subscripted

Fig. 26 Variation of Q_f with concentration of pentanedione in the gas phase at 90°C , $\lambda_{\text{ex}} = 365 \text{ nm}$.



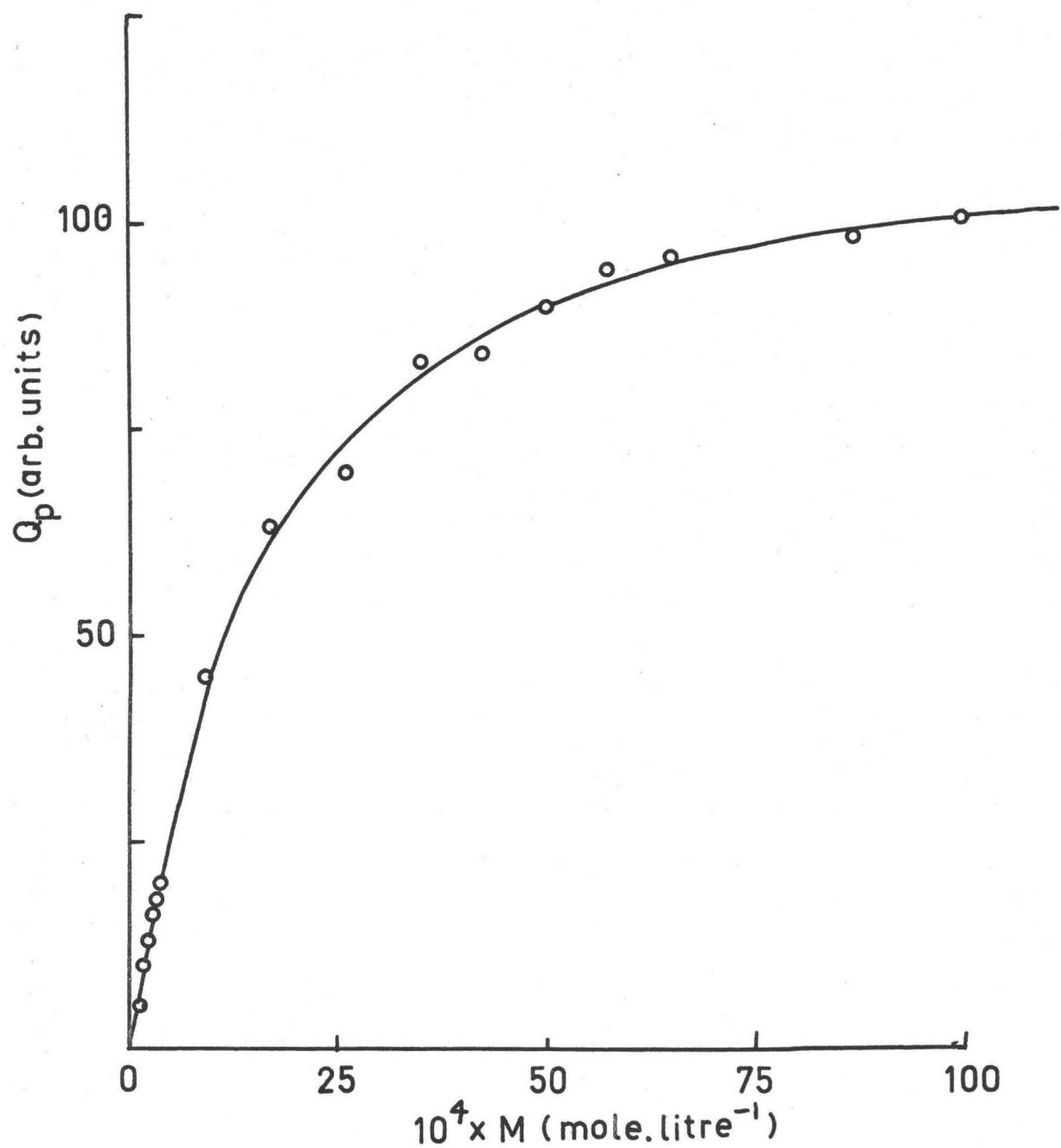


Fig. 27 Variation of Q_p with concentration of pentanedione in the gas phase at 90°C , $\lambda_{\text{ex}} = 365 \text{ nm}$.

TABLE 7. VARIATION OF Q_f , Q_p WITH CONCENTRATION OF PENTANEDIONE
AT 90°C

$10^4 \times (M)$ in M	Q_f arb Units	Q_p arb Units
0.43	41	~ 2
0.85	47	~ 4
1.36	52	7
1.87	57	9
2.39	55	12.0
2.90	58	16.0
3.41	59	16.7
3.92	61	18.5
9.3	84	40
17.0	96	63
26.0	119	70
35.1	125	83
42.3	136	84
50.2	140	90
57.3	151	94
64.9	150	96
86.3	162	98
99.7	166	101
∞	206	

• correspond to the quantities when ~ 1000 torr of methyl chloride was added to the sample at a pressure of 185 torr (1.0×10^{-2} M). Under these conditions of high pressure of added inert gas, vibrational deactivation in the singlet manifold is complete, such that all molecules excited at 365 nm successfully reach the thermally equilibrated vibrational level of the singlet manifold.

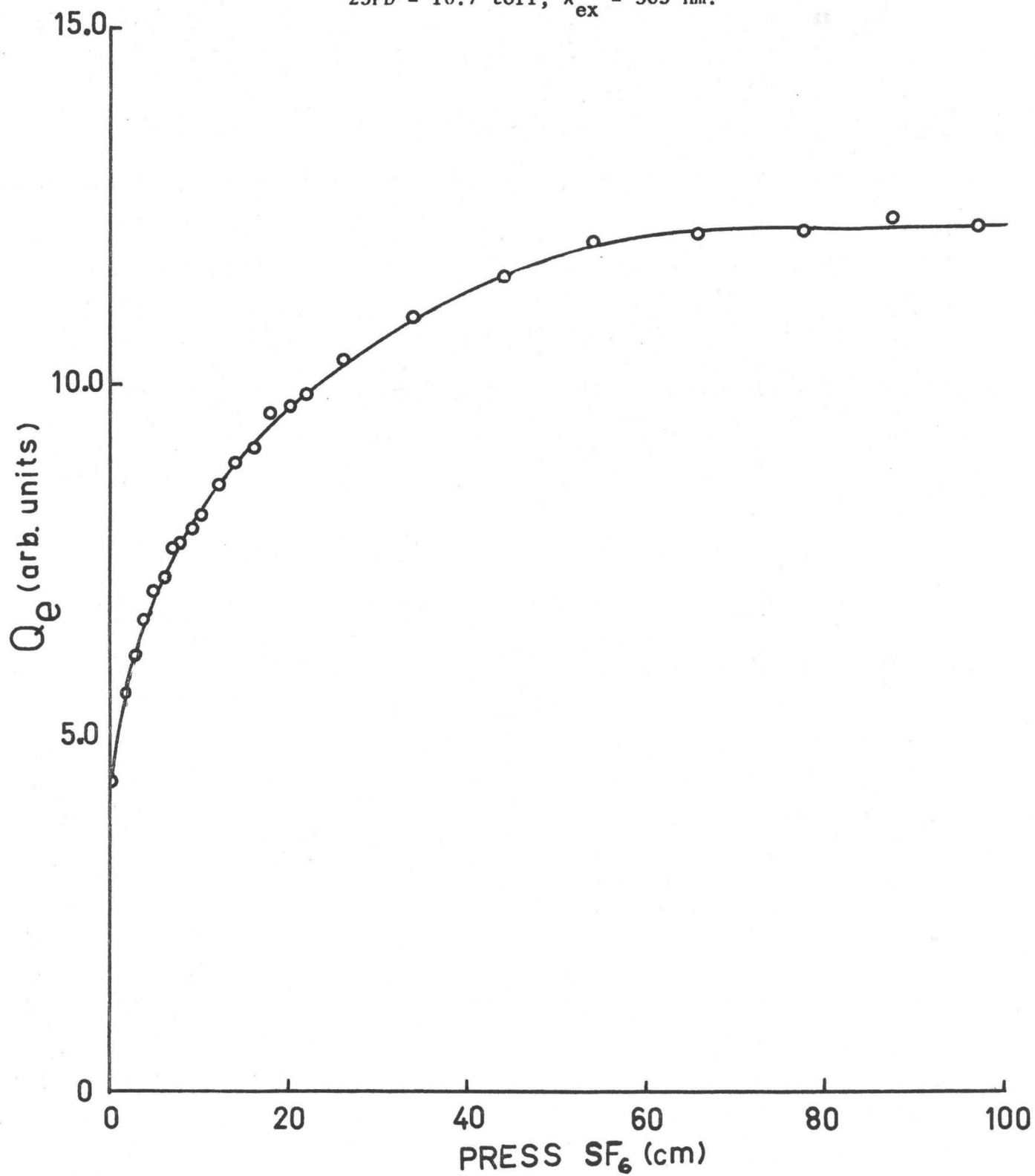
Due to the limited vapour pressure of pentanedione, photolysis at 365 nm at a lower temperature, 30°C , was carried out using a fixed pressure of pentanedione. Measured amounts of sulphur hexafluoride as inert gas were added from a calibrated volume. In this experiment relative quantum yields of total emission were measured using the same apparatus with the modification that a CS-372 filter covered the photomultiplier tube. As the experimentally determined ratio of $Q_f:Q_p$ was found to be ~ 0.05 under these conditions, the value of $Q_{\text{Total emission}}$ is equal to Q_p to a good level of approximation. The pressure of pentanedione was maintained at 10.7 torr throughout the experiment, while the pressure of sulphur hexafluoride was varied from 0 to 1000 torr. The results of this experiment are shown in Fig. 28.

Discussion

The general trend of the data for the experiment at 90°C is consistent with the notion of vibrational deactivation of the initially formed species in the S_1 manifold. This is demonstrated by the smooth increase of Q_f with pressure and the tendency towards a limiting value at high pressure. However, examination of Fig. 26 and Fig. 27 reveals

Fig. 28 Variation of total emission yield with pressure of SF₆ at 30°C,

23PD = 10.7 torr, λ_{ex} = 365 nm.



two striking features.

Firstly, it is found that the variation of Q_f with pressure cannot reasonably be extrapolated to the origin. This implies that at zero pressure, where there is no possibility of vibrational deactivation through collisions, fluorescence emission occurs. This is interpreted as being direct evidence for fluorescence emission from vibrationally excited levels of the singlet manifold.

Secondly, the variation of Q_p with pressure can be smoothly extrapolated to the origin which indicates that the formation of the emitting level of the triplet depends upon a collisional process. These features must be considered in the formulation of any mechanism to describe the system.

Fluorescence Enhancement Models

Attention was focussed initially on the behaviour within the excited singlet manifold. A scheme was devised which comprised the following steps:

Scheme A

1. $S_0^o \xrightarrow{I_{abs}} S_1^v$
 $S_1^v \longrightarrow h\nu_f$ fluorescence emission from vibrationally excited levels of S_1 .
2. $S_1^v \longrightarrow$ radiationless removal
3. $S_1^v + M \longrightarrow S_1^o + M$ vibrational deactivation via single collision.

4. $S_1^0 \longrightarrow hv_f$ fluorescence emission from vibrationally equilibrated level of S_1 .
5. $S_1^0 \longrightarrow T_1^V$ intersystem crossing from the equilibrated level of the S_1 manifold.

Application of the steady state approximation to this system gives,

$$\phi_f = \frac{k_1}{k_2 + k_3(M)} + \frac{k_4 k_3(M)}{k_5(k_2 + k_3(M))}$$

If it is assumed that $k_1 = k_4$ then,

$$\phi_f = \frac{k_1}{k_2 + k_3(M)} \left\{ 1 + \frac{k_3(M)}{k_5} \right\}$$

This expression may be rearranged in several ways to yield a functional dependence which can be tested using the acquired data.

One method is to recognise the limits of this function at high and low pressure.

$$\text{As } M \rightarrow 0, \phi_f \rightarrow \phi_{f_0} = k_1/k_2$$

$$\text{As } M \rightarrow \infty, \phi_f \rightarrow \phi_{f_\infty} = k_1/k_5$$

Inserting these limits give

$$\phi_f - \phi_{f_0} = \frac{k_1 k_3(M) (k_2 - k_5)}{k_2 k_5 (k_2 + k_3 M)}$$

$$\phi_{f_\infty} - \phi_f = \frac{k_1 (k_2 - k_5)}{k_5 (k_2 + k_3 M)}$$

which gives the dimensionless equation,

$$\frac{\phi_f - \phi_{f_0}}{\phi_{f_\infty} - \phi_f} = \frac{k_3}{k_2} (M) = \frac{Q_f - Q_{F_0}}{Q_{F_\infty} - Q_f}$$

The values of Q_f in Table 7 were used to calculate this function. The value of Q_{f_∞} was taken as the relative fluorescence yield of 185 torr pentanedione and ~ 1000 torr methyl chloride. The value of Q_{f_0} was obtained by smoothly extrapolating the experimental curve to zero pressure. A plot of the dimensionless equation above gave Fig. 29. It can be seen from this figure that the dependence is described well by a straight line passing through the origin. The fit is particularly good when it is remembered that the dimensionless quantity $(Q_f - Q_{f_0}) / (Q_{f_\infty} - Q_{f_0})$ contains three experimentally determined quantities and accumulates four times the uncertainty of one experimental determination of Q_f .

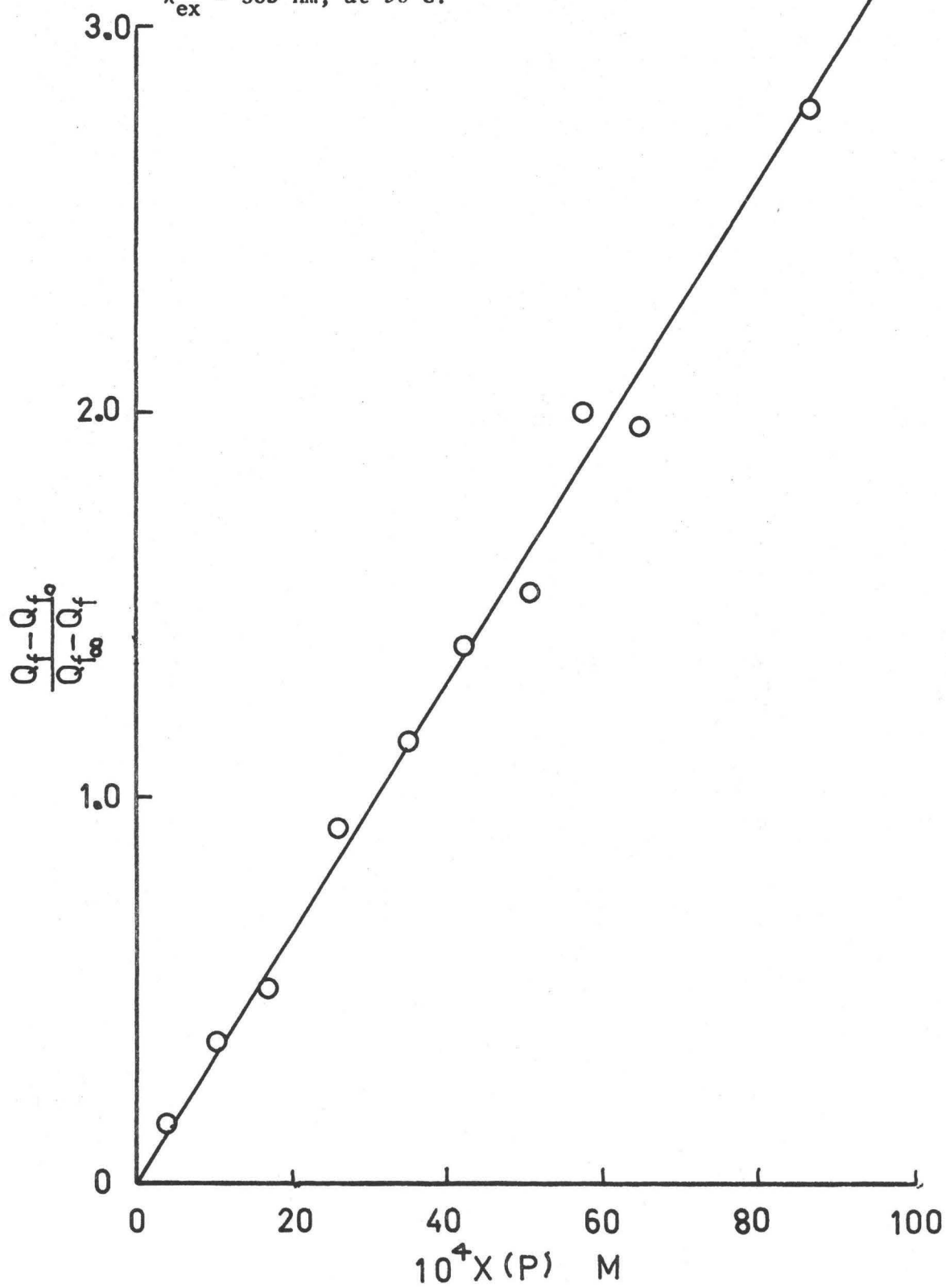
The conclusion from this test is that the fluorescence data fit a collisional deactivation model in which there are two emitting levels in the singlet manifold which are connected through a single strong collision. From the dimensionless equation above, the slope of the line in Fig. 29 is given by k_3/k_2 . This quantity was calculated as $330 \pm 20 \text{ M}^{-1}$.

From the value of k_3/k_2 , it is possible to estimate the collisional deactivation constant k_3 if the constant k_2 is known. The constant k_2 can be derived from the equation,

$$\frac{Q_{f_\infty}}{Q_{f_0}} = \frac{k_2}{k_5} = \frac{206}{47} = 4.4 \quad \text{i.e. } k_2 \sim 4.4 k_5$$

The constant k_5 has already been estimated in Chapter 4 as $\sim 2 \times 10^8 \text{ s}^{-1}$ at 24°C . If it is assumed that this constant does not vary with temperature (see Chapter 8) then,

Fig. 29 The dimensionless fluorescence function for

 $\lambda_{\text{ex}} = 365 \text{ nm}$, at 90°C .

$$k_2 \sim 4.4 \times 2 \times 10^8 = 8.8 \times 10^8 \text{ s}^{-1}$$

In conjunction with the value of k_3/k_2 , this allows the constant k_3 to be calculated as $\sim 2.9 \times 10^{11} \text{ M}^{-1}\text{s}^{-1}$. This value can be compared with the classical kinetic theory collisional frequency which was calculated using ethyl acetate as a model. This molecule was chosen because of the expected similarity in dimensions and because gas phase viscosity data was available (124).



Inserting the value of the viscosity of ethyl acetate at 100°C into the equation (125)

$$\eta = \frac{5}{16 \pi^{1/2}} \frac{(\text{MRT})^{1/2}}{N\sigma^2}$$

gives the collision diameter, σ , as 7.3 \AA .

The collision frequency was then calculated using the ideal gas equation formula (126),

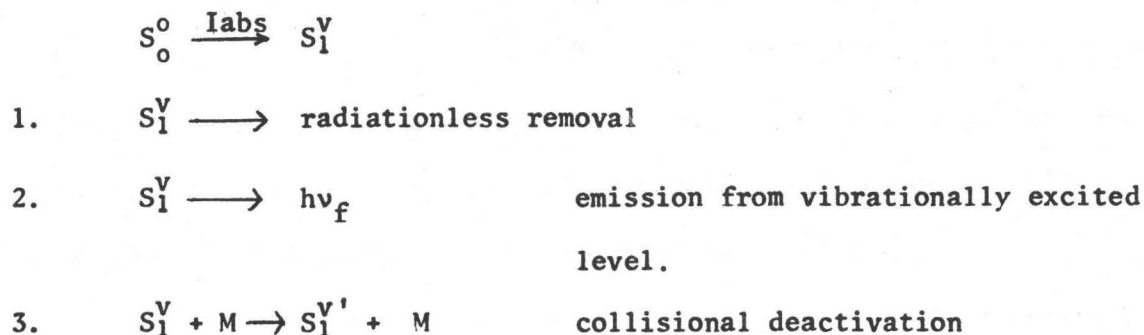
$$Z_{AA} = 2N\sigma^2 \left(\frac{\pi RT}{M} \right)^{1/2}$$

Z_{AA} was found to be $2.0 \times 10^{11} \text{ M}^{-1}\text{s}^{-1}$. This compares well with the derived value of k_3 and indicates that within the context of this mechanism, every collision is successful in producing complete collisional deactivation of the vibrationally excited singlet species.

The subject of collisional deactivation in the gas phase is a controversial issue at the present time. The main point of contention surrounds the removal of vibrational energy in collisions. Mechanisms for this process can involve one collision for equilibration, known as a strong collision theory, or can involve several collisions in which the excess energy is removed sequentially (weak collisions). Fluorescence emission is a particularly useful tool in these studies because the emission can be used as a monitor of the levels in the excited singlet manifold. Much work has been carried out to distinguish between the two categories of behaviour, particularly in the case of hexafluoroacetone (30,127). Kutschke (127) suggests that deactivation occurs by a weak collision mechanism in this compound. However, clear distinction depends upon the acquisition of accurate data, particularly at low pressures where experimental difficulties are increased.

It was decided to construct a mechanism for pentanedione involving more than two levels to discover in what way the fluorescence behaviour would be modified. This weak collision mechanism is shown below.

Scheme B



4. $S_1^{V1} \longrightarrow$ radiationless removal
5. $S_1^{V1} \longrightarrow h\nu_f$ emission from vibrationally excited level
6. $S_1^{V1} + M \rightarrow S_1^0 + M$ collisional deactivation
7. $S_1^0 \longrightarrow h\nu_f$ fluorescence emission from equilibrated level
8. $S_1^0 \longrightarrow T_1$ intersystem crossing to triplet manifold

This situation is considerably more complicated than Scheme A, but can be treated if certain simplifying assumptions are made. These are:

$k_2 = k_5 = k_7$ i.e. the spontaneous emission rate constants are the same from the three levels.

$k_3 = k_6$ i.e. the vibrational quenching efficiency is independent of the level in the singlet manifold.

$k_4 = k_8$ i.e. the intersystem crossing rate constant is the same from the intermediate level as from the thermally equilibrated level.

By setting up the steady state assumptions for the intermediate species, the quantum yield of fluorescence, ϕ_f , is given by:

$$\phi_f = \frac{k_2}{k_1 + k_3M} + \frac{k_2k_3(M)}{(k_1 + k_3M)(k_8 + k_3M)} + \frac{k_2k_3^2(M)^2}{(k_1 + k_3M)(k_8 + k_3M)k_8}$$

Recognising the low and high pressure limits of this function gives,

$$\phi_{f_0} = \frac{k_2}{k_1}$$

$$\phi_{f_\infty} = \frac{k_2}{k_8}$$

The expression for ϕ_f can be rearranged into several forms. One of them is identical with the dimensionless expression derived from Scheme A, i.e.

$$\frac{Q_f - Q_{f_0}}{Q_{f_\infty} - Q_f} = \frac{k_3(M)}{k_1}$$

The reason for this can be seen from the assumptions made above in the simplification of Scheme B. The level $S_1^{V'}$ has the same processes controlling its fate as the level S_1^0 and, therefore, is kinetically indistinguishable from this species. By considering this somewhat trivial extension of the two level Scheme A, it can be seen how introduction of intermediate levels having slightly different rate constants for the collisional deactivation and intersystem crossing can cause small variations in the functional dependence of the fluorescence quantum yield on pressure. Detection of these subtle effects will be extremely difficult in a system such as pentanedione which has a small quantum yield of fluorescence.

This is emphasized by considering Scheme C a minor modification of Scheme B in which k_4 is now set equal to k_1 rather than k_8 . Under these circumstances, retaining the earlier approximations, ϕ_f in Scheme C, is given by;

Scheme C

$$\phi_f = \frac{k_2}{k_1 + k_3 M} + \frac{k_2 k_3 M}{(k_1 + k_3 M)^2} + \frac{k_2 k_3^2 M^2}{k_8 (k_1 + k_3 M)^2}$$

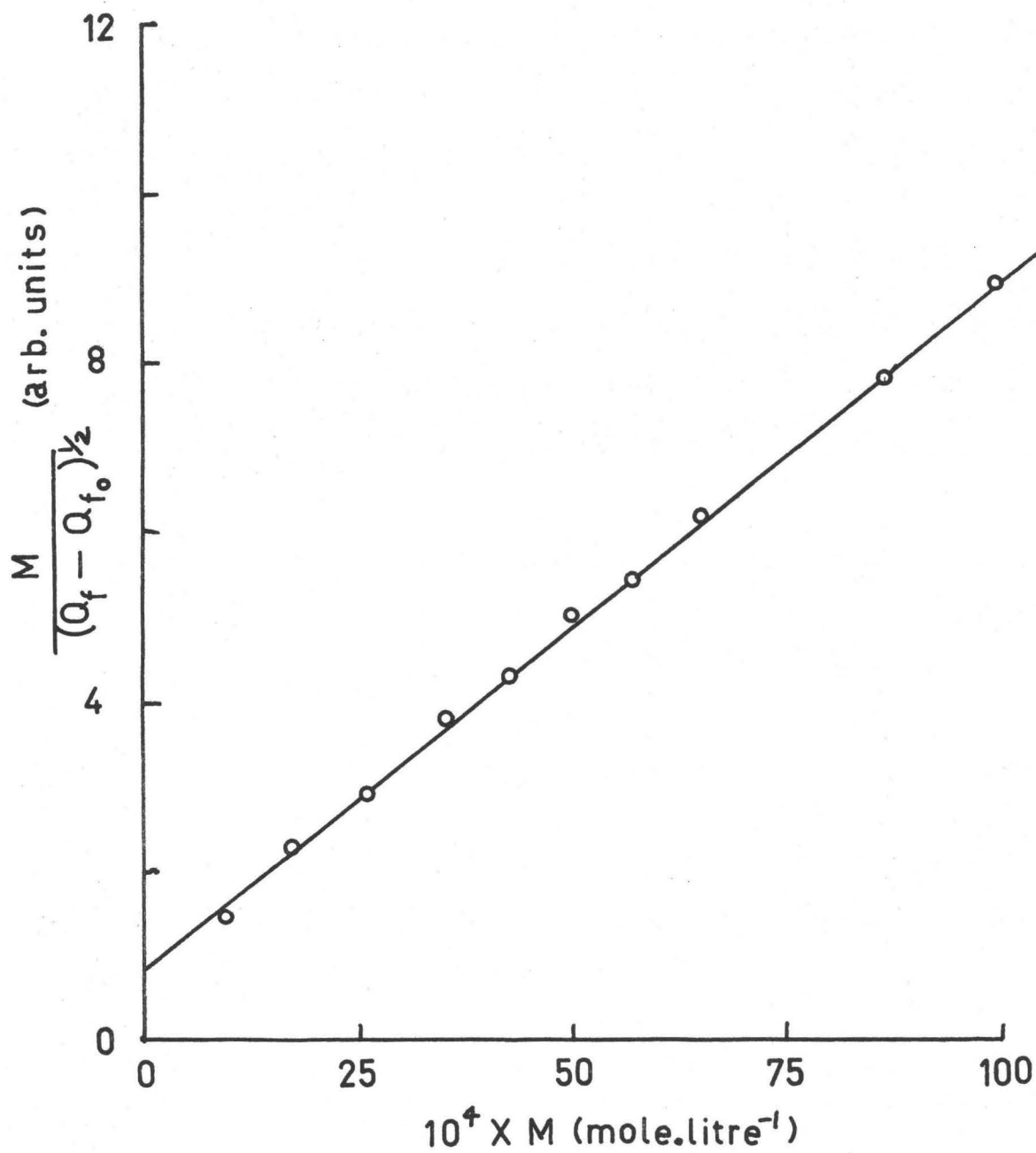
This expression can be rearranged into the form,

$$\frac{1}{\phi_f - \phi_{f_0}} = \frac{k_8 k_1 (k_1 + k_3 M)^2}{k_3 k_2 (k_1 - k_8) (M)^2}$$

It is predicted from this equation that a plot of $\frac{(M)}{(\phi_f - \phi_{f_0})^{1/2}}$ versus (M) should give a straight line. This is tested in Fig. 30 using the data contained in Table 7. A straight line dependence is indeed found which can be considered as qualitative evidence in favour of this scheme. However, as was emphasized previously, subtle modifications in the vibrational deactivation model do not cause dramatic modifications in the behaviour of the fluorescence yield. It **must** be concluded, therefore, that the fluorescence data acquired in this study, although giving agreement with various vibrational deactivation models, is not sufficiently precise to allow a particular model to be chosen. This dilemma is not uncommon in the study of collisional deactivation systems. Of those studied using fluorescence techniques, hexafluoroacetone has received the most attention. In this case only after careful correlation of fluorescence (4,127), phosphorescence (127), decomposition (127), and fluorescence lifetime (129) data is an understanding of the system emerging.

Having attempted to correlate the fluorescence data obtained in this study of pentanedione, attention will now be focussed on the phosphorescence system to deduce the behaviour of species in the triplet manifold.

Fig. 30 Test of the modified three-level fluorescence Scheme C,

 $\lambda_{\text{ex}} = 365 \text{ nm, at } 90^\circ\text{C.}$ 

Phosphorescence Enhancement Models

Scheme A

If it is to be assumed that only those molecules which inter-system cross from the S_1^0 level of the singlet manifold give triplet molecules capable of emitting phosphorescence, then the quantum yield of T_1^V is obtained from

$$\phi_{S_1^0} = \frac{k_3M}{k_2 + k_3M} \quad \phi_{T_1^V} = \frac{k_3M}{k_2 + k_3M} \cdot \frac{k_5}{k_4 + k_5}$$

It is known that $k_4 \ll k_5$, therefore,

$$\phi_{T_1^V} = \frac{k_3M}{k_2 + k_3M}$$

If vibrational deactivation occurs without loss of population in the triplet manifold, then the quantum yield of triplet in the emitting level is given by

$$\phi_{T_1^0} = \frac{k_3M}{k_2 + k_3M}$$

The important processes responsible for the removal of the triplet state in its vibrationally equilibrated level have been elucidated earlier. They can be summarised by,

- (a) $T_1^0 \xrightarrow{k_p} h\nu_p$ phosphorescence emission
- (b) $T_1^0 \longrightarrow S_0$ intersystem crossing to ground state manifold
- (c) $T_1^0 \longrightarrow$ unimolecular reaction

(d) $T_1^0 + M$ (where M is pentanedione) \rightarrow removal

The sum of the rates of processes (a) - (d) is given by the reciprocal of the phosphorescence lifetime, $1/\tau_{\text{phos}}$. The quantum yield of phosphorescence is given by,

$$\phi_p = k_p \tau_{\text{phos}} \phi_{T_1^0}$$

$$\phi_p = k_p \tau_{\text{phos}} \frac{k_3 M}{k_2 + k_3 M}$$

Rearranging gives,

$$\frac{1}{\phi_p} = \frac{1}{k_p \tau} \frac{k_2}{k_3} \cdot \frac{1}{(M)} + 1$$

This expression predicts that the variation of $1/\phi_p$ with $1/(M)$ should be linear neglecting variation of τ with M. It is tested in Fig. 31 using the relative phosphorescence quantum yield data in Table 7. It can be seen that the dependence is indeed linear at low pressures while deviation occurs at higher pressures. This deviation can be reconciled with the self-quenching described in Chapter 5 which gives rise to a reduced triplet lifetime. As the data is in the form of relative quantum yields, a direct comparison of slopes and intercepts cannot be made constant with the predicted form above. An estimate can be found using constant $k_p = 47 \text{ s}^{-1}$ and the value of τ_0 found in Chapter 5 to give the value of $k_p \tau_0$ as 2×10^{-3} at 90°C . The extrapolated value of the intercept in Fig. 31, is difficult to estimate accurately due to the comparatively large range over which the extrapolation is carried out. However, if the intercept is estimated as 0.5, then this can be identified as the intercept given by the expression above, i.e. $1/k_p \tau_0$. Comparison of

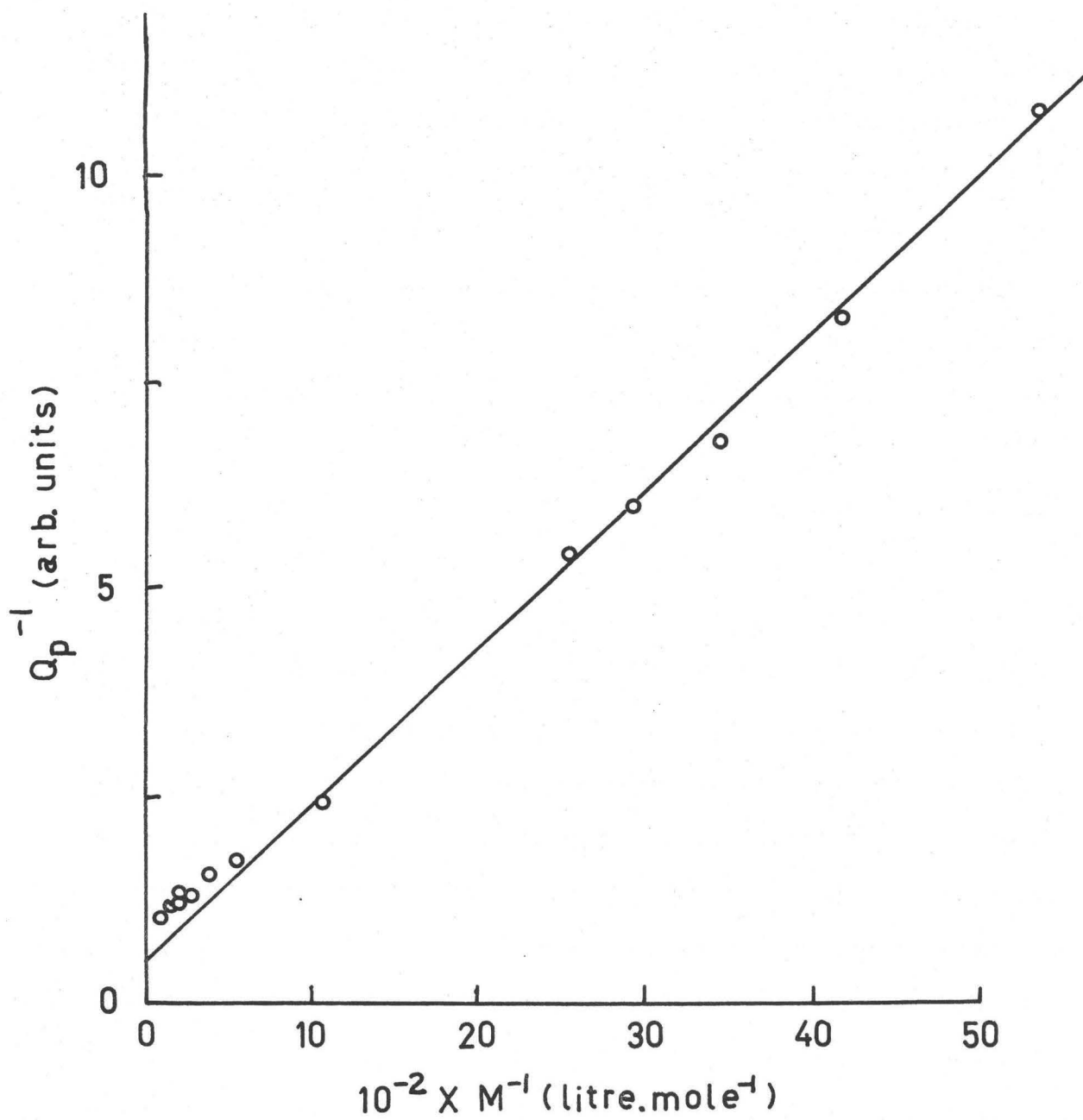


Fig. 31 Variation of Q_p^{-1} with $[M]^{-1}$ at 90°C , $\lambda_{\text{ex}} = 365 \text{ nm}$.

these quantities allows the conversion factor between the arbitrary units of Fig. 31 and the absolute quantity ϕ_p to be calculated. Taking into account the other scaling factors in Fig. 31, the value of the slope allows the calculation of k_3/k_2 . This is found to be $250 \text{ M}^{-1}\text{s}^{-1}$. This can be compared directly to the value of k_3/k_2 determined in the fluorescence study, which was found to be $330 \text{ M}^{-1}\text{s}^{-1}$. Considering the approximation involved in the determining the intercept of Fig. 31, the agreement between these quantities is very good and emphasizes the internally consistent nature of Scheme A.

It should be noted that the phosphorescence model in this case assumes that only those triplets molecules which originate from the vibrationally equilibrated level of the singlet manifold successfully reach the emitting equilibrated level of the triplet manifold. This implies that the radiationless process removing the S_1^V species (process (3) in Scheme A) does not yield triplet molecules capable of deactivation to the equilibrated level of the triplet. Such a process of radiationless irreversible removal from the system is consistent with the mechanism accumulated to describe the behaviour of biacetyl for 365 nm photolysis. It should be remembered that excitation at 365 nm injects 78.4 Kcals into the ground state pentanedione molecule. Because the vibrationally equilibrated level of the singlet manifold is estimated at 63 Kcal in biacetyl and pentanedione, the singlet species formed under these conditions has approximately 15 Kcal of excess vibrational energy. It is reasonable to suppose that this represents sufficient energy to allow dissociation along a particular mode of the hypersurface describing the

excited singlet states (130). An alternative interpretation of the process (2) in Scheme A could be that it represents intersystem crossing to a high vibrational level of the triplet manifold. This species would then possess ~ 23 Kcal of excess vibrational energy above the thermally equilibrated level of the triplet manifold. Fragmentation would then have to occur within a time scale, such that competition with collisional deactivation within the triplet manifold cannot be detected. This allows a lower limit to be placed on this rate constant. As $k_{\text{collisional deactivation}}$ is generally $\sim 10^{11} \text{ M}^{-1}\text{s}^{-1}$ and at a pressure of one atmosphere, $\sim 0.05 \text{ M}$, the rate constant for decomposition must be greater than $5 \times 10^9 \text{ s}^{-1}$ at 90°C to avoid detection.

Schemes B and C

It is interesting to see what approximations are necessary in the case of Schemes B and C to provide agreement with the observed phosphorescence behaviour. In both cases it is found that if it is assumed that the S_1^V level is the only level unable to give vibrationally quenchable triplets then the same functional dependence is found as in Scheme A. This point is demonstrated below,

Scheme B

$$\begin{aligned} \phi_{\text{isc}} &= \phi_{\text{isc}_{S_1^V}} + \phi_{\text{isc}_{S_1^O}} \\ &= \frac{k_8 k_3 M}{(k_8 + k_3 M)(k_1 + k_3 M)} + \frac{k_3^2 M^2}{(k_8 + k_3 M)(k_1 + k_3 M)} \\ &= \frac{k_3 M}{k_1 + k_3 M} \end{aligned}$$

which is identical with the intersystem crossing yield found in Scheme A
Scheme C

$$\begin{aligned}\phi_{isc} &= \phi_{iscS_1^V} + \phi_{iscS_1^O} \\ &= \frac{k_1 k_3 M}{(k_1 + k_3 M)^2} + \frac{k_3^2 M^2}{(k_1 + k_3 M)^2} \\ &= \frac{k_3 M}{k_1 + k_3 M}\end{aligned}$$

which is the same as Scheme A.

In each case, to provide agreement with experiment, it is necessary to assume that all molecules which intersystem cross are successfully deactivated to the equilibrated level of the triplet manifold. These deductions concerning Schemes A, B, and C emphasize the inherent ambiguity which exists in the interpretation of data from experiments of this kind. Even though a choice cannot be made at this stage between the three alternatives, it should be noted that there are common features. These are:

- (a) to explain the fluorescence results it is necessary to invoke emission from at least two levels in the singlet manifold;
- (b) to explain the phosphorescence results it is necessary to demand that the highest emitting singlet level should not be capable of giving thermally equilibrated triplet molecules.

Emission Enhancement at 30°C

At this point, the results of the phosphorescence enhancement experiments with sulphur hexafluoride can conveniently be brought into

the discussion of deactivation phenomena in the pentanedione. The situation existing within a mixture of gases is complicated but, within the framework of the strong collision mechanism, i.e. Scheme A, it can be handled in a fashion recommended by Lissi (131). The following steps are considered where added gas is M, and diketone is P,

Scheme A'

1. $S_0^o \xrightarrow{I_{abs}} S_1^v$
2. $S_1^v \longrightarrow$ radiationless removal
3. $S_1^v + M \longrightarrow S_0^l$
4. $S_1^v + P \longrightarrow S_1^o$
5. $S_1^o \longrightarrow T_1$
6. $T_1 \longrightarrow$ phosphorescence
7. $T_1 \longrightarrow$ radiationless removal

It can be shown using the steady state approximations that if $Y = \frac{\phi_{P_0}}{\phi_P}$

where ϕ_{P_0} is the quantum yield of phosphorescence in the absence of M and ϕ_P is this quantity in the presence of M, and if $f = \frac{Y}{1 - Y}$ then,

$$f = \frac{1}{M} \left\{ \frac{k_4 P}{k_3} + \frac{k_4^2 P^2}{k_2 k_3} \right\} + \frac{k_4(P)}{k_2}$$

This expression predicts a straight line relationship between f and 1/M.

What is more, from the slope and intercept of this plot, the ratios

k_4/k_2 and k_4/k_3 can be calculated. This function f is plotted in Fig. 32

using the data from Fig. 28. The values of k_4/k_2 and k_4/k_3 are $1.04 \times 10^3 \text{ M}^{-1} \text{ s}^{-1}$

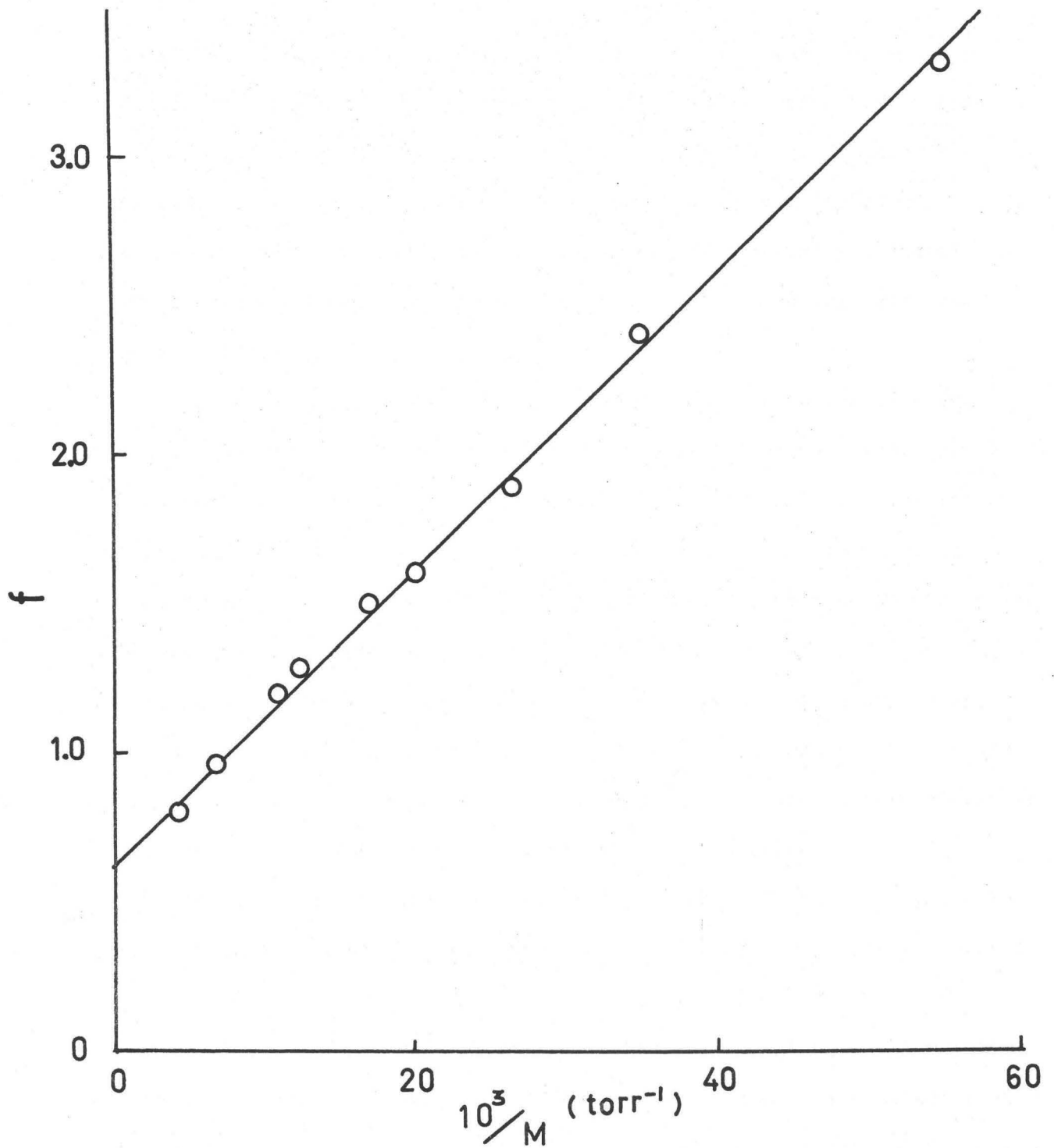


Fig. 32 Variation of f with $[M]^{-1}$ at 30°C , $\lambda_{\text{ex}} = 365 \text{ nm}$.

and 2.94, respectively, at 30°C. This demonstrates that the sulphur hexafluoride molecule is approximately one-third as efficient as the ground state pentanedione molecule in collisionally deactivating the excited singlet species. This inefficiency can be correlated with the dimensions of the molecule and also with the generally observed relationship between vibrational quenching ability and molecular complexity (132).

The derived value of k_4/k_2 at 30°C allows an interesting comparison to be made with the value of this quantity derived from the pure pentanedione emission enhancement experiments at 90°C. The ratio k_4/k_2 was found to be $\sim 330 \text{ M}^{-1}\text{s}^{-1}$ on the basis of the fluorescence enhancement measurements and $250 \text{ M}^{-1}\text{s}^{-1}$ estimated from the phosphorescence enhancement measurements at 90°C. The smaller value at the higher temperature indicates that either k_4 has decreased or k_2 has increased or changes have occurred in both quantities. If the constant k_4 varies in the same fashion as that predicted for the collision number calculated from the classical kinetic theory of gases, an increase of $\sim 10\%$ is expected over the temperature range 30°C to 90°C. Taking this to be the case, the major contributor to the change in the ratio is the rate constant k_2 .

The variation of this radiationless rate constant with temperature is not easily interpreted as the formation of states by absorption at 365 nm is unlikely to give species which obey a Boltzmann distribution law. If dissociation takes place from the S_1^V level then it cannot do so

at a rate greater than $\sim 10^9 \text{ s}^{-1}$. This implies a redistribution of energy within the molecule after the absorption act. This redistribution of energy might be considered as the equivalent of the time lag inherent in the RRKM theory for the description of unimolecular decomposition processes. The difference being that in the thermal system equilibration between the different vibrational modes of a molecule can be assumed, whereas this assumption is not necessarily valid for the species formed by absorption at 365 nm. Application of an Arrhenius law to such a process would not be appropriate.

Assumptions used in Schemes A, B, and C

Before discussing collisional deactivation mechanisms in the broader text of other systems which have been studied, some comment is necessary concerning the approximations used in their derivation.

- (i) It is assumed that the emission rate constants from the various levels of the singlet manifold are the same. While this is a convenient simplification, there is not a priori reason for believing this to be so. In the case of pentanedione, this probability is related to the dipole moment matrix element connecting the initial and final states. The variation of this quantity in different vibrational levels of the singlet manifold is not easy to predict, however, there is evidence from the fluorescence lifetime experiments of Ware (129) that a similar approximation is valid in the case of hexafluoroacetone.
- (ii) Doubts concerning the validity of this first approximation may

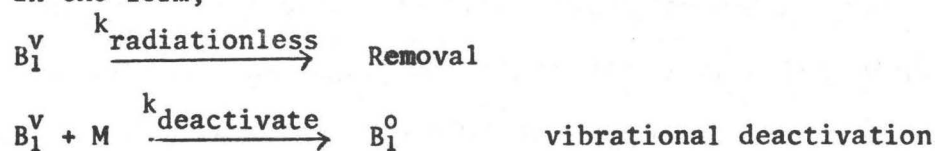
be dispelled to some extent by the subordinate assumption that the fluorescence quantum yield can be treated as the sum of its components. While there is no approximation necessary for this statement, the use of relative quantum yields, Q_f , assumes that the emission signal measured at one wavelength is proportional to the integrated area of the whole fluorescence emission spectrum. This is equivalent to assuming that the emission profile is independent of the pressure and exciting wavelength. There is direct evidence to substantiate this approximation. It was found earlier that the emission profile was independent of the pressure of added inert gas for 365 nm excitation. For any of the three schemes above, it is found that at the pressure of pentanedione used in this experiment there is a considerable contribution to the fluorescence emission from vibrationally excited levels. The fact that no change could be detected in the presence of a large amount of added inert gas, when collisional deactivation will be very efficient, is evidence in favour of this assumption. Furthermore, the insensitivity of the emission profile to exciting wavelength implies that there must be a fast intramolecular redistribution process out of the Franck-Condon state formed on absorption. This conclusion is reached by Ware (129) in his study of hexafluoroacetone, a system which shows properties of emission from vibrationally excited levels of the singlet manifold and insensitivity of fluorescence profile to pressure and exciting wavelength.

It is interesting to note that in the case of hexafluoroacetone, the fluorescent lifetime from the equilibrated singlet level is considerably longer (84×10^{-9} s) than that estimated for pentanedione $\sim 5 \times 10^{-9}$ s. As these lifetimes are effectively governed by the non-radiative rate constants for removal, the intersystem crossing rate constant in hexafluoroacetone is considerably less than that in pentanedione. In the vibrationally excited levels of the singlet it would be expected that these radiationless rate constants would be increased due to higher density of isoenergetic triplet states, but still retain their relative magnitudes. Therefore, it can be understood how pentanedione fluorescence might contain components from vibrationally excited levels at quite high pressures, whereas, in hexafluoroacetone, radiationless processes do not compete as successfully with collisional deactivation and contributions from vibrationally excited levels will be important only at lower pressures.

Comparison with Biacetyl

It would be interesting to compare the behaviour of the fluorescence and phosphorescence found in this study of pentanedione with information compiled on the behaviour of biacetyl. Unfortunately, it seems that no explicit study of the fluorescence behaviour has been carried out over a wide pressure range (134). However, the phosphorescence behaviour for 365 nm excitation has been studied around room temperature by several workers (7,23,24,131,133). In all cases, it was found that the phosphorescence yield extrapolated smoothly to zero at zero pressure

of biacetyl. This is exactly the behaviour found in this study. What is more, the collision deactivation process leading to the formation of the triplet biacetyl could be described by a single collision which successfully removed vibrational energy from the initially formed excited singlet state. The processes controlling the fate of the initially formed vibrationally excited singlet state are radiationless removal and collisional deactivation. There is evidence from the inability of the primary photochemical yield (27) to extrapolate to unity at zero pressure, that the radiationless process is a sum of rates corresponding to internal conversion to the upper levels of the ground state and to fragmentation of the molecule. The ratio $k_{\text{internal conversion}}/k_{\text{decomp.}}$ is estimated at 3 at 90°C from the data of Sheats and Noyes (27). If these processes are represented in the form,

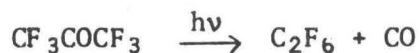


the ratio $k_{\text{deactivate}}/k_{\text{radiationless}}$ has been estimated (73,132) to be in the range $1.2\text{-}2.7 \times 10^3 \text{ M}^{-1}\text{s}^{-1}$ at 28°C. This can be compared to the corresponding ratio in the pentanedione system. From the phosphorescence enhancement experiments at 30°C with 365 nm excitation it was concluded that the ratio $k_{\text{deactivate}}/k_{\text{decomposition}}$ was 1.04×10^3 at 30°C. If the deactivation rate constants are comparable in the two cases, then it can be concluded that the $k_{\text{radiationless}}$ from the S_1^V formed by 365 nm excitation is approximately the same in biacetyl and pentanedione at 30°C.

The description of a system from fluorescence and phosphorescence measurements should be complemented by information derived from decomposition

studies. In the case of biacetyl, the fluorescence yield for 365 nm excitation has been shown to increase as the pressure increases (134), (no detailed study was carried out but the trend was clear), whereas, the primary decomposition yield decreases as the pressure increases (27). These two facts are in agreement with the notion of decomposition from a vibrationally excited level of the singlet manifold. No decomposition studies have been carried out using pentanedione, but by analogy with biacetyl, the decomposition yield might be expected to show the same trend.

The diagnostic use of decomposition data to decide upon the mechanism of vibrational deactivation within the singlet manifold of biacetyl has not been attempted due to the complexity of the decomposition modes. As was pointed out earlier, changes in the mechanism of deactivation can produce subtle changes in the behaviour of the system. A striking example is the case of hexafluoroacetone which has an appealingly simple decomposition mode.



Even in this simple case, decomposition data has been used to support both strong (135,136) and weak collision (137,57) mechanisms for deactivation of the vibrationally excited singlet formed on absorption state. If interpretation of such a simple system as this is open to controversy, then to attempt to apply collisional models to decomposition data from biacetyl or pentanedione would be a much more difficult proposition.

That a simple strong collision model describes the behaviour of biacetyl emission and decomposition is no guarantee that intervening

vibrational levels of the singlet manifold do not enter into the description of the system. This has been emphasized by the consideration of various collisional mechanisms. The same conclusions regarding insensitivity of data to the model of deactivation have been made by Ware in his study of the fluorescence lifetime of hexafluoroacetone (129). He finds that introducing intermediate levels causes little change in the behaviour of the system, although the inclusion of intermediate levels does cause a proportionate reduction in the value of the collisional deactivation rate constant between levels.

Conclusions

In summary, the fluorescence behaviour of pentanedione during 365 nm photolysis with varying pressure is such as to provide direct evidence for emission from vibrationally excited levels of the singlet state. Examination of this variation with pressure does not allow a choice to be made between a strong or weak collision scheme for deactivation in the singlet manifold. An internally consistent model for phosphorescence is proposed which only allows singlet molecules, that are not removed by radiationless processes in the vibrationally excited levels of the singlet, to reach the equilibrated level of the triplet manifold.

CHAPTER 8

VARIATION OF FLUORESCENCE AND PHOSPHORESCENCE YIELDS WITH TEMPERATURE

An adequate description of the major processes controlling the fate of excited singlet and triplet pentanedione molecules must be capable of correlating the variation of quantum yields of fluorescence and phosphorescence with temperature. These quantum yields are proportional to the concentration of species which can emit. This concentration is governed by the rates of formation and removal processes. Variation of temperature will, therefore, provide insight into the nature of these events.

Results

Experiments were conducted using the relative quantum yield apparatus described in Chapter 2. A glass filter, CS3-72, restricted the emitted light such that only wavelengths greater than 470 nm were recorded by the IP28 photomultiplier. Emission readings were taken, for a fixed pressure of pentanedione, at various temperatures up to 100°C in approximately 10° intervals. The contents of the cell were condensed into the U-trap of the cell using liquid nitrogen and approximately 20 torr of oxygen was added. After equilibration, the variation of the emission signal from the pentanedione/oxygen mixture was recorded at various temperatures up to 100°C. In the absence of oxygen, the

emission consists of fluorescence and phosphorescence, whereas in the presence of ~ 20 torr of oxygen, the phosphorescence is effectively completely quenched, leaving the fluorescence as the only emission. The efficiency of the phosphorescence quenching by oxygen will vary through the experiment due to the variation of the phosphorescent lifetime with temperature. However, on the basis of the determined quenching constant for oxygen (Chapter 10) and the previously determined variation of phosphorescent lifetime, it can be calculated that in the presence of 20 torr of oxygen, the correction necessary to the fluorescence readings at high temperature does not exceed 2%. It was, therefore, not taken into account.

As the emission filter only passed wavelengths greater than 470 nm, where the absorption of the diketone is negligible, the "inner filter" correction described earlier was not applied. Corrections were made, however, to take into account fluctuations in incident light intensity, scattered light from the cell and the dark current of the photomultiplier. The variations of the corrected total emission and fluorescence signals were plotted as functions of temperature and smooth curves were drawn through the data. The contribution of phosphorescence in the total emission curve was then calculated at any temperature as the difference between the total emission signal and the fluorescence signal.

This technique was used at different pentanedione pressures and exciting wavelengths in an attempt to detect trends due to possible effects these parameters could have at different temperatures on the

fluorescence and phosphorescence yields. Experiments were conducted at 4.2 torr of pentanedione using 405nm and 365 nm excitation to investigate the effect of low pressures at different wavelengths. Fluorescence and total emission measurements were taken at 405 nm, and are shown in Fig. 33 and Fig. 34. Unfortunately, the weak absorption and low pressure of the diketone at 365 nm caused the intensity of the emission to be weak. The total emission and fluorescence variations were open to errors such that the value of phosphorescence intensity at high temperatures was highly uncertain. The 365 nm photolysis experiment was carried out at a slightly higher pressure, 23 torr, with satisfactory results. These are shown in Fig. 35 and Fig. 36. To investigate the effects of high pressure, an experiment was carried out using a pentanedione sample at 115 torr. Exciting wavelengths of 365 nm and 436 nm were used. The experimental curves and derived variations of phosphorescence intensity are shown in Fig. 37-40. No attempt has been made to relate the individual arbitrary units of the different experiments. Experiments which studied the effect of pentanedione pressure under isothermal conditions at 436 nm and 365 nm excitation have already been described, correlation of the isolated temperature variation experiments was judged unnecessary.

Discussion

It can be seen by inspection of the results of the temperature variation experiments at different wavelengths and pressures that there

Fig. 33 Variation of $Q_p + f$ and Q_f with temperature; 23PD = 4.2 torr,
 $\lambda_{ex} = 405$ nm.

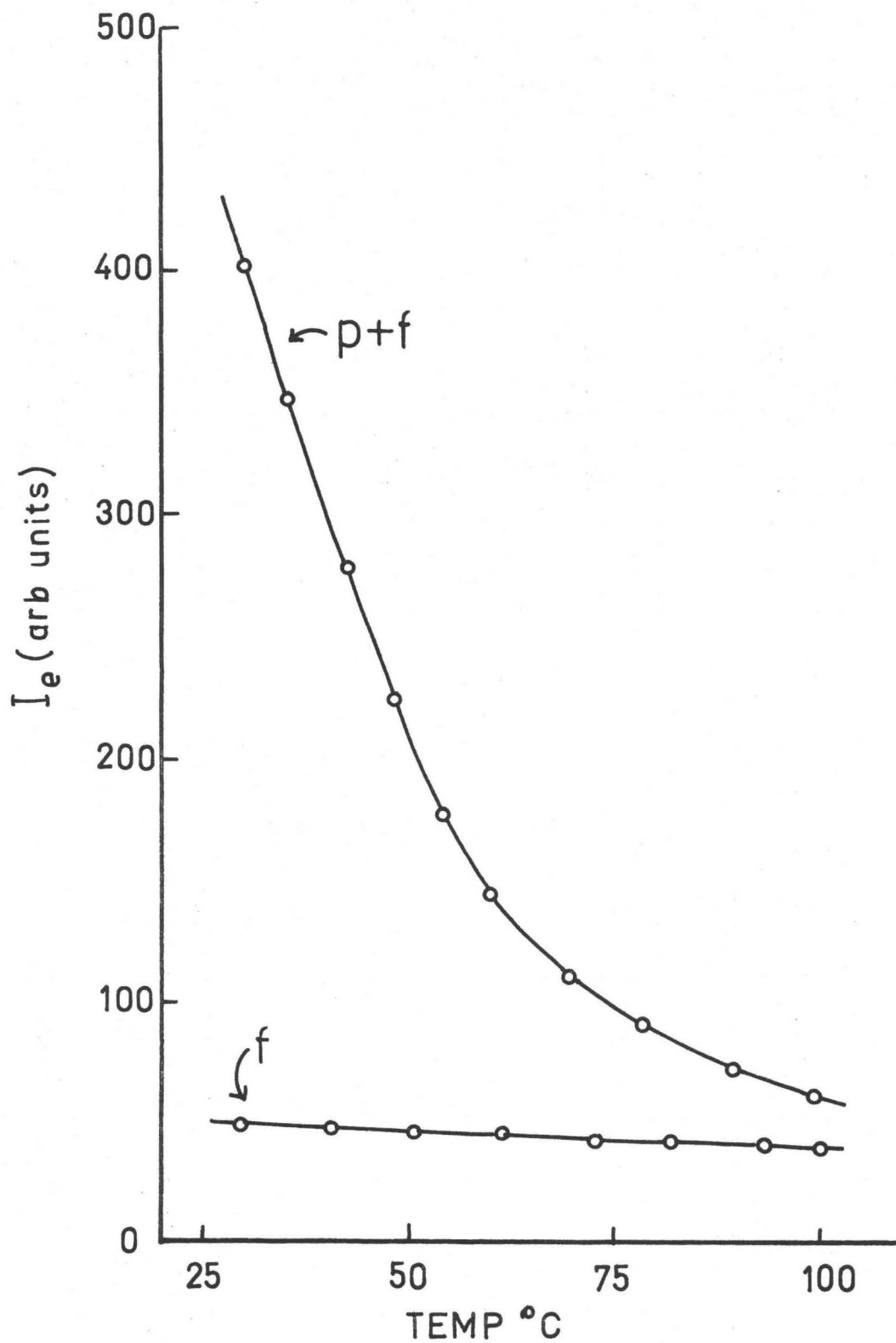


Fig. 34 Continuous line is variation of Q_p with temperature calculated from Fig. 30; 23PD = 4.2 torr, $\lambda_{ex} = 405$ nm. \circ represents variation of τ_p under these conditions.

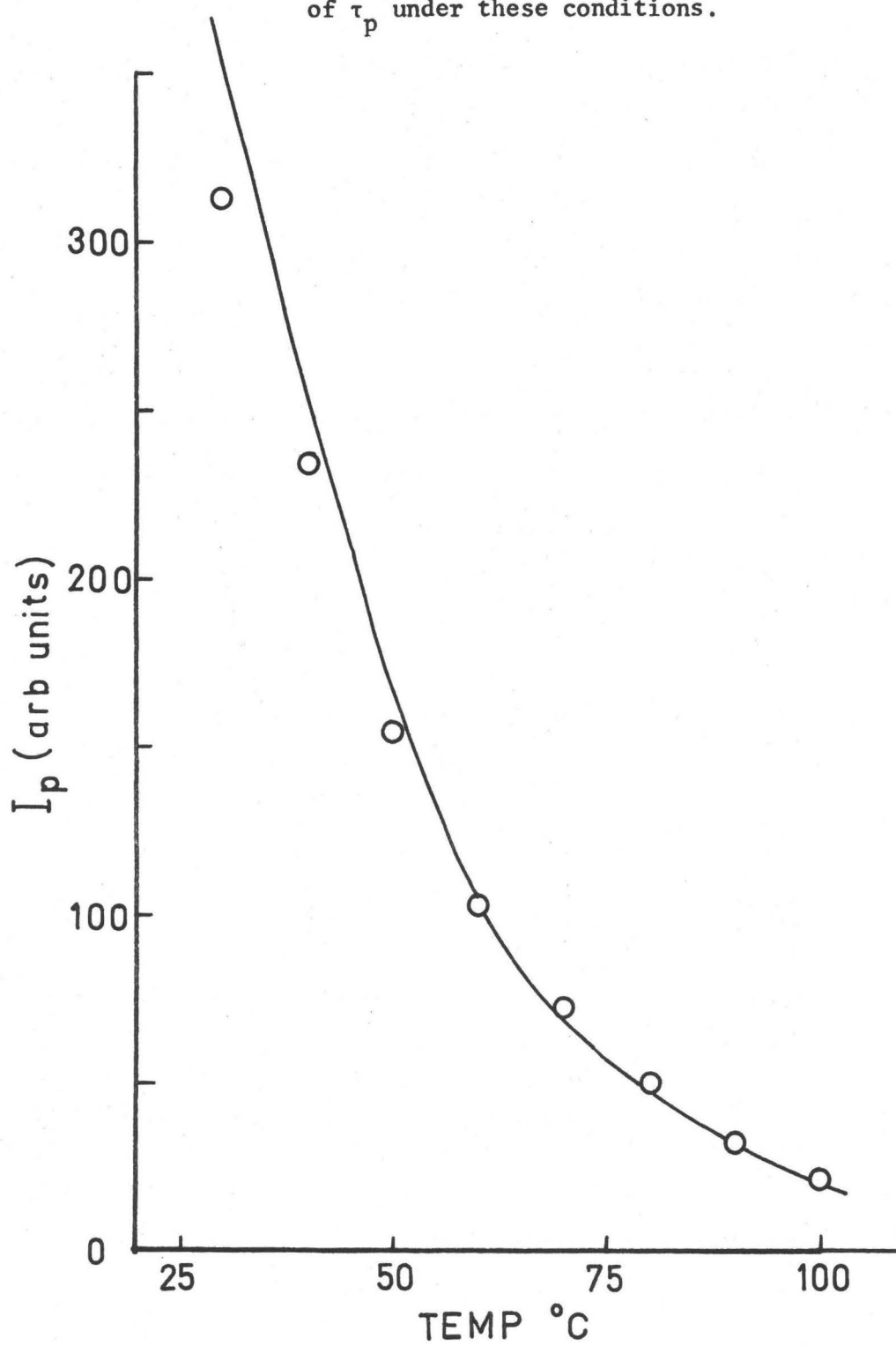


Fig. 35 Variation of $Q_p + f$ and Q_f with temperature; 23PD = 23 150

torr, $\lambda_{ex} = 365 \text{ nm.}$

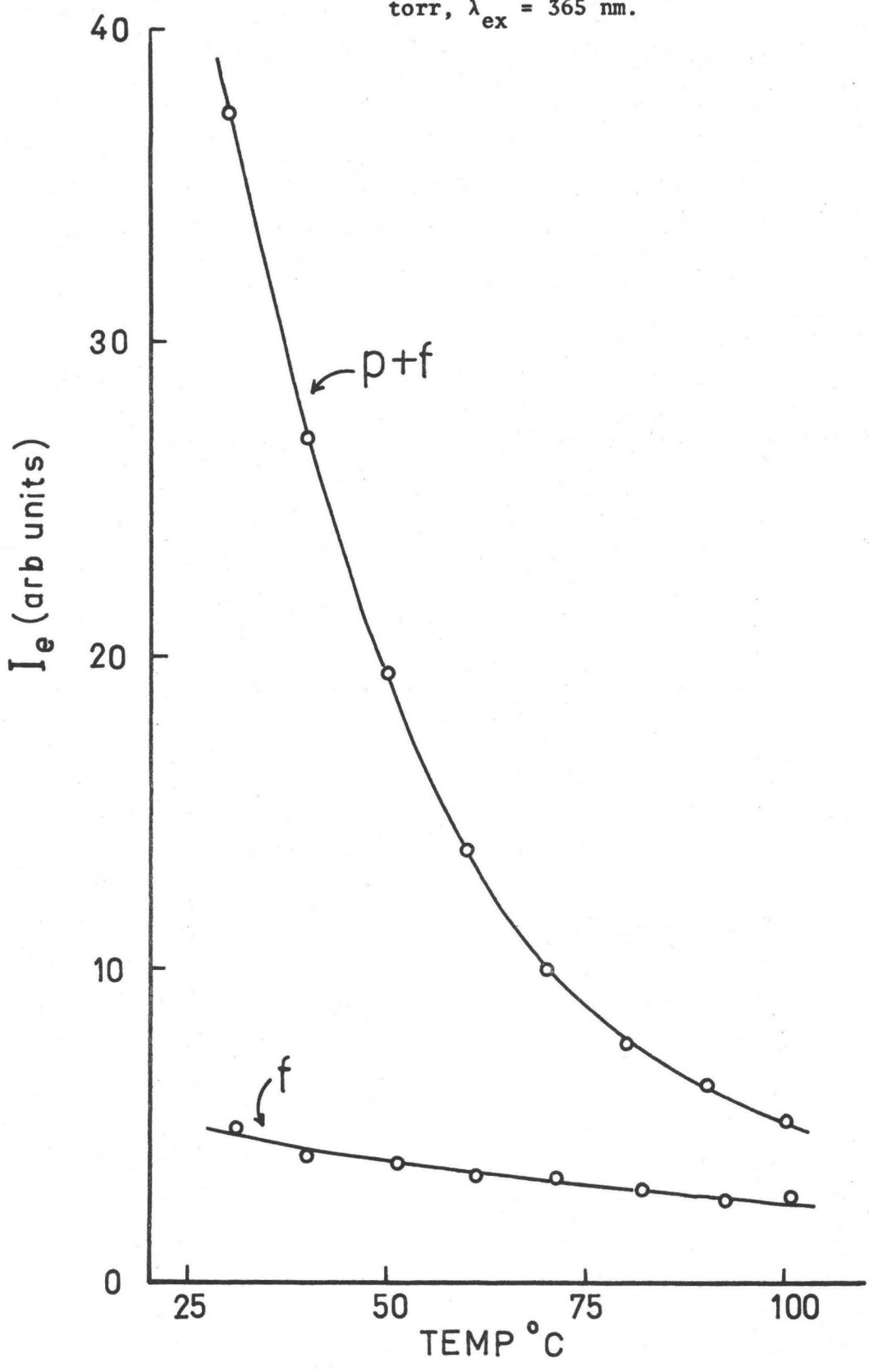


Fig. 36 Continuous line is variation of Q_p with temperature calculated from Fig. 35; 23PD = 23 torr, $\lambda_{ex} = 365$ nm. \circ represents variation of τ_p under these conditions.

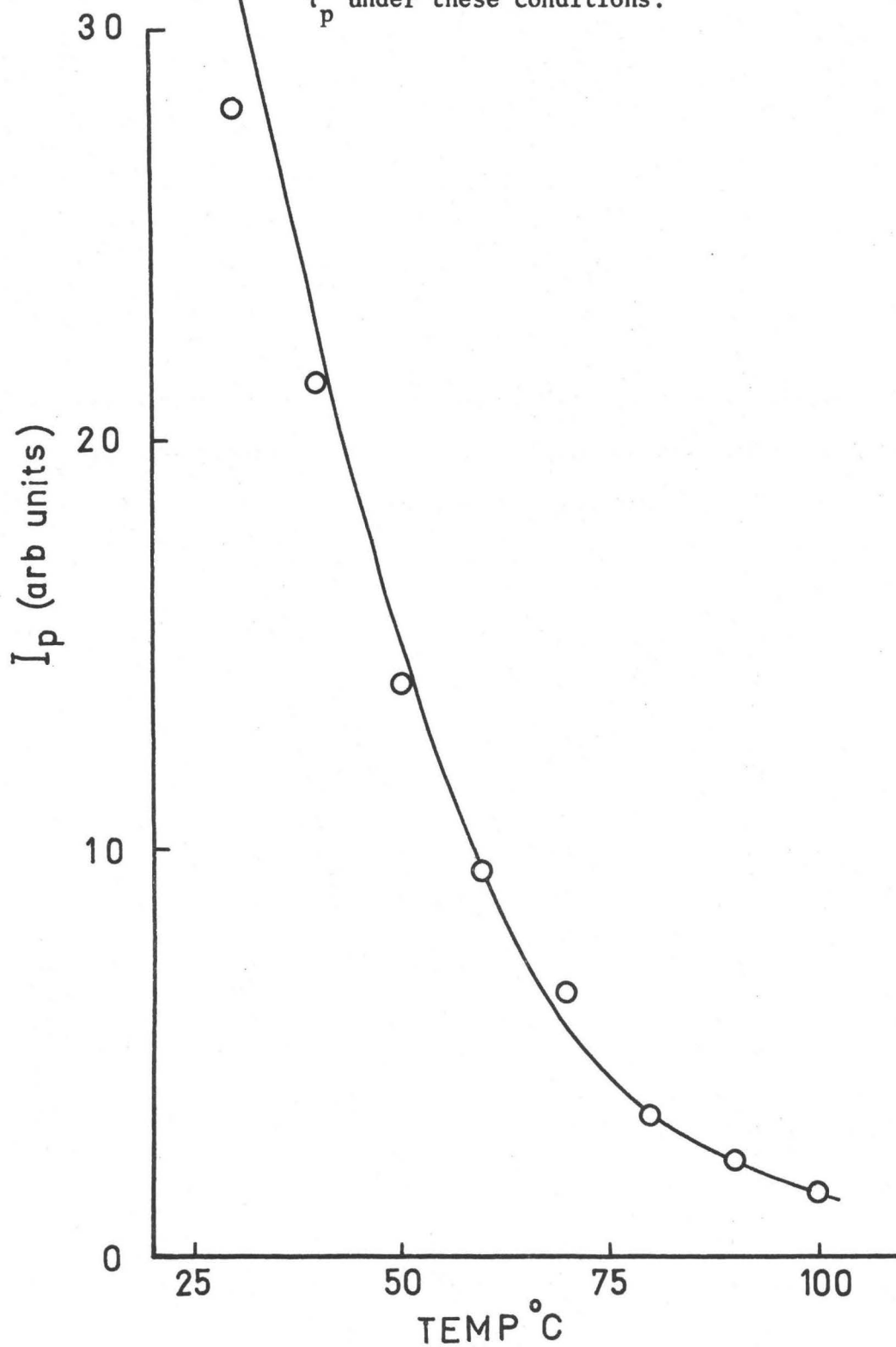


Fig. 37 Variation of $Q_p + f$ and Q_f with temperature; 23PD = 115 torr,
 $\lambda_{ex} = 436$ nm.

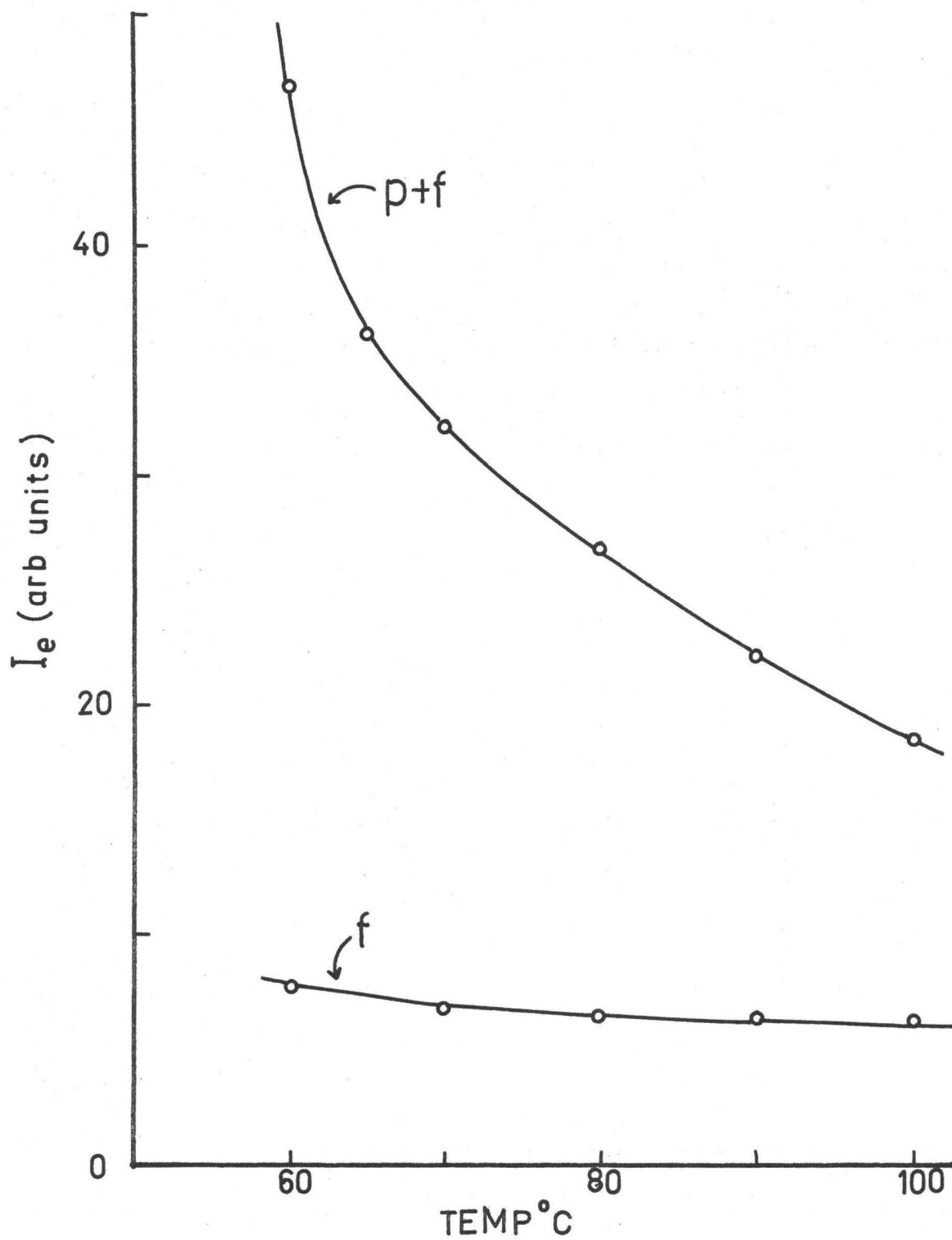


Fig. 38 Variation of Q_p with temperature calculated from Fig. 37;

23PD = 115 torr, $\lambda_{ex} = 436$ nm. \circ represents variation of τ_p
under these conditions.

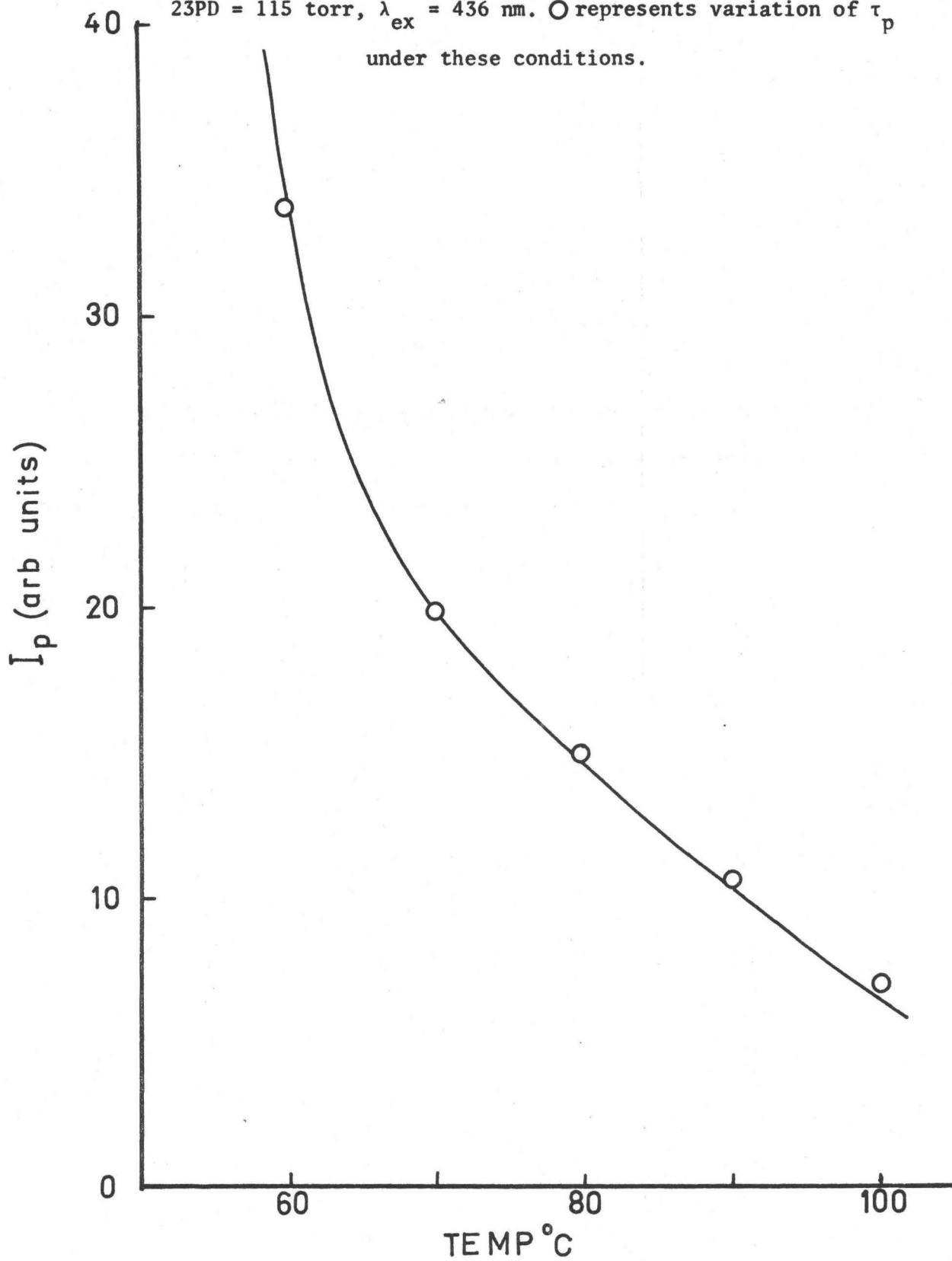


Fig. 39 Variation of $Q_p + f$ and Q_f with temperature; 23PD = 115 torr,
 $\lambda_{ex} = 365$ nm.

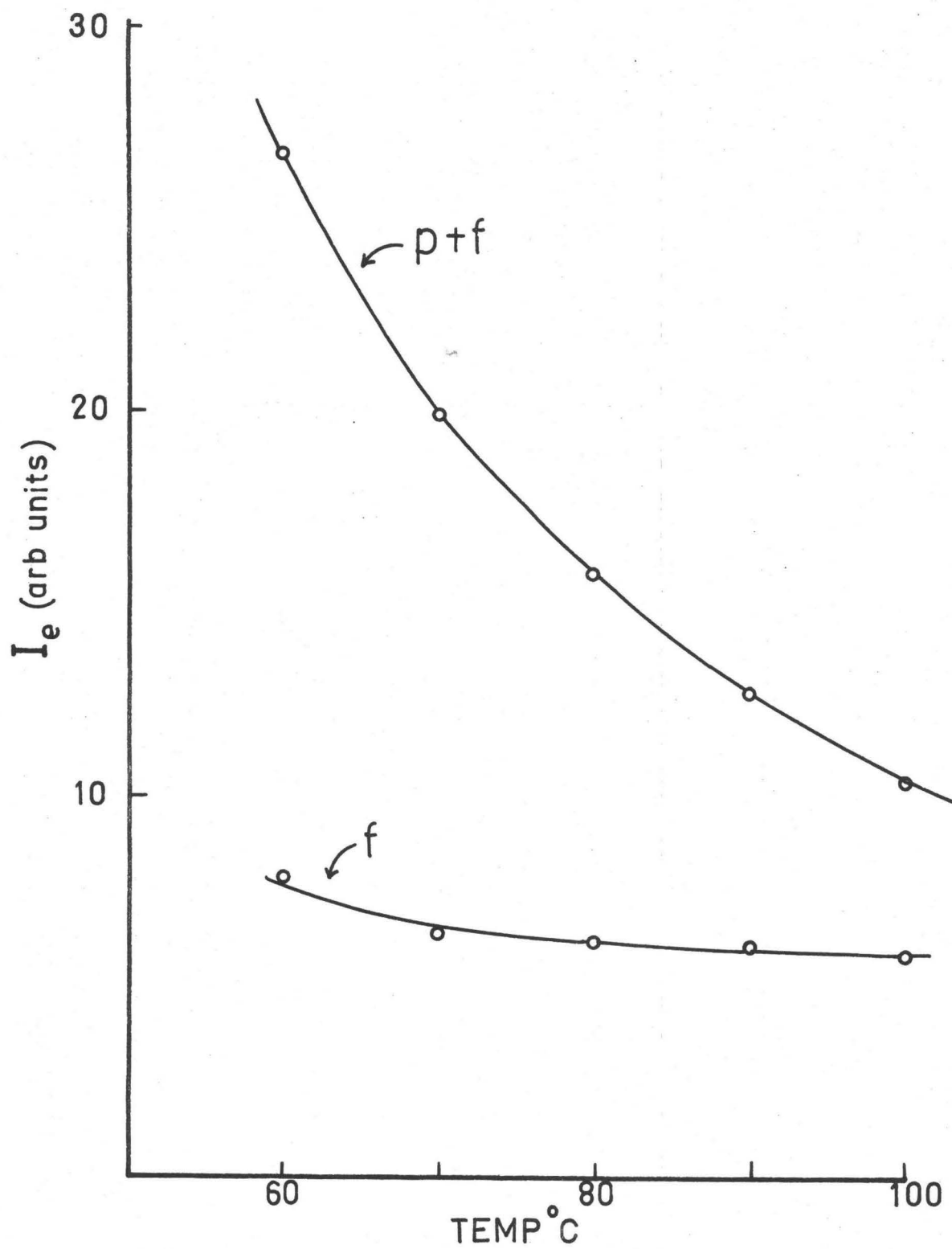
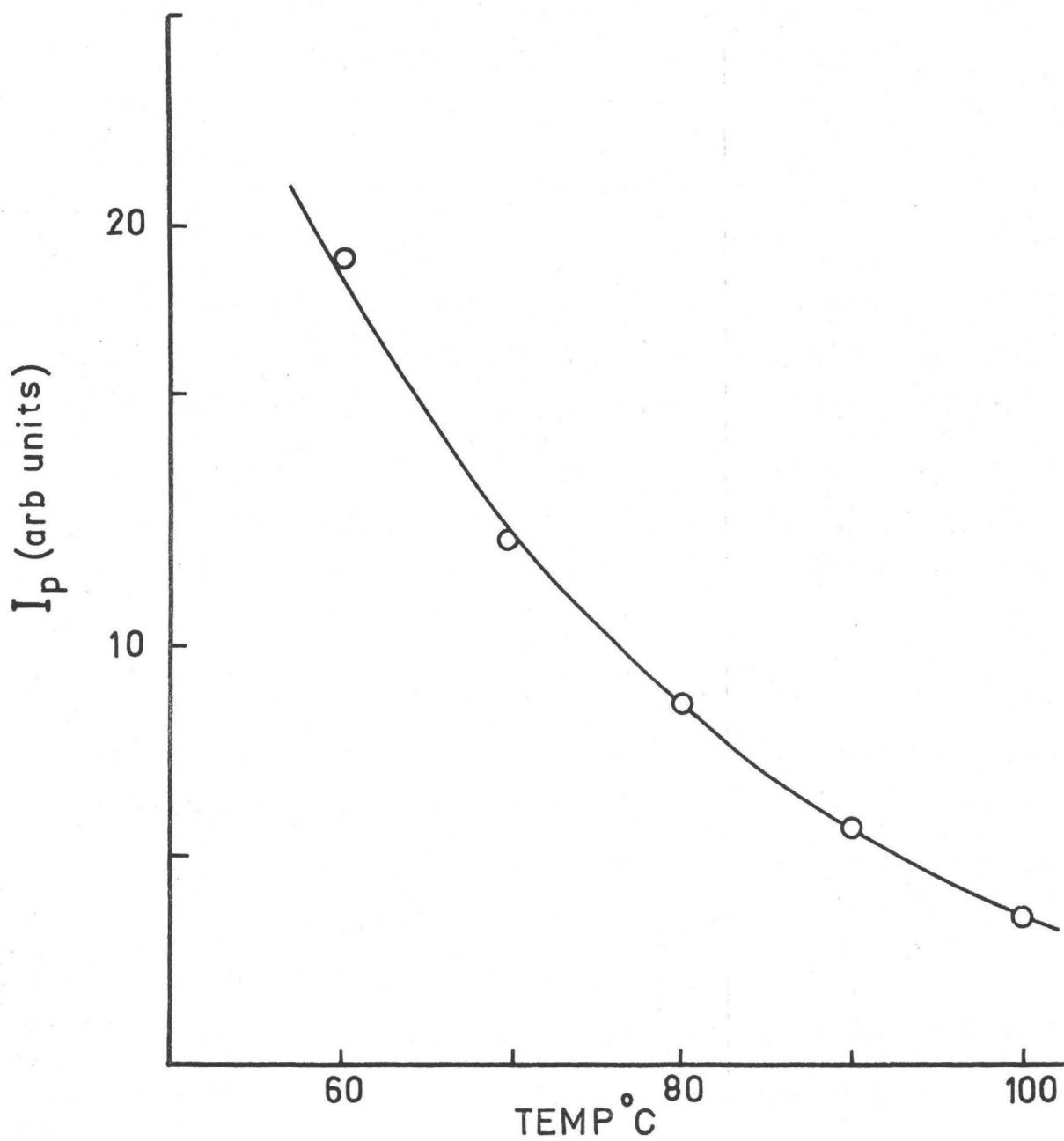


Fig. 40 Variation of Q_p with temperature calculated from Fig. 39;

23PD = 115 torr, $\lambda_{ex} = 365$ nm. \circ represents variation of τ_p under these conditions.



are two common features. Firstly, the fluorescence yield varies only slightly with temperature. Secondly, the phosphorescence yield varies dramatically with temperature.

It is logical to begin consideration of these effects by focussing attention initially on the singlet state, as this is the state formed by absorption and is the precursor to the triplet state.

The Singlet State

It is already known from work earlier in this study that the fluorescence yield is insensitive to the addition of inert gas when excitation is at 405 nm and 436 nm. This indicates that the radiationless processes removing the state formed on absorption are not pressure dependent and that the state is collisionally deactivated without loss to the equilibrated level of the singlet manifold. Therefore, for long wavelength excitation the quantum yield of fluorescence, ϕ_f , is given by,

$$\phi_f = \frac{k_f}{k_{r1}}$$

where k_f is the rate constant for emission of fluorescence and k_{r1} is the sum of the pressure independent rates of radiationless removal of the S_1 state. These radiationless processes are undoubtedly dominated by the term corresponding to intersystem crossing to a vibrational level of the triplet manifold.

The variation in the fluorescence yield with temperature is not large, $\sim 10\%$ between 30° and 100°C , and could be due to a variety of

factors. A reduction in ϕ_f could correspond to a reduction in k_f or an increase in k_{r1} . Experimentally the extinction coefficients at various wavelengths in the absorption spectrum do not vary with temperature and, therefore, a variation in k_f can be excluded.

However, the features controlling the temperature dependence of radiationless processes between different electronic states are not well understood. It has been suggested (95,96) and observed (129) that the radiationless rate constant should increase with temperature for a molecule in the statistical limit. It is quite possible, therefore, that the variation of ϕ_f with temperature is due to the variation of $k_{isc_{S_1 \rightarrow T_1}}$. An alternative explanation could be that the radiationless corresponds to two processes, one of which is large and independent of temperature, i.e. intersystem crossing, while the other is small and has a considerable temperature dependence. Such a process would have to be first order in S_1 and could correspond to a unimolecular decomposition in its high pressure limit. A decision could be made between these alternatives by the variation in the phosphorescence yield, as the first would cause no change in the triplet yield whereas the second would reduce it. It must be remembered, however, that this effect is small and it is doubtful if derived data, such as phosphorescence yields, would be reliable enough to allow a firm decision to be made.

The lack of bimolecular self-quenching of the singlet demonstrated in Chapter 6, is reinforced by the observation, Fig. 33 and Fig. 37, that the proportionate variation of Q_f with temperature is insensitive to pentanedione pressure.

Changing the exciting wavelength to 365 nm might be expected to produce interesting modifications in the behaviour of the fluorescence variation with temperature. Unfortunately in the region where these modifications might be expected to be greatest, the low pressure, the small amount of light absorbed and the reduced fluorescence efficiency, gave rise to unreliable data. However, there was an indication that the proportionate reduction over a particular temperature range, was greater at 365 nm than for long wavelength excitation. At a slightly higher pentanedione pressure, 23 torr, the proportionate change in Q_f over a particular temperature range was the same at 405 and 365 nm excitation. This result is interesting in that the fluorescence and phosphorescence enhancement experiments described in Chapter 7 predicted that for a two level system in the singlet manifold the radiationless process removing the higher level S_1^V , should increase at higher temperatures. The fluorescence variation, at a relatively low pressure of 23 torr, does not show the expected difference in behaviour between 405 and 365 nm excitation predicted by this two level scheme. This could be interpreted as being evidence in favour of the intermediate emitting levels between S_1^V and S_1^O .

As would be expected, at higher pressures of pentanedione, the proportionate variation of the fluorescence efficiencies at 436 and 365 nm are approximately the same, Fig. 37 and Fig. 39. At this higher pressure, collision deactivation of the species formed by excitation at 365 nm, is efficient, although on the basis of the two level emission scheme, some difference in behaviour might have been expected as the contribution

to emission efficiency by the S_1^V level predicted by this scheme is still significant.

The Triplet State

In contrast to the slight variation found in the fluorescence variation with temperature, the phosphorescence variation is indeed dramatic. As the singlet is the precursor of the triplet state, then the contrast in behaviour could be due to:

- (i) the destruction of some intermediate between the emitting levels of the singlet and triplet;
- (ii) some process(es) removing the emitting triplet species.

As it is already known from Chapter 5 that the processes removing the phosphorescing state have a strong temperature dependence, then the second is to be considered the more likely. If long wavelength excitation is considered, then it has been shown that the behaviour can be described by,

1. $S_0 \xrightarrow{I_{abs}} S_1^0$ absorption to give fluorescing level
with unit efficiency
2. $S_1^0 \xrightarrow{k_f} hv_f$ fluorescence
3. $S_1^0 \longrightarrow T_1$ intersystem crossing to give unit
yield of triplet
4. $T_1 \xrightarrow{k_p} hv_p$ phosphorescence
5. $T_1 \longrightarrow$ radiationless removal
6. $T_1 + \text{pentanedione} \longrightarrow$ removal

The yield of phosphorescence, ϕ_p , is given by,

$$\phi_p = \frac{k_p}{k_4 + k_5 + k_6[\text{Pentanedione}]} = \tau_p k_p$$

Therefore, if this mechanism is correct, and k_p does not vary with temperature, the variation of ϕ_p should be described by the variation of τ_p . This has been tested in Figs. 34,36,38,40, where the continuous curve is the experimentally acquired phosphorescence yield and the circles represent the variation of the phosphorescent lifetime at the particular pentanedione pressure, expressed so that $Q_p = \text{const.} \tau_p$. The value of the constant is found by substitution at a temperature approximately in the middle of the temperature range used. Inspection of these graphs shows that the correlation between the variation of the phosphorescence yield and the variation in phosphorescent lifetime is excellent under differing conditions of excitation and pentanedione pressure. Two important conclusions can be drawn from this correlation.

- (i) AS the correlation is so good, it can be concluded that the mechanism shown above is adequate to describe the behaviour at long wavelength excitation. This implies that only the processes removing the triplet state are important. The temperature variation due to decomposition of intermediate states between the S_1^0 and T_1^0 , i.e. T_1^V formed by intersystem crossing from S_1^0 cannot be detected. This conclusion applies equally well to the data for 365 nm excitation, where the correlation indicates that the destruction of vibrationally excited triplet levels which might exist under these circumstances, is unimportant.
- (ii) The correlation is good at low, 4.2 torr, and high, 115 torr, pressures of pentanedione. As the phosphorescent lifetimes were

taken from the plots given in Chapter 5, which demonstrate self-quenching of the triplet state, support is provided for the validity of these results.

The consistent nature of the phosphorescent lifetime variation and the phosphorescence yield variation emphasizes the quality of the proposed mechanism. It should be emphasized that while other processes may occur, they do not reach detectable levels.

Comparison with biacetyl might reveal what these undetectable processes in pentanedione could be. This comparison will also serve to contrast the behaviour of the two compounds in terms of the effect caused by substitution of a methylene group in the biacetyl molecule.

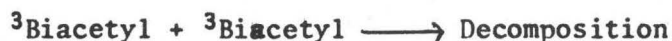
Comparison with Biacetyl

The variation of the fluorescence yield of pentanedione with temperature is similar to that of biacetyl. Groh (67) reports that a reduction of approximately 30% is observed for the fluorescence yield at 200°C compared with 30°C. The variation of the phosphorescence yield with temperature at 436 nm was studied by Coward and Noyes (164). These workers conclude that the variation is complex at temperatures between 30°C and 80°C but shows a definite reduction in the phosphorescence yield. This reduction correlates well with the observed reduction in phosphorescent lifetime between 20° and 80°C (31). Above 80°C, the variation became more regular with temperature. The dependence of the phosphorescence yield over the range 30° to 200°C could be described

by the equation,

$$\frac{1}{\phi_p} = 5 + 3 \times 10^6 \exp(-9000/RT)$$

The variation of the phosphorescent lifetime has not been studied at the higher temperatures used in the study of Coward and Noyes, so the observed dependence for the phosphorescent yield could not be directly associated with a process removing the triplet state. These results are questionable, however, in the view of the elegant experiments of Noyes, Mulac and Matheson (26). In a study carried out using chopped 436 nm excitation, simultaneous measurements of phosphorescence intensity and decomposition yields allowed the source of photochemical decomposition to be identified as the triplet state of biacetyl. At low temperatures, less than 50°C, the major source of decomposition was from the triplet-triplet annihilation reaction,



Whereas, at temperatures above 100°C, the major source of decomposition was due to the thermal decomposition of the triplet biacetyl,



The activation energy for the decomposition was estimated as 15 Kcals mole⁻¹. This value is close to the estimate, 16.5 Kcal mole⁻¹, derived indirectly from photolysis studies at this wavelength (27). The variation of the unimolecular rate coefficient with pressure was such that it was estimated to reach one-half of its limiting high pressure

value at 12 torr. This is a reasonable figure for a molecule containing 12 atoms (118).

It seems then that the variation of the phosphorescence yield with temperature is governed mainly by the thermal decomposition of the triplet state. Conclusions regarding the variation of the fluorescence yield are not based upon such solid experimental facts. The original suggestion (7) that the equilibrated level of the singlet state could thermally decompose with an activation energy of 16 Kcal has since been discarded, leaving the explanation of the effect open to conjecture.

It is interesting to estimate what effect the introduction of a thermally induced decomposition of the triplet pentanedione would have on the description of the system. If it is assumed that the activation energy calculated for biacetyl can be applied, and if the pre-exponential factor for the unimolecular reaction in its high pressure limit is $\sim 10^{13}$ then at 90°C the magnitude of the decomposition rate constant is,

$$k_{\text{unimolecular decomposition}} \sim 10^{13} \exp(-15,000/RT)$$

$$\sim 1 \times 10^4 \text{ s}^{-1}$$

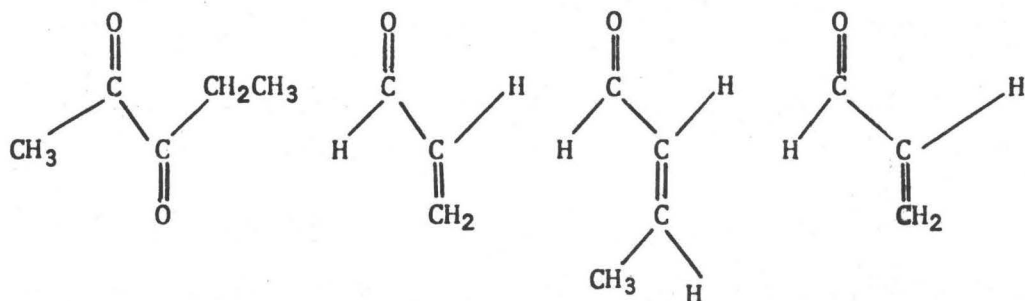
Reference to the phosphorescent lifetime of pentanedione reveals that the radiationless processes removing the triplet pentanedione at low pressures have the magnitude $2.5 \times 10^4 \text{ s}^{-1}$. That it is not necessary to invoke the thermal decomposition of the triplet pentanedione by fragmentation indicates that in the sample calculation above the parameters should be modified for pentanedione so that the magnitude of the rate constant is reduced. The radiationless rate constant which controls the

temperature dependence of the phosphorescent lifetime at low pressures has already been assigned to a unimolecular reaction corresponding to intramolecular hydrogen atom abstraction. This assignment was based on the characteristics of the Arrhenius parameters which described the rate constant and on photochemical evidence. That there might be alternative processes available to the pentanedione molecule illustrates the increased complexity of the system compared to that of biacetyl. The participation of a fragmentation mode in pentanedione, in addition to the intramolecular mode would call for a study of the phosphorescent lifetimes at higher temperatures. Under these conditions the contribution from the fragmentation mode would be enhanced relative to the intramolecular mode and would be more amenable to detection. Unfortunately, the diagnosis of this dual behaviour would present experimental problems in that it would require the measurement of phosphorescent lifetimes $< 10^{-6}$ s at low pressures. It is reasonable to assume that any unimolecular decomposition behaviour in a pentanedione (15 atoms) would be in its high pressure limit at pressures greater than a few torr. This would mean that any deviations due to the introduction of a second unimolecular reaction route would become evident in the lifetime at low pressure.

CHAPTER 9

QUENCHING OF TRIPLET PENTANEDIONE BY α,β UNSATURATED CARBONYL COMPOUNDS

The discovery of the interaction of T_1 pentanedione molecules with ground state diketone molecules prompted the investigation of acyclic α,β unsaturated ketones as possible quenchers. This class of materials were chosen due to the strong structural similarities with the conjugated dicarbonyl system.

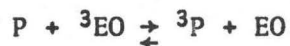


This investigation proved to be fruitful in that the three acyclic conjugated enones shown above were found to quench the phosphorescence of the diketone. The removal of triplet pentanedione molecules by interaction with ground state α,β unsaturated carbonyl compounds was studied using the phosphorescent lifetime apparatus described earlier. The technique involved use of a fixed pressure of diketone and measurement of the increased rate of decay in the presence of variable amounts of the quenching gas. In all cases, the decay of the phosphorescence was described by a simple exponential form indicating that the removal

of the T_1 species was via processes which were first order in the T_1 concentration. The results of experiments using acrolein, crotonaldehyde and methyl vinyl ketone at various temperatures are shown in Fig. 41-44. It should be noted that the available concentration range for a quenching material is limited by its vapour pressure at the temperature of the experiment. In this series of experiments the maximum pressure of quencher was ~ 0.8 x equilibrium vapour pressure, to avoid complications due to non-ideal behaviour.

The values of quenching rate constants, k_Q , for the various quenchers at various temperatures are shown in Table 8. It should be noted that the common feature to the behaviour of all the quenching materials is that the value of k_Q increases as the temperature is increased.

Control experiments were carried out with each quencher to determine if electronically excited triplet eneone molecules formed under these conditions could be capable of transferring electronic energy back to the ground state diketone molecule, i.e.



Despite the use of sensitive detectors, no evidence was obtained for this reaction occurring in the gas phase under the experimental conditions.

Discussion

The results of the quenching experiments are well described by a linear relationship between τ^{-1} and the concentration of the quenching material. The value of the quenching rate constant is derived from the

Fig. 41 Quenching of pentanedione triplet lifetime by acrolein at 42.2°C (23PD = 10 torr) and 50.8°C (23PD = 12.1 torr).

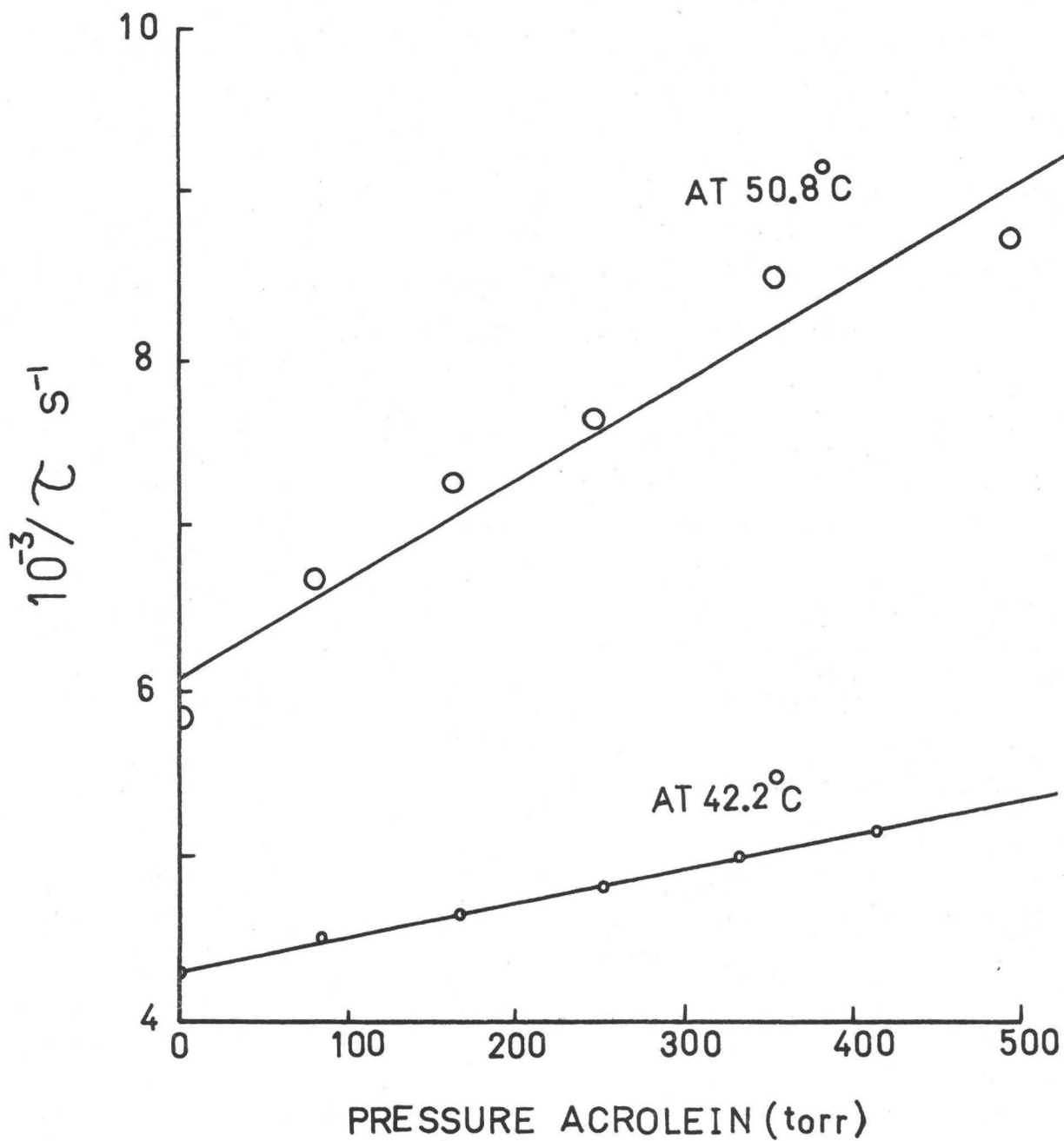
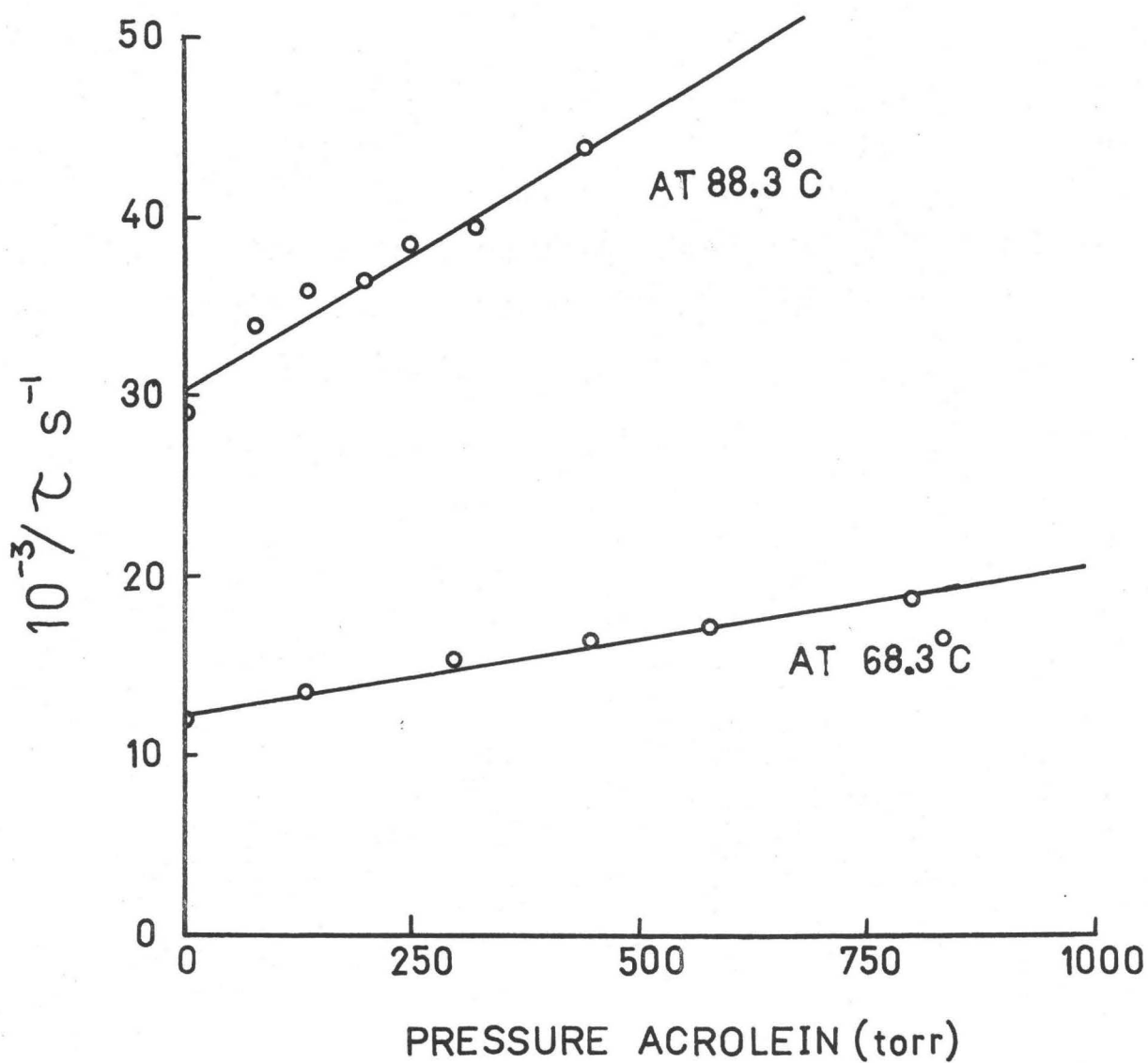


Fig. 42 Quenching of pentanedione triplet lifetime by acrolein at 68.3°C (23PD = 13.5 torr) and 88.3°C (23PD = 15.7 torr).



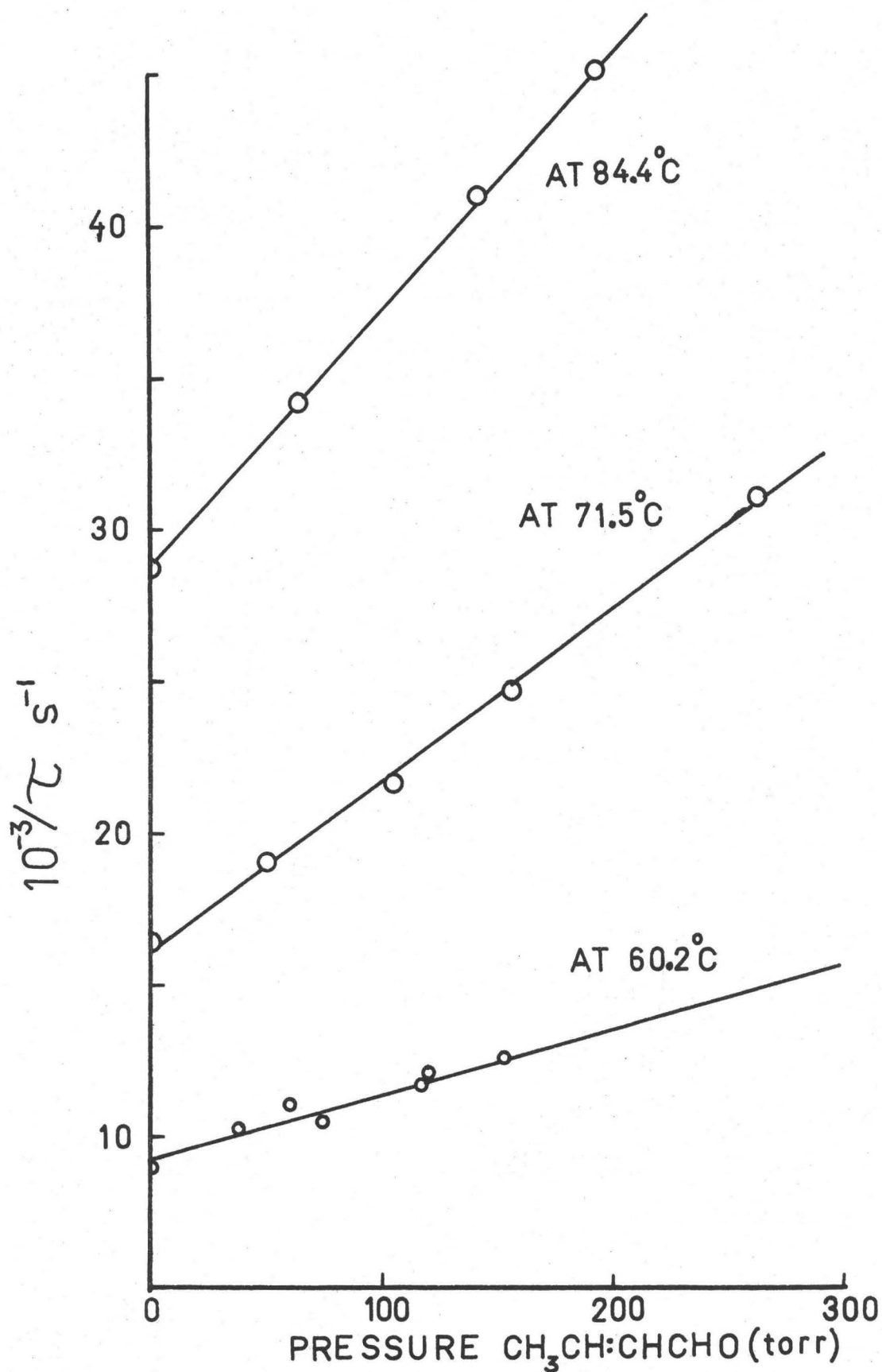


Fig. 43 Quenching of pentanedione triplet lifetime by crotonaldehyde

at 60.2, 71.5, 84.4°C.

Fig. 44 Quenching of pentanedione triplet by methyl vinyl ketone at 62.5, 70.8, 80.5°C.

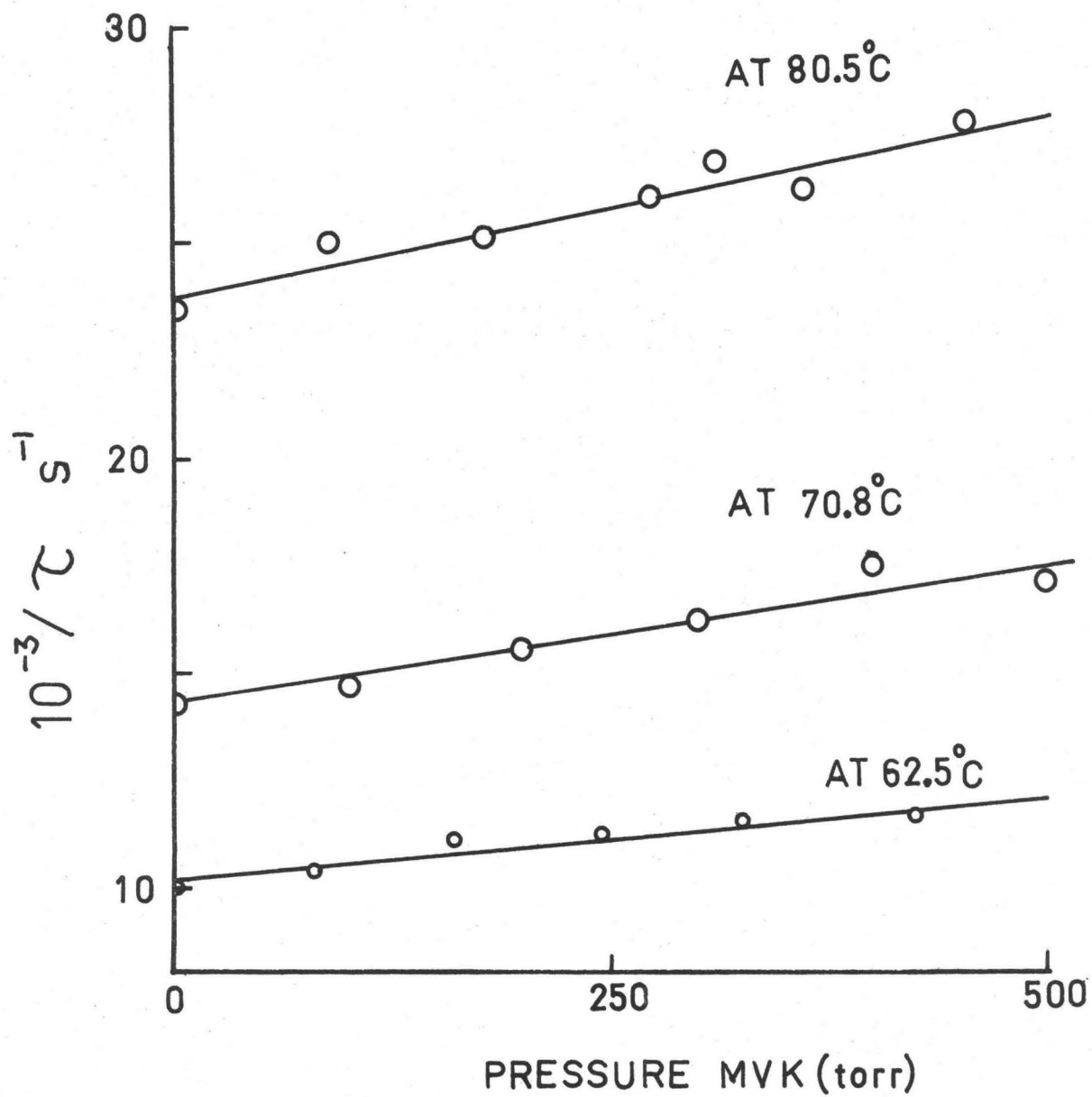


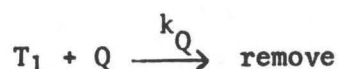
TABLE 8. RATE CONSTANTS FOR QUENCHING OF TRIPLET 2,3 PENTANEDIONE
BY ENEONES

ACROLEIN	CROTONALDEHYDE	METHYL VINYL KETONE
3.8×10^4 at 42.2°	4.6×10^5 at 60.2°	6.8×10^4 at 62.5°
1.1×10^5 at 50.8°	1.0×10^6 at 71.5°	1.1×10^5 at 70.8°
1.5×10^5 at 68.3°	1.6×10^6 at 84.4°	1.5×10^5 at 80.5°
5.5×10^5 at 88.3°		

equation,

$$\tau^{-1} = \tau_0^{-1} + k_Q[Q]$$

where τ_0 is the lifetime of the phosphorescence emission in the absence of quencher, k_Q is the bimolecular quenching rate constant and $[Q]$ is the concentration of the quencher. This expression results from a mechanism whereby the addition of a quencher causes the removal of T_1 by a simple bimolecular process.



When the quenching rate constants for the eneones are plotted in the form $\log k_Q$ vs T^{-1} , Fig. 54, it is found that over the temperature range studied the rate constants can be expressed in the Arrhenius form:

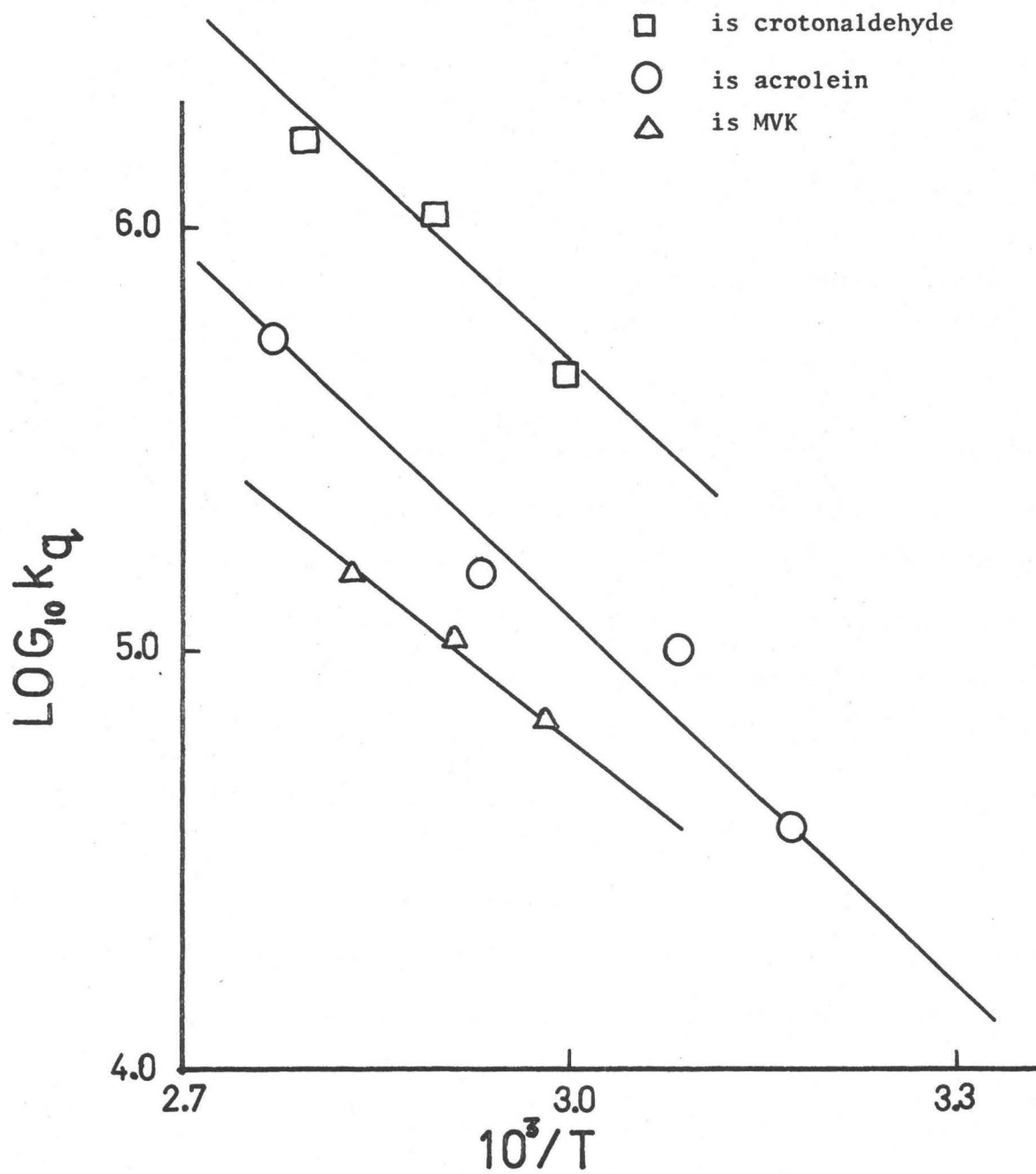
for acrolein $k_Q = 10^{14.0 \pm 1.5} e^{-(13.7 \pm 2.1)/RT} \text{ M}^{-1}\text{s}^{-1}$

for crotonaldehyde $k_Q = 10^{13.8 \pm 1.5} e^{-(12.4 \pm 2.4)/RT} \text{ M}^{-1}\text{s}^{-1}$

for methyl vinyl ketone $k_Q = 10^{11.7 \pm 1.0} e^{-(10.4 \pm 1.5)/RT} \text{ M}^{-1}\text{s}^{-1}$

The errors in the pre-exponential factors and the activation energy are large because only a short temperature range is experimentally accessible. This constraint results from the reduced magnitude of the quenching rate constants at lower temperatures together with the reduced concentration range accessible to the quencher. Under these conditions, detection of the quenching effect becomes difficult. Similarly, at higher temperatures, the lifetime of the pentanedione is inherently shorter, as described in Chapter 5, and detection of the

Fig. 45 Arrhenius plots for eneone quenching rate constants.



quenching effect becomes difficult. Although the quenching rate constants are not large, it is unlikely that impurities could explain the observations; being present in small amounts, they would entail an unrealistically high value for the pre-exponential factor.

Similarities with the self-quenching found in the diketone are displayed by

- (a) the temperature dependence found for the self-quenching constants and for the three eneone quenching systems investigated,
- (b) the high pre-exponential factors found in all cases.

The quenching process of eneone on triplet pentanedione is bimolecular and the temperature dependence of the quenching rate constant indicates that an energy barrier exists for the reaction. This barrier might correspond to an activation energy in a chemical reaction or to the conversion of electronic energy of the diketone and vibrational energy of both molecules into electronic energy of the eneone. These processes could be represented by,



- (i) On the basis of electronic energy transfer, the known reactions of excited triplet carbonyl compounds, two alternatives can be considered for the chemical interaction with eneones. These alternatives are hydrogen atom abstractions by the carbonyl function of the diketone from the substrate molecule, or formation of cyclo addition products with the carbon carbon unsaturated

centre in the eneone molecule. It is known that carbonyl compounds resemble alkoxy radicals in their reactivity towards hydrogenated substrate (106,3). Evidence is available to demonstrate that abstraction of a hydrogen atom occurs in the reaction between tertiary butoxy radicals and acrolein in the solution phase (145); cyclo-addition also takes place in this case, but with reduced efficiency.

Photo-induced reaction between electronically excited diketone compounds and eneones has not been demonstrated in this study as no attempt was made to analyze the products. However, the possibility of photoaddition exists in the light of evidence that triplet biacetyl will form stable products with a variety of unsaturated molecules including 2-methyl-2-butene, furan, indene, and ethyl vinyl ether (146). Similarly, it is known that complex products are isolated from the photolysis in solution of a α -diketone in the presence of dienes (147).

- (ii) The energy of the lowest triplet state of pentanedione has been shown earlier to be about 55 Kcal, however, the triplet energies of the unsaturated ketones are less certain. These uncertainties arise from the lack of direct evidence and, also, complications over the ordering of the $n\pi^*$ states in these molecules. On the basis of spectroscopic evidence (141,142), it has been suggested that the lowest planar triplet state of acrolein is $n\pi^*$ with $E_T = 69$ Kcals. There is a report that the $n\pi^*$ triplet energy of crotonaldehyde is similar (143). Unfortunately, no information

is available concerning the triplet energy of methyl vinyl ketone. To argue by analogy using the substitution effects found in aliphatic compounds is unreliable due to the sensitivity of the triplet $n\pi^*$ and $\pi\pi^*$ levels in eneones to substitution effects (144). However, it is possible that there is a planar triplet of methyl vinyl ketone with lower energy than that of acrolein. Therefore, it is possible that the activation energies found for the quenching processes in these compounds could correspond to endothermic energy transfer. If energy transfer were the mode of quenching in this case, then reverse energy transfer from the triplet state of the eneone to the ground state of the diketone could complicate the kinetics.



Here P represent diketone and EO represent the eneone. This possibility was explored by irradiating a sample of the diketone with the eneone in the gas phase at 313 nm, at the temperature of the quenching experiment. This caused excitation of the eneone almost exclusively. It is known that intersystem crossing from the S_1 manifold to the T_1 manifold is efficient in conjugated eneones (106). Therefore, irradiation at 313 nm forms T_1 eneone species in the gas phase. Depending on the lifetime of this species and the probability of energy transfer from the eneone $E_T \sim 70$ Kcal to the ground state diketone $E_T \sim 54$ Kcals, sensitized phosphorescence emission of the diketone may be observed. As has been explained earlier, control experiments showed that the sensitized emission

of pentanedione could not be detected. This is presumably due to the very short lifetime of the planar triplet eneone which has been shown to relax to a twisted form whence intersystem crossing to the ground state is very efficient (144).

As will be discussed later in Chapter 11, the mechanism of energy transfer is not completely understood but some deductions can be made for the process if it involves thermal activation. The conversion of the deficit in electronic energy from vibrational energy of the pair must necessarily involve the perturbation of the isolated molecule description such that the Born-Oppenheimer approximation is invalid. The conditions necessary for this breakdown could be a perturbation resulting from charge transfer, dipole-dipole attraction or Van der Waals interactions. The fate of the encounter complex between acceptor and donor depends upon the rates of the various radiationless processes available to it. These could be 'intra-molecular' transfer of electronic energy, corresponding to the energy transfer process, radiationless decomposition corresponding to an uneventful encounter or bond making or breaking leading to a stable or metastable intermediate(s).

CHAPTER 10

QUENCHING OF THE TRIPLET STATE BY A VARIETY OF MOLECULES

The interaction of the triplet pentanedione molecule with different compounds was investigated to demonstrate the existence of different quenching modes for excited molecules. The compounds were chosen so that they represented a variety of different molecular properties and functional groups. They are classified below according to their particular characteristics, together with the experimental method by which the quenching efficiency was found.

Oxygen

This molecule is known to exist in a triplet ground state (55) which is, therefore, paramagnetic. The ability of this compound to quench a wide variety of triplet organic molecules is of current interest (148). The quenching rate constant with triplet pentanedione was determined by measuring Q_p , the relative quantum yield of phosphorescence of a fixed amount of pentanedione in the presence of varying amounts of oxygen using the apparatus described in Chapter 2. Radiation of wavelength 405 nm was used. Complications due to the possible interference of collisional deactivation phenomena within the singlet manifold were overcome by carrying out the experiment in the presence of ~ 400 torr of sulphur hexafluoride.

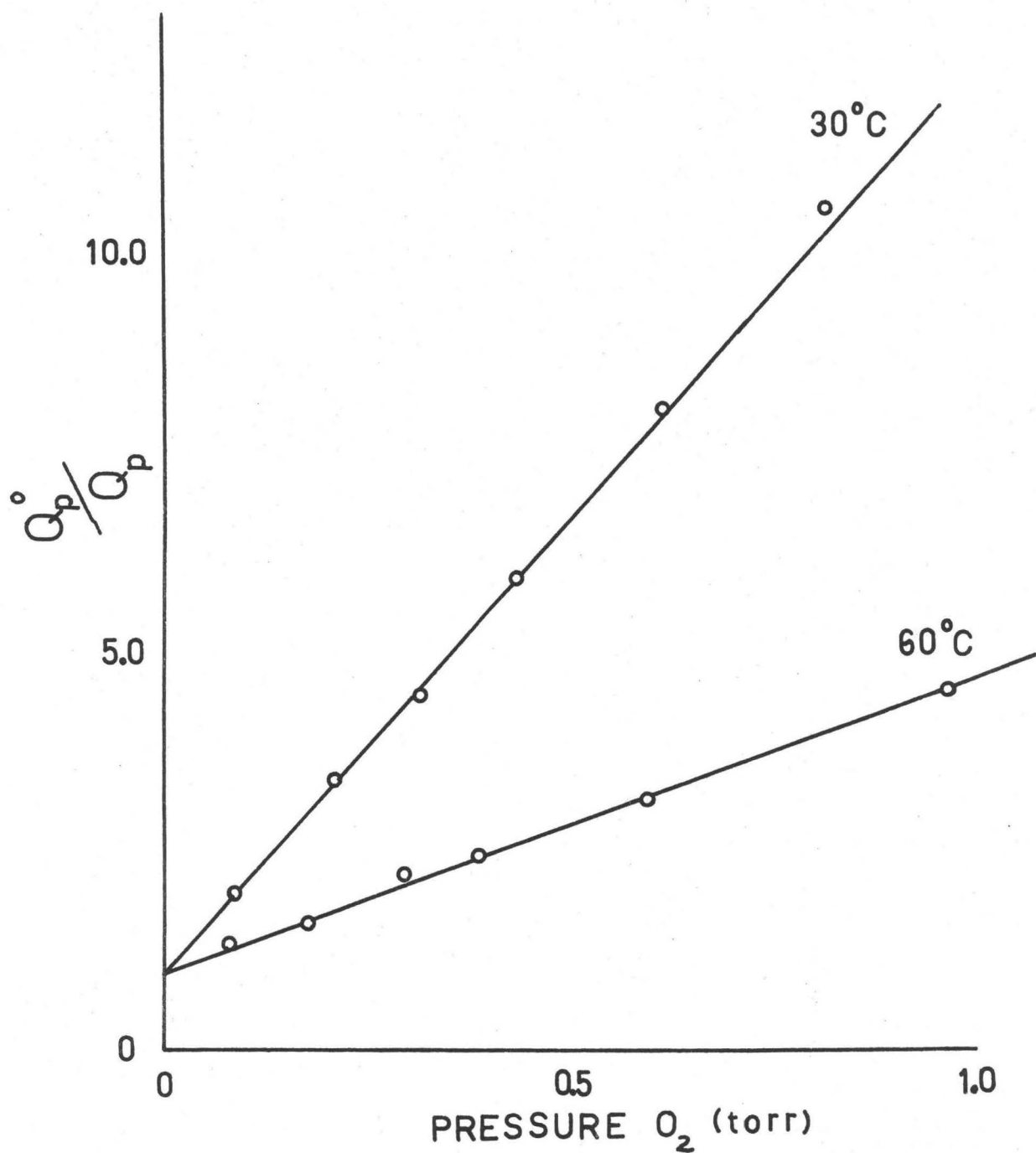


Fig. 46 Quenching of Pentanedione Triplet by O_2 at 30°C and 60°C.

The results of these experiments at 30°C and 60°C are presented in Fig. 46 as Stern-Volmer quenching plots.

Xenon

At the time this research was being carried out, a report appeared in the literature (149) of a quenching effect of xenon on the phosphorescence yield of biacetyl. This could have been interpreted in terms of increased spin-orbit interaction between the triplet state and the ground state due to a collision with a heavy atom. It was decided to investigate this effect in pentanedione. The experimental method involved measurement of the phosphorescent lifetime of pentanedione in the presence of varying amounts of xenon. The results of this experiment, carried out at 30°C, are presented in Fig. 47.

Isobutane

It is well known (106) that one of the characteristic reactions of the triplet carbonyl compounds is abstraction of a hydrogen atom from a substrate molecule. Isobutane might represent a substrate in such a reaction. The experiment was conducted by measuring the phosphorescence lifetime in the presence of various amounts of added quencher. The results of experiments carried out at 30°C and 50°C are shown as reciprocal lifetime variations in Fig. 48.

Germane

As hydrogen atom abstraction by the triplet diketone is a chara-

Fig. 47 Effect of Xenon on the Triplet Lifetime of Pentanedione at 30°C.

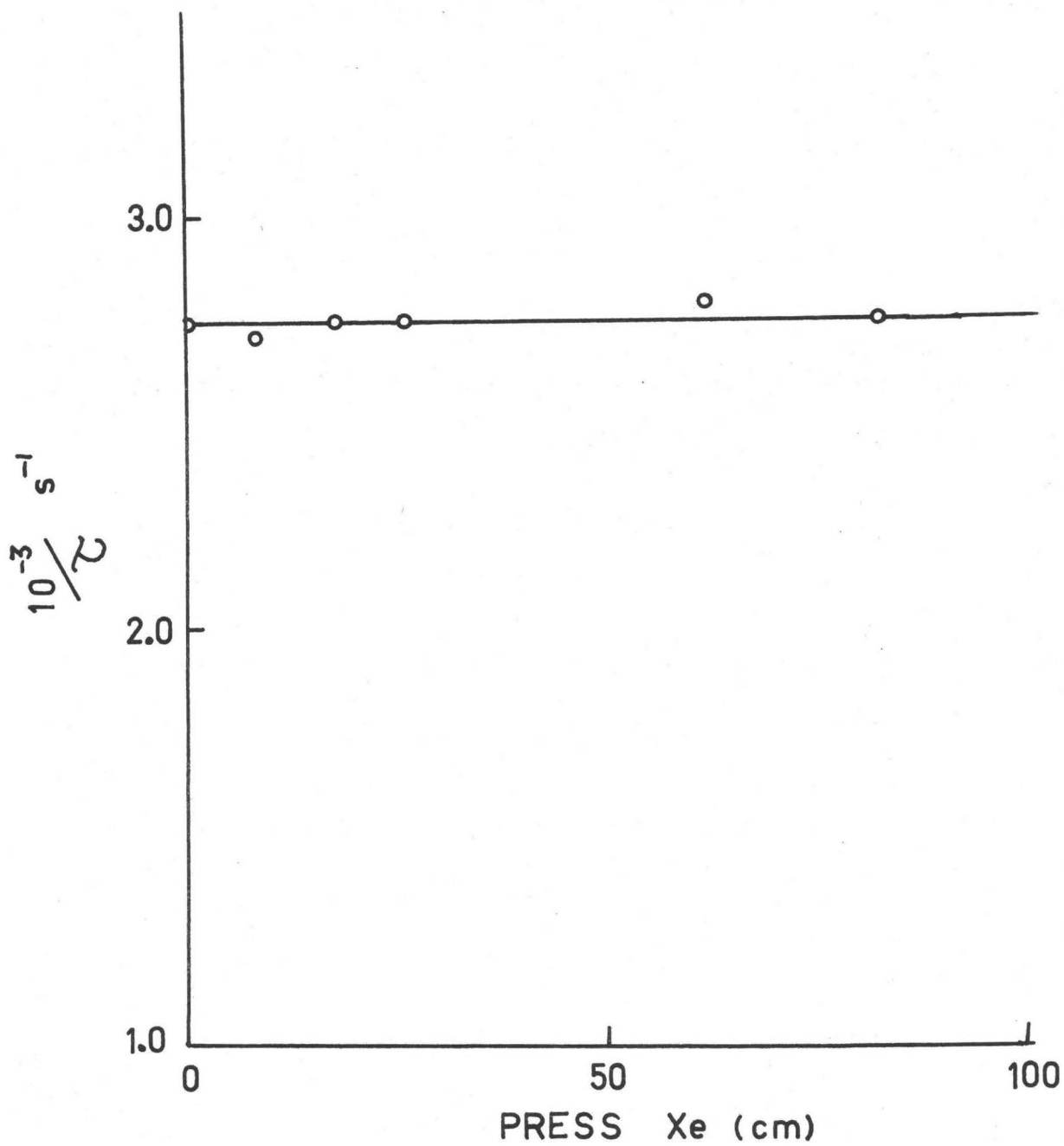
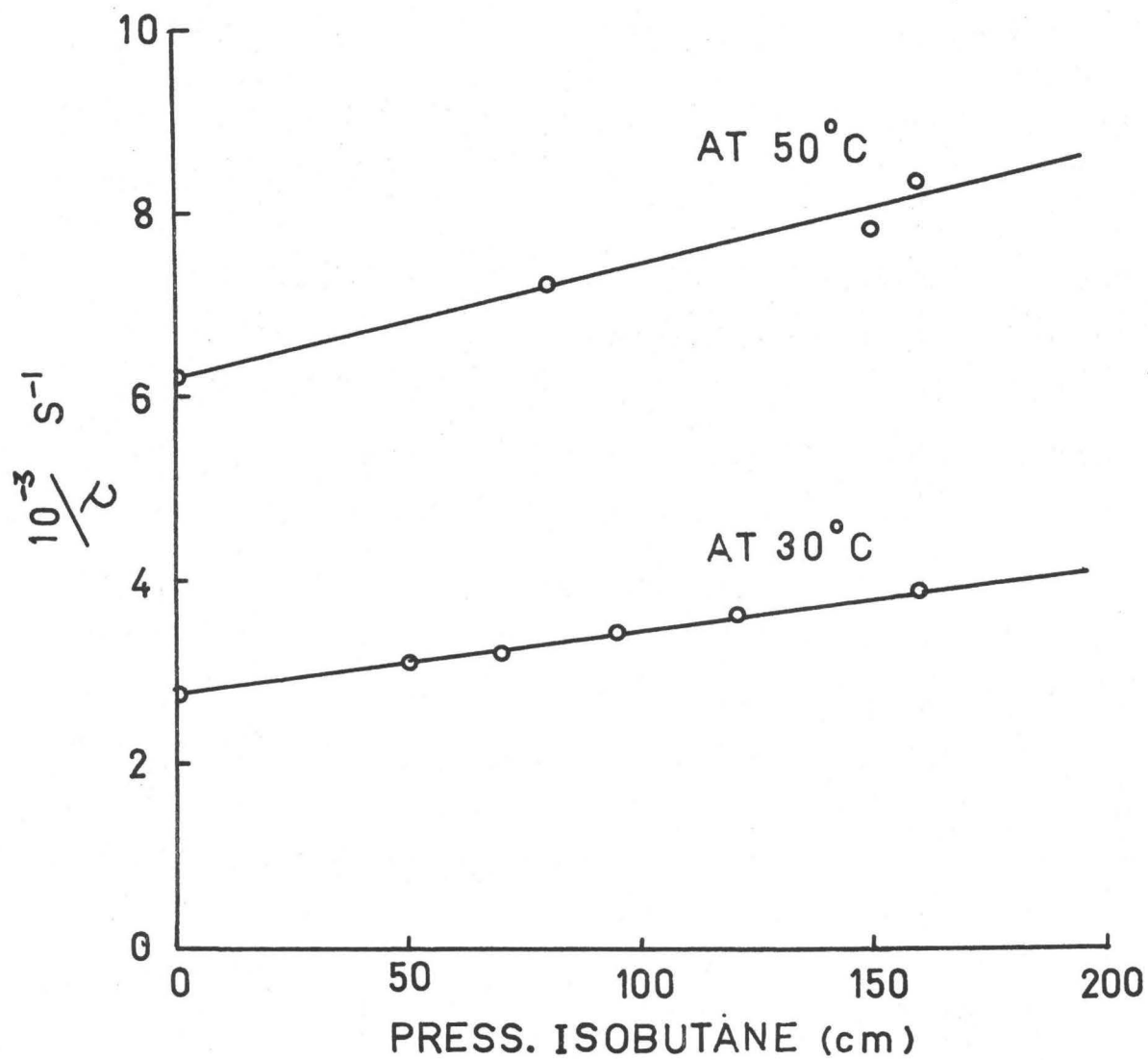


Fig. 48 Quenching of Pentanedione Triplet by Isobutane at 30°C and 50°C.



characteristic reaction, the ease of this reaction might depend upon the bond energy of the hydrogen atom to be abstracted. It was thought that germane would represent a suitable test molecule as the average bond energy has been estimated at 69 Kcal (150) which can be compared with the t-Butyl-H bond energy of 91 Kcal (124). The phosphorescent lifetime technique was used to detect quenching of the triplet state of pentanedione. The results of experiments carried out at 22°C and 68°C are shown in Fig. 49.

Furan

The quenching ability of dienes towards diketones is well known and has been studied in another part of this work (Chapter 11). The substitution of an oxygen atom for the CH₂ entity in cyclopentadiene is an interesting structural modification. The effect of this modification on the quenching characteristics may give insight into the general aspects of the interaction of electronically excited molecules with ground state molecules. Experiments were conducted using the phosphorescent lifetime apparatus with variety of pressures of furan at 30°C and 72.4°C. The results of the experiments are shown in Fig. 50.

Perfluorobutene-2

The weak quenching ability of olefins towards diketone triplet molecules is already known (151). It was decided to study the effect of temperature on this process using perfluorobutene-2. This compound was chosen so that possible complications due to competing hydrogen atom

Fig. 49 Quenching of Pentanedione Triplet by Germane at 30°C and 67.8°C.

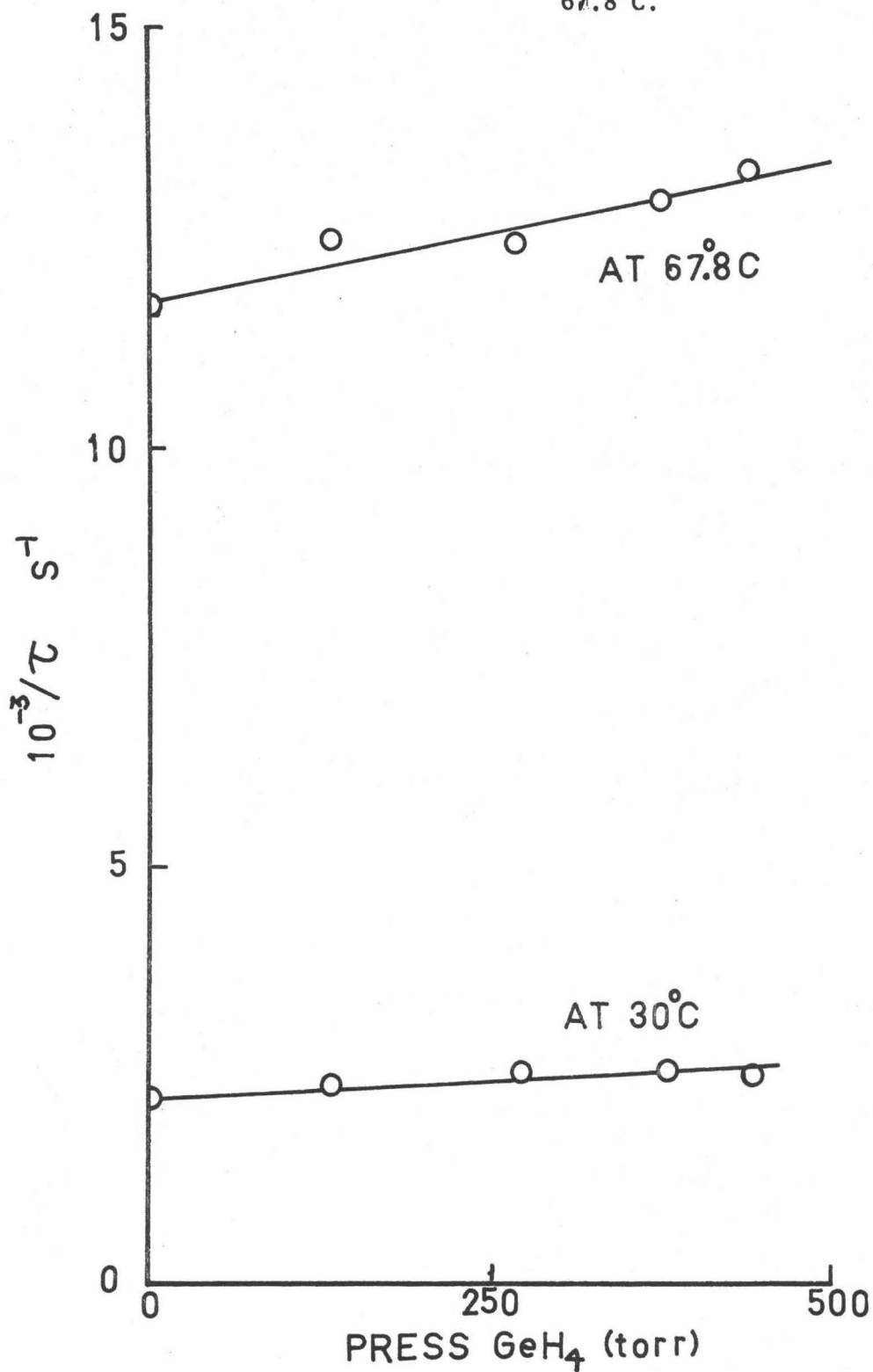


Fig. 50 Quenching of Pentanedione Triplet by Furan at 30°C and 72.4°C.

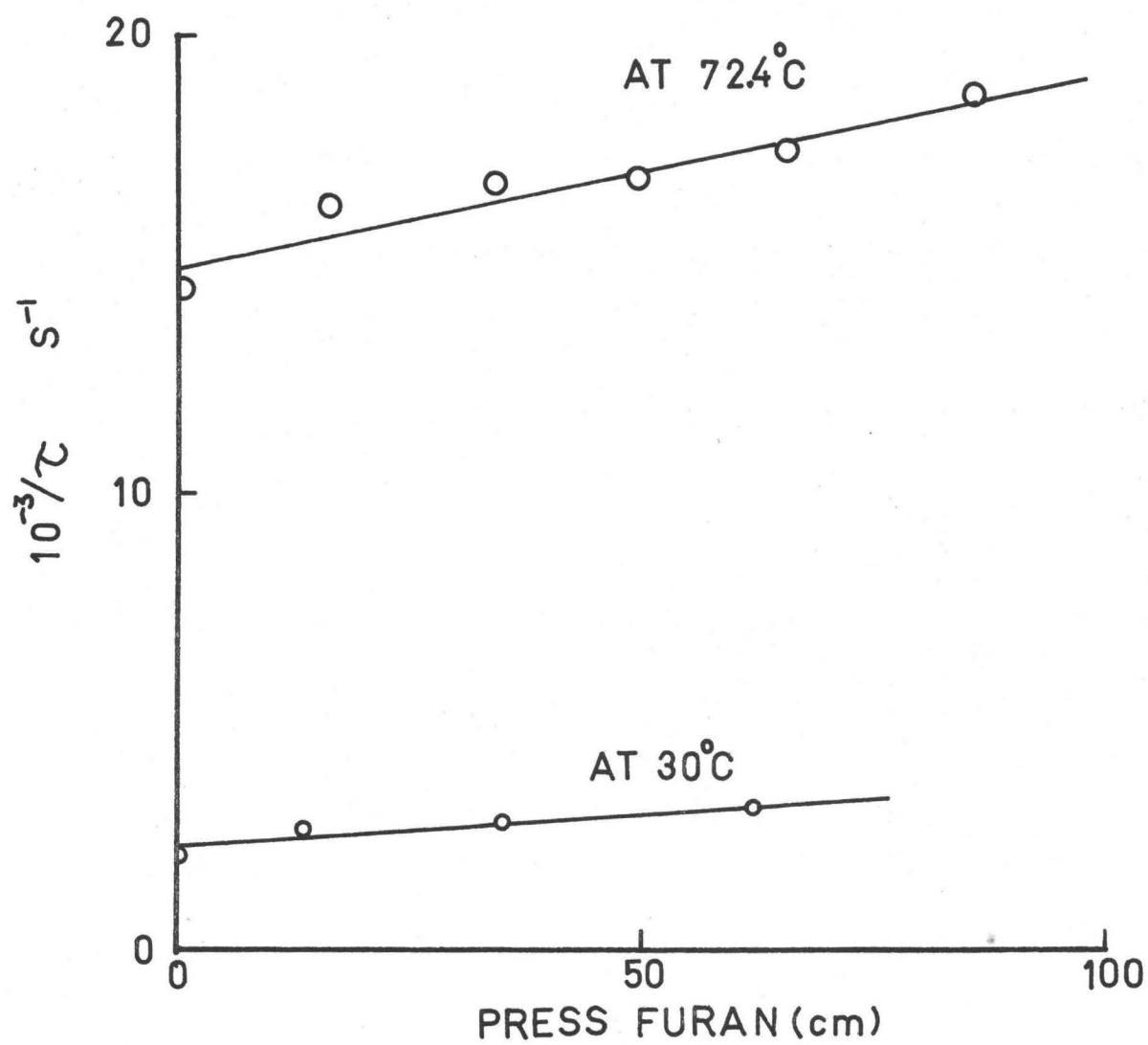
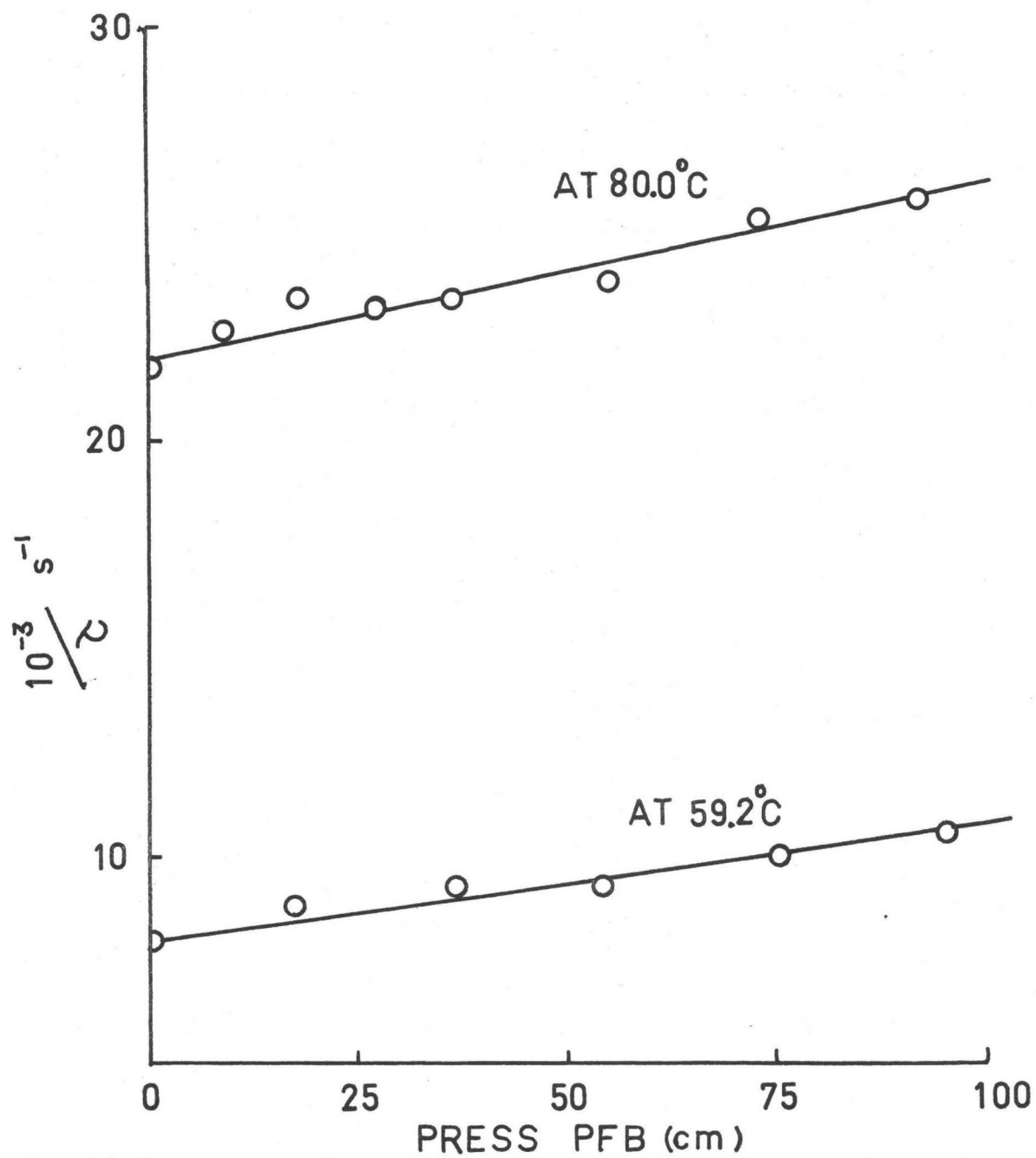


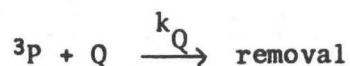
Fig. 51 Quenching of Pentanedione Triplet by Perfluorobutene-2 at 59.2°C and 80.0°C.



abstraction reactions by the diketone could be dismissed. The phosphorescent lifetime technique was used at 59°C and 80°C. The results of these experiments are shown in Fig. 51.

Discussion

The values of the bimolecular quenching rates constants found in this study have been collected for convenience in Table 9. They were derived from a mechanism in which the interaction of the quenching molecule with the triplet molecule was a simple bimolecular step.

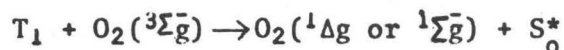


$$\tau^{-1} = \tau_o^{-1} + k_Q[Q]$$

The quenching ability of the various compounds will be discussed separately except where comparisons are useful.

Oxygen

The ability of oxygen to quench the triplet states of many organic molecules is well known (148). This property could be attributed to enhanced spin-orbit coupling in the triplet organic molecule in the presence of the oxygen molecule or to a pseudo-annihilation process, namely,



where S_o^* is a vibrationally excited level of the ground state.

This problem has been studied theoretically by Kawaoka and Kearns (152) who conclude that the annihilation process is 10^2 or 10^3

TABLE 9. QUENCHING CONSTANTS FOR VARIOUS SUBSTRATES.

Substrate	Quenching Constant $M^{-1}s^{-1}$
Oxygen	$(5.5 \pm 0.3) \times 10^8$ at $30^\circ C$
	$(5.6 \pm 0.3) \times 10^8$ at $60^\circ C$
Isobutane	$(1.20 \pm 0.2) \times 10^3$ at $30^\circ C$
	$(2.2 \pm 0.3) \times 10^4$ at $50^\circ C$
Germane	$(\sim 8 \times 10^3)$ at $22^\circ C$
	$(6 \pm 2) \times 10^4$ at $67.8^\circ C$
Furan	$(8.4 \pm 2.6) \times 10^3$ at $30^\circ C$
	$(7.8 \pm 1.0) \times 10^4$ at $72.4^\circ C$
Perfluorobutene-2	$(3.5 \pm 0.6) \times 10^4$ at $59.2^\circ C$
(PFB)	$(7.8 \pm 1.1) \times 10^4$ at $80.0^\circ C$

more important than the contribution from enhanced spin-orbit coupling within the organic triplet molecule. What is more, the efficiency of the annihilation reaction depends entirely on Franck-Condon factors between the T_1 and S_0^* states. The agency by which energy is transferred to the oxygen molecule depends less on exchange interactions than on the intervention of charge transfer virtual states.

In the case of pentanedione, $E_T \sim 55$ Kcal, it can be predicted that the annihilation reaction will proceed so as to give $\sim 90\%$ $^1\epsilon\bar{g}$ ($E_S = 38$ Kcal) (55) and $\sim 10\%$ $^1\Delta_g$ ($E_S = 23$ Kcal) (55). This is the limiting distribution for interaction with organic molecules having triplet energies greater than 50 Kcal. According to the Kearns theory, the inherent inefficiency of the quenching process, i.e. its deviation from the classical collision frequency, will be governed by the Franck-Condon factors between T_1 and S_0^* .

This allows an interesting comparison to be made between pentanedione and biacetyl in the ability of their triplet states to be quenched by oxygen. In both cases, the quenching rate constant is independent of temperature (134), and has the same value. The average value of the oxygen quenching constant for biacetyl triplets taken from the literature (31,132,134) is $5.2 \times 10^7 \text{ M}^{-1}\text{s}^{-1}$ which can be compared with the value of $5.5 \times 10^7 \text{ M}^{-1}\text{s}^{-1}$ found for pentanedione in this study. This implies that the Franck-Condon factors in the two molecules are approximately the same. This result is not surprising as the excess energy to be dissipated as vibrational energy in S_0 is approximately the same in both cases. What is more, the interaction of the oxygen

molecule, which is small, is likely to involve only the dicarbonyl function, which can be expected to retain approximately the same vibrational characteristics in biacetyl and pentanedione.

Xenon

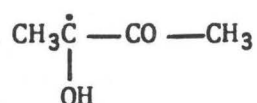
It can be seen from Fig. 47 that the phosphorescent lifetime of pentanedione does not change in the presence of xenon at 30°C. This is consistent with any enhancement of the intersystem crossing rate $T_1 \rightarrow S_0$ being small. The lifetime of the pentanedione and the accessible pressure range allow an upper limit of $\sim 5 \times 10^3 \text{ M}^{-1}\text{s}^{-1}$ to be placed on the magnitude of the bimolecular rate constant. Subsequent experiments (153) with biacetyl contradicted the original report of a quenching effect. It has since been discovered (154) that the original quenching effect observed in the biacetyl system was due to impurity. It would have been surprising if there had been an effect with xenon as the spin-orbit coupling is already large in dicarbonyl compounds (70,155) and would have called for an uncharacteristically high perturbation by the xenon atom.

Isobutane

The quenching ability of isobutane on the triplet pentanedione molecule is displayed in Fig. 48. The derived values of the bimolecular quenching constant at 30°C and 50°C are not large but display a definite temperature effect. Substitution into the Arrhenius equation gives the

parameters of k_Q as $\log A = 8.5 \pm 0.8$, $E_a = 6.1 \pm 2.6$ Kcal mole⁻¹.

It is known that triplet diketones will undergo photoreduction in the gas phase (156) and in solution phase (106) in the presence of a suitable hydrogenated substrate. An intermediate in the solution phase photoreduction of biacetyl has been identified as the semidione radical (156,157),



This is strong evidence in favour of a chemical interaction between the triplet diketone and the hydrogenated substrate resulting in hydrogen atom abstraction. It is suggested that the gas phase quenching by isobutane of pentanedione triplets occurs by this mechanism. The derived Arrhenius parameters are not inconsistent with a reaction of this kind. It is interesting to note that the gas phase quenching of biacetyl triplets by isobutane has been observed recently by Lissi (131). The value of the bimolecular quenching constant was 3.7×10^3 M⁻¹s⁻¹ at 25°C compared with the value of 1.2×10^4 M⁻¹s⁻¹ at 30°C for pentanedione triplet quenching found in this work.

Germane

The quenching of pentanedione triplets observed on the addition of germane is not large and the data show a good deal of scatter. Therefore, precise conclusions are not possible in this system. There is an indication, however, that the bimolecular quenching rate constant varies

with temperature.

The effect of changing the bond strength in the hydrogen containing substrate on the quenching efficiency towards triplet diketones has been observed by Turro and Engel (86). These workers found that tri-n-butylstannane quenched the phosphorescence of biacetyl with a rate constant of $1.5 \times 10^7 \text{ M}^{-1}\text{s}^{-1}$ in benzene solution at 25°C. This is a factor of 5×10^3 greater than the corresponding rate constant for isopropanol under the same conditions. It is difficult to place this effect on a quantitative basis, however, as the bond energy of the tin-hydrogen bond is not known.

The bond energy of the substrate bond which is broken in the abstraction reaction is not likely to be the only factor controlling the efficiency of the process. Stabilising features in the transition state and the stability of the radical pair produced will also influence the efficiency of the reaction.

Furan

The quenching behaviour of furan towards pentanedione triplets is particularly interesting as there is a structural resemblance between furan and cyclopentadiene,

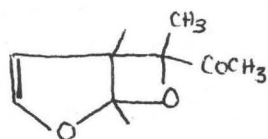


and the absorption systems in the far ultra-violet show strong similarities

(158). The quenching ability of cyclopentadiene towards pentanedione triplets will be demonstrated and the possibility exists that furan may display the same properties. Unfortunately, the first triplet level of this molecule has not been reported and, therefore, speculation concerning the possibility of energy transfer has to be limited.

It can be seen from Table 9, that the quenching rate constant is not large and does vary with temperature. Use of the Arrhenius equation, gives a value of $E_a = 11 \pm 2$ Kcal, and $\log A = 11.8 \pm 1.1$. In the cases of butadiene and cyclopentadiene, it is found that the quenching rate constant, attributed to energy transfer, did not vary with temperature (Chapter 11). Whether the quenching of furan corresponds to energy transfer is a moot point in the absence of an estimate of the triplet energy of this molecule.

An explanation of the quenching effect of furan is provided by the observation that furan will form 1:1 photoadducts with biacetyl (146). This adduct had the structure,



The multiplicity of the reacting state of biacetyl was not determined, neither was the stereochemistry of the product.

If it is the triplet state of biacetyl which is forming the oxetane with furan, then a similar reaction with pentanedione can be expected. The experimentally observed activation energy could correspond

to the formation of the 1,4 diradical which has been found to be a convenient intermediate to postulate in oxetane formation mechanisms. No activation energy information is available to allow comparisons.

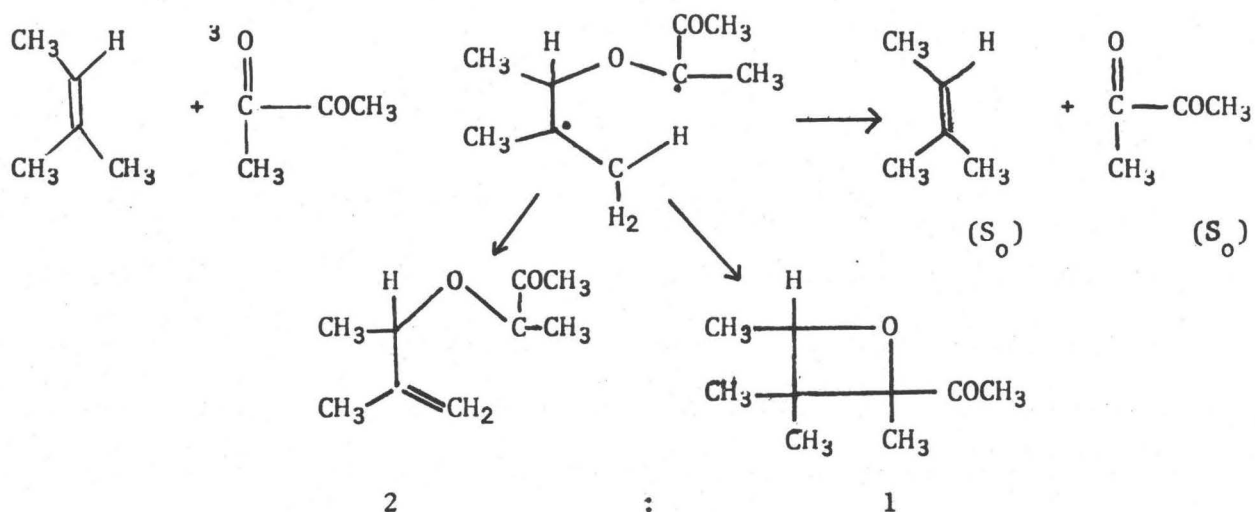
The formation of oxetane has been shown to occur between several triplet monoketones and alkenes (159-161). It has been suggested that it occurs when the alkene has a triplet energy comparable to or higher than the carbonyl compound so that energy transfer to the alkene is inhibited.

Perfluoro-2-butene

The quenching ability of perfluorobutene-2 with pentanedione triplets is demonstrated by inspection of Fig. 51. Experiments at 59.2°C and 80.0°C reveal that the bimolecular quenching rate constant has a definite temperature dependence. Insertion of the appropriate rate constants into the Arrhenius equation gives $E_a = 9 \pm 2$ Kcal and $\log A = 13 \pm 2$.

The behaviour of alkenes towards diketones was indicated by the work of Rebbert and Ausloos (151), who found the bimolecular quenching rate constant for 2,3-dimethyl-butene-2 with biacetyl triplets at 32°C was $2 \times 10^4 \text{ M}^{-1}\text{s}^{-1}$. These workers interpreted this inefficiency as being due to the large energy discrepancy, ~ 17 Kcal, between the triplet levels of the quencher and the quenchee in the energy transfer process. This interpretation is in doubt, however, in the light of evidence for chemical reaction between ketones and alkenes (19), when

the energy discrepancy is such that energy transfer cannot take place. In particular, it has recently been shown (146), that 1:1 photoaddition products are formed between excited biacetyl and alkenes. With 2-methyl-2-butene, the main products were an acyclic ether and an oxetane in the ratio 2:1. It is proposed that the reaction proceeds via the formation of a 1,4 diradical.



This species can then cyclize to give the oxetane or undergo a novel intramolecular hydrogen atom abstraction to give the unsaturated ether. It has been pointed out (3) that reactions of this kind, which have been reported for monoketones, can be reduced in efficiency due to competing reactions of hydrogen atom abstraction by the carbonyl group.

By analogy with the monoketone case, this photoaddition probably proceeds through the triplet state of the diketone. If this is the case, then an explanation is offered for the observed quenching of perfluoro-2-butene. What is more, the reaction if successful, can only proceed to

the oxetane product. This is because perfluorination of the molecule not only eliminates intermolecular hydrogen atom abstraction, but also prevents the formation of the unsaturated ether from the intermediate. The observed activation energy might then correspond to the formation of the 1,4 diradical intermediate. It should be noted that the close similarity proposed for the quenching by furan and perfluoro-2-butene is reflected in similar activation energies.

Conclusions

Quenching of the triplet state of pentanedione has been demonstrated for a variety of different compounds. Mechanisms have been proposed to explain the observations. The only compounds to show a significant variation of quenching efficiency with temperature are furan and perfluoro-2-butene. It is suggested that these compounds quench via 1:1 photoaddition reactions.

A more complete discussion of the quenching modes described above must await a detailed analysis of the photoproducts of these quenching reactions.

CHAPTER 11

QUENCHING OF TRIPLET PENTANEDIONE BY CONJUGATED DIOLEFINS

Results

The removal of triplet pentanedione molecules in the gas phase by interaction with conjugated diolefins was studied using the apparatus described earlier. The object was to determine the efficiency of this process and its variation with temperature. The increased rate of removal of T_1 species in the presence of a quenching material was measured by the decreased phosphorescent lifetime. In all cases, the decay was described by a simple exponential form, indicating that the removal of the T_1 species proceeded by processes which were first order in T_1 .

1,3-Butadiene

The results of experiments using 1,3-butadiene at 30°C and 70°C are presented as Stern-Volmer quenching plots of the phosphorescent lifetime in Fig. 52 and Fig. 53. At both temperatures, the variation of τ^{-1} with concentration is linear, indicating a simple bimolecular process for the removal of the T_1 species. The value of the quenching rate constant is derived from the equation,

$$\tau^{-1} = \tau_0^{-1} + k_Q[Q]$$

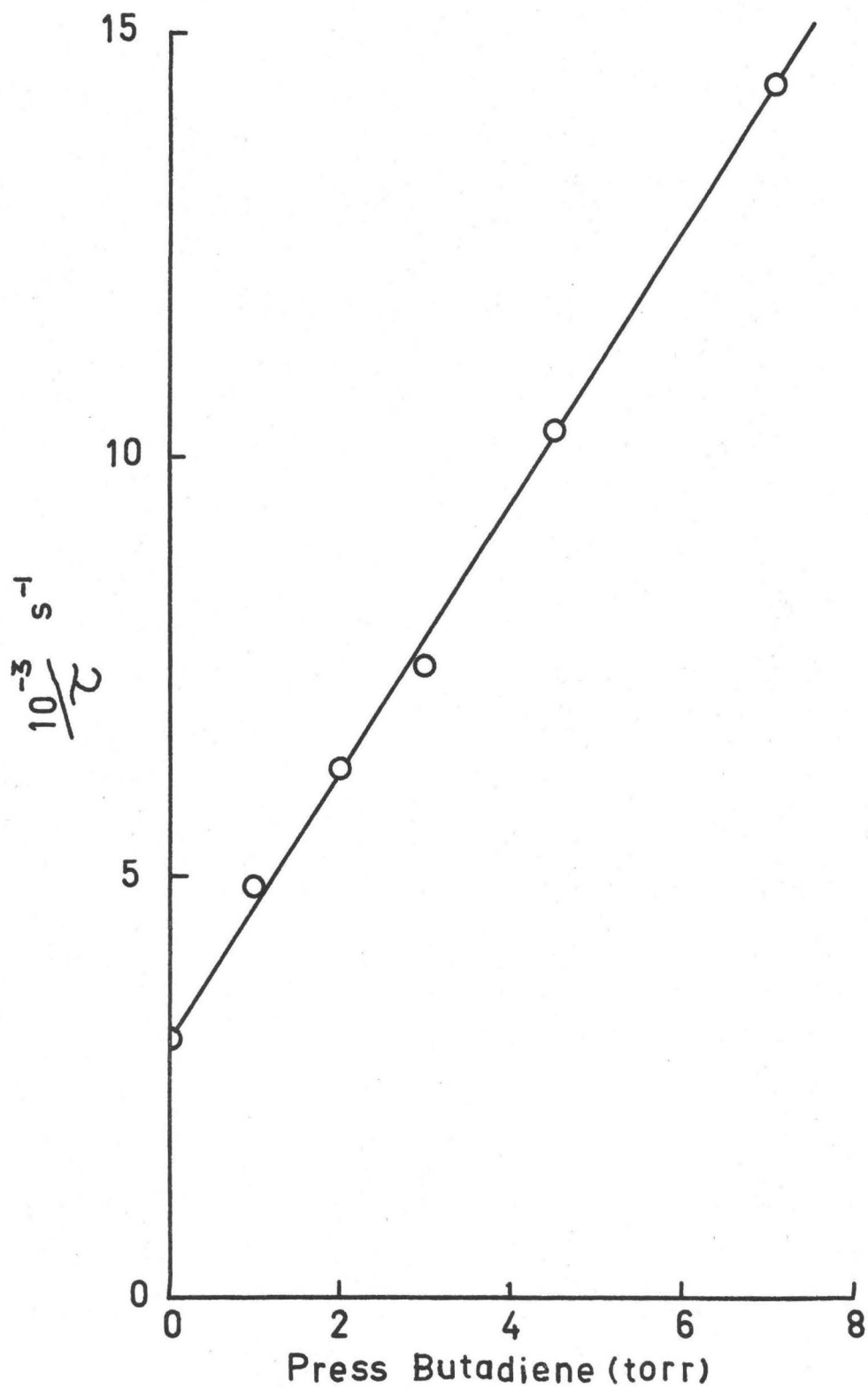
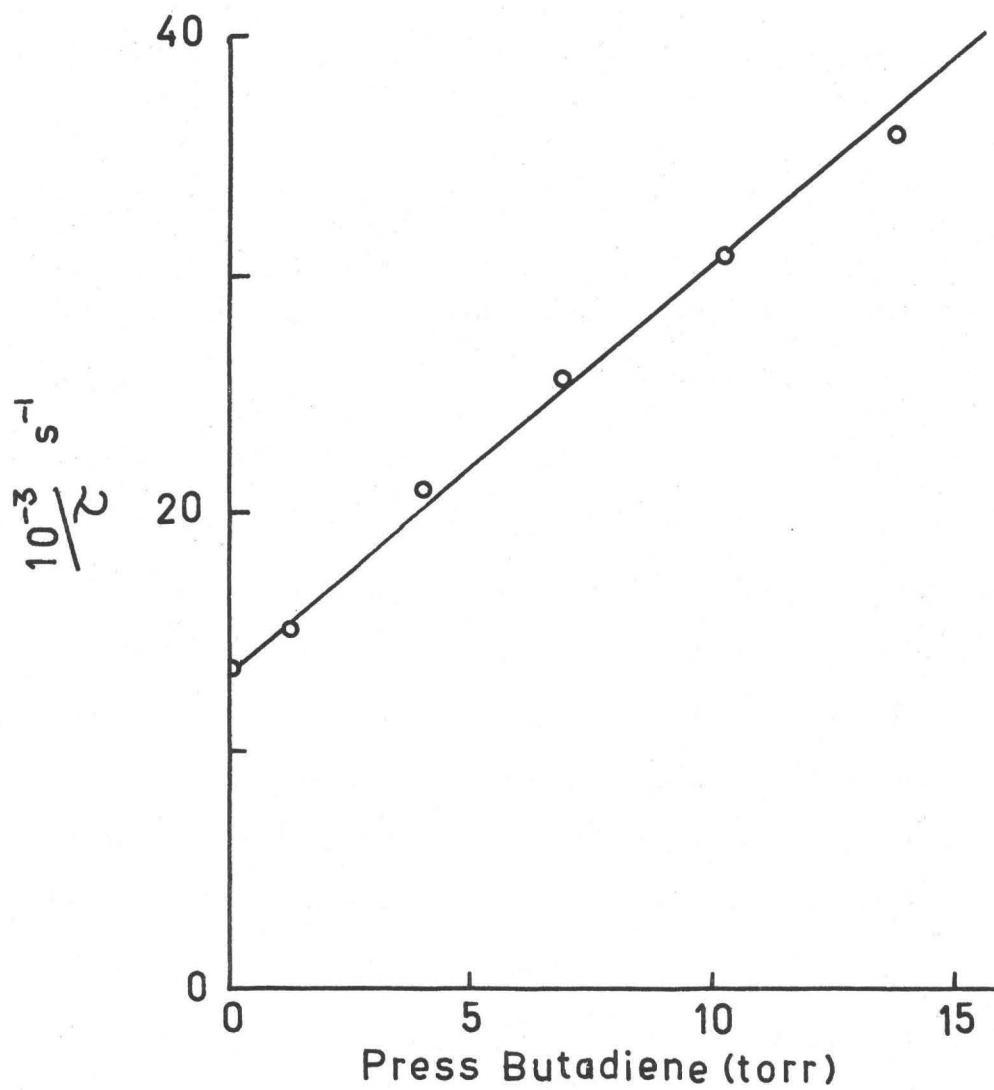


Fig. 52 Quenching of Triplet Pentanedione by 1,3 butadiene at 30°C;
(23PD = 10.9 torr).

Fig. 53 Quenching of Triplet Pentanedione by 1,3 butadiene at 70°C;
(23PD = 13.0 torr).



where τ_0 is the lifetime in the absence of quencher, k_Q is the bimolecular quenching rate constant and $[Q]$ is the concentration of quencher. The values of k_Q determined are $2.9 \times 10^7 \text{ M}^{-1}\text{s}^{-1}$ at 30°C and $3.1 \times 10^7 \text{ M}^{-1}\text{s}^{-1}$ at 70°C .

Cyclopentadiene

The effect of structure in the conjugated diolefin was investigated using cyclopentadiene (CPD) which had been freshly distilled before each experiment. This precaution was necessary due to the known high tendency of dimerisation (166) at room temperature. The determination of the quenching efficiency was made using the same method as for butadiene. At 68°C and 83°C , the decay of the phosphorescence was described by an exponential form and the quenching plots which were derived were linear. These are shown in Fig. 54. The values of the quenching rate constants derived from the simple equation given above are:

$1.53 \times 10^7 \text{ M}^{-1}\text{s}^{-1}$ at 68°C and $1.66 \times 10^7 \text{ M}^{-1}\text{s}^{-1}$ at 83°C .

The quenching behaviour at 30°C was, however, more complex. The decay of the phosphorescence was described by an exponential form, but the Stern-Volmer plots of τ^{-1} vs Cyclopentadiene concentration were not linear. The nature of this dependence was explored by performing quenching experiments using different concentrations of diketone. The results of these runs are shown in Fig. 55-59.

Discussion

The object of this study was to determine the nature of the interaction between the excited triplet diketone molecules and ground state

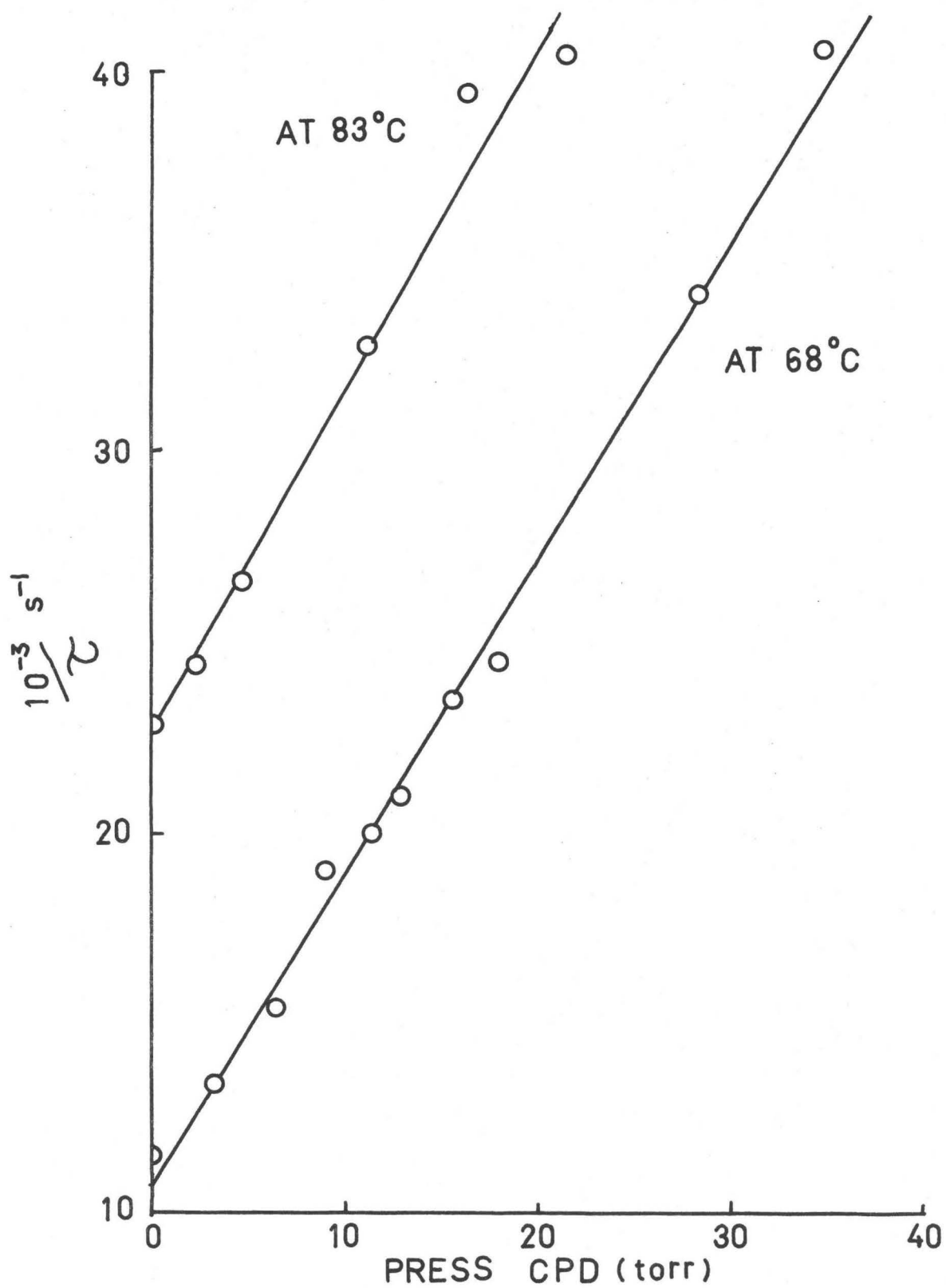


Fig. 54 Quenching of Triplet Pentanedione by Cyclopentadiene at 68°C (23PD = 7.0 torr) and at 83°C (23PD = 8.4 torr).

Fig. 55 Quenching of Triplet Pentanedione by Cyclopentadiene at 30°C,
23PD = 6.1 torr.

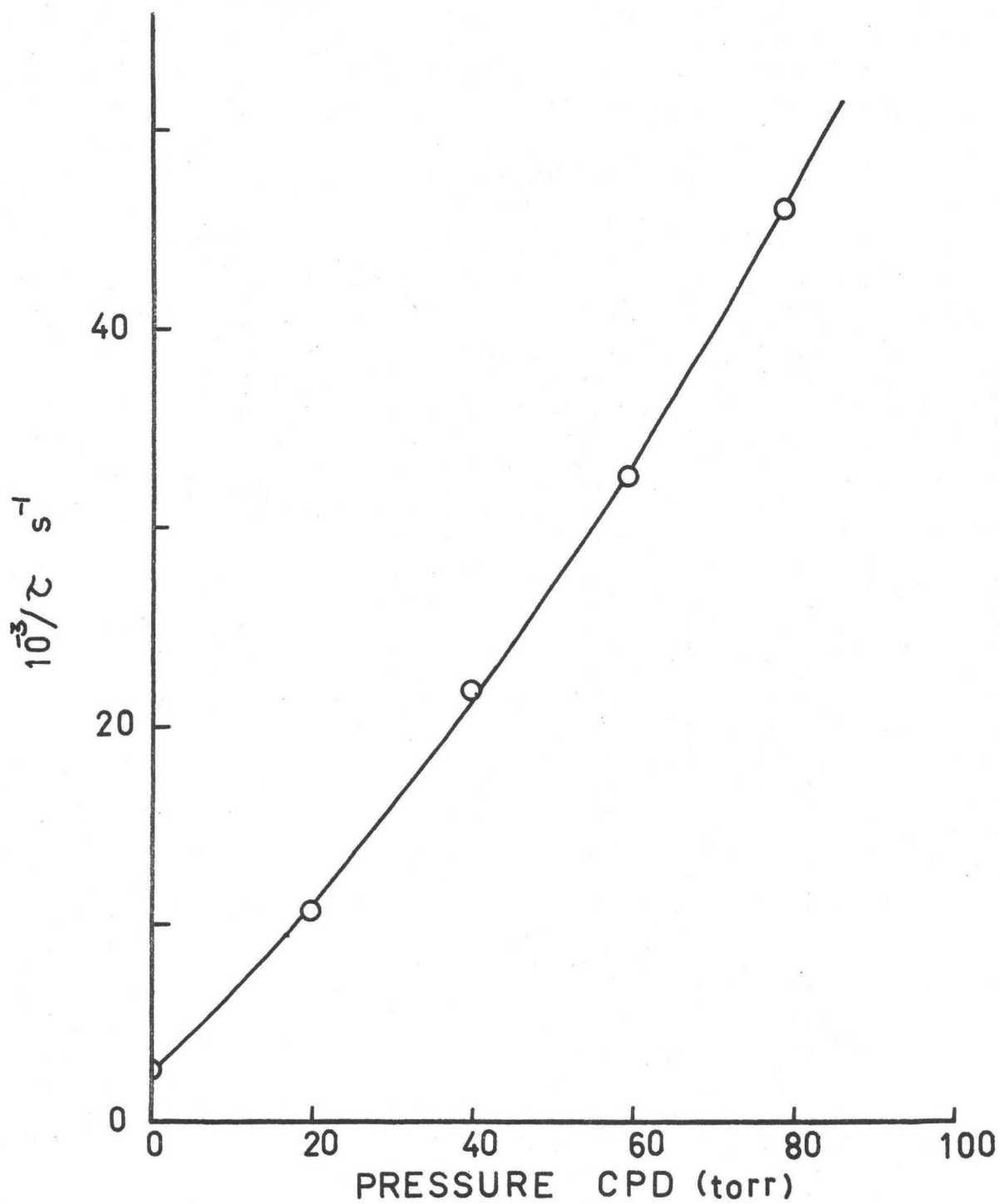
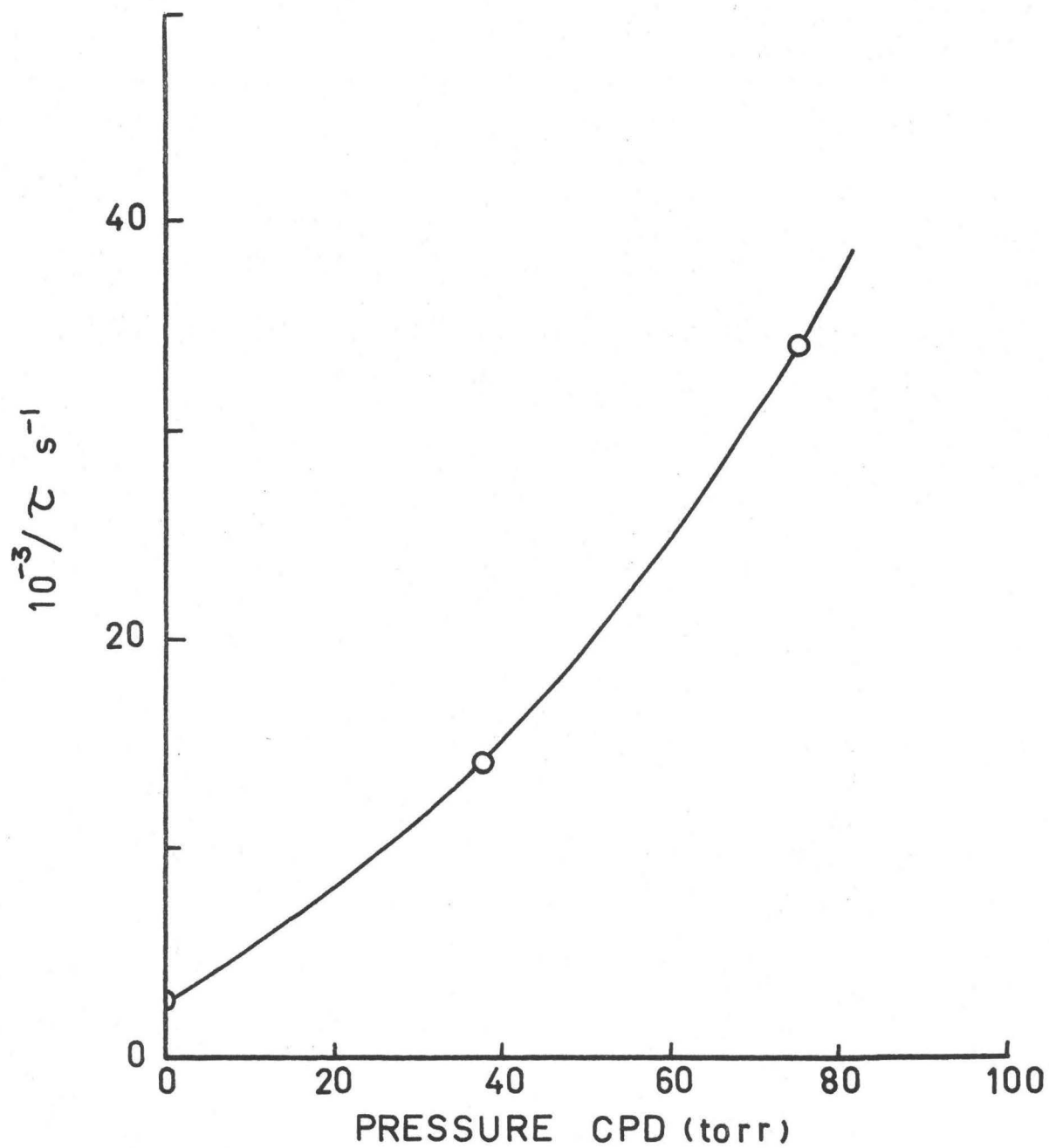


Fig. 56 Quenching of Triplet Pentanedione by Cyclopentadiene at 30°C,
23PD = 12.1 torr.



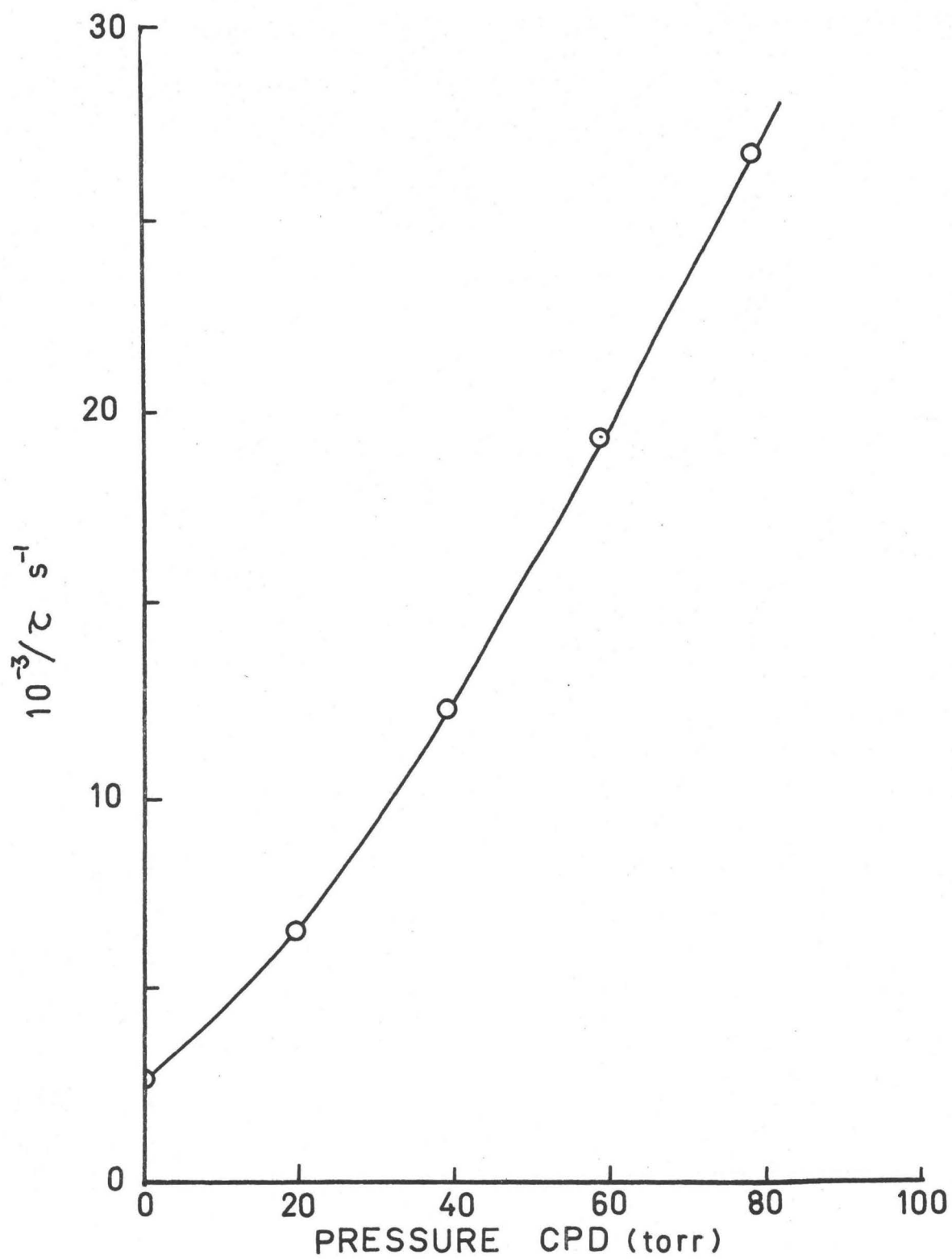


Fig. 57 Quenching of Triplet Pentanedione by Cyclopentadiene at 30°C,

23PD = 20.2 torr.

Fig. 58 Quenching of Triplet Pentanedione by Cyclopentadiene at 30°C,

23PD = 26 torr.

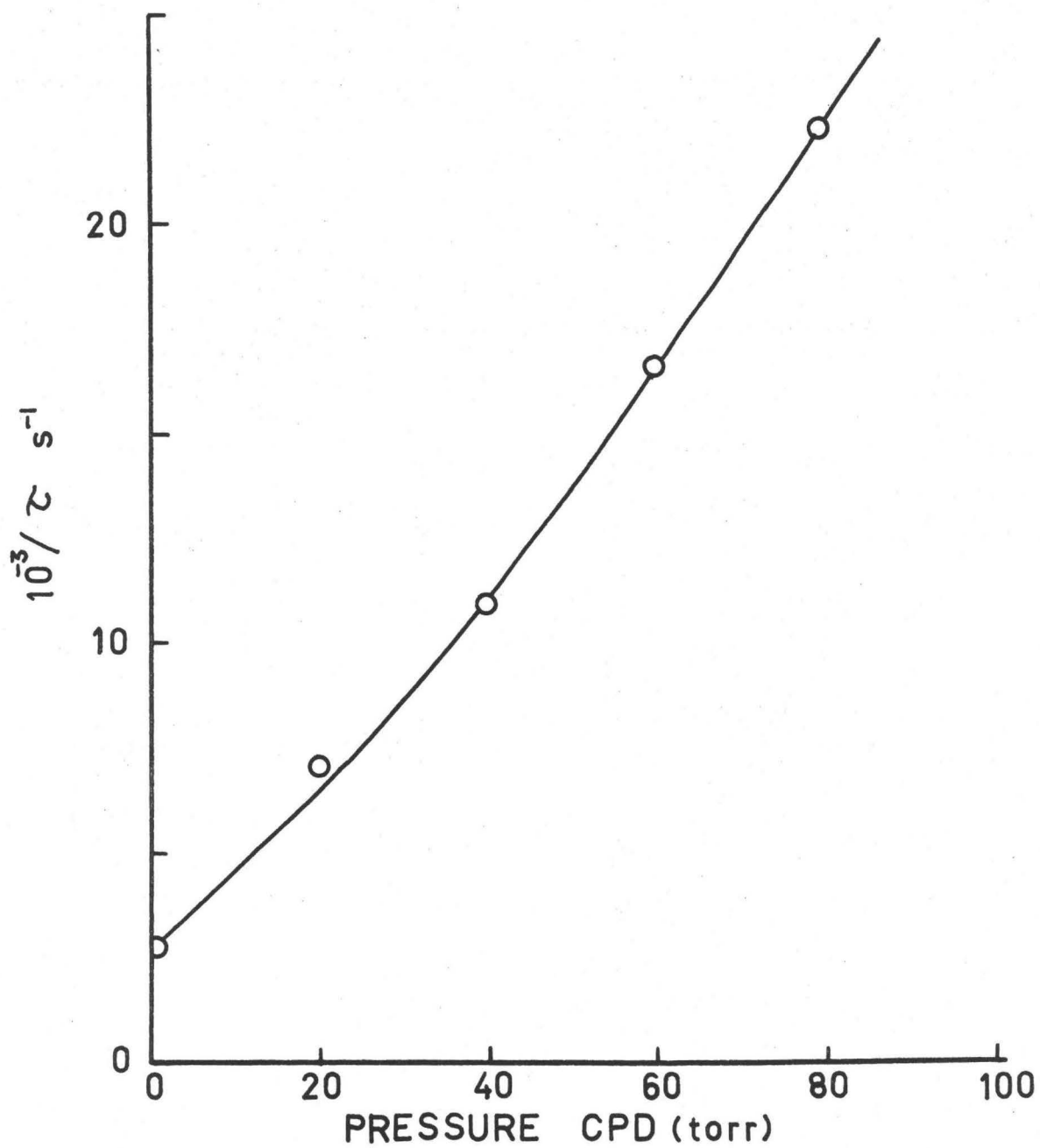
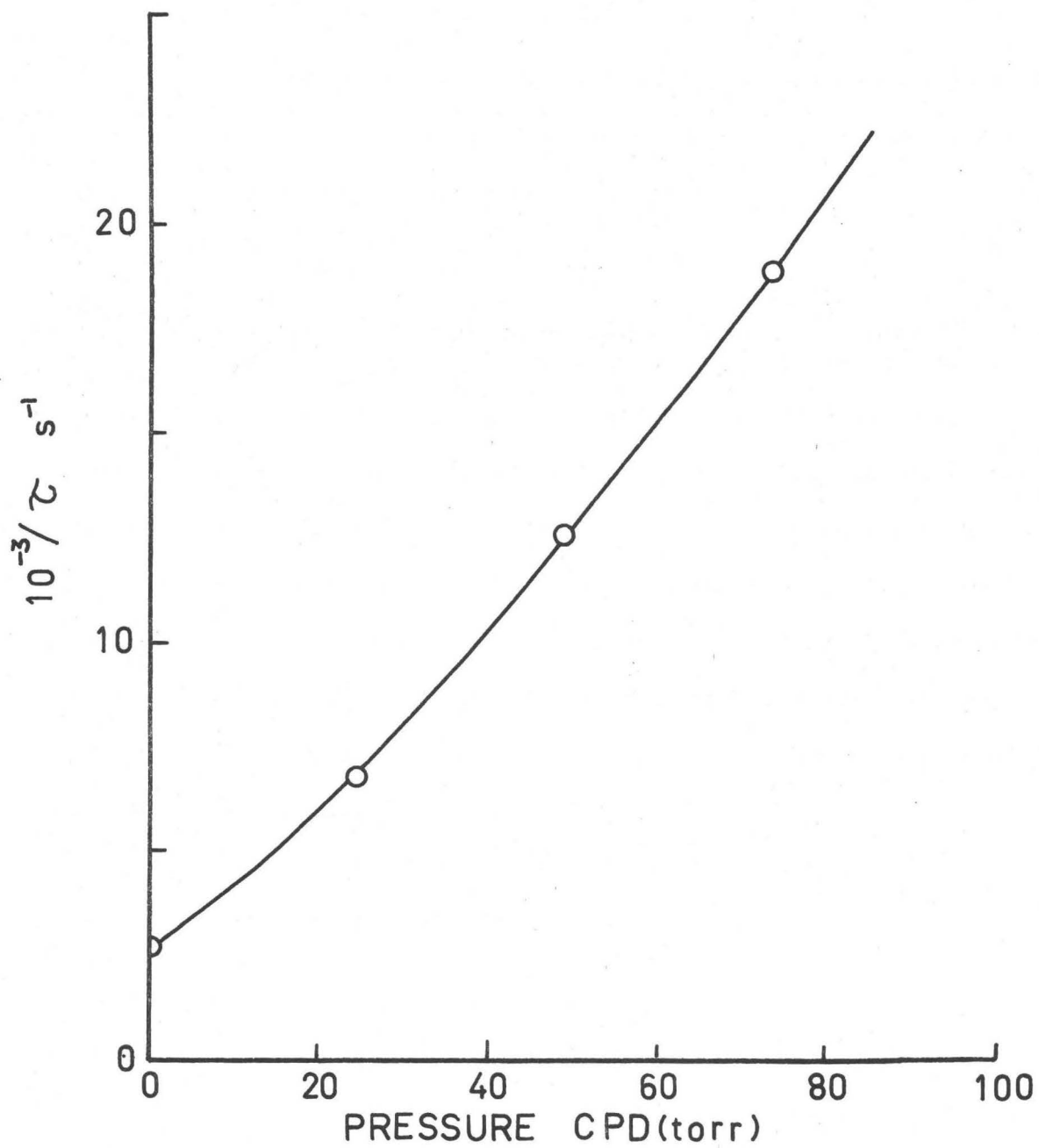


Fig. 59 Quenching of Triplet Pentanedione by Cyclopentadiene at 30°C,

23PD = 32 torr.



conjugated diolefin molecules. The diolefins 1,3-butadiene and cyclopentadiene were chosen so as to reflect the effect of structure on the quenching process.

1,3-Butadiene as Quencher

The results of the experiments with 1,3-butadiene were interesting in that the behaviour was that of a simple quencher for which linear Stern-Volmer plots were found at 30°C and 70°C.

Cyclopentadiene as Quencher

The behaviour of cyclopentadiene was unexpected, in that non-linear Stern-Volmer quenching plots were found at 30°C and linear quenching plots at 68°C and 83°C. The low temperature dependence was studied in detail at 30°C by carrying out quenching experiments with cyclopentadiene (0-80 torr) with various pressures of diketone (6-32 torr). The data from these experiments, presented in the form of τ^{-1} as ordinate and concentration of cyclopentadiene as abscissa, revealed that for a particular pressure of cyclopentadiene, low pressures of diketone were quenched more efficiently than higher pressures.

The dependence between the lifetime of the triplet, τ , and the pressure can temporarily be expressed in the form,

$$\tau^{-1} = \tau_0^{-1} + "k_Q" [\text{CPD}]$$

where τ_0 is the lifetime of the triplet pentanedione in the absence of cyclopentadiene and " k_Q " is a function of cyclopentadiene and pentanedione

concentrations. The expression can be rearranged into the form,

$$(\tau^{-1} - \tau_0^{-1})^{-1} = 1/k_Q \text{ [CPD]}$$

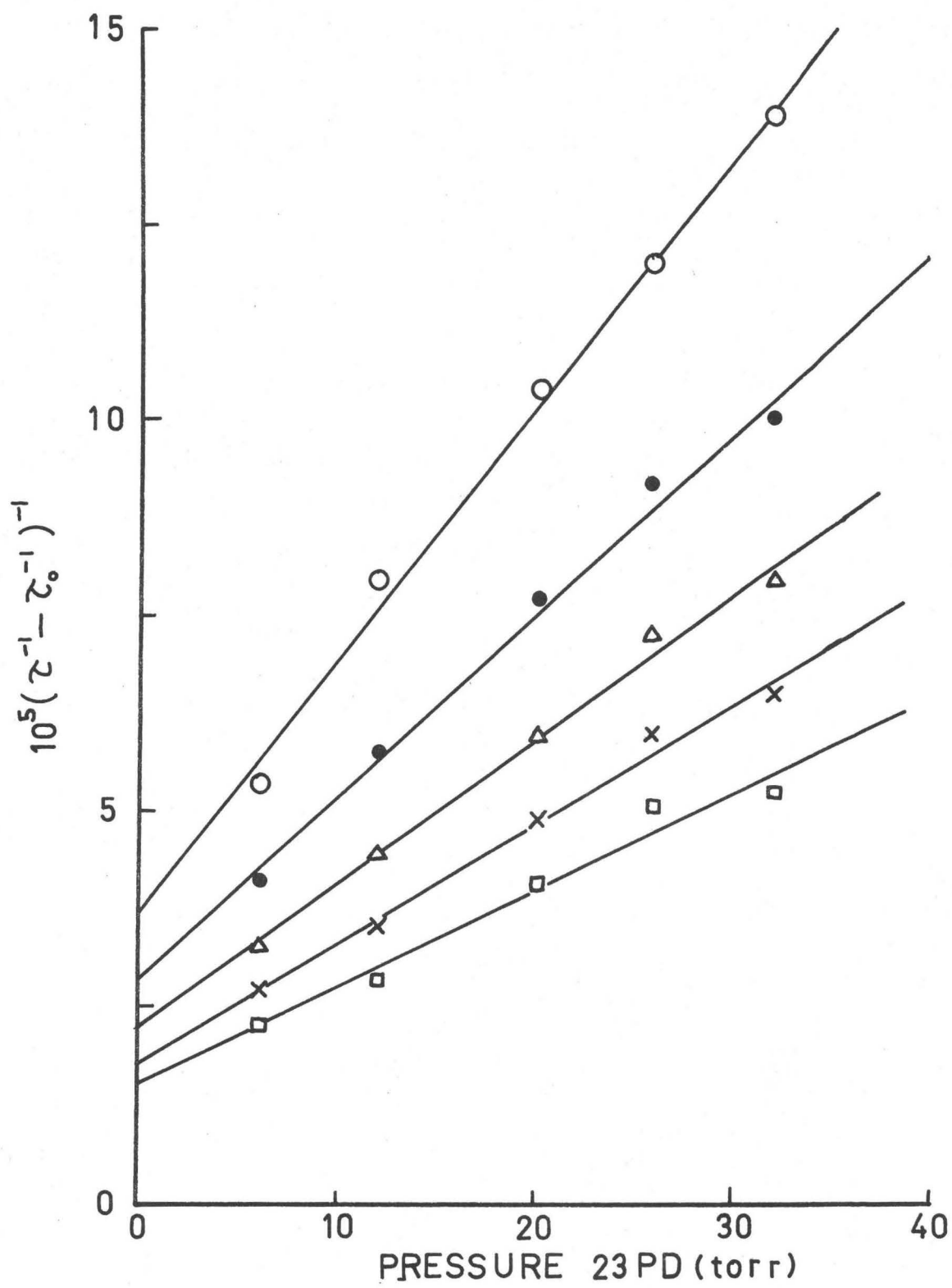
It was found that at a particular pressure of cyclopentadiene, a plot of $(\tau^{-1} - \tau_0^{-1})^{-1}$ vs [Pentanedione] was linear. The data used in the construction of these plots was obtained from Fig. 55-59 by interpolation. Furthermore, at high pressures of cyclopentadiene, the slope and the intercept of the plot was smaller than the slope and intercept at lower pressures. These characteristics are shown in Fig. 60 and 61.

Proposed Mechanism for Cyclopentadiene Quenching

At this point, a mechanism is proposed which accounts for the observations concerning the pentanedione/cyclopentadiene system. In this way, the derivation of other properties of the system will become evident. The quenching ability of diolefins interacting with triplet diketone molecules in the gas phase has been shown by several workers (151,132,166). In the case of biacetyl triplets with butadiene, the original suggestion of Rebbert and Ausloos (151) was that the diolefin molecule had a low lying triplet energy level which was approximately compatible with the excitation energy available in the diketone molecule. Collision between a triplet biacetyl molecule and a ground state diolefin would allow the non-radiative transfer of this electronic excitation energy. This concept was enlarged by Lee and co-workers (166) who attempted to explain the transfer of energy to various conjugated olefins in terms of the exchange theory of Dexter (167). This theory will be discussed in detail later.

Fig. 60 Variation of $(\tau^{-1} - \tau_0^{-1})^{-1}$ with pentanedione pressure at 30°C. Data derived from Fig. 55-59.

- CPD = 40 torr
- CPD = 50 torr
- △ CPD = 60 torr
- × CPD = 70 torr
- CPD = 80 torr



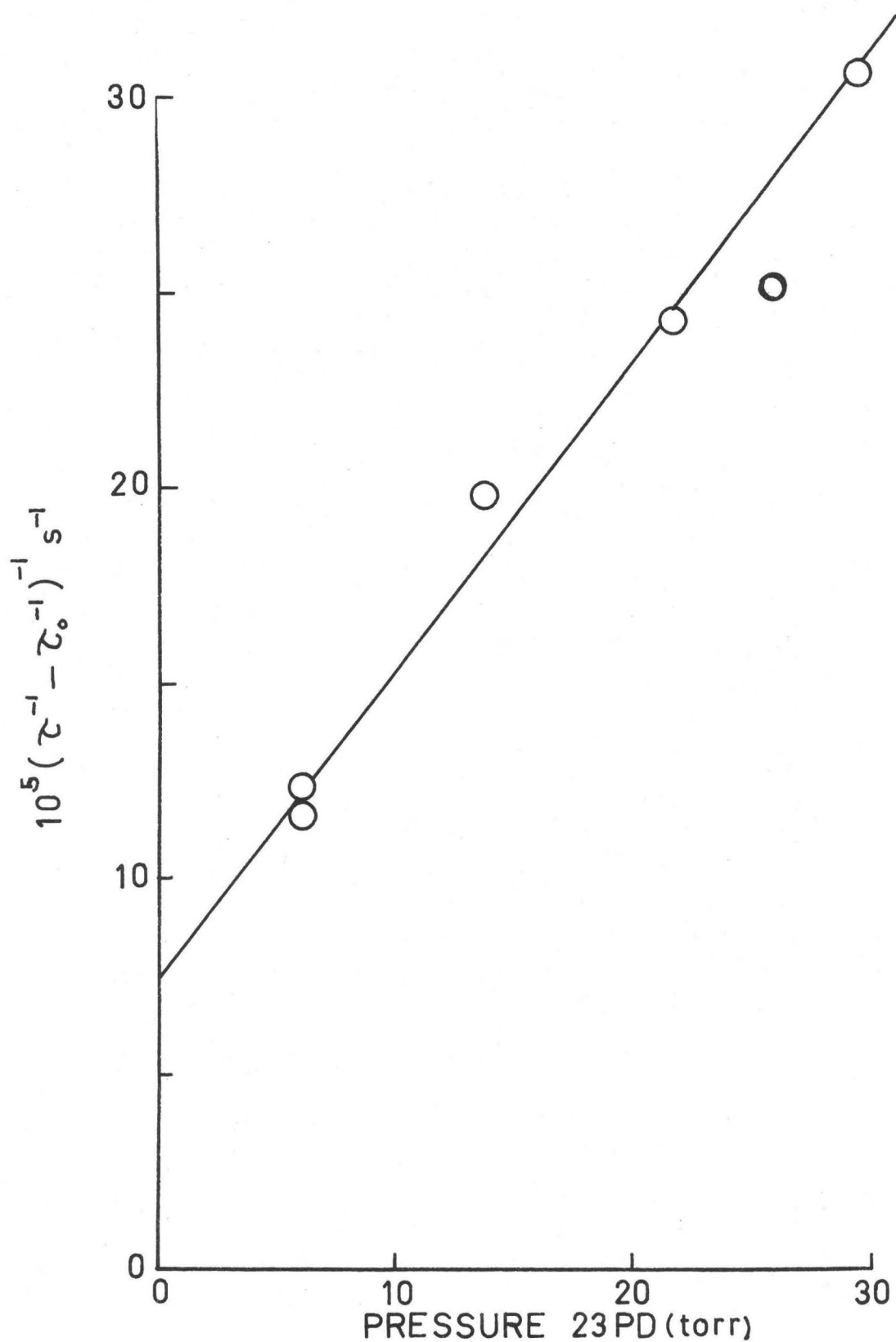
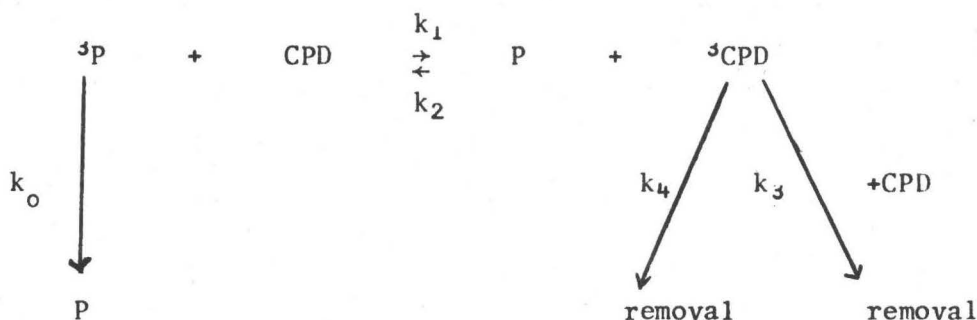


Fig. 61 Variation of $(\tau^{-1} - \tau_0^{-1})^{-1}$ with Pentanedione Pressure at 30°C; CPD pressure is 20.0 torr. Directly acquired data, experiment where the pressure of CPD was fixed and the pressure of pentanedione was varied.

Having adopted the notion of energy transfer as being a likely mechanism for the quenching interaction, the following scheme was devised for the pentanedione/cyclopentadiene system.



Here, P represents ground state pentanedione, CPD represents ground state cyclopentadiene and the superscript 3 indicates lowest triplet state. If the steady state approximation is valid for the processes occurring after the flash excitation to give 3P ,

$$\text{For } {}^3\text{CPD: } k_1[{}^3P][\text{CPD}] = k_2[{}^3\text{CPD}][P] + k_4[{}^3\text{CPD}] + k_3[{}^3\text{CPD}][\text{CPD}]$$

$$\text{i.e. } [{}^3\text{CPD}] = \frac{k_1[\text{CPD}][{}^3P]}{k_2[P] + k_4 + k_3[\text{CPD}]}$$

The rate of removal of 3P is given by,

$$-\frac{d[{}^3P]}{dt} = k_0[{}^3P] + k_3[{}^3\text{CPD}][\text{CPD}] + k_4[$$

Substituting for $[{}^3\text{CPD}]$,

$$-\frac{d[{}^3P]}{dt} = k_0[{}^3P] + \frac{(k_3[\text{CPD}] + k_4)k_1[\text{CPD}][{}^3P]}{(k_2[P] + k_4 + k_3[\text{CPD]})}$$

which is first order in 3P . The lifetime of the 3P is then given by,

$$\tau^{-1} = k_0 + \frac{k_1(k_3[\text{CPD}] + k_4)[\text{CPD}]}{(k_2[P] + k_4 + k_3[\text{CPD]})}$$

Recognising that $k_0 = \tau_0^{-1}$

$$\tau^{-1} - \tau_0^{-1} = \frac{k_1(k_3[\text{CPD}] + k_4)[\text{CPD}]}{(k_2[\text{P}] + k_4 + k_3[\text{CPD}])} \quad (1)$$

Rearranging,

$$(\tau^{-1} - \tau_0^{-1})^{-1} = \frac{k_2[\text{P}]}{k_1(k_3[\text{CPD}] + k_4)[\text{CPD}]} + \frac{1}{k_1[\text{CPD}]} \quad (2)$$

This equation can now be tested using the data in Table 10 which has been derived from Fig. 60 and Fig. 61.

Tests of the Mechanism

- (1) A straight line relationship is predicted between $(\tau_0^{-1} - \tau^{-1})^{-1}$ and the concentration of pentanedione at a constant cyclopentadiene concentration. This is found for a range of values of the cyclopentadiene concentration. Furthermore, as the cyclopentadiene concentration increases, the magnitudes of the slope and the intercept should decrease. This is confirmed by inspection of Fig 60 and Fig. 61.
- (2) If equation (2) is valid, then the intercepts of Fig 60 and 61 should vary directly as the inverse of [CPD]. This is tested in Fig. 62 using the data in Table 10, which was derived from Fig. 60 and Fig. 61. Within the uncertainties (one standard deviation) of the intercept values, the agreement with the predicted form is good.
- (3) According to equation (2) above, the slope of the lines in Figs. 60 and 61 at constant [CPD] is given by,

TABLE 10. SLOPE AND INTERCEPT DATA FROM FIG. 60 AND FIG. 61
UNITS ARE THOSE USED IN FIG. 60 AND FIG. 61 AND SUBSEQUENT FIGURES.

[CPD] in torr	SLOPE	INTERCEPT
20	0.79 ± 0.04	7.5 ± 0.8
40	0.321 ± 0.015	3.71 ± 0.33
50	0.232 ± 0.014	2.84 ± 0.30
60	0.183 ± 0.009	2.25 ± 0.19
70	0.153 ± 0.009	1.79 ± 0.20
80	0.124 ± 0.012	1.52 ± 0.27

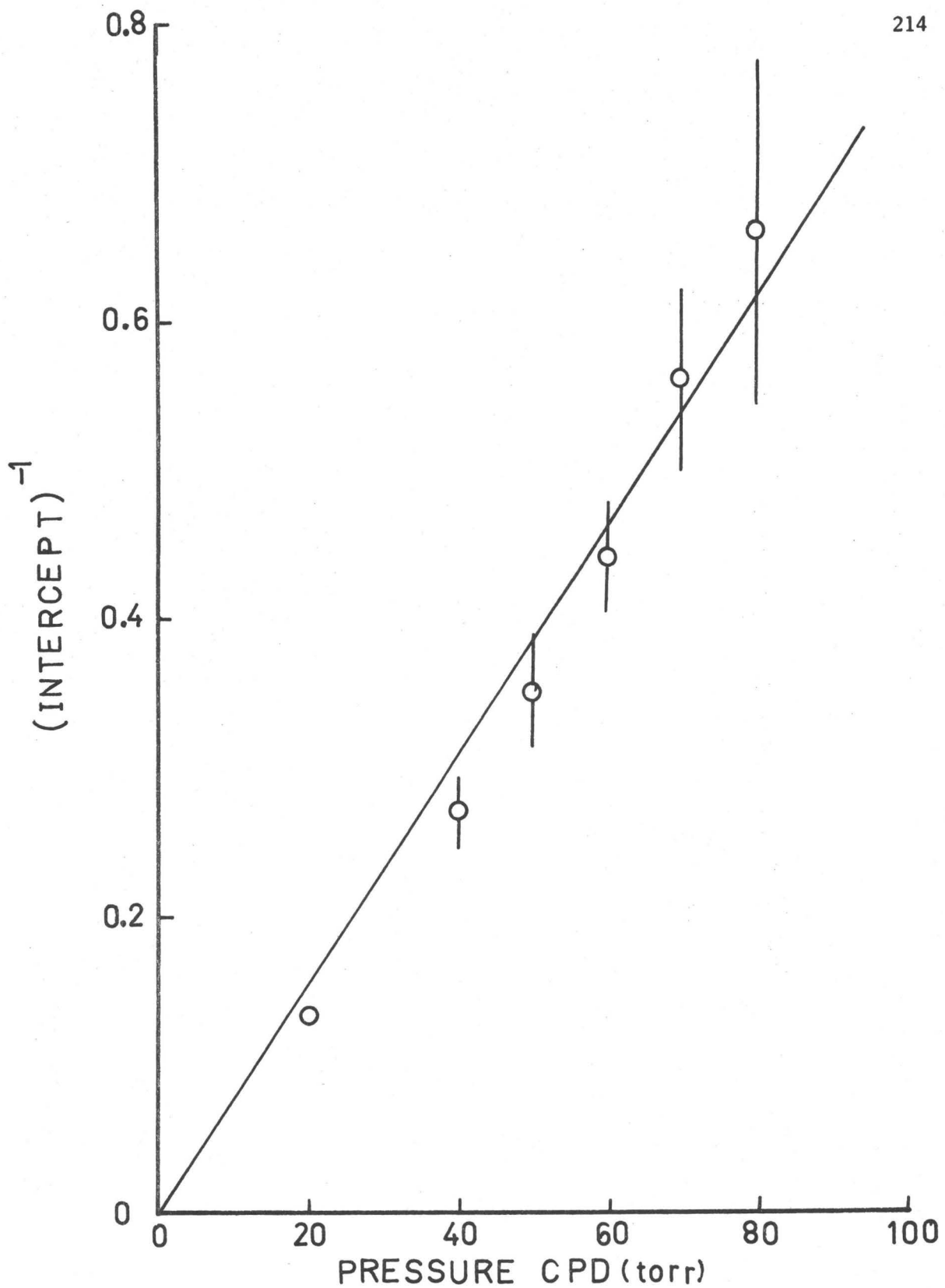


Fig. 62 [Intercept from Figs. 60 and 61]⁻¹ vs CPD pressure.

$$\text{slope} = \frac{k_2}{k_1[\text{CPD}](k_3[\text{CPD}] + k_4)}$$

$$\text{i.e. } \frac{1}{\text{slope} \times [\text{CPD}]} = \frac{k_1}{k_2} (k_3[\text{CPD}] + k_4) \quad (3)$$

This prediction is tested in Fig. 63 using the data in Table 10. It can be seen that the derived data points are well described by a straight line variation. The vertical error bars correspond to one standard deviation for the uncertainty in the value of the slope given in Table 10.

We can conclude on the basis of these tests that the mechanism described above accounts very well for the observed behaviour of the pentanedione/cyclopentadiene system at 30°C. The values and ratios of some of the rate constants of this mechanism can be derived:

(1) From Fig. 62, representing the variation of 1/intercept vs [CPD], the derived value of k_1 is $1.42 \times 10^7 \text{ M}^{-1}\text{s}^{-1}$.

(2) From Fig. 63 and equation (3),

$$\text{Slope of Fig. 63} = \frac{k_1 k_3}{k_2} = (1.12 \pm 0.07) \times 10^6 \text{ M}^{-1}\text{s}^{-1}$$

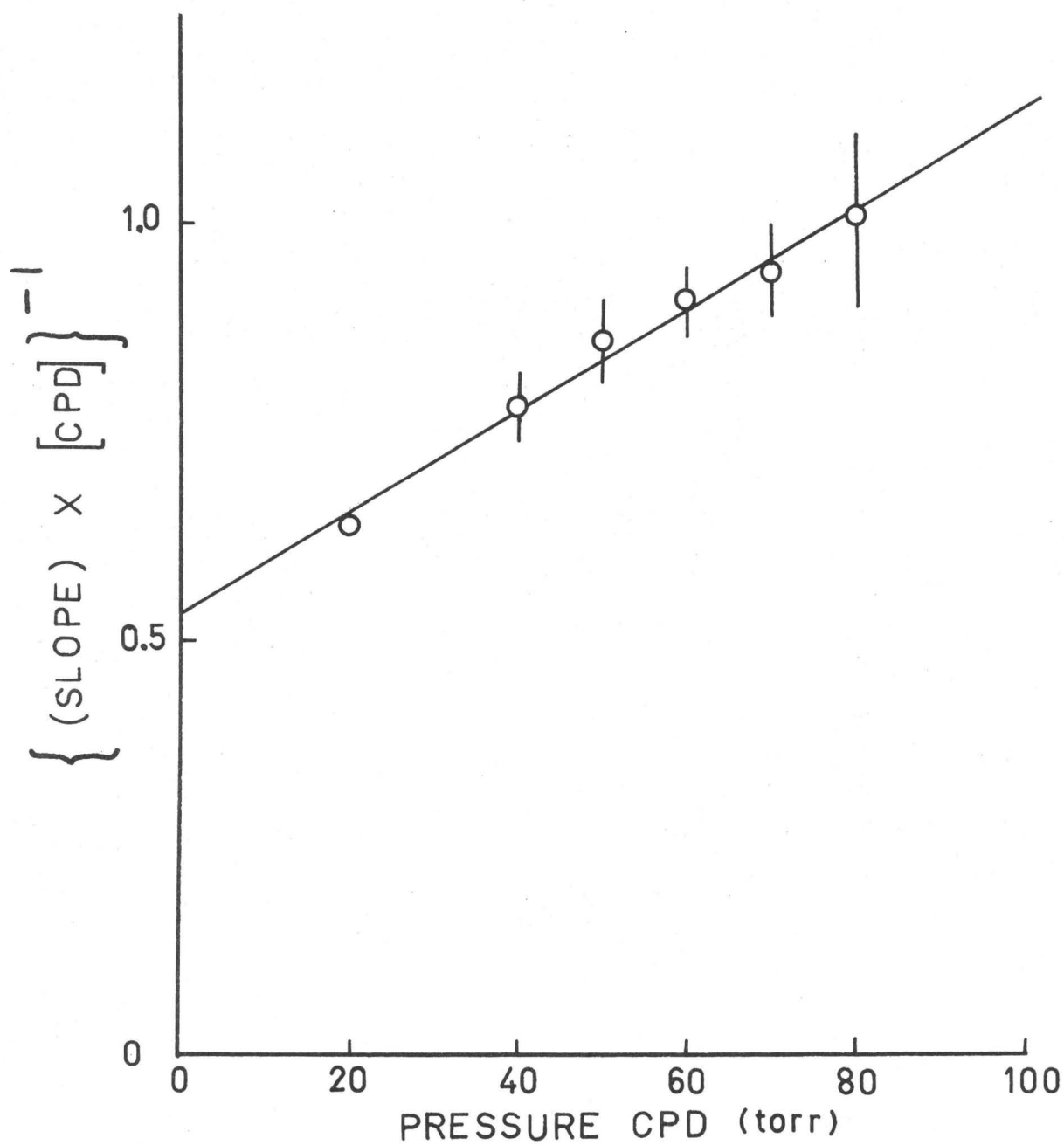
$$\text{Intercept of Fig. 63} = \frac{k_1 k_4}{k_2} = (5.3 \pm 0.2) \times 10^3 \text{ s}^{-1}$$

$$\therefore \frac{k_3}{k_4} = (2.1 \pm 0.2) \times 10^2 \text{ M}^{-1}$$

Variation with Temperature

The values of these rate constants now allow an explanation of the behaviour of the system at various temperatures. The quenching at elevated temperature gave linear Stern-Volmer plots which yield values

Fig. 63 $\left\{ \left[\text{Slope of Figs. 60 and 61} \right] \times [\text{CPD}] \right\}^{-1}$ vs CPD pressure.



of k_Q of $1.53 \times 10^7 \text{ M}^{-1}\text{s}^{-1}$ at 68°C and $1.66 \times 10^7 \text{ M}^{-1}\text{s}^{-1}$ at 83°C .

The agreement between these values and the constant k_1 at 30°C is striking.

Inspection of equation (1) shows how the high temperature behaviour could arise.

If at higher temperatures,

$$k_3[\text{CPD}] + k_4 \gg k_2[\text{P}]$$

then equation (1) develops the form,

$$\tau^{-1} = \tau_0^{-1} + k_1[\text{CPD}]$$

This is exactly the behaviour found. Furthermore, the temperature variation of k_1 over the temperature range 30°C to 83°C is not large. This behaviour also indicates that the term $k_4 + k_3[\text{CPD}]$ has a considerable temperature dependence, as at 30°C $k_4 + k_3[\text{CPD}] \sim k_2[\text{P}]$, whereas at the higher temperatures, $k_4 + k_3[\text{CPD}] \gg k_2[\text{P}]$.

The existence of step (3) in the mechanism is particularly crucial to the interpretation of the interaction. This step is immediate evidence for the intermediacy of a species of cyclopentadiene other than the ground state, having an independent existence. What is more, this species is a product of the interaction between a triplet pentanedione molecule and a ground state cyclopentadiene molecule. The pentanedione/cyclopentadiene system has been studied in fluid solution by Hammond and co-workers (40). It was found that excitation of the pentanedione caused the photosensitised dimerisation of cyclopentadiene to give the products shown on page 18.

It is, therefore, reasonable to associate the formation of these products with the process (3) in the mechanism. It is unlikely that these products would interfere with the measurements in these experiments because, being unconjugated olefins, they would be expected to have a low quenching efficiency (Chapter 10).

Demonstrating the intermediacy of what is presumably the triplet state of cyclopentadiene is critically important, in that it directly demonstrates the nature of the triplet pentanedione/ground state cyclopentadiene interaction, i.e. energy transfer. This important conclusion can be used as a basis for the discussion of the relative efficiencies of butadiene and cyclopentadiene in this process. The description of the triplet-triplet energy transfer process is not well understood, however, most interpretations of this phenomena have used as their basis, the theory of Dexter.

Dexter Theory of Triplet-Triplet Energy Transfer

The quenching of triplet diketone molecules by diolefins in the gas phase was originally associated (151) with the exchange of electronic excitation energy. This concept was adopted by Lee who attempted to correlate the quenching efficiency of various diolefins with biacetyl triplet molecules. According to the theory of Dexter at short distances, the interaction between an electronically excited molecule and a ground state molecule by overlap of molecular orbitals is such as to allow the radiationless transfer of energy by an exchange mechanism. In particular, the process represented by,



termed triplet-triplet transfer, is allowed. The probability of this transfer is proportional to the square of an exchange integral given by,

$$P(^3D \rightarrow ^3A) \propto |\int \psi_{D^*} \psi_A H' \psi_D \psi_{A^*} d\tau|^2$$

Here, $\psi_{D^*} \psi_A$ and $\psi_D \psi_{A^*}$ are the wavefunctions of the initial and final states, respectively, and $H' = e^2/r_{12}$ where r_{12} is the distance between the electrons involved in the transition and e is the electronic charge. This probability will only have appreciable values when r_{12} is small, Dexter has shown that this probability can be expressed as,

$$P(^3D \rightarrow ^3A) = \frac{2\pi}{h} Z^2 \int f_D(E) F_a(E) d(E) \quad (4)$$

where the integral represents the degree of overlap between the normalised emission spectrum of the donor, $f_D(E)$, and the normalised absorption spectrum of the acceptor, $F_a(E)$. The quantity Z^2 is related to the exchange integral given above,

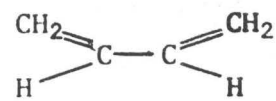
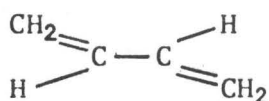
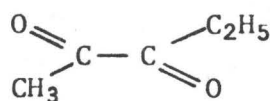
$$Z^2 = \sum_{\text{initial}} \sum_{\text{final}} \frac{e^4}{g_{D^*} g_A} |\int \psi_{D^*} \psi_A H' \psi_D \psi_{A^*} d\tau|^2$$

where g_{D^*} and g_A are the degeneracies of the states D^* and A . The immediate conclusion of this theory is that the probability of radiationless transfer in the gas phase depends on the degree of overlap of the emission spectrum of the donor and the absorption spectrum of the acceptor, but not on their absolute intensities.

To apply this theory to the pentanedione/diene system studied here, requires the knowledge of the characteristics of the $T_1 \leftarrow S_0$ absorption in butadiene and cyclopentadiene. The transitions in these spectra are of very low intensity and have been studied only in the presence of

high pressures of oxygen (168). While this allows the position of the 0-0 transition in butadiene and cyclopentadiene to be established as 59.6 Kcal and 58.3 Kcal respectively, the profiles of the absorptions cannot be ascertained due to interfering absorptions of a diene-oxygen charge-transfer complex (168). However, the positions of the 0-0 band indicate that the overlap of the phosphorescence emission of pentanedione ought to be greater with the cyclopentadiene absorption than with the butadiene spectrum.

The probability of the energy transfer process occurring also depends on the value of the exchange integral between the molecular orbitals involved. It is reasonable to suppose that the magnitude of this term will depend on the proximity of the molecular orbitals involved in the transition. Inspection of the diagram below shown that the interaction can be expected to be greater for the trans form of butadiene than for the cis form of butadiene.



Unfortunately, this must remain as speculation until calculations are carried out to put the effect on a quantitative basis. It is interesting, however, that geometric requirements have been observed in the transfer of triplet energy in solution (168,170) and the solid state (171)

Reversible Energy Transfer

An interesting example of the triplet-triplet energy transfer phenomenon occurs when the triplet levels of the donor and acceptor lie

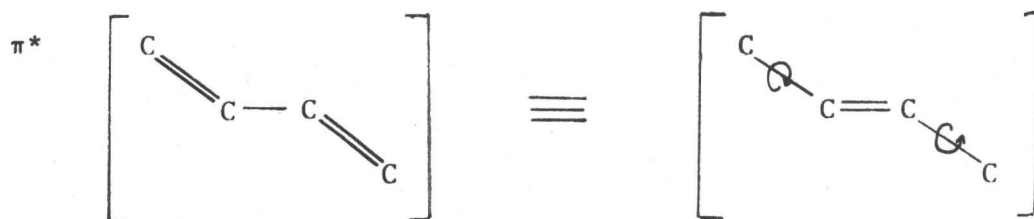
close together. It is then possible that reversible energy transfer may occur, i.e. ${}^3D + A \rightarrow {}^3A + D$, ${}^3A + D \rightarrow {}^3D + A$

This situation has been shown to occur in fluid solution (35). It will give rise to a complicated dependence for the time evolution of the system and detection of this effect will depend upon the lifetime of 3A . If the lifetime of 3A is short, then the reverse process,



will be difficult to detect and the system will display simple Stern-Volmer quenching behaviour.

The relevance of this phenomena to the pentanedione/diene system has been demonstrated above. The difference in the behaviour of cyclopentadiene and butadiene must involve the lifetimes of their triplet states. The longer lifetime of the triplet cyclopentadiene can be reconciled with nature of the radiationless processes which are thought to occur in conjugated dienes. In acyclic conjugated dienes, the electron density in the π - π^* excited state is such as to allow rotation about what were double bonds in the ground state (172,173), i.e.



This freedom of rotation could give rise to the short lifetime of the π^* excited state through favourable Franck-Condon overlap with torsional modes in the ground state. Hammond has suggested that the removal of the triplet diene formed is not to the ground state but by relaxation

through rotation to a twisted geometry (174).

In cyclic dienes, however, and in particular cyclopentadiene, torsional freedom will be greater restricted and it might be expected that the radiationless processes removing the excited state would be less efficient. This will give rise to a longer triplet lifetime and to the detection of reversible energy transfer. It should be noted that the relatively inefficient processes which do remove the triplet cyclopentadiene could be represented by reaction (4) in the proposed mechanism.

Dienes as Quenchers in Other Systems

In spite of the need in Dexter theory of presently inaccessible information concerning the $T_1 \leftarrow S_0$ absorption spectrum of the quencher and values of exchange integrals, striking correlations have been found between what is presumably energy transfer, and the comparability of the triplet energies of donor and acceptor (35,174-176).

A pertinent example is the interpretation given by Hammond (179) of the photosensitized dimerisation of butadiene and isoprene (2-methylbutadiene) in solution, using various sensitizers (donors). The composition of the products varied smoothly with the triplet energy of the sensitizer and allowed certain conclusions to be drawn concerning the nature of the interaction with the diene. It was found that for $E_T > 60$ Kcals, where E_T is the 0-0 energy of the triplet state of the donor derived from its phosphorescence spectrum, the transfer could be considered as taking place to the trans form of the diene. Whereas for $50 \text{ Kcals} < E_T < 60 \text{ Kcals}$ the transfer could be considered as taking place to the cis form of the diene, present in small amount, which is assumed to have an energy of ~ 52 Kcals.

This value is derived by analogy with cyclohexadiene, a prototype cis diene, which has a 0-0 E_T estimated at 52 Kcals (168).

Clearly, this is a possibility in the pentanedione study described above, where the triplet pentanedione ($E \sim 55$ Kcals) can transfer energy to the S-cis form of butadiene. However, this cannot be applied to the case of cyclopentadiene which does not have geometric isomers. Therefore, the situation with respect to S-trans butadiene ($E_T = 60$ Kcal) and cyclopentadiene ($E_T = 58$ Kcal) is that there may be an energy discrepancy between the 0-0 levels of triplets involved.

In the case of butadiene, if the interpretation of Hammond is valid, then energy transfer from triplet pentanedione ($E_T = 55$ Kcal) takes place mainly to the S-cis form of the diene ($E_T \sim 55$ Kcal), or via an endothermic process to the trans form ($E_T \sim 60$ Kcals). It would be expected that varying the temperature would vary the equilibrium distribution of S-cis rotomers, due to the enthalpy difference between the two forms, which has been estimated at +2 Kcals (179). However, the activation energy of k_Q for butadiene found in this study is only 0.2 Kcal. This is not consistent with the estimated value of $\Delta H = 2$ Kcals for the cis-trans isomerisation and indicates that the interaction is not with the S-cis form of the diene. There could be fortuitous compensating variations with temperature affecting the overall efficiency of the process. This compensation could arise if the interaction between triplet diketone and ground state diolefin required the formation of a loosely bound complex having a very short lifetime during which the electronic energy is radiationlessly transferred. At higher temperatures, the stability of this complex could be reduced such that the

radiationless transfer takes place less efficiently than at lower temperatures.

Classical and Non-Classical Energy Transfer

The correlation of energy transfer efficiency and sensitizer energy found in a few well-studied systems has led Hammond to categorize acceptors as classical or non-classical (177). This distinction rests on the behaviour of the variation of the bimolecular energy transfer rate constant and the triplet energy of the sensitizer.

Classical Acceptors

For values of E_T greater than a critical value of the triplet energy of the acceptor, k_Q is constant, and independent of E_T . However, for values of E_T up to 5 Kcals less than the critical value, the dependence of $\log k_Q$ upon E_T is approximately linear, i.e.

$$\frac{\Delta \log k_Q}{\Delta E_T} = \text{const}$$

This is the same conclusion drawn by Sandros (35) for various sensitizers of biacetyl phosphorescence in solution. The existence of this linear relationship is explained by the classical principle of an activation energy for the energy transfer process. This is contrary to the general inefficiency of conversion of energy between electronic and vibrational degrees of freedom in bimolecular collisions (178) which is due to the non-interaction between nuclear and electronic motions in the Born-Oppenheimer approximation for the molecule. This difficulty can be avoided if the potential curves of the donor and acceptor can approach

each other so that perturbations allow interchange of energy between vibrational and electronic degrees of freedom. This is equivalent to the breakdown of the Born-Oppenheimer approximation for this situation.

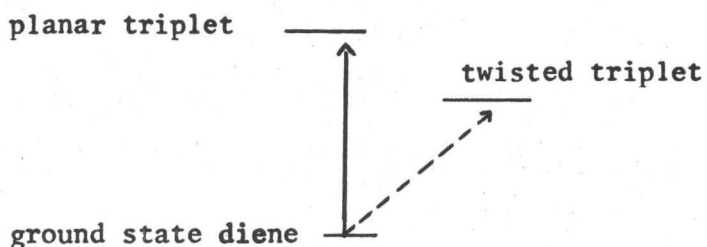
At this point, the rationalization of the behaviour in terms of Dexter's formalism becomes flimsy. To explain this uphill process of energy transfer, overlap would have to occur between the $S_0 \rightarrow T_1$ absorption of the higher energy triplet acceptor and emission from the low energy donor which extends to higher energies than its 0-0 band, i.e. 'hot' band emission.

The classical concept envisaged above, has been derived from isothermal observations in which the energy of the sensitizer was varied. No test has been carried out with a particular sensitizer at various temperatures. The data obtained in this study show that the temperature effect on the efficiency of transfer for butadiene and cyclopentadiene is small over the range 300-350°K. This is interesting for several reasons. Consider first the case of cyclopentadiene, if the system were behaving in the 'classical' manner described above, then one might expect the energy transfer rate constant to vary due to the energy gap between the E_T level of pentanedione (~ 55 Kcal) and the E_T level of cyclopentadiene (~ 58 Kcal). Although these energies are in some doubt, the variation in the bimolecular quenching constant is small and indicates that these energy estimates would have to be altered considerably in order to describe the cyclopentadiene quenching as 'classical'.

Non-Classical Acceptors

The alternative to a 'classical' system is a 'non-classical'

system. This description was applied by Hammond to describe the behaviour of dienes as acceptors when energy transfer occurred from donors with triplet energy considerably less than either the S-cis or S-trans forms. It was proposed that during the time of the interaction, the geometry of the dienes changed from planar to one in which rotation had occurred around a double bond. This twisted form had an energy compatible with the lower energy available in the donor. In terms of the formalism of Hammond, this was described as a 'non-vertical' or non-spectroscopic transition. Support for this suggestion is gained from the earlier re-



ference to the relatively long lifetime of triplet dienes in solution (174), together with their inability to transfer energy back to transfer energy back to the lower energy triplet state of the original donor.

Unfortunately, introducing the concept of non-vertical transitions still does not immediately explain the behaviour of the cyclopentadiene system. No spectroscopic information is available concerning the structure of the triplet species and no detailed study has been carried out to determine the acceptor properties of the ground state in sensitization reactions. It is possible that the relaxed structure of the excited cyclopentadiene is non-planar due to contributions of the type shown

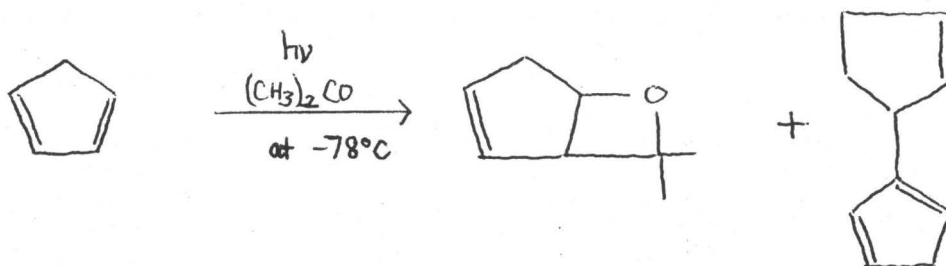
in the $\pi\pi^*$ state, directly analogous to the case of acyclic dienes (180).

This implies the existence of a loose chemical complex between the diketone and the diene such that the Born-Oppenheimer approximation breakdown allows the necessary changes in geometry to be concerted with electronic energy transfer. The lack of temperature effect on the transfer constant could be explained as for butadiene in terms of the coincidental cancelling of temperature effects between the extra vibrational energy of the triplet diketone and the reduced stability of the loose complex. Comparison with the observations of the sensitized dimerisation of cyclohexadiene, presumed to go via a triplet hexadiene intermediate $E_T \sim 52$ Kcals, reveals that only sensitizers with energy greater than or equal to the triplet energy of the triplet hexadiene brought about efficient energy transfer (181). When sensitizers of slightly lower energy were used, addition between donor and acceptor took place. The somewhat tortuous arguments used here to explain the diene data reflect the complexity and current understanding of the triplet-triplet energy transfer process (18).

Chemical Interaction

One feature of the energy transfer process which has been mentioned several times in this discussion is a chemical interaction between donor and acceptor. The importance of this aspect is emphasized by the isolation of 1:1 addition products between acceptor and donor in some cases. The formation of a metastable complex between donor and acceptor has formed the basis of a mechanism for the sensitized dimerisation (183). However, the general application of this theory

is doubtful and the existence of this kind of interaction has been definitely disproved for the pentanedione/cyclopentadiene case at 30°C. It is of direct interest, however, that sensitization of cyclopentadiene at -78°C with acetone ($E_T \sim 73$ Kcal) goes via an unexpected course (183).



Not only does another dimer of cyclopentadiene not found at higher temperatures become an important product, but the formation of an oxetane by cycloaddition is direct evidence for the chemical interaction of donor and acceptor under these conditions. Extending the analogy of triplet acetone-cyclopentadiene oxetane formation to triplet pentanedione-cyclopentadiene oxetane formation is an intriguing possibility, especially in the light of the known ability of diketones and diolefins to form complex products, though admittedly in low yield (147).

Conclusions

The conclusions of the quenching experiments with butadiene and cyclopentadiene are difficult to summarize. Triplet-triplet transfer of electronic energy almost certainly occurs on collision; the explanation of the inefficiency (one collision in $\sim 10^4$) depends on the mechanism

chosen to describe the interaction. The strictly physical picture described by Dexter and developed by Hammond is undoubtedly valuable. Although the behaviour of borderline cases of energy matching between donor and acceptor is not satisfactorily explained, the alternative postulation of chemical interaction in all borderline cases is not justified on the basis of the diverse chemical character of the sensitizers used.

Possibly the description is a composite of both extreme views. The encounter between a donor and an acceptor must involve severe perturbations of their isolated quantum mechanical descriptions. The consequences of this upon the various selection rules governing the behaviour of this encounter complex have been pointed out by Matsen (71). If this transient species is thought of in the same terms as a stable electronically excited system, then there will be many possibilities for the processes which will cause its destruction. The 'simple' case of energy transfer, where $E_T \text{ donor} \approx E_T \text{ acceptor} + \text{up to } 10 \text{ Kcal}$, could be thought of as an 'intramolecular' redistribution of electronic energy, with a subsequent or simultaneous radiationless transition to a description corresponding to the decomposition of the supermolecule. The facility of this process will reflect the triplet energy levels of the isolated molecules. However, the existence of perturbations in the supermolecule can be expected to cause distortion of these isolated levels. When the downhill energy discrepancy is too great, the necessary dissipation of the extra energy between the vibrational modes of the system, particularly in the gas phase, does not take place efficiently (151,166). The description of borderline and uphill transfer cases

would require a time lag for the necessary redistribution of energy in the supermolecule; similar to that in the RRKM description of unimolecular decompositions. The efficiency of this process will, therefore, reflect its success in the face of competition from other radiationless process in the supermolecule. In the general case, these would correspond to decomposition of the supermolecule (an unsuccessful chemical encounter), or bond formation leading to addition products between acceptor and donor.

CONCLUSIONS

This work has been arranged in such a fashion as to allow conclusions to be drawn from experiments at the time they are described. It is necessary, however, to make some remarks which will allow a perspective to be taken.

The measurement of fluorescence and phosphorescence yields in the pentanedione system has proved to be a powerful tool in the elucidation of mechanism. In Chapter 4, the value of the fluorescence yield when compared with that of biacetyl has allowed comments to be made concerning the intersystem crossing process from the S_1 to the T_1 manifold. Whereas in Chapter 5 the value of temperature variation is revealed in that the Arrhenius parameters for the radiationless processes removing the triplet state have been calculated.

In Chapter 7, the use of fluorescence measurements in demonstrating the magnitude of radiationless processes occurring in higher levels of the singlet manifold is stated. In particular the inherent ambiguities present in the interpretation of fluorescence data do not allow a firm conclusion to be reached concerning the collisional deactivation mechanism within the singlet manifold. Chapter 8 provides a pleasing correlation of the properties of the system which had been deduced from preceding experiments. It also points out the consistent nature of the proposed mechanism which does not call for grossly temperature dependent processes removing the excited singlet state.

The interactions of the triplet state with other chemical species have been investigated in Chapters 9-11. Again variation of temperature allows interesting speculations to be made about the form of the interactions in the different cases. It is of special importance that the complex quenching behaviour found for cyclopentadiene at 30°C calls for the independent existence of the electronically excited triplet cyclopentadiene molecule. This immediately reveals the interaction to be electronic energy transfer. The lack of a temperature effect on the endothermic transfer efficiency is intriguing and can at best be explained by invoking fortuitous compensations. Clearly, the nature of the electronic energy transfer process is complex and this complexity can only be enhanced when the triplet levels of donor and acceptor are approximately the same. Chemical bonding interactions seem to become important and the formation of stable or metastable species is favoured.

Appendix A

2,3-Pentanedione (Eastman Kodak and Eastern Chemical Company) was purified (99.8%) by gas-liquid chromatography on a 6m 30% SE-30 on Chromosorb W column at 70°C and stored in a blackened bulb at 77°K. Mass spectral analysis showed no species with $m/e > 100$, and all fragments could be derived from 2,3-pentanedione. Only very pure pentanedione gave reproducible experimental results.

Biacetyl (Matheson Coleman and Bell Chromatoquality Reagent) was distilled at -35°C and collected at -78°C. The middle third fraction was used.

Chlorobiacetyl was prepared by the method of Oglobin and Potekhin (184) and purified by gas-liquid chromatography on a 6m 30% SE-30 on Chromosorb W column at 100°C.

Quinine sulphate (N.F. Grade) was supplied by Fisher and used without further purification.

Oxygen (Matheson Bone Dry Grade) was used as supplied.

Sulphur hexafluoride (Matheson Research Grade) was distilled from -112°C and collected at -135°C.

Perfluoroethane (Matheson Reagent Grade) was distilled at -112°C and collected at -142°C.

Acrolein (BDH Reagent Grade) was purified by distillation at -45°C and collected at -78°C.

Crotonaldehyde (Matheson Coleman and Bell Reagent Grade) was purified by distillation at -35°C and collected at -63°C. Subsequent GLC analysis showed the purity to be better than 99.9%.

Methyl vinyl ketone (Matheson Coleman and Bell Reagent Grade) was purified by distillation at -35°C and collected at 63°C.

Xenon (Airco Research Grade) was degassed and used without further purification.

Furan (Matheson Coleman and Bell Reagent Grade) was purified by distillation at -45°C and collected at -63°C .

Perfluorobutene-2 (Matheson Instrument Grade) was purified by distillation at -95°C and collected at -142°C .

Germane has been prepared by reduction of germanium tetrachloride. Purification was by distillation at -126°C .

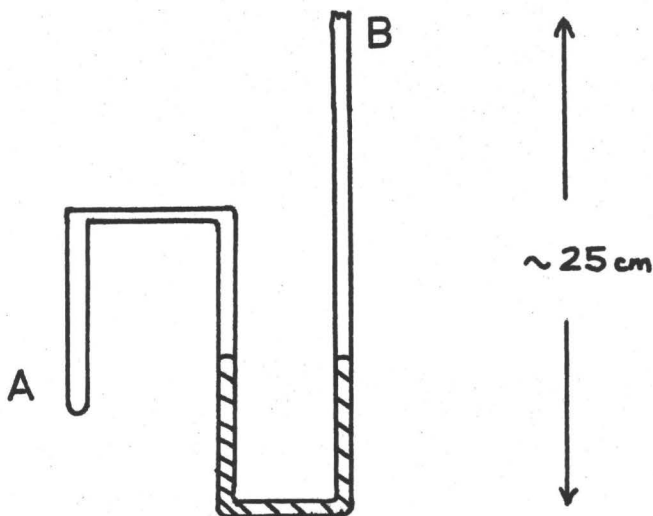
Isobutane (Matheson Research Grade) was distilled at -142°C and collected at -196°C .

Butadiene (Matheson Instrument Grade) was distilled from -78°C into -112°C , the middle one-half fraction was used.

Cyclopentadiene was prepared from the dimer (supplied by Eastman Organic) by thermal cracking over glass chips. Subsequent distillation at -35°C and collected at -78°C .

Appendix B

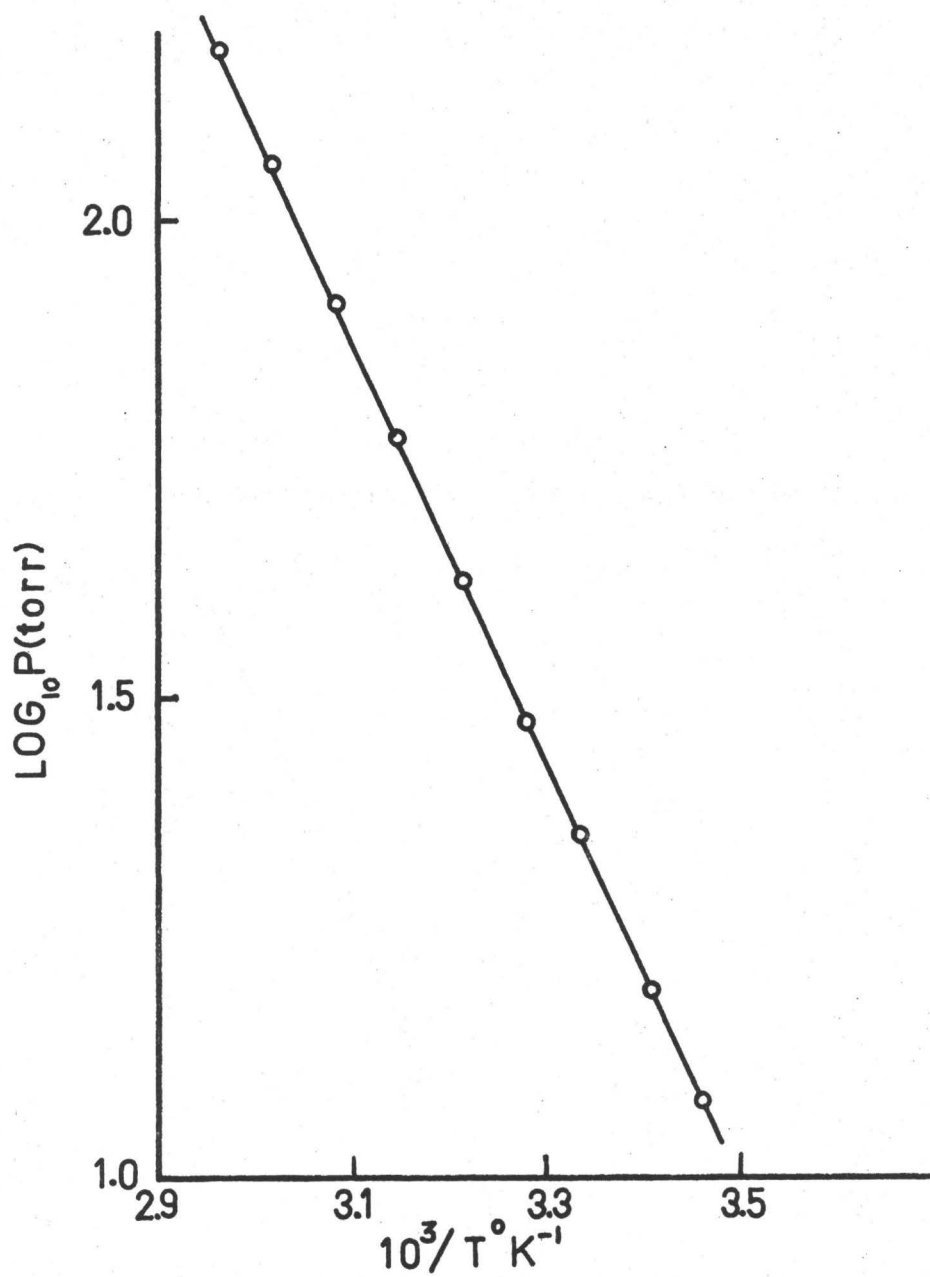
The vapour pressure of pentanedione was determined using the simple apparatus shown below.



The trap, constructed from 5mm Pyrex tubing was attached to the vacuum rack and evacuated. A small sample of pentanedione was condensed into A. Mercury was then allowed to enter the U-tube and fill it to a convenient level. The tubing was then sealed under vacuum at B.

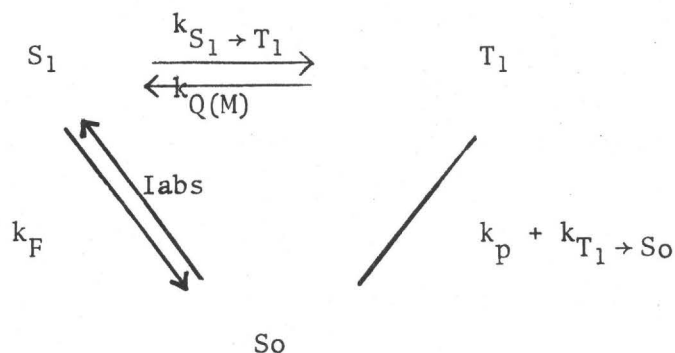
The apparatus was then completely immersed in a thermostated water bath and readings of the pressure head of the manometer were taken at temperatures from 25 to 65°C with a cathetometer. The results obtained are shown in the form of the variation of $\log p$ with $1000/T$ in Fig. 64. The heat of vapourisation, ΔH , was calculated as 9.4 Kcal. mole⁻¹.

Fig. 64 Clausius-Claypyron plot for 2,3 pentanedione in region 300-370°K



Appendix C

The system of delayed fluorescence is considered to be described by



Activation of T_1 to the S_1 manifold is through collisions with added M. If the system is excited by a short pulse of light at time equals zero, the evolution of the system will be governed by the coupled differential equations below.

$$\frac{-d(T_1)}{dt} = k_{T_1 \rightarrow S_0}(T_1) + k_p(T_1) + k_Q(M)(T_1) - k_{S_1 \rightarrow T_1}(S_1)$$

$$\frac{-d(S_1)}{dt} = k_{S_1 \rightarrow T_1}(S_1) + k_F(S_1) - k_Q(M)(T_1)$$

The coupled differential equations can be solved (120) to give for (T_1) ,

$$(T_1) = \text{const}_1 e^{+D_1 t} + \text{const}_2 e^{+D_2 t}$$

where const_1 and const_2 are constants and D_1 and D_2 are the roots given by

$$-(k_{T_1 \rightarrow S_0} + k_p + k_Q(M) + k_{S_1 \rightarrow T_1}) \pm (k_{T_1 \rightarrow S_0} + k_p + k_Q(M) + k_{S_1 \rightarrow T_1}) \sqrt{\frac{1 - 4(k_{T_1 \rightarrow S_0} + k_p)k_{S_1 \rightarrow T_1}}{(k_{T_1 \rightarrow S_0} + k_p + k_Q(M) + k_{S_1 \rightarrow T_1})^2}}$$

2

Comparing the magnitude of the terms under the square root

$$(k_{T_1 \rightarrow S_0} + k_p + k_Q(M) + k_{S_1 \rightarrow T_1}) \sim (10^3 + 10^2 + 10^4 + 10^8) \sim (k_{S_1 \rightarrow T_1})^2 \sim 10^{16}$$

and,

$$4(k_{T_1 \rightarrow S_0} + k_p)k_{S_1 \rightarrow T_1} \sim 4(10^2 + 10^3)10^8 \sim 10^{11}$$

Therefore, the binomial expansion of the square root term is valid. By neglecting squared terms and Higher, the complete expression gives,

$$D_{1,2} = -(k_{T_1 \rightarrow S_0} + k_p + k_Q(M) + k_{S_1 \rightarrow T_1}) \pm (k_{T_1 \rightarrow S_0} + k_p + k_Q(M) + k_{S_1 \rightarrow T_1}) \left\{ \frac{1 - 2(k_{T_1 \rightarrow S_0} + k_p)k_{S_1 \rightarrow T_1}}{(k_{T_1 \rightarrow S_0} + k_p + k_Q(M) + k_{S_1 \rightarrow T_1})^2} \right\}^{1/2}$$

The two roots are given by

$$D_1 = \frac{-(k_{T_1 \rightarrow S_0} + k_{\text{phos}})k_{S_1 \rightarrow T_1}}{(k_{T_1 \rightarrow S_0} + k_p + k_Q(M) + k_{S_1 \rightarrow T_1})} \approx -(k_{T_1 \rightarrow S_0} + k_{\text{phos}})$$

$$D_2 = (k_{T_1 \rightarrow S_0} + k_p + k_Q(M) + k_{S_1 \rightarrow T_1}) + \frac{(k_{T_1 \rightarrow S_0} + k_p)k_{S_1 \rightarrow T_1}}{(k_{T_1 \rightarrow S_0} + k_p + k_Q(M) + k_{S_1 \rightarrow T_1})}$$

$$\approx -k_{S_1 \rightarrow T_1} - k_Q(M)$$

Inserting the boundary conditions, $t = 0$, $S_1 = (S_1)_0$, $T_1 = 0$ gives,

$$T_1 = -(S_1)_0 e^{-k_{S_1 \rightarrow T_1} t} + (S_1)_0 e^{-(k_p + k_{T_1 \rightarrow S_0}) t}$$

The second term is the part governing the decay of the species over relatively long times, and as can be seen, it does not contain any terms in $k_Q(M)$. Therefore, one can conclude that even if delayed E-type fluorescence did occur in this system it would not affect the phosphorescence lifetime. In terms of the model, this can be associated with the large value of $k_{S_1 \rightarrow T_1}$, so that even if species are removed by excitation back to S_1 , they are returned within a time which is small compared to the lifetime of the triplet species.

REFERENCES

1. Genesis 1, vv 3.
2. J. G. Calvert and J. N. Pitts, "Photochemistry" (New York: Wiley 1966).
3. N. J. Turro, "Molecular Photochemistry" (New York: Benjamin 1967).
4. G. S. Hammond, *Advances in Photochemistry*, 7, 373 (1970).
5. P. de Mayo and S. T. Reid, *Quart. Revs.*, 15, 393 (1961).
6. P. Borrell, *Ann. Reports Chem. Soc. London*, 60, 62 (1963).
7. W. A. Noyes Jr., G. B. Porter and J. E. Jolley, *Chem. Rev.*, 56, 49 (1956).
8. B. R. Henry and M. Kasha, *Ann. Rev. Phys. Chem.*, 19, 161 (1968).
9. J. Jortner, S. A. Rice and R. M. Hockstrasser, *Advances in Photochemistry*, 7, 149 (1969).
10. M. Bixon and J. Jortner, *J. Chem. Phys.*, 48, 715 (1968).
11. J. Jortner and R. S. Berry, *J. Chem. Phys.*, 48, 2757 (1968).
12. D. P. Chock, J. Jortner and S. A. Rice, *J. Chem. Phys.*, 49, 610 (1968).
13. K. F. Freed and J. Jortner, *J. Chem. Phys.*, 50, 2916 (1970).
14. S. P. McGlynn, T. Azumi and M. Kinoshita, "Molecular Spectroscopy of the Triplet State" (New York: Prentice-Hall 1969).
15. G. Porter, "Techniques of Organic Chemistry", 2nd ed. ed. A. Weissberger (Vol. 8, New York: Interscience, 1963) p. 1055.
16. L. M. Stevenson and G. S. Hammond, *Pure Appl. Chem.*, 16, 125 (1968).
17. H. E. Gunning and O. P. Strausz, *Advances in Photochemistry*, 1, 209 (1963).
18. P. J. Wagner, A.C.S. Symposium on Frontiers of Photochemistry, Oct. 1970, Tarreytown, N. Y.
19. N. J. Turro, "Molecular Photochemistry" (New York: Benjamin 1967) p. 208.
20. J. W. Sidman and D. S. McClure, *J. Am. Chem. Soc.*, 77, 6461 (1955).
21. W. E. Bell and F. B. Blacet, *J. Am. Chem. Soc.*, 76, 5332 (1954).
22. F. B. Blacet and W. E. Bell, *Disc. Faraday Soc.*, 14, 70 (1953; *ibid.*, 14, 131 (1953)).

23. J. Heicklen, *J. Am. Chem. Soc.*, 81, 3863 (1959).
24. H. Okabe and W. A. Noyes Jr., *J. Am. Chem. Soc.*, 79, 801 (1957).
25. H. L. J. Backstrom and K. Sandros, *Acta. Chim. Scand.*, 14, 48 (1960).
26. W. A. Noyes Jr., M. A. Mulac and M. S. Matheson, *J. Chem. Phys.*, 36, 880 (1962).
27. G. F. Sheats and W. A. Noyes Jr., *J. Am. Chem. Soc.*, 77, 1421 (1955);
ibid., 77, 4532 (1955).
28. J. T. Dubois and F. Wilkinson, *J. Chem. Phys.*, 39, 899 (1963).
29. G. P. Porter, *J. Chem. Phys.*, 32, 1587 (1960).
30. A. Gandini and K. O. Kutschke, *Proc. Roy. Soc. Ser. A*, 306, 511 (1968).
31. W. E. Kaskan and A. B. F. Duncan, *J. Chem. Phys.*, 18, 427 (1950).
32. W. H. Urry and D. H. Trecker, *J. Am. Chem. Soc.*, 84, 118 (1962).
33. J. Lemaire, *J. Phys. Chem.*, 71, 2653 (1967).
34. F. Wilkinson and J. T. Dubois, *J. Chem. Phys.*, 39, 377 (1963).
35. K. Sandros, *Acta. Chim. Scand.*, 18, 2355 (1964).
36. H. Ishikawa and W. A. Noyes Jr., *J. Chem. Phys.*, 37, 583 (1962).
37. G. S. Hammond and N. J. Turro, *Science*, 142, 1541 (1963).
38. G. N. Lewis and M. Kasha, *J. Am. Chem. Soc.*, 66, 2100 (1944).
39. W. G. Herkstroeter, A. A. Lamola and G. S. Hammond, *J. Am. Chem. Soc.*, 86, 4537 (1964).
40. G. S. Hammond, P. A. Leermakers and N. J. Turro, *J. Am. Chem. Soc.*, 83, 2395 (1961).
41. W. H. Urry and D. H. Trecker, *J. Am. Chem. Soc.*, 84, 118 (1962).
42. W. H. Urry, D. H. Trecker and D. A. Winey, *Tetra. Letters*, 609 (1962).
43. H. H. Richtol and F. H. Klappmeier, *J. Chem. Phys.*, 44, 1519 (1966).
44. N. J. Turro and T. J. Lee, *J. Am. Chem. Soc.*, 91, 5651 (1969).
45. *Advances in Photochemistry* (in press).

46. H. E. Zimmerman and W. R. Elser, *J. Am. Chem. Soc.*, 91, 887 (1969).
47. C. A. Parker, *Proc. Roy. Soc. Ser. A.* 220, 104 (1953); *ibid.*, A235 518 (1956).
48. R. E. Hunt and T. L. Hill, *J. Chem. Phys.*, 15, 111 (1947).
49. H. L. McMurray, *J. Chem. Phys.*, 9, 231 (1941); *ibid.*, 9, 241 (1941).
50. J. C. D. Brand, *Trans. Faraday Soc.*, 50, 431 (1954).
51. F. W. Birss, J. M. Brown, A. R. H. Cote, A. Lofthus, S. L. N. G. Krishnamachari, G. A. Osborne, J. Paldus, D. A. Ramsay, and L. Watmann, *Can. J. Phys.*, 48, 1230 (1970).
52. S. C. Woo and S. T. Chang, *Trans. Faraday Soc.*, 157 (1945).
53. M. Kasha, *Disc. Faraday Soc.*, 9, 14 (1950).
54. J. N. Murrell "Theory of the Electronic Spectra of Organic Molecules" (New York: Wiley (1929)) p. 168.
55. G. Hertzberg, "Electronic Spectra of Polyatomic Molecules" (Princeton: Van Norstand (1966)) P177.
56. K. G. Kidd and D. P. Santry, unpublished work, McMaster University (1970).
57. R. K. Boyd, G. B. Porter, K. O. Kutschke, *Can. J. Chem.*, 46, 175 (1968).
58. G.M. White, M.Sc. Thesis McMaster University (1971).
59. A. Einstein, *Physik Z.*, 18 121 (1917).
60. J. B. Birks and I. H. Monroe, *Progress in Reaction Kinetics*, 4, 291 (1967).
61. G. J. Small, *J. Chem. Phys.*, 54, 3300 (1971).
62. G. M. Almy and S. Anderson, *J. Chem. Phys.*, 8, 805 (1940).
63. W. H. Melhuish, *J. Opt. Soc. Am.*, 54, 183 (1964).
64. G. M. Almy and P. R. Gillette, *J. Chem. Phys.*, 11, 188 (1943).
65. M. Kasha, *Disc. Faraday Soc.*, 9, 14 (1950).
66. S. P. McGlynn, T. Azumi, and M. Kinoshita, "Molecular Spectroscopy of the Triplet State" (New York: Prentice-Hall 1969) P67.

67. H. J. Groh Jr., *J. Chem. Phys.*, 21, 674 (1955).
68. S. P. McGlynn, T. Azumi, and M. Kinoshita, "Molecular Spectroscopy of the Triplet State" (New York: Prentice-Hall 1969) p. 84.
69. *ibid.*, p. 72.
70. M. A. El-Sayed, *J. Chem. Phys.*, 41, 2462 (1964).
71. F. A. Matsen and D. J. Klein, *Advances in Photochemistry*, 7, 1 (1969).
72. T. F. Hunter, *Trans Faraday Soc.*, 301 (1969).
73. C. A. Parker, "Photoluminescence in Solution" (Amsterdam: Elsevier 1969), p. 44.
74. C. A. Parker and T. A. Joyce, *Chem. Comm.*, 1421 (1968).
75. S. H. Ng, Ph.D. Thesis, University of New Brunswick (1970).
76. N. J. Turro, "Molecular Photochemistry" (New York: Benjamin 1967) p. 156.
77. I. M. Whitemore and M. Szwarc, *J. Phys. Chem.*, 67, 2492 (1963).
78. C. S. Parmenter, *J. Chem. Phys.*, 41, 658 (1964).
79. I. G. Anderson, G. S. Parmenter, H. M. Poland and J. D. Ran, *Chem. Phys. Letters*, 8, 232 (1971).
80. C. S. Parmenter and H. M. Poland, *J. Chem. Phys.*, 51, 1551 (1969).
81. L. G. Anderson and C. S. Parmenter, *J. Chem. Phys.*, 52, 466 (1970).
82. N. J. Turro R. Engel, *J. Am. Chem. Soc.*, 91, 7113 (1969).
83. P. C. Haarhoff, *Mol. Phys.*, 7, 101 (1963).
84. O. Stern and M. Volmer, *Physik. Z.*, 20, 183 (1919).
85. M. E. Garabedian and D. A. Dowes, *J. Am. Chem. Soc.*, 90, 2468 (1968).
86. N. J. Turro and R. Engel, *J. Am. Chem. Soc.*, 91, 7113 (1969).
87. R. B. Cundall and A. S. Davies, *Progress in Reaction Kinetics*, 4, 181 (1967).
88. R. G. Zepp and P. J. Wagner, *J. Am. Chem. Soc.*, 92, 7466 (1970).
89. R. Bakule and F. A. Long, *J. Am. Chem. Soc.*, 85, 2309 (1963).
90. H. Moreu, *Justus Liebigs Ann. Chim.*, 14, 283 (1930).
91. G. Wheland, "Advanced Organic Chemistry" 3rd ed. (New York: Wiley 1960) p. 693.

92. R. B. Woodward and R. Hoffmann, "The Conservation of Orbital Symmetry" (New York: Academic (1970)).
93. S. Strickler and R. A. Berg, *J. Chem. Phys.*, 37, 814 (1962).
94. W. Siebrand, *J. Chem. Phys.*, 47, 2411 (1967).
95. K. F. Freed and J. Jortner, *J. Chem. Phys.*, 52, 6272 (1970).
96. R. Engelman and J. Jortner, *Mol. Phys.*, 18, 145 (1970).
97. P. F. Jones and S. Siegel, "Molecular Luminescence", Edited by E. C. Lin (New York: Benjamin 1969).
98. A. Gandini, D. A. Whytock, K. O. Kutschke, *Proc. Roy. Soc. Ser. A.*, 306, 541 (1968).
99. M. O'Sullivan and A. C. Testa, *J. Am. Chem. Soc.*, 92, 258 (1970).
100. J. P. Byrne, E. F. McCoy and I. G. Ross, *Aust. J. Chem.*, 18, 1584 (1965).
101. J. R. Henderson and M. Muramoto, *J. Chem. Phys.*, 43, 1215 (1965).
102. N. J. Turro and R. E. Engel, *J. Am. Chem. Soc.*, 90, 2989 (1968).
103. J. E. McKintosh and G. B. Porter, *J. Chem. Phys.*, 48, 5475 (1968).
104. S. W. Benson, "Thermochemical Kinetics" (New York: Wiley 1968) p. 101, 167.
105. E. S. Huyser and D. C. Neckers, *J. Org. Chem.*, 29, 276 (1964).
106. P. J. Wagner and G. S. Hammond, *Advances in Photochemistry* 5, (1968).
107. C. Walling and A. Padiva, *J. Am. Chem. Soc.*, 85, 1597 (1963).
108. G. R. MacMillan, J. G. Calvert and J. N. Pitts Jr., *J. Am. Chem. Soc.*, 86, 3602 (1964).
109. N. C. Yang and D. H. Yang, *J. Am. Chem. Soc.*, 80, 2913 (1958).
110. N. C. Yang, S. P. Elliot and B. Kim, *J. Am. Chem. Soc.*, 91, 7551 (1969).
111. H. E. Zimmerman, *Advan. in Photochem.*, 1, 183 (1963).
112. C. Walling, "Free Radicals in Solution", (New York: Wiley 1958).
113. P. Gray, R. Shaw and J. C. J. Thynne, *Progress in Reaction Kinetics*, 4, (1967).

114. R. F. Borkman and D. R. Kearns, *J. Am. Chem. Soc.*, 88, 3467 (1966).
115. N. C. Yang, *J. Am. Chem. Soc.*, 85, 1017 (1963).
116. K. H. Shulte-Elte and G. Ohloff, *Tet. Letters*, 1143 (1964).
117. P. J. Wagner and G. S. Hammond, *J. Am. Chem. Soc.*, 87, 4010 (1965);
ibid., 88, 1245 (1966).
118. N. B. Slater, "Theory of Unimolecular Reactions" (Ithaca: Cornell Univ. Press (1959)).
119. C. W. Larson and H. E. O'Neal, *J. Phys. Chem.*, 73, 1011 (1969).
120. Margenau and Murphy, "Mathematical Methods in Physics and Chemistry".
121. J. T. Dubois and F. Wilkinson, *J. Chem. Phys.*, 39, 899 (1963).
122. N. J. Turro and R. Engel, *J. Am. Chem. Soc.*, 90, 2089 (1968).
123. H. S. Samant and A. J. Yarwood, *Can. J. Chem.*, 48, 2611 (1970).
124. "Handbook of Physics and Chemistry", 48th Ed. Chem. Rubber Co., p. F42.
125. W. Kauzmann, "Kinetic Theory of Gases", (New York: Benjamin (1966)), p. 202.
126. K. F. Laidler, "Chemical Kinetics", 2nd Ed. (New York: McGraw-Hill (1965)).
127. A. Gandini, D. A. Whytock and K. O. Kutschke, *Proc. Roy. Soc. Ser. A.*,
306, 529 (1968); *ibid.*, 306, 537 (1968); *ibid.*, 306, 541 (1968).
128. W. R. Ware and M. L. Dulton, *J. Chem. Phys.*, 47, 4670 (1967).
129. A. M. Halpern and W. A. Ware, *J. Chem. Phys.*, 53, 1969 (1970).
130. F. C. Henriques and W. A. Noyes Jr., *J. Am. Chem. Soc.*, 62, 1038
(1940).
131. E. Caro, J. Grotewold and E. A. Lissi, *Chem. Comm.*, 318 (1969).
132. E. Aubin, J. Grotewold and E. A. Lissi, *J. Chem. Soc. A.*, 516 (1971).
133. S. H. Ng, G. P. Semeluk, and I. Unger, *Ber, der Bunsen-Gas*, 74, 29 (1971).
134. H. J. Groh Jr., *J. Chem. Phys.*, 21, 674 (1953).
135. P. G. Bowers and G. B. Porter, *J. Phys. Chem.*, 70, 1962 (1966).
136. G. B. Porter and K. Uchida, *J. Phys. Chem.*, 70, 4079 (1966).
137. A. N. Strachan, R. K. Boyd and K. O. Kutschke, *Can. J. Chem.*, 42, 1435 (1964).

138. S. P. McGlynn, T. Azumi and M. Kunoshika, "Molecular Spectroscopy of the Triplet State" (New York: Prentice-Hall 1969) p. 284.
139. R. F. Borkman and D. R. Kearns, *J. Chem. Phys.*, 44, 945 (1966).
140. H. S. Samant, Ph.D. thesis, McMaster University (1970).
141. W. H. Eberhardt and H. Renner, *J. Mol. Spectry.*, 6, 483 (1961).
142. J. C. D. Brand and D. G. Williamson, *Disc. Faraday Soc.*, 35, 184 (1963).
143. Y. Amako, M. Akagi and H. Azumi, *Proc. Internat. Symp. on Mol. Spec. and Mol. Struc.*, Tokyo (1965).
144. A. Devanquet and L. Salem, *Can. J. Chem.*, 49, 977 (1971).
145. C. E. Castro and F. F. Rust, *J. Am. Chem. Soc.*, 83, 4928.
146. H. Ryang, K. Shima and H. Sakurai, *Tet. Letters*, 1091 (1970).
147. G. E. Gream, M. Mular and J. C. Price, *Tet. Letters*, 3479 (1970).
148. G. S. Hammond and N. J. Turro, *Advances in Photochemistry*, 1, 2.
149. A. Cook, G. P. Semeluk and I. Unger, *Can. J. Chem.*, 47, 4527 (1969).
150. F. Glocking, "The Chemistry of Germanium" (New York: Academic (1969)) p. 12.
151. R. E. Rebbert and P. Ausloos, *J. Am. Chem. Soc.*, 87, 5569 (1965).
152. K. Kawaoka, A. U. Kahn and D. R. Kearns, *J. Chem. Phys.*, 46, 1842 (1967).
153. A. W. Jackson and A. J. Yarwood, *Can. J. Chem.*, 48, 3763 (1970).
154. Private communication, G. P. Semeluk, University of New Brunswick.
155. L. Vanquickenborne and S. P. McGlynn, *J. Chem. Phys.*, 45, 4755 (1966).
156. H. Zeldes and R. Livingston, *J. Chem. Phys.*, 47, 1465 (1967).
157. S. A. Weiner, E. J. Livingston, and B. M. Monroe, *J. Am. Chem. Soc.*, 91, 6350 (1969).
158. G. Hertzberg, "Electronic Spectra of Diatomic Molecules" (Princeton: Van Norstand (1966)).
159. G. Buchi, J. T. Kofron, E. Koller and D. Rosenthal, *J. Am. Chem. Soc.*, 76, 876 (1956).

160. D. R. Arnold, R. L. Hinman and A. H. Glick, *Tet. Letters*, 1425 (1964).
161. N. C. Yang, M. Nussin, M. J. Jorgensen and S. Murov, *Tet. Letters*, 3657 (1964).
162. C. A. Parker and C. G. Hatchard, *Trans. Faraday Soc.*, 57, 1894 (1961).
163. N. A. Coward and W. A. Noyes Jr., *J. Chem. Phys.*, 22, 1207 (1954).
164. C. R. Noller, "Chemistry of Organic Compounds", (Philadelphia: Saunders 1965).
165. M. W. Schmidt and E. K. C Lee, *J. Am. Chem. Soc.*, 92, 3579 (1970).
166. D. L. Dexter, *J. Chem. Phys.*, 21, 836 (1951).
167. D. F. Evans, *J. Chem. Soc. B*, 1735 (1960).
168. W. G. Herkstroeter, L. B. Jones and G. S. Hammond, *J. Am. Chem. Soc.*, 88, 4777 (1965).
169. E. F. Unman and N. Baumann, *J. Am. Chem. Soc.*, 90, 4158 (1968).
170. J. K. Roy and M. A. El-Sayed, *J. Chem. Phys.*, 40, 3442 (1964).
171. J. Saltiel, L. Metts, and M. Wrighton, *J. Am. Chem. Soc.*, 92, 3227 (1970).
172. N. L. Allinger and M. A. Miller, *J. Am. Chem. Soc.*, 86, 2811 (1964).
173. R. S. H. Liu, N. J. Turro and G. S. Hammond, *J. Am. Chem. Soc.*, 87 3406 (1963).
174. W. G. Herkstroeter, N. J. Turro and G. S. Hammond, *J. Am. Chem. Soc.*, 88, 4769 (1966).
175. W. L. Dilling, R. D. Kroening and J. C. Little, *J. Am. Chem. Soc.*, 92, 928 (1970).
176. W. G. Herkstroeter and G. S. Hammond, *J. Am. Chem. Soc.*, 88, 4769 (1966).
177. A. B. Callear and J. D. Lambert, *Comprehensive Chemical Kinetics*, Vol. 3, Edited by C. H. Bamford and C. F. H. Tipper Elsevier (1969).
178. J. G. Aston and G. Szacs, *J. Chem. Phys.* 14, 67 (1946).
179. H. E. Simmons, *Progress in Phys. Org. Chem.*, 7, 1 (1970).

181. D. Valentine, N. J. Turro and G. S. Hammond, J. Am. Chem. Soc., 86, 5202 (1964).
182. E. H. Gold and D. Ginberg, Angew. Chem. Intern. Ed. Engl., 5, 246 (1966).
183. G. O. Shenck and R. Steinmetz, Bull. Soc. Chim. Benges., 71, 781 (1962).
184. K. A. Oglobin and A. A. Potekhin, Zhurnal Obshekei Khimii, 34, 2688 (1964).